Notch signalling in intestinal homeostasis and cancer: orchestrator of stemness

Erika López Arribillaga

TESI DOCTORAL UPF 2016

Thesis supervisors:
Dr. Lluís Espinosa Blay
Dr. Anna Bigas Salvans

Programa de Recerca en Càncer,
Institut Hospital del Mar d'Investigacions Mèdiques

Zuei, beti neregan sinisteagatik

"[Cancer cells] have somehow lost the ability to stop dividing. Every cell in the body, after all, is descended from an unbroken line of billions of generations of germ-line cells that have not stopped dividing. Suddenly being asked to become a somatic cell [...] and learn the act of not dividing, has never happened before in the entire history of the cell's ancestors!"

Richard Dawkins – The Ancestor's Tale,
a Pilgrimage to the Dawn of Life (2004)

ACKNOWLEDGEMENTS

ACKNOWLEDGEMENTS

Todo doctorando al que le preguntas te dice que la parte más difícil de escribir de una tesis es la Discusión. Pero se equivocan. Lo más difícil es escribir los agradecimientos. Cómo resumir cinco o seis años de trabajo en un libro es la parte fácil. Hacer los experimentos es la parte divertida (sí, incluso los que no salen). Pero… ¿Cómo agradecer a toda esa gente que te ha acompañado a lo largo de este camino…? ¡Eso sí que es difícil!

Primero me gustaría dar las gracias a mis directores de tesis, Lluís y Anna. Por una parte, por la confianza que depositaron en mí desde el principio, y por otra, por haberme guiado y haber sabido exprimir lo mejor de mí en un entorno científico. Lluís, tú siempre tuviste fama de ser "un jefe duro", pero yo no entiendo el trabajo en el laboratorio de otra manera. Hacemos un buen equipo. Un gran equipo. Gracias por haberme enseñado tantas cosas, pero sobre todo gracias por haberme enseñado a aprender. Y a enseñar. Gracias por hacerme darles mil vueltas a las presentaciones, porque al final, todos los cambios merecen la pena. Y gracias por toda la paciencia que has tenido conmigo. Que no ha sido poca. Por entender cuando me enfado, y enseñarme a ser más fuerte. Anna, tú no sólo me has ayudado a lidiar con Lluís en muchas ocasiones, sino que también has estado siempre ahí, con los mejores consejos. Gracias por enseñarme a ser mejor científica y por ser un modelo a seguir. Gracias a los dos por hacerme ser crítica no sólo con el trabajo de los demás, sino con el mío propio. En gran parte gracias a vosotros me he convertido en la científica que soy hoy, y por ello os estaré eternamente agradecida.

A mis mentoras del Bigas Lab, Júlia, Mari y Vero… Gracias por enseñarme todo lo que sabíais. Júlia, sin ti los primeros días en el laboratorio hubiese estado perdida. Contigo no sólo aprendí las técnicas básicas y a preparar todas las soluciones habidas y por haber en el laboratorio… De ti aprendí a enseñar. Siempre fuiste mi ejemplo a seguir. Mari, estoy convencida de que es por tu filosofía que he llegado tan lejos, *"feina feta no fa destorb"*… Gracias por las tardes interminables en el laboratorio. La compañía era lo mejor. Y Vero… Gracias por enseñarme todo lo que sabías sobre las "inmunos", los intestinos y las *stems*… Dejaste un gran legado en el laboratorio y yo sólo espero haber estado a la altura.

A las chicas del Bigas Lab (bueno, Bigas/Espinosa ahora)… ¿Por dónde empiezo? Cristina, tu tesis fue la primera que viví en el laboratorio (y dejaste el listón muy alto). Seis años hace ya de aquel día. Recuerdo perfectamente tus ensayos, tus nervios… Y yo pensaba, "¡pero si lo tiene todo controlado!". Y ahora me toca a mí. Parecía que el día no iba a llegar nunca… Gracias por todos los ánimos que me has dado siempre. Tal vez tú no lo recuerdes, pero cuando antes del primer *Journal Club* que iba a presentar estábamos en una *Beer Session* y yo te conté lo preocupada y nerviosa que estaba, tus palabras de ánimo me alegraron la tarde. Yo, que ni siquiera había acabado la carrera, y tú a punto de doctorarte diciendo que no me preocupara que lo haría genial… Pues eso. Gracias. Roshani, you're next in line! There's little I could say here that you already don't know. I will never forget the day that I went looking for you in the middle of Barcelona… without knowing you! I'm so happy our paths crossed. I admire your endless efforts to make your project work. You're tireless! I will be forever grateful for our walks and talks and our little coffee breaks. Please, don't ever change. You're beautiful and I'm sure wonderful things await for you in the future. Carlota, angel, tu llegada al Espinosa Team fue un

respiro. ¡Por fin alguien con la personalidad que hace falta! Gracias por acompañarme en las aventuras Rin4, por todas las risas, y por ayudarme con los organoides… ¡La que nos espera con el biobank! Mucha suerte con tu tesis (que no está tan lejos), estoy segura de que lo harás genial… Laura, cómo me recuerdas a mí hace unos años… Verte con miles de GSTs haciendo *pull-downs* cada día… Te deseo mucha suerte, pero estoy segura de que te irá genial. Espero poder echarte una mano cuando pase todo esto… Y me alegro de que alguien siga con el proyecto de IκBα (lo siento, Lluís, ¡yo no puedo con todo, pero Laura lo hará fantásticamente!). Cristina P, you're an inspiring woman. When I become a post-doc I want to be like you. Thank you for your kind words, always. Christos, I'm really happy I got to share the Notch Meeting experience with you. You're really talented and I'm sure you'll do great things. Joan, a ti gracias por todo el interés que muestras por todo, tus ganas de saber son contagiosas. A Gemma, nuestra última incorporación, desearte muchos ánimos. Sé que no lo crees, pero todos nos hemos sentido como tú te sientes ahora al principio. Pero todo llega y todo pasa. A veces la ciencia es un poco complicada, y aunque tire de tópicos manidos, "la paciencia es la madre de la ciencia". David, esperamos que vuelvas pronto al lab, ¡te echamos de menos!

A los ex-Bigas/Espinosa lab… Pol, ver una cara conocida al llegar al laboratorio fue un alivio. Me alegro de haber compartido unos cuantos años de nuestras respectivas tesis… Verte convertido en una pequeña estrella… Lo que no habrás tenido que aguantar de todas las chicas del lab… Desde luego tienes el cielo ganado. Mil gracias por todo lo que me has ayudado durante todo este tiempo, y sobre todo ahora en la recta final, por estar siempre ahí, incluso en la distancia. Leonor, gracias por tus sonrisas, tus curiosidades y la alegría que trajiste al lab. Jordi y Teresa, vosotros sí que formáis un gran equipo dentro y fuera del laboratorio. Jordi, espero ver pronto un artículo tuyo de ISCs, y Teresa, estoy convencida de que algún día llegarás a tener tu propio laboratorio. Bing, you came at what was probably one of the hardest times of my PhD, in the middle of our revisions. But you helped me a lot, and for that I am grateful. I still use some of the slides you cut! Thank you for being so thorough and for the most fun conversations! You were an amazing company! And thank you for your patience too, I'm sure I was a bit too hard on you sometimes, I hope you forgave me! Eva, Jessica V, Dylan, Cristina Rius, Ricard, Berta… ¡Gracias por los momentos compartidos!

A todos mis estudiantes, gracias por vuestra paciencia… Y en especial a Gemma, con tu interés, esfuerzo y ganas por aprender estoy segura de que llegarás lejos. ¡Gracias por tus visitas al lab!

Lierni, tu paso por el Espinosa Lab fue más fugaz de lo que nos hubiese gustado, pero seguro que algún día volveremos a trabajar juntas. Mientras tanto, me conformo con que vengas a visitarnos de vez en cuando. Gracias por confiar en mí para tantas cosas dentro y fuera del laboratorio.

¿Y me dejo a alguien? Pues sí, porque lo mejor se deja para el final. Falta mi compañera de laboratorio "number one". Jessi, no sólo eres fantástica en tu trabajo y siempre estás dispuesta a ayudar. Siempre. Sino que además, siempre vas más allá. Eres la persona a la que más me gusta explicarle cómo funcionan los experimentos. Eres la mejor. Mi confidente. Mi compañera de ordenador y de batallas. Nos entendemos sólo con la mirada. Gracias por estar ahí siempre. Gracias por hacer de mis horas interminables en el laboratorio algo ameno. Gracias por el TGIF. Por las risas y más risas. Contigo hasta pasar 5 horas en el estabulario marcando ratones es divertido. Con palabras no se puede agradecer todo lo que ha significado tenerte a mi lado estos seis años. Sólo espero que ya lo sepas. Gracias, amiga.

Por supuesto también agradecer a los Snail y demás gente del departamento… Sandra, Raúl, Alba, Estel, Lorena, Jelena, Jordina, Ane, gracias por estar ahí y por vuestras palabras de ánimo, que no sólo de reactivos vive el científico. Lorena, gracias especialmente a ti por toda tu ayuda en esta recta final. Silvia, Conchi, Neus, Joan… una conversación con cualquiera de vosotros en el pasillo es lo que necesito para alegrarme el día.

A todos los jefes del Departamento de Cáncer del IMIM, en especial a Antonio, por ser mi tutor de tesis y un gran profesor. A Silvia G, gracias por tu eficacia a la hora de resolver todos los problemas, por ser siempre tan rápida y eficiente en tu trabajo. Pero sobre todo, gracias por tu disponibilidad y saber escuchar cuando más falta me ha hecho.

A nuestros colaboradores, especialmente a Pura y a Susana, por toda vuestra ayuda con los *Bmi1* KOs. Y a Mar, por siempre hacer lo posible porque nos lleguen las muestras, y por asegurarte de que Lluís cuida de "les seves nenes".

A mis *BioLadies*, Alba L, Anna D, Sandra, Alba Ll, Anna E, Maria, Eva, Helena, Alba M, Estel, Raquel, Rakel, Mercè… Ya sabéis que sin vuestra compañía a lo largo de la carrera no habría llegado hasta aquí. Gracias. Y en especial a Anna G y Noelia, por todos los momentos compartidos, y porque la distancia no importa. Gracias por acompañarme en este camino. Nere kuadrilari, Naia, Ane, Maria eta Arkaitz, eskerrik asko zuei ere! Iritsi da eguna! Y a ti, Sergio, porque nuestra amistad sobreviviera por encima de todo. Por estar ahí, siempre. Por ayudarme a seguir adelante en los momentos más difíciles. Eskerrik asko.

A Ángel y Olatz, por valorarme como una investigadora más cuando sólo era una estudiante. Con vosotros aprendí de verdad lo que era trabajar en un laboratorio. Y todo sobre las mamosferas! Olatz, milesker erakutsitako guztiagatik eta neregan jarritako konfidantzagatik, beti.

A mis profesores.

Y a mi familia. Porque sin su apoyo este libro no se habría escrito y yo no habría llegado hasta donde he llegado hoy. Gracias a mis aitas. Ama, gracias por ser una mala madre. Has sido y eres la mejor mala madre. Gracias por coserme las alas, por luchar contra viento y marea porque hiciese todos mis sueños realidad. Aita, gracias por quererme siempre cerca pero a la vez ayudarme estando lejos. Gracias por dejar a la ama ser una mala madre. Gracias a los dos por cuidar de mí y enseñarme a ser como soy. Por hacerme incansable, trabajadora, luchadora. Todo eso lo he aprendido de vosotros. Dennis, separarme de ti para venir a vivir a Barcelona fue lo más difícil. Me perdí verte crecer, pero te has convertido en alguien genial, y a quien admiro. Gracias por tus visitas a Barcelona (y a Canadá), por mirarme con esos ojos como platos como sólo un hermano puede mirar a su hermana mayor. Y gracias por apoyarme en todo, relacionado con la ciencia y no. Tu entusiasmo por la vida contagia. Gracias por invertir unas cuantas horas en diseñar la portada de esta tesis. Eres el mejor. Gracias por creer en mí siempre, a los tres. Al resto de mi familia. Izeba, gracias por ser mi fan incondicional. Por acompañarme aquel verano a la residencia, por cuidarme siempre. Y, aunque a regañadientes, por dejarle a la ama ser una mala madre también. Osaba, eskerrik asko zuri ere hitz murritzekin mila gauza esaten dizkidazulako, eta begirada batekin mila hitz esan ezin dutena diozulako. Bioi, izeba eta osaba, mila esker gure familian agertutako hutsuneak betetzeagatik. Amaia, Mikel eta Borja, eduki nitzakeen lehengusurik hoberenak, milesker zuei ere, beti ondoan egoteagatik, nahiz eta urrun izan. Osaba Javier, Patxi, Izaro, Marta, Lu eta Jim, eskerrikasko. Txikiei ere, Eki, Enaitz, Oscar, Adur, Oier eta Luar… Mila esker muxu eta besarkadengatik. A mi amoñi y a mi amona, eskerrik asko.

Eta ez daudenei ere. Bizitzak denbora gutxi utzi zigun batera bizitzeko, baño beti zaituztet gogoan. Aitona, izeba eta Rachel, zer pentsatu eta sentituko ote zenukete ni doktore bihurtzen ikustean…

Y finalmente, a Àlex, por venir un día a verme al laboratorio, sacarme de allí y enseñarme todo lo que hay fuera de él. Gracias por cuidar de mí y abrazarme cuando más lo necesito. Gracias por entenderme tan bien y apoyarme siempre. Gracias a tu familia, mi familia en Barcelona. Y a Carla, me alegro de que formes parte de nuestras vidas, de poder verte crecer y de acompañarte en el camino.

A todos vosotros, gracias. Eskerrik asko.

"No fracasé, sólo descubrí 999 maneras
de cómo no hacer una bombilla."
(Thomas Alva Edison, 1847-1931)

ABSTRACT

ABSTRACT

Wnt/β-catenin and Notch signalling cooperate in regulating the transcription of various genes specifically in the small intestinal stem and progenitor cell compartments. We characterized Bmi1 functionally in this context and showed that it contributes to ISC self-renewal capacity. We postulated that it does so by regulating its classical locus *Cdkn2a* and probably also by supporting DNA damage repair. Yet another level of Notch and Wnt/β-catenin crosstalk was found in colorectal cancer where tumour-associated β-catenin induced *Jagged 1* (*Jag1*) transcription, thus leading to Notch activation. We also investigated which is the contribution of intestinal epithelial Jag1-mediated Notch activation on tumour initiating activity. We found that intestinal-specific deletion of Jag1 greatly decreases tumour formation in the $Apc^{Min/+}$ background, likely due to reduced stemness. Jag1 deletion in preformed spheroids abrogates stemness-related gene expression and proliferation leading to spheroid failure. Jag1 is dispensable for normal stem cells, which rely on Dll1/4 Notch ligands for their maintenance. Together, these results open a new path in personalised CRC therapy, presumably involving Notch inhibition from specific ligands.

RESUMEN

Las vías de señalización de Wnt/β-catenina y de Notch cooperan en la regulación transcripcional de varios genes específicamente en las células madre / progenitoras del epitelio intestinal. Hemos caracterizado la funcionalidad de Bmi1 en este contexto y demostrado que contribuye a la capacidad de auto-renovación de las células madre intestinales. Postulamos que lleva a cabo esta función mediante la regulación de su diana clásica, *Cdkn2a*, pero probablemente también llevando a cabo funciones alternativas ayudando a la reparación del daño en el ADN. Sin embargo, existe otro nivel de cooperación entre las vías de señalización de Wnt/β-catenina y de Notch en el contexto del cáncer colorectal. Aquí, la β-catenina asociada al tumor es capaz de inducir la transcripción de *Jagged1* (*Jag1*), resultando en la activación de la vía de Notch. También hemos investigado cuál es la contribución a la iniciación tumoral de la activación de Notch mediada por Jag1 epitelial. Encontramos que delecionando *Jag1* específicamente en el epitelio intestinal se reducía la formación tumoral en el modelo animal $Apc^{Min/+}$, probablemente debido a una pérdida de las características de célula madre. La deleción de Jag1 en esferoides previamente formados abroga la expresión de genes de célula madre y la proliferación, llevando al colapso de los esferoides. Jag1 es dispensable para las células madre normales, que dependen de los ligandos de Notch Dll1/4 para su supervivencia. En conjunto, estos resultados abren un nuevo camino a las terapias personalizadas en el tratamiento del cáncer colorectal, presumiblemente mediante la inhibición de Notch a partir de ligandos específicos.

PREFACE

PREFACE

Colorectal cancer (CRC) is the second leading cause of cancer related death in developed countries. Thus, understanding the molecular mechanisms leading to CRC generation and progression is of crucial importance to develop new and more specific drugs for treating patients. Notch signalling has long been related to several types of cancer, including CRC, but general inhibition of Notch signalling is very toxic. This is due to the fact that Notch signalling indeed is essential for multiple stem cell compartments. Hence, there is a necessity to better understand how stem cells differ from cancer cells, so that new therapies only affect the latter. My work has been focused on delving into the role of Notch signalling as an orchestrator of stemness in healthy intestinal stem cells (ISCs), in homeostatic conditions, as well as in adenoma cells from the intestine. Not only is it essential to understand how ISCs differ from CRC cells, but their functional characterization is relevant for future studies in regenerative medicine. The second part of my work, on the other hand, focuses on how selective Notch-ligand interactions provide a unique opportunity for intestinal cancer therapy.

I was awarded a grant by the *Obra Social Fundación 'laCaixa'* for my Master studies in 2010 and during my PhD I have been funded by the Department of Education, Universities and Research of the Basque Government (BFI-2011). The IMIM-Institut Hospital del Mar d'Investigacions Mèdiques funded the printing of this thesis.

The image in the cover shows a section of a developing intestine at stage E15.5, stained for ICN1 (green) and Bmi1 (red). Nuclei are counterstained in blue.

TABLE OF CONTENTS

TABLE OF CONTENTS

FIGURES AND TABLES

FIGURES AND TABLES INDEX

INTRODUCTION

MATERIALS AND METHODS

PREVIOUS WORK (PART I)

RESULTS (PART I)

The Bmi1-deficient phenotype mimics that of Notch inhibition with respect to the self-renewal and DNA repair capacity of ISCs

SUPPLEMENTARY FIGURES

PREVIOUS WORK (PART II)

RESULTS (PART II)

Abrogation of Jag1-mediated Notch signalling restrains the stem cell potential of intestinal adenoma cells in vitro

ABBREVIATIONS AND ACRONYMS

ABBREVIATIONS AND ACRONYMS

4-OH-T	4-Hydroxytamoxifen
5-HT	5-hydroxytryptamine, serotonin
ADAM	a disintegrin and metalloproteinase
ANK	Ankyrin repeats
Apc	Adenomatous polyposis coli
ARF	Alternative reading frame
Ascl2	Achaete-Scute family bHLH transcription factor 2
β-cat	β-catenin
β-TrCP	β-transducin repeat containing protein
Bmi1	B cell-specific Mo-MLV integration site 1
BrdU	5-Bromo-2'-deoxyuridine
BSA	Bovine serum albumin
C	Carboxy-terminal
CAII	Carbonic anhydrase II, marker of absorptive cells
CBC	Crypt-base columnar (cell)
ccas3	Cleaved caspase 3
CCK	Cholecystokinin
Cd44	Cluster of differentiation 44
Cdc25	Cell division cycle 25
cDNA	Complementary deoxyribonucleic acid
ChIP	Chromatin immunoprecipitation
CK1	Casein kinase 1
CK18	Cytokeratin-18
CoA	Co-activator
CoIP	co-Immunoprecipitation
CoR	Co-repressor
CRC	Colorectal cancer
CSC	Cancer stem cell
CSL	CBF1 in humans, Supressor of Hairless in Drosophila and LAG in C. elegans, also known as Rbpj
Ctnnb1	Catenin (Cadherin-Associated Protein), Beta 1 (β-catenin)
DAB	3,3'-diaminobenzidine
DAPI	4',6-Diamidino-2-Phenylindole
DAPT	N-[N-(3,5-Difluorophenacetyl)-L-alanyl]-S-phenylglycine t-butyl ester
DCC	Deleted in colorectal cancer
Dclk1	Doublecortin-Like Kinase 1
DEPC	Diethylpyrocarbonate
Dkk	Dickkopf
Dll	Delta-like
DMSO	Dimethyl sulfoxide
DPX	Dibutyl phthalate xylene
DSB	Double strand breaks (DNA damage)
DSL	Delta/Serrate/LAG-2
Dvl	Dishevelled
EC cells	Enterochromaffin cell

ECN1	Extra-cellular Notch1
EDTA	Ethylenediaminetetraacetic acid
EE	Enteroendocrine (cells)
EGF	Epidermal growth factor
EGTA	Ethylene glycol tetraacetic acid
EphB2	Ephrin B2 (receptor)
FBS	Foetal bovine serum
FITC	Fluorescein isothiocyanate
Fz	Frizzled
GALT	Gut-associated lymphoid tissues
GI	Gastrointestinal
GIP	Gastric inhibitory polypeptide
GLP	Glucagon-like peptid
GSK3	Glycogen synthase kinase 3
Gy	Gray, unit of ionising radiation
HAT	Histone acetyltransferase
HD	Heterodimerisation region
HDAC	Histone deacetylase
Hes1	Hairy and enhancer of split 1
Hopx	HOP Homeobox
HRP	Horseradish peroxidase
ICN1	Intra-cellular Notch1, active Notch1
IF	Immunofluorescence
IHC-P	Immunohistochemistry, from paraffin sections
INK4a	Inhibitor of CDK4 (Cyclin-dependent kinase 4)
ISC	Intestinal stem cell
ISH	In situ hybridisation
Jag1	Jagged 1
KRAS	Kirsten Rat Sarcoma
Krt19	Keratin 19
LDCV	Large dense-core vesicles
Lef	Lymphoid enhancer-binding factor
Lgr5	Leucine-rich repeat-containing G-protein coupled receptor 5
LNR	LIN12/Notch repeats
Lrig1	Leucine-Rich Repeats And Immunoglobulin-Like Domains 1
Lrp	Low-density lipoprotein receptor-related protein
LSAB	Labelled Streptavidin-Biotin
LSL	Lox-stop-lox
Lyz	Lysozyme, marker of Paneth cells
Mfng	Manic fringe
MIACs	Mouse intestinal adenoma cells
Msi-1	Musashi-1
mTert	Mouse telomerase reverse transcriptase
Muc2	Mucin2, marker of goblet cells
Myc	Avian Myelocytomatosis Viral Oncogene
N	Amino-terminal
NES	Nuclear export signal

NICD	Notch intra-cellular domain
NLS	Nuclear localisation signal
O/N	Overnight
OCT	Optimal cutting temperature
Olfm4	Olfactomedin 4
P-	Phospho-
PAGE	Polyacrylamide gel electrophoresis
PBS	Phosphate buffered saline
PEST	Proline, glutamic acid, serine, threonine-rich domain
PFA	Paraformaldehyde
PI3K	Phosphatidylinositol-4,5-bisphosphate 3-kinase
pp	primer pair
Ptgs	Prostaglandin-endoperoxide synthase
PVDF	Polyvinylidene fluoride
qRT-PCR	Quantitative real time polymerase chain reaction
RAM	Rbpj associated molecule
Rbpj	Recombination signal Binding Protein for immunoglobulin kappa J region
RNA	Ribonucleic acid
rpm	Revolutions per minute
RT	Room temperature
SDCV	Small dense-core vesicles
SDS	Sodium dodecyl sulphate
SI	Small intestine
SMAD	Small mothers against decapentaplegic
SN	Supernatant
Sox9	SRY (Sex Determining Region Y)-Box 9
Syp	Synaptophysin, marker of EE cells
TA	Transit amplifying
TACE	Tumor necrosis factor-α-converting enzyme
TAD	Transcriptional activation domain
Tcf	T-cell specific factor
TM	Transmembrane
TSA	Tyramide signal amplification
TUNEL	Terminal deoxynucleotidyl transferase (TdT) dUTP Nick-End Labeling
UEA1	*Ulex europaeus* agglutinin-1
Vil	Villin1
WB	Western blot
YFP	Yellow fluorescent protein

INTRODUCTION

I1. The intestine

I1.1. The intestinal tract

The gastrointestinal (GI) tract, by its broadest definition, is the alimentary canal that includes all the structures between the mouth and the anus. The digestive system is a wider term that incorporates the digestive organs and their accessories (such as liver, gallbladder and pancreas) [FIGURE I1]. The GI tract can be divided into foregut, midgut and hindgut, reflecting the embryonic origin of each segment. However, anatomically it can be classified as follows: the *upper GI tract* that consists of the **oesophagus**, **stomach** and duodenum; and the *lower GI tract* that comprises most of the small intestine and the large intestine[1]. In human anatomy, the intestine is the segment of the GI tract extending from the pyloric sphincter of the stomach to the anus and is composed by two segments, the **small intestine** (SI) and the **large intestine**. The small intestine is further subdivided into the duodenum, jejunum and ileum, while the large intestine is subdivided into the cecum (with the appendix), colon (right or ascending, transverse, left or descending and sigmoid), rectum, and anal canal.

I1.2. Functions

The main function of the GI tract is to digest and absorb nutrients from the diet, but it also plays a major role in immunity as a barrier.

Each part of the tract is specialized in a different function:

> **Oesophagus**[2]: consists of a muscular tube through which food (bolus) passes aided by peristaltic contractions, from the pharynx to the stomach.

[1] The boundary between the *upper* and *lower GI tracts* is marked by the suspensory ligament of the duodenum (also known as the Ligament of Treitz), which delineates the embryonic borders between the foregut and midgut.

[2] From the Greek word οισοφάγος *(oisofágos)*, which means "to carry to eat".

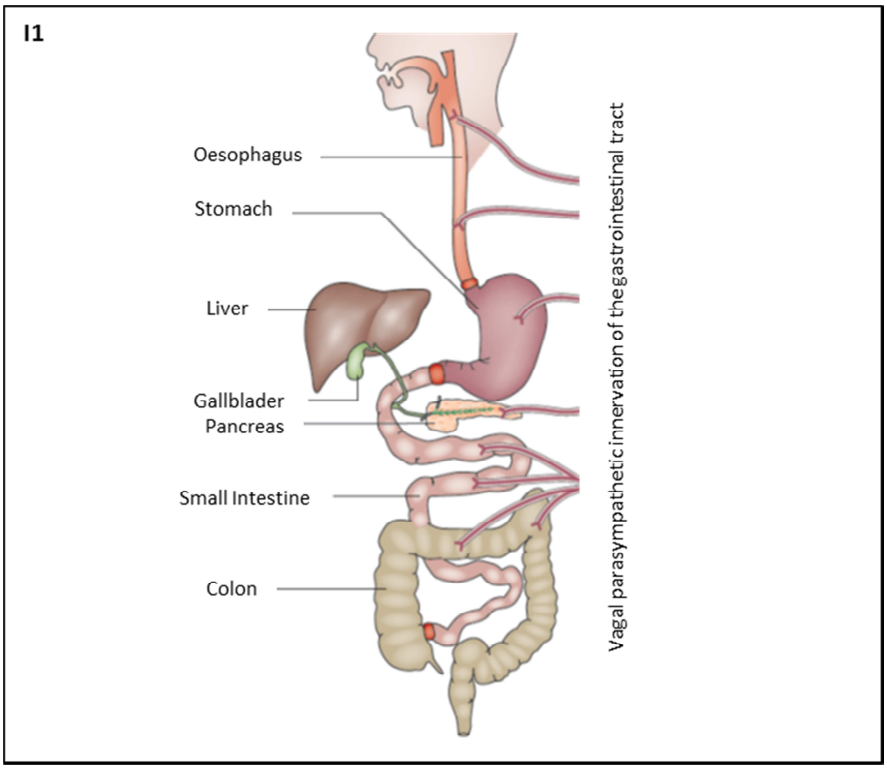

FIGURE I1 | The digestive system. The digestive system is formed by the gastrointestinal tract and the digestive organs and their accessories (such as liver, gallbladder and pancreas). The vagal parasympathetic innervation of the digestive system is also depicted: in the submucosal and mesenteric plexus, the axons coming from the central nervous system contact the enteric nervous system. Adapted from (Klingelhoefer & Reichmann 2015).

Stomach: is a hollow muscular organ, where gastric acid and gastric enzymes are released to digest the food that has arrived (chyme), aided again by peristaltic contractions.

Small intestine: in the duodenum is where the digestive juices from the pancreas, gallbladder and liver are released and its main function is to absorb the products of digestion (namely glucose, aminoacids, fatty acids and vitamins); the jejunum connects the duodenum to the ileum and also has the main function of absorption of the products of digestion; the ileum is the last

section of the small intestine and absorbs mainly vitamin B12 and bile acids, as well as any other remaining nutrients.

Large intestine: mainly absorbs water and electrolytes.

I1.3. Layers of the intestine

The gastrointestinal tract has a specific histology that reflects its functional specialization. The term *gastrointestinal wall* refers to the series of concentric tissue layers surrounding the lumen of the tract [FIGURE I2].

Mucosa: the innermost layer of the gut, in direct contact with the food, responsible for absorption and secretion. It can be further divided into **epithelium** (where most digestive, absorptive and secretory processes occur), **lamina propria** (connective tissue) and **muscularis mucosae** (thin layer of smooth muscle). In the stomach and intestine the epithelium is simple and columnar, but its main functions vary along the tract. For instance and it is specialized in acid and gastric enzyme secretion in the stomach, in absorption of nutrients in the small intestine, and recovering water in the large intestine. It is protected by a layer of mucus secreted by goblet cells from the epithelium (See below).

Submucosa: consists of a dense irregular layer of connective tissue with large lymphatic and blood vessels, as well as nerves branching into the mucosa and muscularis externa (belonging to the submucosal or Meissner's plexus).

Muscularis externa: is composed by an inner circular muscle layer and an outer longitudinal muscle layer. It is responsible for the peristalsis, which is controlled by the myenteric or Auerbach's plexus, located between the two layers.

Serosa (intraperitoneal) or **adventitia** (retroperitoneal): the outermost layer of the gut, consisting of a single layer of mesothelial cells and several strata of connective tissue. Most of the stomach, first part of the duodenum, all of the small intestine, caecum and appendix, transverse colon, sigmoid colon and rectum are intraperitoneal, hence covered by serosa, have a

mesentery and a clear boundary between them and the surrounding tissue. Retraperitoneal regions, on the other hand, such as the oral cavity, esophagus, pylorus, distal duodenum, ascending colon, descending colon and anal canal are covered in adventitia, blend into the surrounding tissue and are fixed in position.

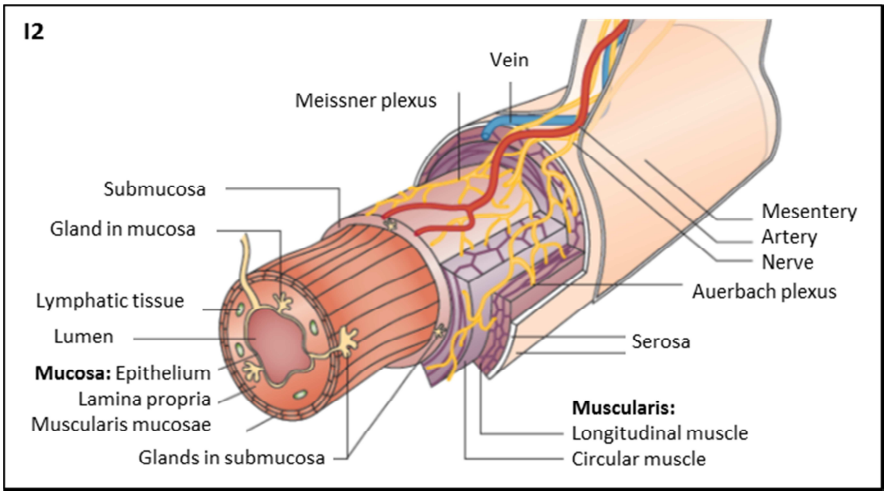

FIGURE I2 | The layers of the small intestine. Drawing depicting the layers of the gastrointestinal wall. Adapted from (Klingelhoefer & Reichmann 2015).

I1.4. Structure of the epithelium and characteristics

The structure of the epithelium in the small and large intestine present many similarities, but their architecture is quite different: in the small intestine, the epithelial layer covers finger-like villus structures and adjacent invaginations called crypts of Lieberkühn, an arrangement that provides a large absorptive area to this epithelium. The colonic epithelium does not contain villi; instead, deeper invaginations represent a compressed version of the crypt-villus architecture.

Since the focus of this work is the intestinal epithelium, the different cell types that compose it are detailed below.

I1.5. Epithelial cell types

Differentiated intestinal epithelial cell types can be classified in two main groups according to their function: absorptive or secretory. In the small intestine, the principal epithelial cell lineage is comprised by the columnar cells termed **enterocytes**. This type of absorptive cells, although in smaller numbers, is also present in the large intestine where they are regarded to as **colonocytes**. They are responsible for the absorption of nutrients from the intestinal lumen and their transport across the epithelium to reach the capillaries of the underlying layer. They are polarized cells with microvilli on the apical surface facing the lumen (visible microscopically as a *brush border*) that increase the absorptive area (Ito 1965). Their apical portion is also covered by a glycocalyx, enriched in digestive enzymes (Bossmann & Haschen 1983). **Microfold (M) cells** can be considered a subtype absorptive cells specifically enriched in the epithelium overlying the organized lymphoid follicles of the gut-associated lymphoid tissues (GALT). They are characterized by unique morphological features, such as the presence of an irregular brush border and reduced glycocalyx and microvilli. M cells are highly specialized for the phagocytosis and transcytosis of macromolecules, antigens and pathogenic or commensal microorganisms from the lumen and across the epithelium, to ensure antigen presentation to lymphocytes and mononuclear phagocytes (located in basolateral pockets), an essential initial step in the induction of the mucosal immune response. [Reviewed in (Mabbott et al. 2013)].

Several cell types can be found within the secretory lineages of epithelial intestinal cells, further classified according to the nature of the secreted molecules. First described by histopathologists at the end of the 19th century (Bizzozero 1892; Sacerdotti 1894), highly-glycosylated-mucin-secreting **goblet cells** are scattered among the enterocytes, their frequency increasing along the anterior-posterior axis of the gut (Paulus et al. 1993). They are responsible for generating a protective mucus layer, which not only allows for the smooth passage of the intestinal contents, but also acts as a protective barrier for bacteria (commensal or pathogen). [Reviewed in: (Specian & Oliver 1991; Pelaseyed et al. 2014)]. Recent studies moreover suggest that, in a similar manner to Paneth cells

(See below) goblet cell secreted mucus also plays a role in gut homeostasis through immunoregulation (Shan et al. 2013).

The intestinal epithelium also contains neuroendocrine[3] or **enteroendocrine cells** that secrete peptidic hormones and/or digestive enzymes. They are characterized by the presence of secretory vesicles, which are either large dense-core vesicles (LDCVs) or smaller synaptic-like microvesicles (SLMVs) similar to those found in neurons. Markers: chromogranin A (in LDCVs) and synaptophysin (in SLMVs). Some are found all along the GI tract, and some are intestine-specific, but enteroendocrine cells can be classified according to their main secretory products: somatostastin by D-cells, substance-P and 5-HT EC cells, secretin by S-cells, GIP by K-cells, CCK by I-cells, GLP-1/2 by L-cells, neurotensin by N-cells. [Reviewed in: (Engelstoft et al. 2013)].

Noticing their unique morphology, Järvi and Keyrilainen first described **Tuft cells** in 1955 (Järvi & Keyrilainen 1955). Also regarded as **brush cells**, on a narrow cell apex they have long and blunt microvilli with prominent rootlets and a well-developed tubulovesicular system in the supranuclear cytoplasm. Although some secretory functions have been proposed for this cell type (they produce and secrete opioids such as β-endorphin) (Gerbe et al. 2011), and ability to carry out absorptive functions has not been excluded, their most extensively investigated function is as chemorreceptors (due to their expression of α-gustducin). Markers: CK18, Ptgs, Dclk1; high reactivity with UEA1. [Reviewed in: (Sato 2007; Gerbe et al. 2012)].

Normally residing at the bottom of the crypts of Lieberkühn, **Paneth cells** contain large apical secretory granules and were first described by Gustav Schwalbe and Josef Paneth more than a century ago (Schwalbe 1872; Paneth 1888). These granules mainly contain anti-microbial peptides that are secreted to the lumen, such as lysozyme (Deckx et al. 1967) and α-defensins[4] (Ouellette et al. 1992), making Paneth cells essential players in the innate immune response. Their key role in innate

[3] First termed **neuroendocrine cells**, they were once thought to originate from the neural crest, due to the similarities they share with neurons.

[4] α-defensins are termed cryptdins, for crypt defensins, in mice.

immunity has been extensively studied and reviewed [an example: (Bevins 2004)], but now they are emerging as constituents of the stem cell niche [Reviewed in (Bevins & Salzman 2011; Clevers & Bevins 2013)]. In healthy individuals they are usually confined to the small intestine, but Paneth cells can arise aberrantly at other locations [such as colon (Cunliffe et al. 2001) and oesophagus (Shen et al. 2005)], often associated to chronic inflammation. They are then termed metaplastic Paneth cells.

I1.6. The stem cell niche

The intestine constitutes the most rapidly self-renewing tissue in adult mammals. In the mouse, the intestinal epithelium turns over entirely within 3–5 days (Potten & Loeffler 1987) and the massive rate of cell production by the transit-amplifying (TA) crypt compartment is compensated by apoptosis at the tip of the villus. **Intestinal stem cells** (ISCs) residing at the bottom of the crypts can produce all **transit-amplifying progenitors**, which are capable of differentiating toward all epithelial lineages (Cheng & Leblond 1974) [FIGURE I3]. Maturation of progenitor cells coincides with upward migration. Nevertheless, Paneth cells do not migrate upward; as a result, they accumulate at the bottom of crypts, where they remain in contact with the stem cells, constituting their niche. In the colonic crypts where there are no Paneth cells, $CD24^+$ (Sato et al. 2011) and/or c-Kit^+ (Rothenberg et al. 2012) cells residing between $Lgr5^+$ cells may represent their functional equivalents.

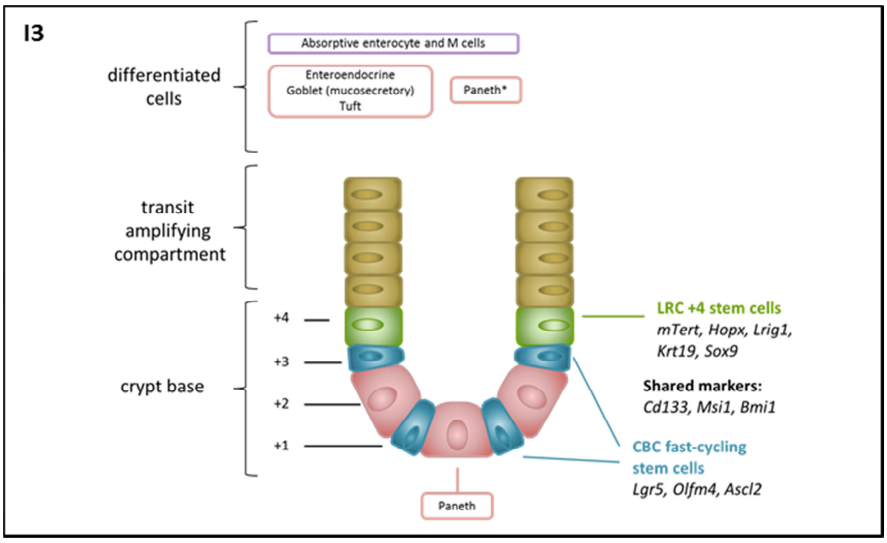

FIGURE I3 | The intestinal stem cell niche. ISCs reside at the bottom of the crypts in the intestinal epithelium. Paneth cells are thought to provide niche signals for their maintenance.

I1.7. Intestinal stem cells

In 1974 Cheng and Leblond first described the **crypt-base columnar cell** population (CBCs), located at the bottom of the crypts intermingled with the Paneth cells, and proposed them as the proliferating intestinal stem cell compartment (Cheng & Leblond 1974) [FIGURE I3]. Later, CBCs were described to be marked by expression of Lgr5 (Barker et al. 2007). Lineage tracing has shown that $Lgr5^+$ cells behave as a long-lived and cycling multipotent stem cell population (Barker et al. 2007). The establishment of 3D techniques for ex-vivo culture of intestinal stem proved that one single $Lgr5^+$ cell could form a long-lived, self-renewing "minigut" in culture (Sato et al. 2009). Although a few years later more intricate studies showed that $Lgr5^+$ cells form miniguts more efficiently when co-cultivated with Paneth cells, since they rely on Wnt and Notch ligands provided by them (Sato et al. 2011).

In 1981, Bjerknes and Cheng demonstrated the existence of an intestinal stem cell compartment located at the **+4 position** above the crypt base (Bjerknes & Cheng 1981). Later, using in vivo lineage tracing, other

studies showed that cells expressing Bmi1 predominantly marked the +4 position and were able to give rise to all epithelial lineages (Sangiorgi & Capecchi 2008). It was proposed that these $Bmi1^+$ cells were slowly cycling stem cells, whereas cells expressing the stem cell marker Msi-1 that were found in the same position might also represent the quiescent stem cell population (Li & Clevers 2010). However, this "quiescence" might have been wrongly described due to the nature of the experiments. Rather, the most plausible explanation is that these cells retain DNA-labelling dyes, due to an **asymmetric segregation of chromatids**, as a mechanism of protecting the stem cell DNA from replication-induced mutations. The non-stem daughter cell would receive the newly synthesised DNA strand, while the old (template) would be sorted into the stem cell (Potten et al. 2002). Nevertheless, new studies challenge this possibility (Escobar et al. 2011; Schepers et al. 2011).

$Lgr5^+$ stem cells are distinct from +4 label-retaining cells in that $Lgr5^+$ stem cells do not retain DNA labels and are sensitive to CDC25 inactivation, supporting their proliferative state (Lee et al. 2009). Thus, it could be said that the intestine contains a cycling $Lgr5^+$ stem cell population among the Paneth cells, in charge of maintaining the self-renewal of the epithelium under homeostatic conditions and a "reserve" stem cell population at the +4 position, which would rapidly replenish the $Lgr5^+$ pool (and hence the rest of the epithelial lineages) when the system is challenged (Tian et al. 2012). Yet the possibility that both ISC populations are interchangeable is not completely discarded (Takeda et al. 2011). Takeda and colleagues have showed that *Hopx* is a specific marker of +4 cells, which can give rise to $Lgr5^+$ CBCs, and vice versa. Other proposed markers are mTert (Montgomery et al. 2011), Lrig1 (Powell et al. 2012), Krt19 (Asfaha et al. 2015) and Sox9 (Roche et al. 2015) for "quiescent" or reserve radioresistant stem cells; Olfm4 (van der Flier, Haegebarth, et al. 2009) and Ascl2 (van der Flier, van Gijn, et al. 2009) for actively cycling ISCs; and Msi-1 and CD133 for ISCs and progenitors (Potten et al. 2003; Snippert et al. 2009) [**FIGURE I3**]. However, individual crypt cells can simultaneously express several of these markers (Itzkovitz et al. 2011). Interestingly enough, most of these stem cell genes are under the transcriptional control of Wnt and/or Notch pathways. The controversy remains alive with the possibility that

even secretory (van Es et al. 2012) or absorptive (Tetteh et al. 2016) progenitors could revert to $Lgr5^+$ ISCs upon crypt damage.

Lgr5 – a functional stem cell marker?

Lgr5 is a leucine-rich repeat-containing G protein-coupled receptor (Hsu et al. 1998) and a known target of Wnt signalling both in colorectal cancer (Van de Wetering et al. 2002) and normal intestinal crypts (Barker et al. 2007). R-spondin (Rspo) family proteins are ligands of Lgr5 (de Lau et al. 2011; Glinka et al. 2011; Carmon et al. 2011). The exact function of the Lgr5 receptor remains unknown, but it is thought to act as an intrinsic negative regulator of Wnt signalling. Inhibition of Wnt by LGR5 is removed in the presence of RSPO (Walker et al. 2011), although it is also possible that the LGR5:RSPO complex enhances Wnt signalling by interacting with the cell-surface transmembrane E3 ubiquitin ligases ZNRF3 and/or its homolog RNF43 (Hao et al. 2012), implicated in fine-tuning Wnt signalling in the ISC compartment (Hao et al. 2012; Koo et al. 2012) by targeting the Fz receptors. It was recently demonstrated that RNF43 can even inhibit the Wnt pathway downstream of oncogenic mutations that activate the pathway by interacting with and sequestering TCF4 to the nuclear membrane (Loregger et al. 2015).

Bmi1 – not so '+4'

We may no longer consider the Bmi1 protein a marker of the +4 position or of any specific stem cell population, due to the development of more specific antibodies that show homogeneous expression throughout the crypts of the small intestine as well as the colon, as we and others have demonstrated (Muñoz et al. 2012). However, this crypt-restricted expression suggests an intestinal stem or progenitor cell specific role for Bmi1.

Bmi1 is a member of the Polycomb group (PcG) of transcriptional repressors[5], the function of which in the intestine remains unknown. It is

[5] PcG form multiprotein complexes called polycomb repressive complex 1 and 2 (PRC1/2). They are responsible for gene silencing through post-translational histone modifications. PRC1 accounts for monoubiquitylation of lysine 119 of histone H2A and PRC2 is involved in di- and tri-methylation of lysine 27 of histone H3.

an essential regulator of hematopoietic (Oguro et al. 2006), neural (Bruggeman et al. 2005; Molofsky et al. 2005), lung (Zacharek et al. 2011) and muscle stem cells (Sousa-Victor et al. 2014). For instance, it has long been known that *Bmi1* gene deficiency in mice causes skeletal, neural and hematopoietic abnormalities (Van Der Lugt et al. 1994). The role of Bmi1 has been most extensively studied in hematopoietic stem cells (HSCs). Specifically in HSCs, their self-renewal ability is affected. Bmi1 is known to regulate proliferation and senescence through the $p16^{INK4a}/p19^{ARF}$ locus (also known as *Cdkn2a*), since deletion of the locus rescues the lymphoid and neurological defects seen in Bmi1-deficient mice (Jacobs et al. 1999). The self-renewal capacity of *Bmi1-/-* HSCs is also rescued by deletion of *Cdkn2a* (Oguro et al. 2006). On the other hand, increased $p16^{INK4a}$ levels found in old mice induce an aging-associated decrease in HSC self-renewal (Janzen et al. 2006). Bmi1 null mice do not show any other evident developmental defect than posterior transformation (which implies an important role during embryonic development), but they die prematurely (around 2-3 months of age), likely associated with a progressive decrease in the number of hematopoietic cells and neurological abnormalities (Van Der Lugt et al. 1994). Bmi1 functions in cancer have also been attributed to transcriptional repression of the *Ink4a/Arf* locus [Reviewed in (Sherr 2001; Valk-Lingbeek et al. 2004; Sharpless et al. 2004)].

Alternative functions of Bmi1 – DNA damage repair

Bmi1 carries out its PRC1-related function by forming a heterodimer with Ring1B/Rnf2 and stimulating its ubiquitin ligase activity toward lysine 119 of histone 2A (H2A-K119) (Cao et al. 2005; Buchwald et al. 2006). However, there is a series of studies that propose additional functions for Bmi1 apart from its classical role in regulating the *Cdnk2a* locus this way. Faccino and colleagues showed that after gamma irradiation BMI1 is redistributed on the chromatin of glioma cells, where it colocalizes and interacts with ATM and γH2A.X, and that BMI1 inactivation impairs recruitment of DNA double strand break (DSB) repair machinery (Facchino et al. 2010). At the same time, Ismail and colleagues confirmed that in the absence of BMI1 53BP1, BRCA1 and RAP80 are not efficiently recruited to the DSB sites and that the cells accumulate γH2A.X foci

(Ismail et al. 2010). They postulate NBS1 (member of the MRN complex consisting of MRE11, RAD50 and NBS1) as the scaffold for BMI1 and RING2[6] (also a member of the PRC1) in DSB sites, where BMI1 would act as a H2A/ɣH2A.X E3 ubiquitin ligase (with a similar role to RNF8). Other works also support and further explore these alternative functions (Ginjala et al. 2011; Pan et al. 2011; Nacerddine et al. 2012).

The functionality of other stem cell markers

Hopx is an atypical homeobox protein which does not bind DNA. In cardiac growth and development acts via its interaction with SRF (serum response factor) and prevents SRF-dependent transcription either by inhibiting SRF binding to DNA or by recruiting histone deacetylase (HDAC) proteins (Shin et al. 2002; Chen et al. 2002). ***mTert*** encodes for the murine Telomerase Reverse Transcriptase, ribonucleoprotein polymerase that maintains telomere ends by addition of the telomere repeat TTAGGG and plays a role in cellular senescence (Harley et al. 1990). Interestingly, mTert directly modulates Wnt/beta-catenin signalling by serving as a cofactor in a beta-catenin transcriptional complex in the intestine (Park et al. 2009). **Lrig1** is a negative-feedback regulator of the ErbB receptor family through a mechanism that involves enhancement of receptor ubiquitination and accelerated intracellular degradation (Wong et al. 2012; Gur et al. 2004). This way controls the size of the ISC niche. **Krt19** is the smallest known acidic cytokeratin, intermediate filament proteins responsible for the structural integrity of epithelial cells. Interestingly, it is not expressed on $Lgr5^+$ CBCs (Asfaha et al. 2015). **Sox9** seems to confer radiation-resistance to reserve ISCs and limits their proliferation (Roche et al. 2015). **Olfm4** is a secreted extracellular matrix glycoprotein that facilitates cell adhesion (Liu et al. 2006). It seems to be of functional relevance in inflammatory bowel disease, possibly by binding defensins in the mucus layer (Gersemann et al. 2012), however its functional relevance for ISCs remains unknown. Similarly to Lgr5, **Ascl2** also modulates Wnt/β-catenin dependent transcription in the $Lgr5^+$ ISC compartment (Schuijers et al. 2015). **Msi-1** (Musashi-1) is a negative regulator of Paneth cell differentiation, and may contribute to

[6] RING2 is also known as RING1B encoded by the gene *RNF2*.

maintaining ISCs in an undifferentiated state (Murayama et al. 2009). **Cd133**, also known as Prominin1 (Prom1), is often expressed on adult stem cells, where it is thought to function in maintaining stem cell properties by suppressing differentiation through regulation of other signalling pathways (Takenobu et al. 2011), but again its function in the intestine remains unclear.

I2. Notch signalling pathway

I2.1. Members

The Notch pathway mediates signals between adjacent cells and relies on cell-cell contacts. Already a century has passed since the *Notch* mutant *Drosophila* was described by T. H. Morgan's[7] group: in heterozygous female flies the wing margin was serrated or "perfectly notched" (Dexter 1914). Subsequent cloning of the **Notch** gene identified it as a receptor involved in cell-cell interactions (Artavanis-Tsakonas et al. 1983). Soon after, two fly ligands were identified: **Delta** (Vässin et al. 1987) and **Serrate** (Fleming et al. 1990). In Drosophila, two nuclear downstream effectors –**Suppressor of Hairless** [Su(H)] and **mastermind** (mam)– and Helix-Loop-Helix Notch target genes encoded by the **Enhancer of split** [E(spl)] locus, complete the basic elements of the Notch signalling pathway.

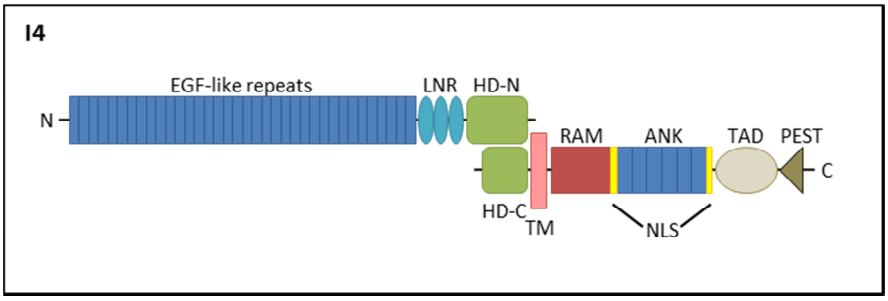

FIGURE I4 | Schematic diagram of a Notch1 receptor. This diagram shows the domain organisation of a Notch1 receptor, and how it would lay, heterodimerised, in the plasma membrane. Abbreviations: EGF, epidermal growth factor; LNR, LIN12/Notch repeats; HD, heterodimerisation region; N, amino-terminal; C, carboxy-terminal; TM, transmembrane region; RAM, Rbpj associated molecule; NLS, nuclear localisation signal; ANK, ankyrin repeats; TAD, transcriptional activation domain; PEST, proline, glutamic acid, serine, threonine-rich domain, a motif that mediates proteolytic cleavage by the proteasome.

[7] Thomas Hunt Morgan, American evolutionary biologist, geneticist, embryologist, and science author who won the Nobel Prize in Physiology or Medicine in 1933 for discoveries elucidating the role that the chromosome plays in heredity. The *Morgan* is now the unit of measurement of distances along all chromosomes.

In mammals, there are four Notch receptors (Notch1-4). They are type I transmembrane proteins composed of (1) an extracellular domain (NECD) containing ~30 epidermal growth factor (EGF)-like repeats, three LIN-12/Notch repeats (LNR) and a heterodimerization (HD) region (the LNR and HD regions together constitute the NRR, negative regulatory region); (2) a transmembrane domain; and (3) an intracellular portion with a RAM domain, seven ankyrin repeats flanked by two nuclear localization signals (NLS), a transactivation domain (TAD) and a carboxy-terminal PEST sequence [**FIGURE I4**].

Notch receptors are usually present in the cell surface in a cleaved, heterodimeric form (Blaumueller et al. 1997). Although they are codified by a single mRNA molecule that translates into a polypeptide, in the trans-Golgi apparatus mammalian Notch proteins are cleaved by furin-like pro-protein convertases (Logeat et al. 1998) at the "site 1" ("S1") cleavage (Kopan et al. 1996). This cleavage results in an N-terminal portion (N^{EC}, containing the extracellular domain) and a C-terminal portion (N^{TM}, including the transmembrane and intracellular domains) that are held together in the membrane, forming the Notch receptor heterodimer. Blaumueller and colleagues proposed that the two fragments were linked via disulphide bridges, since the interaction was sensitive to reducing agents. However, Rand and colleagues later demonstrated that the association between N^{EC} and N^{TM} was non-covalent, since it was sensitive to ionic detergents (0.1% SDS) and divalent cation chelators such as EDTA, under reducing or non-reducing electrophoretic conditions (Rand et al. 2000).

There are at least five canonical Notch ligands in vertebrates: three orthologs to the *Drosophila* Delta (Delta or Delta-like [Dll] 1, 3, and 4) and two to the Drosophila Serrate (Jagged 1 and 2). Notch ligands also exhibit a modular domain arrangement, with an N-terminal MNNL (Module at the N-terminus of Notch Ligands) domain, followed by a Delta-Serrate-LAG2 (DSL) domain. In some ligands, including all Serrate homologs and Dll1 in mammals, the DSL domain is followed by two variant EGF-like repeats also referred to as the "DOS" (Delta and OSM-11-like) domain. Then all ligands present a variable number of additional EGF-like repeats before the transmembrane segment and a C-terminal cytoplasmic tail. Serrate ligands differ from Delta ligands in the presence of a cysteine-rich

domain (CRD) between the EGF-like tandem repeats (that are usually more abundant) and the TMD.

Non-canonical Notch ligands

There is a repertoire of non-canonical Notch ligands that lack the DLS domain necessary to interact with Notch. They can be integral membrane-bound proteins (such as Dlk-1/Pref-1 or DNER); GPI-linked membrane-bound proteins (such as F3/Contactin1 or NB3/Contactin6); or even secreted proteins (such as scabrous or MAGP-1/2). Dlk-1 is thought to inhibit Notch receptors (Baladrón et al. 2005) most likely in *cis* (Bray et al. 2008), while DNER binds and activates Notch through a Deltex-dependent pathway (Eiraku et al. 2005). Contactins 1 and 6, which are membrane bound in a GPI-dependent manner also activate Notch through Deltex (Hu et al. 2003; Cui et al. 2004). And microfibril-associated glycoprotein (MAGP) family of proteins, MAGP-1 and MAGP-2, are secreted ligands that seem to activate Notch in *cis*, but they can act as negative modulators in some systems (Miyamoto et al. 2006; Albig et al. 2008).

Other proteins that participate in the regulation of Notch signalling are summarized in TABLE I1 and explained below:

	Drosophila	*C. Elegans*	*Mus musculus*
Receptor	Notch (N)	lin-12, glp-1	Notch1-4
Ligands:			
Canonical	Delta (Dl); Serrate (Ser)	lag-2, apx-1, dsl-1	Dll1,3,4; Jag1,2
Non-canonical (non-DSL)	Scabrous (Sca), Wingless (Wg), weary (wry)	osm-11, osm-7, dos-1, dos-2, dos-3	Dlk-1, CCN3, MAGP-1/2,
Nuclear effectors:			
DNA-binding TF	Supressor of Hairless [Su(H)]	lag-1	Rbpj
Transcriptional co-activator	mastermind (mam)	sel-8 (or lag-3)	Maml 1-3
Other transcr. co-activators	nejire (nej)	cbp-1	HATs (p300, PCAF)
Transcriptional co-repressors	Hairless (H) groucho (gro) Smrter (Smr)	 unc-37* gei-8*	Hr* TLE1-4 CIR, FLH1C/KyoT2 NCoR/SMRT SHARP/ MINT/SPEN
Receptor proteolysis:			
Furin-convertase (S1 cleavage)	Furin-1/2 (Fur1/2)*	kpc-1*	Furin
Metalloprotease (S2 cleavage)	kuzbanian (kuz) Tace (Tace)	sup-17 adm-4	Kuzbanian/Adam10 Tace/Adam17
ɣ-secretase (S3 cleavage)	Presenilin (Psn) Nicastrin (nct) anterior pharynx defective (aph-1) presenilin enhancer (pen-2)	sel-12 aph-2 aph-1 pen-2	Psen 1-2 Ncstn Aph-1a-c Psenen (or Pen-2)
Glycosyltransferases:			
O-fucosyl-transferase	O-fucosyltransferase (O-fut1)	C15C7.7	Pofut1
β1,3-GlcNAc-transferase	fringe (fng)	?	Lfng (Lunatic Fringe) Mfng (Manic Fringe) Rfng (Radical Fringe)
O-glucosyltransferase	rumi (rumi)	?	Poglut1
Endosomal sorting / Membrane trafficking regulators:			
Ring Finger E3 Ubiquitin ligase (ligand endocytosis)	mind bomb 1 (mib1) mind bomb 2 (mib2) neuralized (neur)	mib-1* F10D7.5*	Mib1 Mib2 Neurl1a/b(2)
Ring Finger E3 Ubiquitin ligase (receptor endocytosis)	deltex (dx)	?	Dtx1-4
HECT Domain E3 Ubiquitin ligase (receptor endocytosis)	Nedd4 (Nedd4) Suppressor of deltex [Su(dx)]	Y92H12A.2* wwp-1*	Nedd4 Itch
Negative regulator	numb (numb)	num-1*	Numb, Numbl
Other endocytic modifiers	sanpodo (spdo)	?	?
NICD degradation:			
F-Box Ubiquitin ligase	archipielago (ago)	sel-10	Fbxw7
bHLH repressor targets	Enhancer of split [E(spl)] deadpan (dpn), hairy (h) HES-related (Her) Hairy/E(spl)-related with YRPW motif (Hey)	ref-1 lin-22 hlh-25-29	Hes3, Hes7 Hes1 Hes5 Hey2 (Herp1), Hey1 (Herp2)

TABLE I1 | Core components and modifiers of the Notch signalling pathway. Asterisks indicate orthologs that have been predicted but whose role in Notch signalling in the species has not been confirmed yet. Orthologs were found at http://flybase.org/ and http://wormbook.org/.

I2.2. Regulation of ligand-receptor interactions

Receptor glycosylation

O-linked glycosylation of Notch receptors is essential for Notch activity in flies (Okajima & Irvine 2002) and mammals (Shi & Stanley 2003). The first step of the sugar modifications of the Notch receptor is carried out by an O-fucosyltransferase called O-Fut1 (Pofut1 in mammals), and consists of the transference of an O-fucose moiety to a serine or threonine residue right before the third cysteine of an EGF repeat (Wang et al. 1996; Wang et al. 2001). O-fucose residues are then recognized by Fringe β-1,3-N-acetylglucosaminyltransferases, which elongate the glycosaminoglycan chain by the addition of N-acetylglucosamines (Brückner et al. 2000; Moloney et al. 2000). In mammals, there are three Fringe proteins: Lunatic fringe (Lfng), Manic fringe (Mfng) and Radical fringe (Rfng) (Johnston et al. 1997). More recently, Rumi in Drosophila (Acar et al. 2008) and its ortholog Poglut1 in mammals (Fernandez-Valdivia et al. 2011) have been identified as O-glucosyltransferases for Notch EGF-like repeats; the O-glucose is then further modified by a xylosyltransferase (Sethi et al. 2010) [**FIGURE I5**].

O-Fut1 has chaperone effects on Notch (it is necessary for its correct folding), and the O-fucose is required for proper receptor-ligand interactions and trafficking of Notch to the membrane. Indicating the functional relevance of Notch O-fucosylation, intestinal specific *Pofut1* mutant mice (Guilmeau et al. 2008) or mice lacking 3,5-epimerase/4-reductase (FX) (Waterhouse et al. 2010), an enzyme necessary for the synthesis of the Pofut1 substrate GDP-fucose, show a phenotype resembling Notch loss of function in the intestine. Rumi is also essential for Notch function, as it seems to be required for conformational changes in Notch that occur subsequent to ligand binding and promote cleavage. Glycosylation mediated by Fringe potentiates the interaction between Notch and Delta in Drosophila, while reducing responsiveness for Serrate. The increased number of players in mammals increases the complexity of the system, but it is believed that modifications by Fringes make Notch1 at least behave similarly with greater affinity towards Delta-like ligands [**FIGURE I5**]. The functional significance of glycosylation

of the Notch receptors has been extensively reviewed by Pamela Stanley (Stanley 2007; Stanley & Okajima 2010).

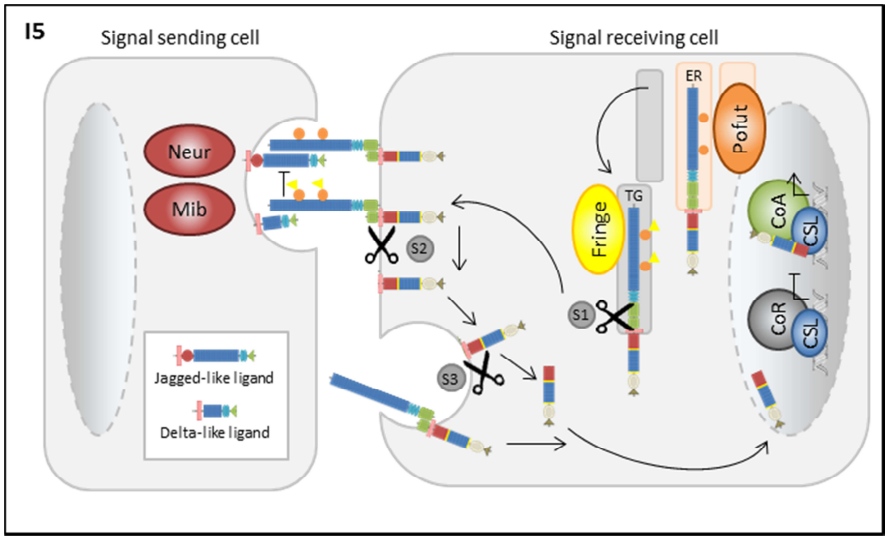

FIGURE I5 | Regulation of Notch receptor-ligand interactions. Simplified representation of some of the post-translational modifications that regulate Notch receptor-ligand interactions. The newly synthesised Notch receptor gets O-fucosylated by Pofut in the ER. Then, in the Golgi, O-fucose moieties (orange circles) are further modified by addition of N-acetylglucosamines (GlcNAc, yellow triangles). Glycosylation by Fringe proteins favours interaction with Delta-like ligands while reducing responsiveness to Jagged. Modifications by Poglut and xylosyltransferases are not represented. In addition to sugar modifications, Notch receptors also get cleaved in the Golgi, by furin-like convertases at the S1 site. Neuralized and Mindbomb are ubiquitin ligases that modify DSL ligands, contributing through their endocytosis to Notch activation. Abbreviations: Neur, Neuralized; Mib, Mindbomb; S1, cleavage site by furin-like convertase; S2, cleavage site by ADAM-TACE (see I2.3); S3, cleavage site by γ-secretase (see I2.3); CoA, (transcriptional) co-activator; CoR, (transcriptional) co-represor; CSL, CBF1 in humans, Supressor of Hairless in *Drosophila* and LAG in *C. elegans*, also known as Rbpj.

Ligand and receptor endocytosis and trafficking

Endocytosis is usually considered to play a negative role in signalling pathways by removing receptors from the membrane. However, more and more evidence suggests that endocytosis can also play a positive part. In fact, signalling can also occur in endosomes and several signalling pathways have been shown to depend on endocytosis for their full

activation [reviewed in (Sorkin & von Zastrow 2009)], including Notch signalling.

Endocytic trafficking of the DSL ligands plays a critical role in enhancing their signalling ability and it is triggered by monoubiquitination mediated by the E3 ubiquitin ligases Neuralized and Mindbomb (Koo et al. 2005; Lai 2005; Pitsouli & Delidakis 2005) [**FIGURE I5**]. There are two current theories for how ligand endocytosis can enhance signal, including the "ligand activation" model (by means of clustering of ligands, trafficking into lipid microdomains, proteolytic cleavage, or other posttranslational modification) and the "pulling force" model [transendocytosis of DSL ligands may generate a physical force to separate the Notch heterodimer that is linked by non-covalent interactions, exposing the "S2" site that is subsequently cleaved by ADAM metalloproteases (Nichols et al. 2007; Gordon et al. 2015)], but they are not mutually exclusive [Reviewed in (Yamamoto et al. 2010)].

Inactive Notch receptors undergo constitutive endocytosis, trafficking and degradation in the lysosomes. HECT domain E3 ligases that ubiquitinate Notch and promote its internalization are Suppressor of deltex [Su(dx)]/Itch[8] (Qiu et al. 2000; Chastagner et al. 2008) and DNedd4 (Sakata et al. 2004; Wilkin et al. 2004). Although this is primarily used as a mechanism to restrict protein levels at the cell surface, receptors can be recycled into the membrane, and ligand-independent activation can also occur due to the release of NICD after partial degradation in the endosomal pathway. RING finger E3 ligase Deltex (dx) has also been shown to ubiquitinate Notch receptors, with positive effects upon signalling (Hori et al. 2011).

Numb is a negative regulator of Notch in most systems; it does so by inhibiting the Sanpodo-induced endocytic turnover of Notch receptors (Couturier et al. 2013). Although the exact mechanism by which it does so remains largely unknown, it could be through interaction with [Su(dx)]/Itch and promoting lysosomal degradation of Notch (McGill et al. 2009).

[8] Itch can inhibit Notch signalling at yet another level, by ubiquitinating and sending Deltex to degradation by the lysosome (Chastagner et al. 2006).

I2.3. Activation cascade

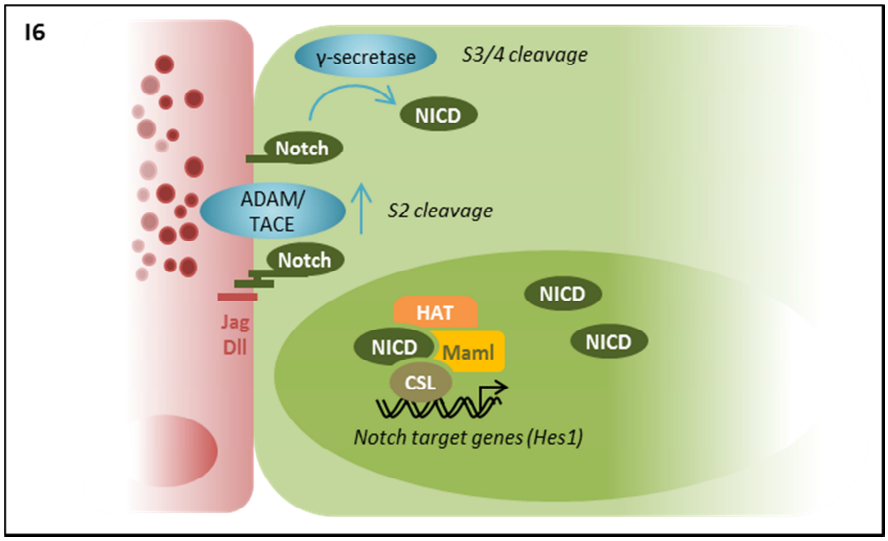

FIGURE I6 | Notch signalling activation cascade. Upon binding of the ligand presented by the signal sending cell (red) with the receptor in the signal receiving cell (green), a proteolytic cascade is initiated. Notch receptors are subsequently cleaved by ADAM/TACE metalloproteases and a γ-secretase complex, releasing the intracellular domain of Notch that translocates to the nucleus. Here, it displaces the co-repressors bound to CSL and recruits co-activators of transcription to activate target gene expression. Abbreviations: Dll, Delta-like ligand; Jag, Jagged; ADAM, a disintegrin and metalloproteinase; TACE, tumor necrosis factor-α-converting enzyme; NICD, Notch intracellular domain; HAT, histone acetyl transferase; Maml, Mastermind-like; CSL, CBF1 in humans, Supressor of Hairless in *Drosophila* and LAG in *C. elegans*, also known as Rbpj; Hes1, Hairy and Enhancer of Split homolog 1.

Signalling is triggered by interaction of the DSL (Delta/Serrate/LAG-2) ligands with the Notch receptors, which initiates a proteolytic cascade that results in the release of the intracellular portion of the receptor (NICD). The first cleavage occurs within the extracellular domain (at the "S2" site) and is mediated by ADAM metalloproteases ADAM10/kuzbanian or ADAM17/TACE (Brou et al. 2000; Mumm et al. 2000). Then a progressive cleavage starts from the "S3" to the "S4" sites within the transmembrane domain, which is mediated by the γ-secretase activity of the multi-protein complex termed Presenilin (PS) complex, which includes Presenilin, Nicastrin, APH-1 and PEN-2 (De Strooper et al. 1999; Struhl & Greenwald 1999; Wolfe et al. 1999; Ye et al. 1999; Okochi

et al. 2002). The released intracellular domain of Notch (NICD) translocates into the nucleus and binds to the transcription factor RBPj (also referred to as CSL[9]) (Jarriault et al. 1995) and a transcriptional coactivator of the Mastermind family (Doyle et al. 2000; Petcherski & Kimble 2000; Wu et al. 2000; Wu et al. 2002), displacing the co-repressors. In the absence of signalling, CSL is sitting at Notch target genes, but functions as a transcriptional inhibitor by interacting with corepressors, such as CIR, FLH1C/KyoT2, NCoR/SMRT, and SHARP/ MINT/SPEN [Reviewed in (Bray 2006)][10]. The transcriptional activation complex that forms upon signalling then engages additional coactivators such as p300 to recruit the transcription machinery (Fryer et al. 2002; Wallberg et al. 2002). Thus, expression of downstream target genes is turned on.

Nevertheless, sustained NICD accumulation can be oncogenic [an example: (Weng et al. 2004)] so the cell needs a mechanism to downregulate Notch signalling. Indeed, Maml not only acts as a transcriptional coactivator, but also recruits CycC:CDK8, that in turn phosphorlylates NICD at the PEST domain (Fryer et al. 2004). This phosphorylation allows recognition and ubiquitination of NICD by the E3 ubiquitin ligase Fbx7 and targets it for degradation by the proteasome (Tsunematsu et al. 2004; O'Neil et al. 2007; Thompson et al. 2007). Another mechanism that has been postulated to regulate Notch protein levels is autophagy or lysosomal degradation (Wu et al. 2016). Notch signalling is further fine-tuned also at the transcriptional target level. In the somite clock, where oscillating signalling levels are required, the Notch targets themselves (Hes1 and Hes7) inhibit their own transcription (Hirata et al. 2002; Bessho et al. 2003).

[9] RBPj is also known as CSL, which stands for CBF1 in humans, Supressor of Hairless in *Drosophila* and LAG in *C. elegans*.

[10] In *Drosophila*, in the absence of Notch signalling Su(H) is interacting with Hairless, which binds Groucho and CtBP corepressors to keep target genes silenced (Nagel et al. 2005). But strikingly up to date, no homologs of Hairless have been found in mammals.

Non-canonical Notch signalling

To make things more complicated, it has also been shown that in certain contexts, Notch signalling activity can be mediated through a CSL-independent pathway, which is usually referred to as non-canonical Notch signalling[11]. Notch can signal independently of CSL for example through Deltex (Ordentlich et al. 1998; Ramain et al. 2001), by regulating JNK signalling pathway at the plasma membrane (Zecchini et al. 1999), through a PI3K/Akt-mTOR-STAT3 axis (Androutsellis-Theotokis et al. 2006) or by interacting with Disabled and Trio in *Drosophila* (Le Gall et al. 2008).

I2.4. Target genes

Among the Notch targets, the best characterized are the bHLH (basic-helix–loop–helix) genes of the Enhancer of Split [E(Spl)] family in *Drosophila* and Hes (Hairy and Enhancer of Split) family in mammals, which encode for repressor proteins that usually inhibit cell-fate promoting genes. Also related and well characterized are the Hey/Herp proteins [Hairy/E(spl)-related with YRPW motif or Hairy/E(spl)-related repressor proteins]. The Hes family comprises seven members (*Hes1-7*) but only Hes1, 5 and 7 are established targets of canonical Notch signalling (Iso et al. 2003), although Hes3 is also downstream of DSL/Notch through a PI3K/Akt-mTOR-STAT3 axis (Androutsellis-Theotokis et al. 2006). They exert their repressor activity by recruiting HDACs and Groucho/TLE proteins [reviewed in (Fischer & Gessler 2007)]. Hey proteins, on the other hand, lack the WRPW motif necessary to bind Groucho/TLE proteins, but they can efficiently interact with NCoR and mSin3A, which directly recruit HDAC-1.

Although Hes and Hey families are the best known and most universal Notch target genes (and effectors), RBPj binding sites have been identified in many other gene promoters and several have been identified as Notch target genes. Examples include pro-proliferative

[11] Not to be confused with "non-canonical Notch ligands". Non-canonical Notch ligands can modulate Notch in a CSL-dependent (canonical signalling) or in a CSL-independent (non-canonical signalling, through Deltex, for instance) way.

genes Myc (Klinakis et al. 2006; Palomero et al. 2006; Weng et al. 2006), CyclinD (Ronchini & Capobianco 2001), string/CDC25 (Krejcí et al. 2009) and CDK5 (Palomero et al. 2006); cell cycle inhibitors p21 (Rangarajan et al. 2001). Other genes include Gata2 (Robert-Moreno et al. 2005), Gata3 (Amsen et al. 2007) and Cdca7 (Guiu et al. 2014).

Moreover, adding a higher level of complexity, many components of the Notch pathway are themselves direct transcriptional targets of Notch signalling: Deltex1 (Kishi et al. 2001), and in invertebrates Serrate (Yan et al. 2004; Martinez et al. 2009), Su(H) (Barolo et al. 2000), and neuralized, numb and kuzbanian (Krejcí et al. 2009). In addition, Notch can even promote its own expression (Weng et al. 2006; Yashiro-Ohtani et al. 2009), in a positive feedback loop.

I3. Wnt signalling pathway

I3.1. Members

The mouse *Wnt1* gene, originally named *Int-1*, was identified in 1982 by Nusse and Varmus as a proto-oncogene (Nusse & Varmus 1982). The *Drosophila wingless (wg)* gene had already been identified (Nüsslein-Volhard & Wieschaus 1980), but it was later shown to be the fly homolog of *Wnt1* (Rijsewijk et al. 1987).

Wnt ligands are cysteine-rich secreted proteins. There are roughly 20 of them in mammalians, which can be divided into 12 conserved Wnt subfamilies. To be secreted, Wnt proteins need (1) to be palmitoylated in the endoplasmic reticulum (ER) by the action of the palmytoyl-transferase porcupine (Zhai et al. 2004); (2) the presence of *wntless (wls)* (Bänziger et al. 2006) [also described as *evenness interrupted (evi)* (Bartscherer et al. 2006)], initially found in Drosophila, but conserved in worms and mammals (Wls, also referred to as Gpr177); and (3) the presence and activity of the retromer complex (Coudreuse et al. 2006; Yang et al. 2008; Belenkaya et al. 2008; Port et al. 2008).

The receptors for secreted Wnt proteins are the Frizzled (Fz) proteins, seven-pass transmembrane receptors with an extracellular N-terminal cysteine-rich domain (CRD) (Bhanot et al. 1996). And the co-receptors are arrow in *Drosophila* (Wehrli et al. 2000) and LRP5 and -6 in vertebrates (Pinson et al. 2000; Tamai et al. 2000), single span LDL receptor-related proteins.

There are agonists of Wnt/Fz/LRP, such as Norrin (Xu et al. 2004) and R-spondins (Kim et al. 2005); but also antagonists, such as secreted Dickkopf (Dkk) proteins (Glinka et al. 1998) or Wise (Itasaki et al. 2003).

In the absence of Wnt signalling, cytoplasmic levels of the effector of the pathway β-catenin are regulated by a **destruction complex**. The tumour suppressor protein Axin acts as a scaffold of this complex as it is able to directly interact with all the other components: β-catenin, Apc, and the two kinase families CK1α, -δ and -ε and GSK3α and -β (Ikeda et al. 1998; Kishida et al. 1998; Liu et al. 2002; Sakanaka et al. 1998). β-catenin that is not present in adherens junctions is sequentially phosphorylated by CK1 and GSK3 (Liu et al. 2002), and the phosphorylated form of β-catenin is

recognized by the F-box/WD repeat E3 ubiquitin ligase β-TrCP (Kitagawa et al. 1999). As a consequence, β-catenin is ubiquitinated and degraded by the proteasome (Aberle et al. 1997). But CK1 and GSK3 play paradoxical roles in the Wnt signalling pathway: by phosphorylating β-catenin, they are acting as antagonists of the pathway, but upon recognition of Wnt ligands by the Fz/LRP coreceptor complex, they phosphorylate LRP and have an agonist effect [Reviewed in (Wu & Pan 2010)].

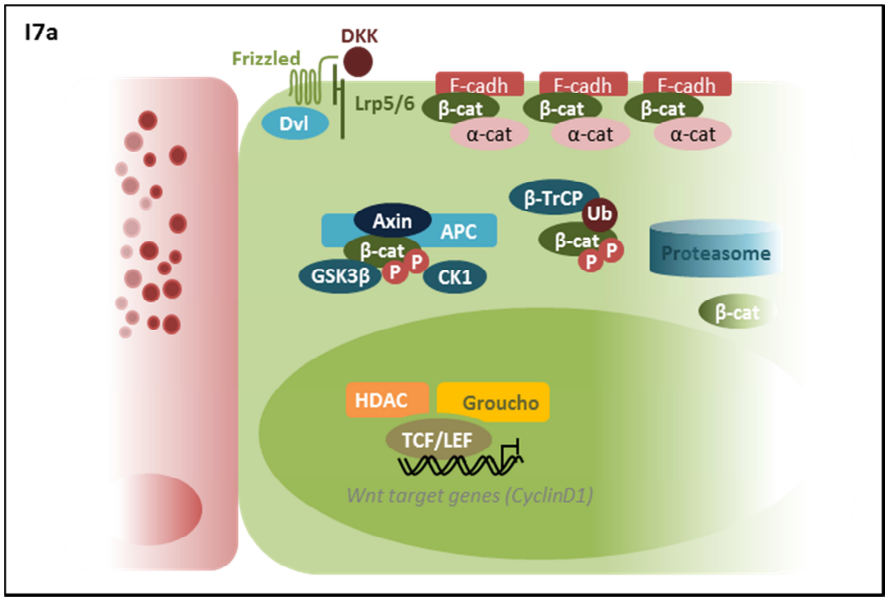

FIGURE I7a | Canonical Wnt signalling in its OFF state – the cytoplasmic destruction complex of β-catenin. In basal conditions, in the absence of Wnt ligands (or in the presence of the antagonist Dkk), there is no free β-catenin in the cytoplasm of the cells. All the β-catenin is either in the adherens junctions, or being sent to degradation in the proteasome by a cytoplasmic destruction complex composed by Apc, Axin and the kinases Gsk3β and CK1. β-TrCP is the substrate recognition subunit of the SCF (Skp1-Cullin-F-box protein) ubiquitin-protein ligase complex; it recognises phosphorylated β-catenin and after its ubiquitination, it is degraded by the proteasome. Abbreviations: Dkk, Dickkopf; Dvl, Dishevelled; Lrp, Low-density lipoprotein receptor-related protein; cadh, cadherin; cat, catenin; Apc, Adenomatous polyposis coli; Gsk3β, glycogen synthase kinase 3β; CK1, Casein kinase 1; β-TrCP, β-transducin repeat containing protein; HDAC, Histone de-acetylases, Tcf/Lef, T-cell specific factor / Lymphoid enhancer-binding factor; P, phosphorylation; Ub, Ubiquitination.

Apc seems to play an essential role in the turnover of the destruction complex. In resting conditions, while β-catenin is being phosphorylated by CK1 and GSK3, Apc is also phosphorylated. Phosphorylated β-catenin and Apc now interact with more affinity, and since Apc can also interact with β-TrCP (Hart et al. 1999; Su et al. 2008), ubiquitination of β-catenin and subsequent degradation by the proteasome occurs. This means that removal of β-catenin from the destruction complex is simply achieved by proteasomal degradation, and the destruction complex is ready for another round of β-catenin degradation. Furthermore, it seems that Apc also plays a role in the translocation of β-catenin to and/or from the nucleus (see below).

	Drosophila	*C. Elegans*	*Mus musculus*
Receptor	frizzled (fz) 1-4	lin-17, cfz-2, mig-1, mom-5	Fzd1-10
Coreceptor	arrow (arr)	rme-2*	LRP5/6
Ligands:			
Canonical	wingless (wg)	egl-20, mom-2, cwn-1, lin-44	Wnt1,2,3,8a,8b,10a,10b
Non-canonical		cwn-2 (=Wnt5b)	Wnt4,5a,5b,6,7a,7b,11
Ligand modulation:			
Ligand palmytoylation	porcupine (por(c))	mom-1	Porcn
Ligand secretion	wntless (wls) / (evi)	mig-14 (or mom-3)	Wls
Nuclear effectors:			
Signal transductor	armadillo (arm)	bar-1	β-catenin
DNA-binding TF	pangolin (pan)	pop-1	Tcf/Lef
Transcriptional co-activator	pygopus (pygo)	?	Pygo1/2
Adaptor	legless (lgs) / BCL9	?	Bcl9
Other transcr. co-activators	nejire (nej)*	cbp-1*, cbp-2*, F40F12.7*	CBP/p300
Transcriptional co-repressors	groucho (gro)	unc-37*	TLE1-4
Receptor activation:			
Kinases	shaggy (sgg) / GSK3*	gsk-3*	CKγ, GSK3α/β
Adaptor (canonical)	dishevelled (dsh)	mig-5, (dsh-1, dsh-2)	Dishevelled
Destruction complex:			
Scaffold	Axin (Axn)	pry-1 / axl-1	Axin
	APC-like (Apc)	apr-1	Apc
Kinases	Casein kinase Iα (CkIα)	kin-19 (non-canonical)	CKα
	shaggy (sgg) / GSK3	gsk-3	GSK3α/β
β-cat degradation:			
F-Box Ubiquitin ligase	supernumerary limbs (slmb)	lin-23	β-TrCP
Transcriptional target:	naked cuticle (nkd) (ex)	mab-5 (ex)	Axin2/conductin (ex)

TABLE I2 | Core components and modifiers of the Wnt signalling pathway. Asterisks indicate orthologs that have been predicted but whose role in Wnt signalling in the species has not been confirmed yet. The transcription targets indicated are examples (ex) and they are not homologs to one another. Orthologs were found at http://flybase.org/ and http://wormbook.org/.

I3.2. Activation cascade

Currently, three different pathways are believed to be activated upon Wnt receptor activation: the canonical Wnt/β-catenin cascade, the noncanonical planar cell polarity (PCP) pathway [Reviewed in (Katoh 2005)], and the Wnt/Ca^{2+} pathway [Reviewed in (Kohn & Moon)].

Once bound by Wnt ligands, the Fz/LRP coreceptor complex activates the canonical signalling pathway [Reviewed in (Clevers 2006) and (MacDonald et al. 2009)]. Fz interacts with Dishevelled (Dsh) and LRP is phosphorylated by membrane anchored CK1γ (Davidson et al. 2005) and GSK3 (Zeng et al. 2005), and interacts with Axin. Once bound to their respective membrane (co)receptors, Dsh and Axin heterodimerize. For several years, this step (the recruitment of Axin to the membrane upon receptor activation) was thought to result in the disassembly of the destruction complex, giving rise to an accumulation of non-phosphorylated (active) β-catenin in the cytoplasm that could then translocate into the nucleus to activate transcription of its target genes.

Recent discoveries, however, emphasizing the analysis of endogenous proteins, argue that upon activation the cytosolic destruction complex is not disassembled, its composition remains the same. Instead, through interaction of Axin with phosphorylated LRP, the whole complex is translocated to the plasma membrane and prevents the interaction of β-TrCP. Phosphorylated β-catenin, still bound to Axin, is no longer ubiquitinated or degraded and saturates the destruction complex. Hence, newly synthesised non-phosphorylated β-catenin can accumulate and translocate to the nucleus to activate transcription of its target genes (Li et al. 2012).

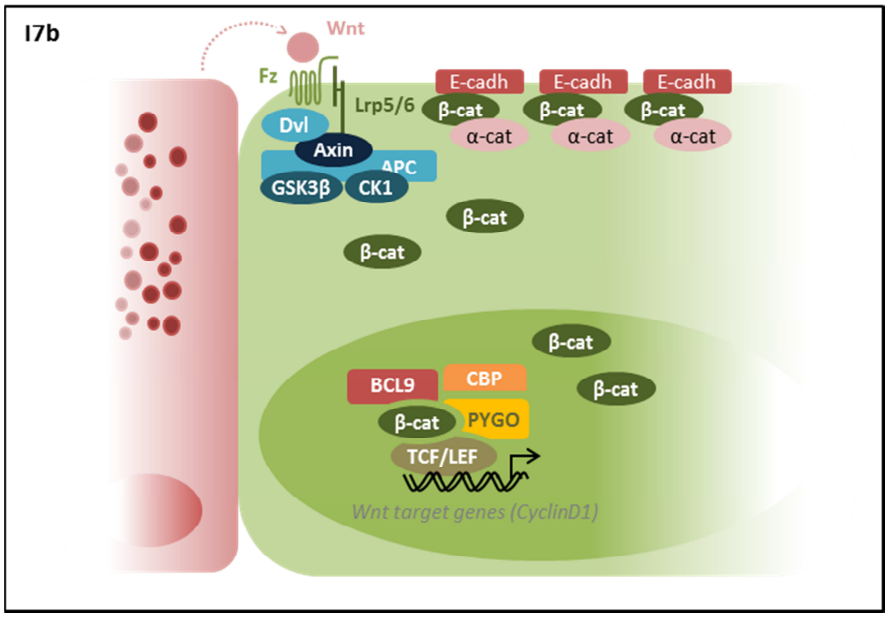

FIGURE I7b | Canonical Wnt signalling in its ON state. Upon ligand binding, the cytosolic destruction complex is disassembled (or rather, recruited to the membrane) a step that prevents engagement of β-TrCP. Thus, β-catenin is free to accumulate in the cytoplasm and translocate into the nucleus, where it can interact with its transcription factors Tcf/Lef and displace the transcriptional co-repressors. At the same time, it recruits co-activators of transcription to activate target gene expression. Abbreviations: Fz, Frizzled; Dvl, Dishevelled; Lrp, Low-density lipoprotein receptor-related protein; cadh, cadherin; cat, catenin; Apc, Adenomatous polyposis coli; Gsk3β, glycogen synthase kinase 3β; CK1, Casein kinase 1; β-TrCP, β-transducin repeat containing protein; Tcf/Lef, T-cell specific factor / Lymphoid enhancer-binding factor; CBP (CREB (cAMP response element-binding protein) binding protein, a histone acetyl transferase); BCL9, B-cell CLL/lymphoma 9; Pygo, Pygopus.

Be as it may, what is clear is that the accumulation of non-phosphorylated (active) β-catenin in the cytoplasm leads to its translocation into the nucleus. The mechanisms by which β-catenin accumulates in the cytoplasm and then translocates to the nucleus remain unclear, but an essential step is the dissociation from E-cadherin in the adherens junctions. It seems that phosphorylation of both β-catenin (Roura et al. 1999) and E-cadherin (Dupre-Crochet et al. 2007) plays a role in their dissociation. With regard to the nuclear translocation of β-catenin (which does not contain classical NLS or NES sequences), there are reports that suggest that this step is regulated by Apc (Roura et

al. 2003; Wang et al. 2014), but appears to be Ran/importin/exportin independent (Fagotto et al. 1998; Yokoya et al. 1999; Eleftheriou et al. 2001). Rather, it could be mediated by direct contact with the nuclear pore (Sharma et al. 2012).

In the nucleus, β-catenin binds members of the Tcf/Lef (T-cell specific factor /Lymphoid enhancer factor) family of HMG box transcription factors (Behrens et al. 1996; van de Wetering et al. 1997). In a similar fashion to Notch signalling, In the absence of Wnt signals, Tcf acts as a transcriptional repressor by forming a complex with Groucho/TLE proteins (Cavallo et al. 1998). The interaction of β-catenin with Tcf physically displaces Groucho (Daniels & Weis 2005) and binds coactivators such as Pygopus (Pygo) [through the adaptor protein Legless Lgs], histone deacetylases CBP/p300 and Brm/Brg-1, a component of the SWI/SNF chromatin remodeling complex [Reviewed in (Städeli et al. 2006)].

I3.3. Target genes

Wnt/β-catenin target genes seem to be cell type-specific, and have pleiotropic effects that range from cell proliferation and tissue expansion to cell fate determination of postmitotic cells. However, what seems to be conserved among cell types is the autoregulation of signalling at the transcriptional level. One of the most robust Wnt/β-catenin targets is Axin2/conductin (Jho et al. 2002)[12]. But Frizzled, LRP and Tcf/Lef expression is also controlled by β-catenin/TCF.

[12] Axin2/conductin is an Axin ortholog with a more restricted expression pattern but with an interchangeable function.

I4. Colorectal cancer

I4.1. Incidence & lethality

The normal intestinal epithelium is capable of continuous and perpetual renewal, while maintaining an exquisite balance between proliferation, differentiation, cell migration and cell death, as mentioned above. Intestinal tumorigenesis is initiated when any of these mechanisms becomes altered, leading to increased proliferation, reduced differentiation and altered tissue homeostasis.

According to the last Globocan Project report from 2012 (Ferlay et al. 2013), in developed regions of the world **colorectal cancer** (CRC) is the third most common cancer in men (340.000 cases 12.4%) and second in women (338.000 cases, 12% of the total) [FIGURE I8][13]. It is only outranked by breast cancer in females and prostate and lung cancers in males.

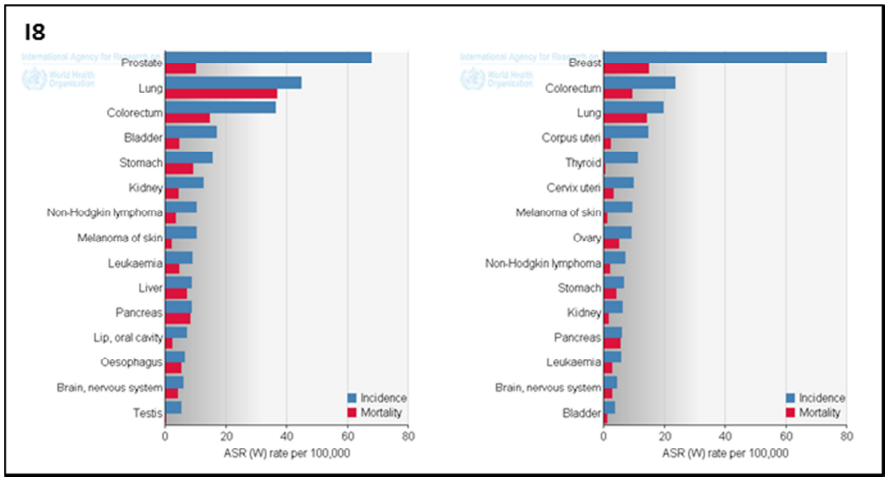

FIGURE I8 | Colorectal cancer incidence and mortality. Estimated age-standardised incidence (blue) and mortality (red) rates for men (left) and women (right). Analysed population: "more developed regions". Adapted from (Ferlay et al. 2013).

[13] Worldwide, colorectal cancer is also the third most common cancer in men (746.000 cases, 10% of the total) and second in women (614.000 cases, 9.2% of the total). And almost 55% of the cases occur in more developed regions.

Regarding its mortality, it is the second leading cause of death due to cancer in men (175.000 deaths, 11% of the total) and third in women (158.000 deaths, 12.3% of the total).

I4.2. The adenoma-carcinoma sequence

Colorectal carcinomas arise through a series of well-characterized histopathological changes as a result of specific genetic 'hits' in a handful of oncogenes and tumour-suppressor genes. The earliest manifestations of colorectal neoplasia are the **aberrant crypt foci** that can progress and become a **polyp** – a benign tumour mass that protrudes into the lumen from the intestinal epithelium. Polyps can be classified into two different subtypes: **hyperplasic** (nondysplasic) or **adenomatous** (dysplasic). Hyperplasic polyps preserve their normal architecture and cellular morphology, whereas adenomatous polyps are characterized by the presence of abnormalities in both inter- and intracellular organization. Adenomatous polyps can evolve to **invasive carcinomas** if they acquire further mutations [FIGURE I9] (Fodde et al. 2001).

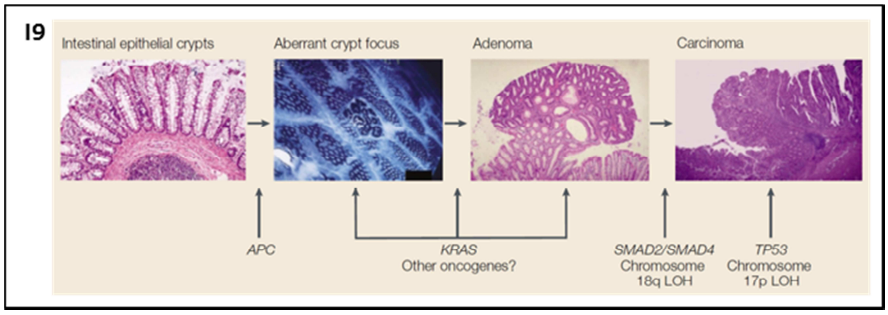

FIGURE I9 | Histopathology of colorectal cancer: the adenoma-carcinoma sequence. This is an oversimplified model of colorectal carcinogenesis evolution, but it aligns observed clinicopathological changes with genetic abnormalities in the progression of CRC. The initial step in tumorigenesis is the appearance of aberrant crypt foci upon APC loss. Larger adenomas acquire mutations in the small GTPase KRAS, followed by loss of chromosome 18q with SMAD4, which is downstream of transforming growth factor-β (TGFβ), in early carcinomas. Mutations in TP53 appear in carcinoma. From (Fodde et al. 2001).

In 1990 Fearon and Vogelstein proposed a **genetic model for colorectal tumorigenesis**, describing the genetic alterations that lead to the multistep progression of this type of cancer. In this model, inactivation of the adenomatous polyposis coli (*APC*) gene is one of the earliest events in both hereditary and non-hereditary colorectal carcinogenesis (Fearon & Vogelstein 1990; Levy et al. 1994). Germline mutation of the *APC* gene, leading to the deregulated activation of the Wnt/β-catenin pathway, provides a substrate for the subsequent somatic mutation of the second *APC* allele in the inherited familial adenomatous polyposis syndrome (FAP) (Ichii et al. 1993; Albuquerque et al. 2002; Crabtree et al. 2003), characterized by the presence of hundreds to thousands of colonic adenomatous polyps. Moreover, the overwhelming majority (80%) of early adenomas from sporadic cases of CRC also bear truncating mutations in *APC* (Gregorieff & Clevers 2005). Activating mutations in the oncogene K-Ras represent the second step in the progression of the malignancy (Fearon & Vogelstein 1990). Interestingly, mutant KRAS alone failed to initiate intestinal tumorigenesis in mice (Luo et al. 2007; Luo et al. 2011; Feng et al. 2011), or to induce highly invasive carcinomas when transduced into organoids (Drost et al. 2015), the latter requiring SMAD4 loss. In accordance with this, loss of the 18q chromosome (containing DCC and Smad2/4, among others) is frequently observed in human CRC (Fearon & Vogelstein 1990). Finally, loss of tumour suppressor p53 at a late stage may account for invasive carcinoma formation, associated with escape from cell cycle arrest and apoptosis (Sui et al. 2015), and for therapy resistance (Benhattar et al. 1996; Bunz et al. 1999) [**FIGURE I10**]. It seems that while mutation events are stochastic, the sequence in which they accumulate is non-random, supporting the argument that only certain mutations confer a selective advantage at a given stage of a tumour's natural history.

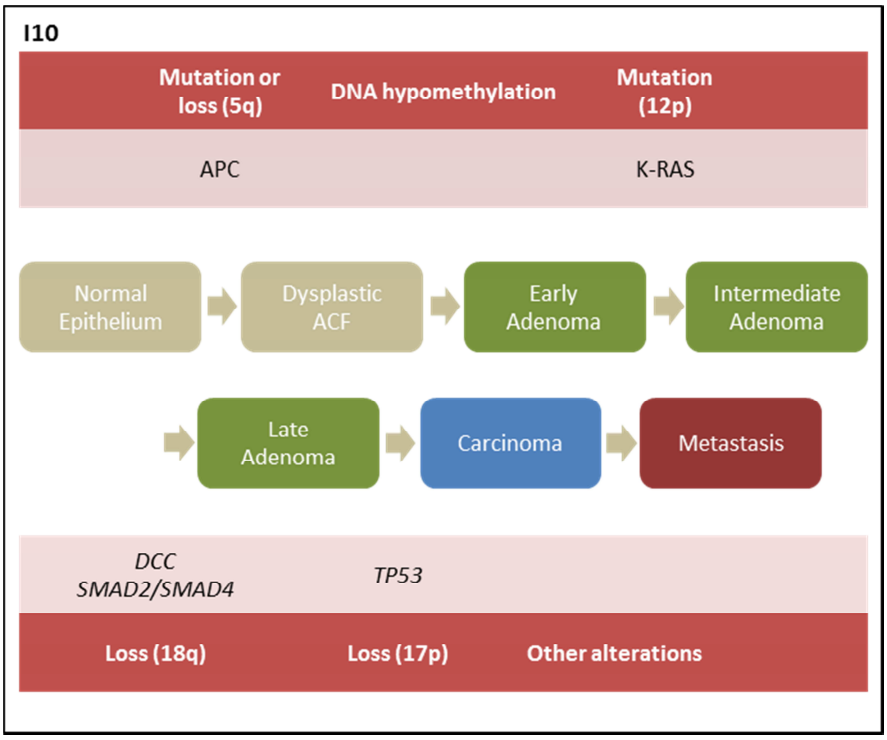

FIGURE I10 | A genetic model for colorectal tumorigenesis. Adapted from (Fearon & Vogelstein 1990). Numbers and letters indicate chromosomal location.

Little has changed from the model that Fearon and Vogelstein proposed 25 years ago [FIGURE I10], and many works have validated it ever since. State-of-the-art techniques, such as CRISPR/Cas9 for targeted genome editing, have confirmed the CRC progression model where oncogenic mutations in *KRAS*, *APC*, *SMAD4* and *P53* play a critical role (Drost et al. 2015; Matano et al. 2015). Notably, the expansion of the epigenetics field has given some insights in **epimutations** in addition to mutations that can also contribute to the model of CRC progression. A recently published review by Eric R. Fearon himself revisited the model and included miRNAs, although the backbone remains the same (Fearon 2011). As recent example, miR-135b downstream of APC loss, PTEN/PI3K pathway deregulation, and SRC overexpression promotes colorectal transformation and tumour progression (Valeri et al. 2014).

I4.3. Therapy

Surgery is the primary choice of treatment for non-metastatic CRC patients and adjuvant therapies consist of the classical **chemotherapy** and/or **radiotherapy**. Typically, the first-line drug regimens used in the treatment of CRC consist of 5'-fluorouracil (5-FU) together with leucovorin and irinotecan and/or oxaliplatin[14] (Aparicio et al. 2005; Masi et al. 2006), which can also be combined with bevacizumab, a monoclonal antibody that inhibits VEGF, acting as an antiangiogenic (Cohen et al. 2007). Cetuximab and panitumumab, monoclonal antibodies against EGFR, are also an effective treatment in combination with irinotecan for patients with metastatic colon cancer (Van Cutsem et al. 2009; Bokemeyer et al. 2009; Douillard et al. 2010), but their use is restricted to RAS wildtype patients (Pietrantonio et al. 2015). However, despite local recurrences being under control due to more invasive surgery (transmesorectal excision) and pre-operative adjuvant chemotherapy or radiotherapy, distant recurrences after surgery (~30% of stage II or III patients) still present a major problem and are often the ultimate cause of death for CRC patients (Boland & Fakih 2014; Pita-Fernández et al. 2015).

I4.4. Cancer stem cells

Currently, there is considerable evidence that most cancers, including leukaemia and solid tumours, are mainly heterogeneous, organized and sustained by a subpopulation of self-renewing cells that can generate the full repertoire of tumour cells (both tumorigenic and non-tumorigenic cells) [Reviewed in (Dick 2008; Visvader & Lindeman 2008; Clevers 2011)]. There are two models that are currently proposed to explain tumour heterogeneity. The **stochastic model** predicts that a tumour is

[14] Abbreviated FOLFIRI (a combination of FOLic acid or leucovorin, a vitamin B derivative that increases the cytotoxicity of 5-Fluororacil a pyrimidine analog which incorporates in the DNA and stops synthesis, and IRInotecan, a topoisomerase inhibitor that prevents DNA from uncoiling and duplicating) or FOLFOXIRI (that in addition to the previous three chemotherapeutic agents includes OXaliplatin, a platinum-based anti-neoplasic that causes crosslinking of the DNA inhibiting its repair and synthesis).

biologically homogeneous and the behaviour of cancer cells is influenced by intrinsic or extrinsic factors, resulting in differences in cell surface marker expression, entry to cell cycle or tumour initiation capacity. In contrast, the **hierarchy model** predicts that the tumour mimics the normal tissue development retaining a hierarchical organization with **cancer stem cells** (CSCs) at the apex (a distinct population that can be isolated) (Dick 2008). The essential difference is that in the stochastic model cancer stem cells arise randomly and every tumour cell has the potential to behave like a cancer stem cell, whereas in the hierarchy model there is only a distinct subset of cells that has the potential to behave like cancer stem cells.

The clinical implication of the hierarchy model is the possibility to specifically target CSCs as an effective method to revert tumour growth and avoid relapse. This is because CSCs not only have self-renewal capacity and the ability to generate all the populations of the heterogeneous tumour mass, but also may account for relapses and show resistance to conventional anti-cancer therapies [Reviewed in (Colak & Medema 2014)]. The clinical implication of the stochastic model, on the other hand, is that CSC removal needs to occur along with removal of all the rest of the cancer cells, because all of them have the potential to behave like CSCs. Nevertheless, if we take cellular plasticity and the role of the microenvironment into account, this dichotomy between the stochastic and hierarchical model is not so clear [Reviewed in (Plaks et al. 2015)].

The validation of the subsets of tumour cells as CSCs can be done by different approaches. There is an in vivo approach involving the purification of specific cell populations (by the presence of cell surface markers) and testing their tumour formation ability in serially-transplantable **xenografts** in mice. Alternatively, an in vitro approach can be used by culturing CSCs as **spheroids** in non-adherent serum-free conditions.

In CRC, the stem cell-driven tumorigenesis model has received substantial support from the recent identification and phenotypic characterization of specific subpopulations of colon cancer cells able to initiate tumour growth and to reproduce human colon carcinomas when

transplanted into mice. However, in a parallel way with normal ISCs, there is no clear consensus on what the intestinal CSCs are, as multiple subpopulations follow these same criteria. CD133 (O'Brien et al. 2007; Ricci-Vitiani et al. 2007), CD44 (Dalerba et al. 2007; Todaro et al. 2014), ALDH1 (Huang et al. 2009), CD26 (Pang et al. 2010), EphB2 (Merlos-Suárez et al. 2011), Lgr5 (Schepers et al. 2012) , Dclk-1 (Nakanishi et al. 2013) Krt19 (Asfaha et al. 2015), SOX2 (Neumann et al. 2011), CDCP1 (Gao et al. 2013) and CD110 (Gao et al. 2013; Wu et al. 2015) (the latter three mediating organ-specific metastasis) have been proposed as human and/or murine colorectal cancer stem cell (CSC) markers.

Although the terms '**tumour initiating cell**' (TIC or 'cancer initiating cell', CIC) and CSC have been used interchangeably, the TIC more aptly denotes the cell of origin. In human colorectal cancer, TICs have been described to express the markers CD133 (Zhu et al. 2009), Lgr5 (Barker et al. 2009), and Krt19 (Asfaha et al. 2015) in a similar fashion to CSCs. In all these cases, the cells of origin have been described using a Cre recombinase under the control of that specific marker promoter to induce deletion of *Apc* or overexpression of a constitutive active form of β-catenin. However, CSCs as cells with properties to initiate tumours in xenograft assays have been the most extensively studied because of their clinical implications: if they are not eliminated with therapy or become resistant, they would have the ability to re-grow the tumour and account for relapse.

I5. Wnt and Notch in intestinal homeostasis

Notch and Wnt/β-catenin pathways are essential regulators of stem cells in multiple tissues, including the intestine (Korinek et al. 1998; Ireland et al. 2004; Riccio et al. 2008; VanDussen et al. 2012; Pellegrinet et al. 2011). Korinek and colleagues showed the requirement of Wnt/β-catenin signalling in the intestine by deleting the DNA-binding HMG box in the *Tcf7l2* gene (encoding for the Tcf4 transcription factor), resulting in null mutations. Homozygous mutants were born at Mendelian ratios but died within 24 hours of birth. The only abnormality they showed was the epithelial organization of the small intestine, with reduced number of villi and less epithelial cellularity in intervillous regions (Korinek et al. 1998).

However, the defect was only seen in the small intestine, but they argued that redundant expression of *Tcf7l1* may account for the lack of a more severe and extended phenotype. Ireland and colleagues confirmed later that specifically deleting β-catenin in the gastrointestinal tract led to crypt ablation and increased apoptosis, but the epithelium was rapidly repopulated by non-recombinant cells (Ireland et al. 2004). The molecular mechanism by which Wnt/β-catenin signalling supports intestinal homeostasis is thought to be through the maintenance of the ISC program through c-Myc and $p21^{CIP1}$ (Pinto et al. 2003).

The most notable effect of Notch activity in the intestinal epithelium is the specification of the absorptive lineage. The first evidence that Notch signalling played this role was reported in Hes1 knockout mice (Jensen et al. 2000). In cells where Notch is active, Hes1 is expressed (Jarriault et al. 1995) – a basic helix-loop-helix (bHLH) repressor of gene transcription (Sasai et al. 1992). With Hes1 expression, repression of *Math1* (*ATOH1*) ensues. Math1, also a bHLH transcription factor, is required for secretory lineage commitment (Yang et al. 2001). Hence, Notch inhibition leads to extreme differentiation into the secretory lineage (van Es et al. 2005). This extraordinary phenotype has hindered the discovery of the role of Notch signalling specifically in stem cells, since exhaustion of the stem cell compartment due to forced differentiation into the secretory lineage is difficult to exclude. Nevertheless, genetic data indicate that Notch signalling could be playing a critical role specifically in intestinal stem/progenitor cells. Two sets of work by the laboratory of Freddy Radtke, in collaboration with others, have shown that (1) Notch1- and/or Notch2-mediated Hes1 expression supports the proliferative crypt compartment, by transcriptionally repressing the CDK inhibitors *p27Kip1* and *p57Kip2* (Riccio et al. 2008) and (2) Dll1 and Dll4 are the Notch ligands responsible for the maintenance of stem and progenitor cells (Pellegrinet et al. 2011). Unexpectedly, Jagged1, which is ubiquitously detected in most of the intestinal epithelial cells including the stem and progenitor compartments, does not contribute to Notch activation in the normal intestine or in the maintenance of intestinal homeostasis. The mechanism regulating Notch ligand selectivity in the intestinal epithelium are primarily unknown, but they may involve the activity of Fringe

glycosyltransferases that are distinctively expressed at particular intestinal compartments (Schröder & Gossler 2002).

I6. Wnt and Notch in colorectal cancer

For many years the most widely used model for the study of intestinal tumorigenesis has been the Apc^{Min} mouse, which was generated by random ethylnitrosourea mutagenesis (Su et al. 1992). Apc^{Min} carries a nonsense mutation in the codon 850 of the *Apc* gene, leading to a truncated *Apc* polypeptide of approximately 95 kDa (the wildtype protein is about 310 kDa). Heterozygous $Apc^{Min/+}$ (Min) animals develop more than 100 intestinal tumours per animal, mainly located in the upper gastrointestinal tract. When this animal was generated, it was already known that germline mutations in the APC gene were responsible for the familial adenomatous polyposis (FAP) syndrome, where patients develop multiple benign colorectal tumours. In both cases the mutation is autosomal dominantly inherited. But it was not until the year after that Apc was known to interact with β-catenin (Rubinfeld et al. 1993; Su et al. 1993). Yet two more years passed before Apc was regarded as a negative regulator of β-catenin (Munemitsu et al. 1995), but it was still unclear how β-catenin, at the moment thought to only act in adherens junctions, could exert a signalling function. Munemitsu and colleagues hypothesised that the deletion of Apc and the activation of Wnt1 (Hinck et al. 1994) could be promoting tumour growth in part due to a common outcome: the accumulation of cytoplasmic β-catenin. The clear and functional association of APC, β-catenin and TCF-mediated signalling with CRC did not come until a few years later (Korinek et al. 1997; Morin et al. 1997).

Even though Notch activity is found and known to be important in CRC (Zagouras et al. 1995; Reedijk et al. 2008; Chu et al. 2010; Zhang et al. 2010), mutations in members of the Notch signalling pathway are not commonly identified in these tumours. Still, they are not completely unheard of (Arcaroli et al. 2012). The absence of Notch mutations can be partly explained by the fact that activation of the Wnt signalling pathway is sufficient to activate Notch through the transcriptional activation of Jagged1 (Rodilla et al. 2009) (see below for further information on Wnt and Notch pathway crosstalk). Moreover, endothelial cells can also

produce a soluble form of Jagged1 that activates Notch and enhances the stem cell phenotype of CRC cells (Lu et al. 2013). Additional mechanisms that explain the absence of Notch mutations in CRC are the activating mutations in the Notch (and β-catenin) target gene CMYC (see RESULTS below) and inactivating mutations in the negative regulator of Notch FBXW7 that have been identified in a significant proportion of human CRC cases [Reviewed in (Fearon 2011)].

Notch signalling is not only involved in neoplasic transformation and tumorigenesis[15] in the intestine (Fre et al. 2009), but also plays a major role in tumour progression and metastasis (Zhang et al. 2010; Sonoshita et al. 2011; Chanrion et al. 2014; Sonoshita et al. 2015), as well as in angiogenesis (Noguera-Troise et al. 2006; Ridgway et al. 2006). For instance, Notch signalling abrogation in the $Apc^{Min/+}$ mouse model imposes differentiation of the adenoma cells into the secretory lineage, thus limiting tumour progression (van Es et al. 2005). Genetic deletion of *Aes*, a negative regulator of Notch activation, promotes tumour progression and metastatic invasion in the presence of mutant Apc (Sonoshita et al. 2011). The way Notch signalling promotes invasion of colorectal cancer cells is thought to be by transcriptionally activating DAB1 that elicits a cascade involving ABL and the RAC/RHOGEF protein TRIO (Sonoshita et al. 2015). Importantly, Notch1 depletion is sufficient to promote apoptosis and inhibit formation of tumour spheres in human CRC cell lines (Zhang et al. 2010). Moreover, *Jagged1* knockdown induced G0/G1 phase cell cycle arrest and reduced the migratory and invasive capacity of CRC cells in vitro, and reduced tumour growth, proliferation and expression of metastasis markers in a xenograft mouse model in vivo (Dai et al. 2014). Notch can promote cell proliferation by repressing *Krüppel-like factor 4* (*KLF4*) (Ghaleb et al. 2008; Zheng et al. 2009). It also increases the levels of the stem cell marker CD44 and promotes the transcriptional induction of Snail and Slug, mediators of EMT in several tissues and tumour types including CRC (Timmerman et al. 2004; Fender

[15] Overactivation of Notch signalling in the Wnt/β-catenin-active Apc^{Min} mouse model induces a greater number of adenomas and at an earlier age, but it seems that the progression of the adenomas is limited. It remains unclear whether Notch has tumor-initiating properties but at the same time anti-tumor-progression effects or whether this could be due to the complex interplay between Wnt and Notch signalling pathways.

et al. 2015). Combined detection of the Notch target proteins HEY1, HES1 and SOX9 significantly predicts reduced survival after chemotherapy in a study including 441 CRC patients, when compared with each marker alone (Candy et al. 2013).

I7. Wnt and Notch pathway crosstalk

Several examples of co-regulatory crosstalk have been described for Wnt and Notch signalling, in different systems and at various levels [Reviewed in (Collu et al. 2014)]. As Collu and colleagues propose, the levels of crosstalk can be divided into three categories: (1) **cooperative regulation of transcriptional targets**, (2) **transcriptional targets of one pathway affecting another**, and (3) **direct molecular crosstalk between the signal-transduction machineries**. Indeed, Wnt and Notch signalling pathways are so intertwined during development that the term "Wntch" has been proposed to refer to the integrated macro-pathway (Hayward et al. 2008).

One of the first pieces of evidence of an interaction between Notch and Wnt signalling pathways was the discovery that Notch and Wingless (the first Wnt ligand identified in *Drosophila*) together regulate expression of *vestigial* in the fly wing (Klein & Arias 1999). Other examples of cooperative regulation of transcriptional target genes are the works of Jin et al and Yamamizu et al (Jin et al. 2009; Yamamizu et al. 2010). Yamamizu and colleagues identified a complex comprised of RBPj, NICD and β-catenin at RBPj binding sites within the enhancer or promoter elements of several arterial genes. In contrast, recent work by Kim and colleagues show a negative regulation of Wnt signalling by Notch as a result of NICD recruiting transcriptional corepressors to β-catenin/TCF-4 binding sites within Wnt target genes (Kim et al. 2012).

There are many examples of transcriptional targets of one pathway affecting the other in the literature. Oscillations in gene expression that drive somitogenesis are due in part to LEF1-mediated regulation of Dll1 (Galceran et al. 2004). In hair follicle stem cells, *Jagged1* has been identified as a direct transcriptional target of β-catenin (Estrach et al. 2006). And in both breast and colorectal cancer, Wnt signalling activates Notch by inducing Notch ligand expression (Ayyanan et al. 2006; Rodilla

et al. 2009). However, this level of crosstalk is not restricted to transcription of Notch or Wnt (Rulifson & Blair 1995; Jayasena et al. 2008) ligands; in HSCs, Notch/RBPj activate expression of Frizzled receptor, an essential step in differentiation into dendritic cells (Zhou et al. 2009). In the developing *Drosophila* eye, Frizzeld/Dsh activates expression of Neuralized, which in turn promotes Delta function (and therefore Notch activity) (del Alamo & Mlodzik 2006). Epigenetic mechanisms of regulation of transcription have been recently brought into the picture of Wnt and Notch crosstalk: in mammary stem cells Wnt signalling inhibits Notch activity through a β-catenin/Pygopus2-dependent remodelling of the chromatin at the Notch3 locus, preventing expression of the gene (Gu et al. 2013).

Proof of direct molecular crosstalk between the signal-transduction machineries is also abundant. In *Drosophila*, interaction of Dishevelled with Notch inhibits Notch signalling (Axelrod et al. 1996) and Notch can suppress the activity of Armadillo/β-catenin by promoting its degradation (Hayward et al. 2005), likely mediated by Axin (Hayward et al. 2006). Another proposed mechanism by which Notch can inhibit Armadillo/β-catenin is by an RBPj- and ligand-independent control of trafficking: membrane-bound Notch associates with Armadillo at the adherens junctions and as Notch is endocytosed it sequesters "active" Armadillo (Sanders et al. 2009). In vertebrates, a similar trafficking model exists for β-catenin antagonism by Notch, in the differentiation of cardiac progenitor cells, embryonic stem cells and colon cancer cells (Kwon et al. 2009; Kwon et al. 2011).

In addition, it has been proposed that the Notch co-activator MAML1 could also work as a co-activator for β-catenin-mediated transcription (Alves-Guerra et al. 2007). In mammalian cells the negative regulation of Notch by Dishevelled has also been described and it is proposed that it does so by binding and sequestering RBPj away from the nucleus (Collu et al. 2012). In mammalian cells as well, GSK3β has been shown to interact with and phosphorylate the intracellular domain of two Notch paralogues, with two opposite outcomes. GSK3β phosphorylates and stabilizes N1IC, promoting Notch signalling (Foltz et al. 2002). However, it does not affect the stability of N2IC; instead it reduces its ability to signal (Espinosa et al. 2003), maybe owing to a decrease in the ability to bind

co-factors, as a result of the juxtaposition of the binding sites for GSK3β and the coactivator CBP.

As mentioned above, in the undifferentiated compartment of the intestinal epithelium both Wnt and Notch signalling pathways are active and necessary for the maintenance of the stem/progenitor cells. In particular, Paneth cells are thought to provide the essential signals for activating these pathways – they express Wnt3 and Dll4 (Sato et al. 2011) – and thus it is widely accepted that they constitute the ISC niche. This simultaneous activation of both pathways in a specific subpopulation of cells creates an exceptional scenario for studying new levels of crosstalk.

OBJECTIVES

OBJECTIVES

Based on previous data from others and our group, our general objective was to study the role of Notch signalling in intestinal homeostasis and cancer. Divided in specific subjects:

1. Analyse the requirement Notch (and Wnt) signalling for maintaining intestinal homeostasis
2. Characterise the functional relevance of Bmi1 expression downstream of Notch (and Wnt) for the maintenance of the ISC compartment
3. Explore canonical and alternative functions of Bmi1 in the ISC compartment
4. Establish the differential requirement for the Notch ligand Jag1 in normal vs. tumorigenic intestine
5. Evaluate the requirement of Notch signalling for adenoma cells
6. Evaluate specifically the requirement of Jag1-mediated Notch signalling for adenoma cells
7. Investigate possible candidates that mediate the differential requirement for Jag1 in intestinal adenomas

MATERIALS AND METHODS

MM1. Animals

Animal models or **model organisms** are widely used in biomedical research to investigate human diseases or biological processes. The classical vertebrate model is the house mouse (*Mus musculus*), which shares around 95% of its genome with humans. Mice can be genetically manipulated to mimic human diseases or conditions and can be inbred to maintain uniformity within strains, allowing for more accurate and repeatable experiments. They have an accelerated lifespan and an entire life cycle can be studied within 2-3 years. And they are a cost-effective and efficient research tool (they are small, reproduce quickly and are relatively easy to house and transport).

In summary, these were the strains used:

Mouse strain	Alternative name	Description	Bg	Reference
Vil*-CreER-T2	Tamoxifen-inducible Cre recombinase under the control of the *Villin1* promoter: expressed in the intestinal epithelium, active upon tamoxifen administration		C57BL/6	(el Marjou et al. 2004)
***Vil*-Cre**	Constitutively active Cre recombinase under the control of the *Villin1* promoter: expressed in the intestinal epithelium		C57BL/6	(el Marjou et al. 2004)
β-*actin*-Cre-ERT	Tamoxifen-inducible Cre recombinase under the control of the β-*actin* promoter: expressed in all the cells, active upon tamoxifen administration		C57BL/6	(Hayashi & McMahon 2002)
Rbpj*^{lox}	*Rbpj*^{lox} (Notch OFF)	Deletion of RBP	C57BL/6	(Han et al. 2002)
Ctnnb1*$^{lox(ex3)}$	*Ctnnb1*^{active} (Wnt ON)	Expression of a non-degradable form of β-catenin	C57BL/6	(Harada et al. 1999)
Ctnnb1*^{lox}	*Ctnnb1*^{lox} (Wnt OFF)	Deletion of β-catenin	C57BL/6	(Huelsken et al. 2001)
R26-LSL-ICN1*	ICN1 (Notch ON)	Expression of the active form of Notch1	C57BL/6	(Murtaugh et al. 2003)
Bmi1$^{-/-}$	Bmi1 null	General Bmi1 null mice	FVB/NJ	(Van Der Lugt et al. 1994)
Bmi1^{lox}	Bmi1^{lox}	Deletion of Bmi1	C57BL/6	(Arranz et al. 2012)
***Jag1*$^{lox(ex4)}$**	*Jag1*^{lox}	Expression of a Jag1 unable to interact with Notch receptors	C57BL/6	(Kiernan et al. 2006)
R26-LSL-YFP	YFP	YFP reporter of Cre activity	C57BL/6	(Srinivas et al. 2001)
***Apc*$^{Min/+}$**	Truncated form of *Apc*, similar to hereditary human CRC. Animals develop polyps in the small intestine predominantly.		C57BL/6	(Su et al. 1992)
C57BL/6	BL6 (WT)	Wildtype animals	C57BL/6	Jackson Laboratories

Table MM1 | Mouse strains. Asterisks indicate mice manipulated by Dr. Verónica Rodilla in her stay at the *École polytechnique fédérale de Lausanne* (EPFL) at Dr. Radtke's Lab. For those, the Service Vétérinaire Cantonal of Etat de Vaud approved all procedures.

All animal work was conducted according to the guidelines from the Animal Care Committee at the Generalitat de Catalunya, and these studies were approved by the Committee for Animal Experimentation at the Institut Hospital del Mar d'Investigacions Mèdiques (Barcelona).

Crossed with the Villin-CreERT2 line, the Cre recombinase was activated by intraperitoneal injection of tamoxifen (10mg/kg body weight in corn oil) [Sigma] in 2-3 week old mice for 3 consecutive days. Mice were killed 2-3 days after treatment.

Bmi1 null mice were euthanised before any obvious sign of disease was detected, around 2-3 months of age.

MM2. Intestine sample: embedding in paraffin

The first step in the histological characterization of any tissue is the preparation of the sample. In this case, many of the analyses of the intestines were performed using histological techniques. In that regard, a fast and proper collection and preparation of the intestinal sample was essential to preserve the epithelial architecture.

Sample preparation

- Collect intestine in ice-cold phosphate buffered saline (PBS) [Biological Industries Ref. 02-023-1A]
- Remove fat and mesentery and flush carefully with help of a syringe
- Place in cassette in "Swiss Roll" shape
- Fix in 4% paraformaldehyde (PFA) rocking overnight (O/N) at room temperature (RT) [Sigma Ref. P6148, 4% in PBS]
- 2x wash in PBS 1x 15min rocking at RT
- 25% ethanol rocking 15min at RT [Merck Ref. 1.00983.2500]
- 50% ethanol rocking 15min at RT
- 75% ethanol rocking O/N at 4°C
- 90% ethanol rocking 30min at RT
- 3x absolute ethanol rocking 1h at RT
- 3x xylene rocking 1h at RT [VWR Ref. 28975.325]
- Place tissue in embedding mould and incubate in paraffin 1h at 65°C [Leica Ref. 39602004]
- Change paraffin and incubate O/N at 65°C

- Change paraffin and cool down at RT
- Store at 4°C

MM3. HE staining

Haematoxylin and Eosin staining is the most widely used staining in histology. After preparation of each sample for histological analysis, HE staining is normally performed to confirm the integrity of the tissue and its cellular composition and organisation.

Haematoxylin is a dark blue/violet stain that is basic (positive). It binds to basophilic substances, such as the DNA and RNA (which are acidic and negatively charged). Eosin is a red/pink stain that is acidic (negative). It binds to acidophilic (also known as eosinophilic) substances, such as positively charged amino acid side chains. Most proteins in the cytoplasm and in the extracellular matrix are basic (positively charged due to arginine or lysine amino acidic residues), so they stain in varying degrees of pink.

Starting material is usually 4% PFA-fixed 4µm paraffin sections:

Dewax and rehydrate

- Heat slides 1-2h at 65°C (if slides have been re-paraffined, place at 65°C the night before), until paraffin is melted
- Xylene I and II 15min each
- Absolute ethanol I and II 10min each
- 96% - 70% - 50% ethanol 10min each
- Distilled water 10min

Staining

- Haematoxylin 30sec [Merck Ref. 1092530500]
- Tap water 5min
- 80% ethanol 0.15% HCl 30sec
- Distilled water 30sec
- Ammonia water [NH_3(aq)] 0.3% 30sec
- Distilled water 30sec
- 96% ethanol 5min
- Eosin 3sec [Bio-Optica Ref. 05-10003/L]

- 3x absolute ethanol 1min each

Dehydrate and mount

- Absolute ethanol I and II 5min each
- Xylene I and II 5min each
- Mount in DPX [Merck Ref. 1.01979.0500]
- Pictures were obtained with an Olympus BX61 microscope, using the CellSens software

MM4. Immunohistochemistry (paraffin, IHC-P)

Histology, together with advanced knowledge in immunology and biochemistry, evolved into immunohistochemical techniques that allow us to visualise the distribution and localisation of specific cellular components within cells and in the proper tissue context. Immunohistochemistry is based in the recognition of target antigens by specific antibodies tagged (directly or most commonly indirectly) with a visible tag.

Starting material is usually 4% PFA-fixed 4µm paraffin sections:

Dewax and rehydrate

- Heat slides 1-2h at 65°C (if slides have been re-paraffined, place at 65°C the night before), until paraffin is melted
- Xylene I and II 15min each
- Absolute ethanol I and II 10min each
- 96% - 70% - 50% ethanol 10min each
- Distilled water 10min

Antigen retrieval

Depending on the antibody, a different antigen retrieval protocol was used [see **Table MM2**]

A) Tris-EDTA (pH 8.0, 40mM Tris, 1mM EDTA) 50min at 100°C without pressure
B) Sodium citrate (pH 6.0, 1.9mM citric acid monohydrate [$C_6H_8O_7.H_2O$], 8.8mM tri-sodium citrate dihydrate [$C_6H_5Na_3O_7.2H_2O$]) 20min at 100°C without pressure

C) Sodium citrate (pH 6.0) 20min in autoclave (liquid programme, 60Hz)

- Retain in buffer 1h allowing cooling down to RT
- 3x wash in PBS rocking 5min at RT

Peroxidase blockage

- 0.3% H_2O_2 in PBS 20min rocking at RT [Sigma Ref. H1009-500ML]
- 3x wash in PBS rocking 5min at RT

Permeabilisation and blocking

For most of the antibodies, the permeabilisation and unspecific binding blockage is done simultaneously in one step

- 0.3% Triton X-100 [Surfactant Amps, Thermo Scientific Ref. 28340], 1% bovine serum albumin (BSA) [Sigma Ref. 3912-500G] in PBS 1h at RT
- 3x wash in PBS rocking 5min at RT

For ICN1 and Bmi1 detection, this step is done separately:

- 2x 0.3% Triton X-100 in PBS 10min rocking at RT
- 3x wash in PBS rocking 5min at RT
- Histoblock solution 2h at RT

Histoblock solution: 3% BSA, 5% foetal bovine serum (FBS) [Biological Industries 04-007-1A], 0.3% Tween 20 [Merck Ref. 8.22184.1000], 20mM $MgCl_2$ in PBS)

Primary antibody

- Incubate overnight at 4°C in 0.05% BSA in PBS (see specific dilutions in **Table MM2**)
- 5x wash in PBS rocking 5min at RT

For ICN1 and Bmi1 detection:

- Incubate overnight at 4°C in histoblock solution
- 2x wash in 0.3% Triton X-100 in PBS 5min rocking at RT
- 3x wash in PBS rocking 5min at RT

Secondary antibody

Using the universal LSAB System-HRP [Dako Ref. K0690] and following the manufacturer's instructions, briefly:

- Biotinylated link universal (yellow solution) 30 min at RT
- 5x wash in PBS rocking 5 min at RT
- Streptavidin-HRP (red solution) 30 min at RT
- 5x wash in PBS rocking 5 min at RT

For ICN1 and Bmi1 detection:

- Envision+ System HRP Labelled Polymer anti-Rabbit [Dako Ref. K4003] 90min at RT
- 5x wash in PBS rocking 5 min at RT

Develop (DAB)

- Develop with 3,3'-diaminobenzidine (DAB) [Dako Ref. K3468], which forms a very stable, brown end-product at the site of the target antigen
- 5x wash in PBS rocking 5 min at RT

Several times, after Ki67 staining, mucopolysaccharides were stained with alcian blue. For that, stop after this step and continue with the protocol described in MM4.

Otherwise, samples were counterstained with haematoxylin, as follows:

- Distilled water 5min
- Haematoxylin 30sec
- Tap water 5min
- 80% ethanol 0.15% HCl 30sec
- Distilled water 30sec
- 50% - 70% - 96% ethanol 5min each
- Absolute ethanol I and II 5min each
- Xylene I and II 5min each
- Mount in DPX [Merck Ref. 1.01979.0500]
- Pictures were obtained with an Olympus BX61 microscope, using the CellSens software

Develop (TSA):

- Develop with TSA-FITC 1:500 in amplification diluent [Perkin Elmer Ref. NEL753001KT]
- 5x wash in PBS rocking 5 min at RT
- Mount in Vectashield with DAPI (4',6-Diamidino-2-Phenylindole, to counterstain the nuclei) [Vector Ref. H-1200]
- Pictures were obtained with a TCS SP5 Upright Confocal Microscope, using the Leica Application Suite software

Antibody	Company	Reference	Species	Dilution	Antigen retrieval
Ki67	Novocastra (Leica)	NCL-L-Ki67-MM1	Mouse	1:500	TE 50min
Lysozyme	Dako	A0099	Rabbit	1:5000	TE 50min
Bmi1	abcam	ab14389	Mouse	1:100	TE 50min
Bmi1	Cell Signalling	#6964	Rabbit	1:200	Citrate autoclave
p16 (F-12)	Santa Cruz	sc-1661	Mouse	1:200	Citrate 20min
γH2A.X	Cell Signalling	#2577	Rabbit	1:200	Citrate 20min
ICN1	Cell Signalling	#4147	Rabbit	1:200	Citrate autoclave
BrdU	abcam	ab6326	Rat	1:250	Citrate 15min*

Table MM2 | Antibodies used in IHC-P. *For BrdU IHC-P see specific protocol in MM7.

MM5. Mucopolysaccharide staining

Alcian blue stains acid mucopolysaccharides and glycosaminoglycans, therefore it is one of the most used cationic dyes; the stained parts are blue to bluish-green. It binds by electrostatic forces to the negatively charged macromolecules. Gradual increases in the electrolyte concentration used to wash the bound dye selectively identify neutral, sulphated, and phosphated mucopolysaccharides.

Following Ki67 immunohistochemistry:

- Immerse in 3% acetic acid in water 3min at RT
- Immerse in Alcian blue (10mg/mL pH 2.5) [Merck Ref. 1.01647.0500] 2-10 min at RT
- Wash with running water and then with distilled water
- Counterstain with Nuclear Fast Red solution [Kernechtrot, Sigma Ref. N3020-100ML] 5-10 min at RT
- Wash with running water and then with distilled water

- Dehydration and mounting: 2min in each solution of 50% - 70% - 96% ethanol, absolute ethanol I and II, and xylene I and II; mount in DPX
- Pictures were obtained with an Olympus BX61 microscope, using the CellSens software

MM6. Immunohistochemistry (frozen, IHC-F)

Embed in OCT (Optimal Cutting Temperature compound):

- Collect intestine in ice-cold PBS
- Remove fat and mesentery and flush carefully with help of a syringe
- Cut in 1cm pieces
- Fix in 4% PFA rocking O/N at RT
- 5x wash in PBS 1x 5min rocking at RT
- Incubate in 10% sucrose in PBS [Sigma Ref. 84097-1KG] 30min rocking at RT (until the pieces do not float anymore)
- Place in OCT in embedding mould, snap frozen [Tissue-Tek Ref. 4583]
- Store at -80°C

Immunostaining from 8µm frozen sections:

- Fix the sections in pre-chilled absolute methanol 20min at -20°C [Merck Ref. 1.06018.2500]
- 5x wash in PBS 1x 5min rocking at RT
- Block and permeabilise in 10% FBS 0.3% Triton X-100 5% milk in PBS 1h at 4°C
- 5x wash in PBS 1x 5min rocking at RT
- Incubate primary antibodies in 10% FBS 5% non-fat milk in PBS O/N at 4°C (See specific dilutions in **Table MM3**)
- 5x wash in PBS 1x 5min rocking at RT
- Incubate secondary antibodies in 10% FBS 0.1% BSA in PBS 2h at RT
- 5x wash in PBS 1x 5min rocking at RT
- Mount in ProLong® Diamond with DAPI [Thermo Scientific Ref. P36971]
- Pictures were obtained in a Nikon Eclipse Ni-E Upright Motorized Microscope, using the NIS-Elemets software

Category	Antibody	Company	Reference	Species	Dilution
Primary	**Mfng (A-19)**	Santa Cruz	sc-8237	Goat	1:100
	Mfng	Biorbyt	orb157845	Rabbit	1:100
Secondary	**DαG-488**	Life Technologies	A-11055	Donkey	1:1000
	DαR-488	Life Technologies	A-21206	Donkey	1:1000

Table MM3 | Antibodies used in IHC-F.

MM7. BrdU injection and detection

Cell proliferation can be measured with the thymidine analog BrdU (5-bromo-2'-deoxyuridine) following its incorporation into newly synthesized DNA that occurs during S phase prior to cell division and its subsequent detection with an anti-BrdU antibody.

BrdU [Sigma Ref. B5002] was injected intraperitoneally (50mg / kg body weight) and animals were killed 2h or 24h after injection. Intestines were collected and processed as described above. IHC-P was performed following a slightly different protocol after the dewaxing and rehydration protocol.

Antigen retrieval

- In sodium citrate buffer (see **MM4**) 15min with pressure
- Allow to cool down in the sodium citrate buffer
- 3x wash in PBS rocking 3min at RT

Peroxidase blockage

- 2x 3% H_2O_2 in PBS rocking 30min at RT
- 3x wash in PBS rocking 3min at RT

DNA hydrolysis

- Incubate slides in pre-warmed 2N HCl 6min at 37°C in a water bath
- Incubate slides in borate buffer (0.1 M sodium borate pH 8.5) 5min rocking at RT
- 3x wash in PBS rocking 3min at RT

Blocking

- Incubate in blocking solution (5% goat serum [Dako Ref. X0907] 1% BSA in PBS)

Primary antibody

- Incubate with primary antibody 2h at RT in blocking solution (see **Table MM2** for concentration)
- 3x wash in PBS rocking 3min at RT.

Secondary antibody

- Incubate with secondary antibody, biotinylated rabbit anti-rat [Dako Ref. E0468] 1:600 in PBS 1h at RT
- 3x wash in PBS rocking 3min at RT
- Incubate with ABC solution [Vectastain ABC Kit, Vector Labs Ref. PK6100] 10min at RT
- 3x wash in PBS rocking 3min at RT

Develop and counterstain

Develop with DAB and counterstain with haematoxylin as described in the general IHC-P protocol (See **MM4**).

MM8. In situ Hybridisation (ISH)

ISH is a versatile and robust method for monitoring gene expression. The basic principle of ISH relies on the detection of hybridized RNA species using radiolabeled or hapten-conjugated nucleic acid probes. In brief, the method involves hybridization of formalin-fixed, paraffin-embedded intestinal sections with digoxigenin-labeled RNA probes and subsequent detection of hybrids with alkaline phosphatase coupled anti-digoxigenin antibodies.

Generation of digoxigenin-RNA probes

The RNA probes were obtained from complementary DNA of mouse *Lgr5*, *Olfm4*, and *Ascl2,* and were generated through in vitro transcription with a Digoxigenin RNA Labeling Kit [Roche Ref. 11175025910] according to the manufacturer's instructions.

Dewaxing and rehydration

The starting material is 4% PFA-fixed 8µm paraffin sections. As described in the general IHC-P protocol (See **MM4**), rinsing twice in DEPC (diethylpyrocarbonate)-treated H_2O in the last step.

Pre-treatment

- Pre-treat the samples with 0.2 N HCl 15min at 37°C in a water bath
- Incubate the samples with proteinase K (30µg/mL) 20min at 37°C in a water bath
- Stop reaction by adding 0.2% glycine in PBS
- 2x wash in PBS rocking 3min at RT

Re-fixing

- Re-fix the samples with 4% PFA in PBS 10min at RT
- 3x wash in PBS rocking 3min at RT
- 2x incubate in acetic anhydride solution (0.25% acetic anhydride in 0.1M Triethanolamine pH 8.0) 5min
- 5x wash in PBS rocking 3min at RT

Pre-hybridisation

- 2x rinse in 2x SSC solution (3M NaCl, 0.3M sodium citrate dihydrate, pH 4.5)
- Place slides in a covered box humidified with 50% formamide/2xSSC pH4.5 and cover them with hybridisation solution (50% formamide, 5x SSC pH4.5, 2% blocking reagent [Roche Ref. 11096176001], 0.05% CHAPS (3-[(3-cholamidopropyl)dimethylammonio]-1-propanesulfonate), 5mM EDTA, 50µg/mL heparin, 1µg/mL yeast RNA)
- Incubate them at least 1h at 65°C

Hybridisation

- Incubate slides with hybridisation solution plus 500ng/mL probe in an oven 24h at 65°C
- 2x rinse in 2xSSC solution
- 3x wash in 50% formamide/2xSSC pH4.5 20min at 65°C
- 5x wash in Tris-NaCl solution (0.1M Tris-HCl pH 7.5, 0.15 M NaCl, 0.1% Tween 20) rocking 3min at RT

Immunological detection

- Incubate in blocking solution (1% blocking reagent in Tris-NaCl solution) 30min at RT
- Incubate sheep anti-digoxigenin antibody 1:2000 in blocking solution O/N at 4°C

- 7x wash in Tris-NaCl solution rocking 3min at RT
- 3x wash in NTM buffer (0.1M NaCl, 0.1M Tris pH9.5, 0.05M MgCl2) rocking 3min at RT
- Add NBT/BCIP solution (NTM Buffer + 0.33µg/µL NBT [4-Nitro blue tetrazolium chloride] + 0.175µg/µL BCIP [5-Bromo-4-chloro-3-indolyl phosphate]); incubate 24h at RT
- 2x wash in PBS rocking 3min at RT
- Mount the sections in 50% Glycerol [Sigma Ref. G5516] in PBS or proceed with BrdU IHC-P (See **MM7**), without counterstaining with haematoxylin

MM9. Crypt/MIAC isolation

Obtaining a cell suspension enriched in intestinal crypts is essential for analysing the ISC compartment. Likewise, obtaining a similar population enriched in adenoma cells is of paramount importance. Both these enriched fractions can be used for analysis by RNA extraction and qRT-PCR, flow cytometry and most importantly 3D culture that favours growth of cells with stem cell properties (See **MM10**). Crypts are obtained by mechanical dissociation and murine intestinal adenoma cells (MIACs) from the *Apc*$^{Min/+}$ mouse model are obtained through a combination of mechanic and enzymatic dissociation. The protocol that we use was adapted from (Sato et al. 2009):

Crypt isolation

- Collect the small intestine in ice-cold PBS with 5x antibiotics [Pen-Strep solution, Biological Industries Ref. 03-031-1B (normally used 1:100, dilute it 1:20 instead)]
- Remove fat and mesentery
- Cut open longitudinally
- Wash repeatedly in PBS 5x Pen/Strep until there are no remaining particles stuck to the intestine
- Carefully scrape the villi under a magnifying lens
- Collect villi-free tissue sections to PBS 5x Pen/Strep
- Wash 1x in PBS 5x Pen/Strep
- Cut the sections to 2-4mm pieces and transfer to 50mL tube

- Add 10mL PBS 5x Pen/Strep and pipet up and down with a 10mL pipette; remove supernatant and add fresh PBS; repeat until supernatant is clear; if tissue pellet is not settled by gravity, centrifuge 5min at 800rpm at 4°C
- Add 10mL 2mM EDTA [Titriplex III, Merck Ref. 1370041000] in PBS 5x Pen/Strep
- Incubate 1-2h rocking at 4°C or 30min rocking at RT
- Let settle and remove supernatant
- Add 10mL PBS 5x Pen/Strep 10% FBS; pipet up and down 5-10 times and collect the supernatant after passing it through 100µm pore diameter nylon mesh (cell strainer) [Falcon Ref. 352360]
- Spin down the crypt fraction by centrifuging 10-20min at 800rpm at 4°C to remove single cells (mostly lymphocytes)
- Resuspend crypt unit pellet in 5mL PBS 5x Pen/Strep and count

MIAC isolation

- Collect the small intestine in ice-cold PBS with 5x antibiotics [Pen-Strep solution, Biological Industries Ref. 03-031-1B (normally used 1:100, dilute it 1:20 instead)]
- Remove fat and mesentery
- Cut open longitudinally
- Wash repeatedly in PBS 5x Pen/Strep until there are no remaining particles stuck to the intestine
- Carefully scrape the villi under a magnifying lens (this step is not essential for MIAC isolation, but helps find small adenomas better)
- Dissect adenomas carefully with a blade under a magnifying lens
- Wash adenomas 3x in HBSS [Gibco Ref. 14025] 5x Pen/Strep rocking 5min at RT; let settle and discard the SN
- Incubate adenomas in 8mM EDTA in HBSS 5x Pen/Strep rocking 5min at RT
- Shake vigorously 3x 10 times: the supernatant is the first fraction (collect, add 5% FBS and keep on ice); keep the pellet for obtaining following fractions
- Cut the adenomas with a blade (to small pieces, do not mince them)

- Incubate adenoma pieces in 8mM EDTA in HBSS 5x Pen/Strep rocking 20min at 4°C
- Shake vigorously 3x 10 times: the supernatant is the second fraction (collect, add 5% FBS and keep on ice); keep the pellet for obtaining following fractions
- Incubate adenoma pieces in 0.4mg/mL Dispase I [Sigma Ref. D4818] in HBSS 5x Pen/Strep shaking 20min at 37°C
- Shake vigorously 3x 10 times
- Centrifuge all fractions 5min at 1200rpm at 4°C; discard the SN
- Resuspend the pellet(s) in 1.25mg/mL collagenase I [Sigma Ref. C0130] in HBSS 5x Pen/Strep shaking 20min at 37°C
- Shake vigorously 3x 10 times: the supernatant is the last fraction; centrifuge 5min at 1200rpm at 4°C; discard the SN
- Resuspend the cells in ice-cold HBSS 5x Pen/Strep 140nM ROCK inhibitor [Y-27632, Sigma Ref. Y0503]
- Filter the cells through 100µm-70µm-40µm pore diameter cell strainers [Falcon Refs. 352360/50/40]
- Centrifuge 5min at 1200rpm at 4°C; discard the SN
- Resuspend the cells in ice-cold HBSS 5x Pen/Strep 140nM ROCK inhibitor
- Count, checking viability by Trypan Blue dye exclusion

MM10. Organoid/spheroid culture and reagents

Once we have a crypt enriched suspension or isolated MIACs we can seed them embedded in basement membrane extract matrices, such as Matrigel® [BD Biosciences, now Corning Ref. 354234]. Cells that grow in serum-free conditions and without attachment to a plate are thought to have stem-cell characteristics. Indeed, these 3D cultures can be maintained indefinitely with serial passaging (Fatehullah et al. 2016).

Adapted from (Sato et al. 2009):

- Optimal seeding conditions: 5.000-10.000 crypt units or 50.000 MIACs per 50µL matrigel drop in 24-well plate with 500µL complete organoid medium.
- Refresh growth factors (adding 50µL to each well) every 2 days and change fresh complete organoid medium every 4 days.
- Composition of the complete organoid medium:
  In Advanced DMEM/F12 [Gibco Ref. 12634028]
    - 100U/mL Penicillin and 0.1mg/mL Streptomycin [Pen/Strep Solution, Biological Industries Ref. 03-031-1B]
    - 2mM L-Glutamine [Biological Industries Ref. 03-020-1B]
    - 1x B27 supplement [Gibco Ref. 17504044]
    - 1x N-2 supplement [Gibco Ref. 17502048]
    - 140nM ROCK inhibitor [Y-27632, Sigma Ref. Y0503]
    - 100ng/mL Noggin [Peprotech Ref. 250-38]
    - 100ng/mL R-spondin1 [R&D Systems Ref. 3474-RS]
    - 50ng/mL EGF [Sigma Ref. E9644]
    - 20ng/mL basic FGF [Peptrotech Ref. 450-33B]
- When seeding MIACs, at the moment of plating also add 100ng/mL Wnt3A [R&D Systems Ref. 1324-WN]. It is not necessary when replating or at subsequent passages.

<u>Passaging 3D cultures</u> [adapted from (VanDussen et al. 2012)]

- With ice-cold 1mL tips, 7x pipet up and down both matrigel and medium in the well, making sure all the matrigel is dissolved and trying not to make many bubbles
- Transfer to eppendorf tube placed on ice

- Add an extra 500µL of ice-cold DMEM-F12 (supplemented with antibiotics and L-glutamine, DF12++ hereon) to give volume
- Pass the suspension 4x through a 30G needle [yellow, BD Microlance Ref. 304000] placed in a 1mL syringe
- Depending on the organoid/spheroid count, splitting the culture 1/3 is recommended: divide in desired tubes and give volume with DF12++ to help wash matrigel out
- Centrifuge at 1200rpm 20min at 4°C; discard the SN and keep the tubes constantly on ice
- On ice and with ice-cold tips resuspend each pellet in 50µL thawed matrigel
- Quickly place matrigel drops without bubbles onto pre-warmed (1-2h at 37°C) 24-well plate
- Incubate 1-2 minutes at RT
- Incubate 10-20 minutes at 37°C
- Add 450µL complete sphere medium (see composition above) on top of solidified matrigel drops
- Refresh factors at 3rd day and passage at 5th or 6th day is recommended

Reagents used in the 3D cultures are the following: 50µM DAPT [ɣ-secretase inhibitor IX from Calbiochem, now at Merck Millipore Ref. 565770], 0.66µM PKF115-584 [β-catenin/Tcf-Lef inhibitor, kindly given by Novartis], 5µM (Z)-4-hydroxytamoxifen (4-OH-T) [Sigma Ref. H7904] and 800ng/mL soluble Jag1-Fc chimera [R&D Systems Ref. 599-JG-100]. All of them were added to the complete organoid medium, except for the soluble Jag1, that was added directly to the matrigel while cells were being resuspended.

MM11. Organoid/spheroid immunostaining

Following a slightly modified protocol from (Dow et al. 2015), for performing immunostaining of 3D structures grown in matrigel, these were previously seeded onto round glass coverslips, instead of onto the well directly, so that they could be mounted on a slide in the last step.

Fixation

- Aspirate the medium and add 500µL 4% PFA /well; incubate 20min at RT
- 2x wash in PBS 3min at RT
- Add 500µL DTT buffer /well (100mM Tris pH9.4, 10mM DTT in H_2O). Incubate 25min at RT.
- 3x wash in PBS 3min at RT

Permeabilisation

- Add 500µL permeabilisation buffer /well (0.5% Triton X-100 in PBS); incubate 10min at RT
- 3x wash in PBS 3min at RT

Blocking

- Add 500µL blocking buffer /well (2% BSA, 0.3% Triton X-100 in PBS); incubate at least 30min at RT, 1h is preferable (>2h at +4°C)

Primary antibody

- Without washing, add the primary antibodies diluted in blocking buffer, 500µL /well (See **Table MM4** for details)
- Incubate O/N at 4°C
- 3x wash in PBS 5min at RT
- 3x wash in 0.3% Triton X-100 in PBS 5min at RT

Secondary antibody

- Add directly labelled secondary antibodies in 0.05% BSA in PBS, 500µL /well; incubate 2h at RT, protected from light
- 3x wash in PBS 5min at RT, protected from light

Nuclei counterstaining and mounting

- Add 500µL DAPI 1:2000 in water / well [5mg/mL Invitrogen Ref. D1306]; incubate 10min at RT, protected from light
- 3x wash in PBS 5min at RT, protected from light
- Mount in ProLong® Diamond (with DAPI) [Thermo Scientific Ref. P36971] onto a slide
- Pictures were obtained with a TCS SP5 Upright Confocal Microscope, using the Leica Application Suite software

Category	Antibody	Company	Reference	Species	Dilution
Primary	Bmi1	abcam	ab14389	Mouse	1:100
	γH2A.X	Cell Signalling	#2577	Rabbit	1:200
	Ecadh	BD Biosciences	610181	Mouse	1:100
	EphB2	R&D Systems	AF467	Goat	1:200
	CD44	abcam	ab65829	Rabbit	1:250
	ECN1	Acris	AM00349PU-N	Mouse	1:50
	Dll4	abcam	ab7280	Rabbit	1:1000
	Jag1 (C-20)	Santa Cruz	sc-6011	Goat	1:500
	CA-II	Rockland	200-401-136	Rabbit	1:2000
	Lyz1	Dako	A0099	Rabbit	1:5000
	Muc2	(kindly given by Dr. C. de Bolós)		Rabbit	1:400
	Syp	Dako	A0010	Rabbit	1:500
	Ki67	Novocastra (Leica)	NCL-L-Ki67-MM1	Mouse	1:500
	ccas3	Cell Signalling	9661	Rabbit	1:500
	Mfng (A-19)	Santa Cruz	sc-8237	Goat	1:100
	Mfng	Biorbyt	orb157845	Rabbit	1:100
Secondary	DαM-488	Life Technologies	A-21202	Donkey	1:1000
	DαR-488	Life Technologies	A-21206	Donkey	
	DαG-488	Life Technologies	A-11055	Donkey	
	DaM-568	Life Technologies	A-10037	Donkey	
	DaR-546	Life Technologies	A-10040	Donkey	
	GaR-Cy3	Jackson Immunoresearch	111-165-144	Goat	

Table MM4 | Antibodies used in 3D immunostainings

MM12. TUNEL / ccas3 double staining

We used Promega's DeadEnd® Colorimetric Apoptosis Detection System [Promega Ref. G7360] to label DNA breaks. The test measures nuclear DNA fragmentation, a biochemical indicator of apoptosis. However, the fragmented DNA is end-labeled using a modified TUNEL (TdT-mediated dUTP Nick-End Labeling) assay, so it is staining any DNA breaks. Indeed, they have now changed the name of the commercial kit and removed "apoptosis" from the title – the product is now called "DeadEnd® Colorimetric TUNEL System". Using a slightly modified protocol from what the manufacturers indicated, we performed a double staining for TUNEL and cleaved caspase 3 as a marker for apoptotic cell death. This way, in "old" *Bmi1* KO organoids we could conclude that cells that were still in the epithelial layer and looked phenotypically intact were indeed accumulating DNA breaks ($TUNEL^+$ $ccas3^-$) and not apoptotic (unlike the cells that are normally secreted to the lumen of the organoids when they become apoptotic, $TUNEL^+$ $ccas3^+$). The protocol that we followed was:

Cell recovery

- Using a Recovery Solution [BD Biosciences Ref. 354253, now available at Corning], depolymerise matrigel by gently rocking 2h at 4°C
- Centrifuge organoids/spheroids 5min at 800rpm at 4°C; discard SN
- 1x wash in HBSS 5min at RT
- Cytospin organoids/spheroids onto poly-L-lysine coated slides (1000rpm 3min)

Fixation

- Fix cells in 4% PFA (in PBS) 25min at RT
- 2x wash in PBS 5min at RT

Permeabilisation

- Permeabilise cells in 0.2% Triton X-100 in PBS 5min at RT
- 2x wash in PBS 5min at RT

Equilibration and labelling

- Add 100µL equilibration buffer and incubate 5-10min at RT

- Add 100µL reaction mix (1µL biotinylated nucleotide mix, 1µL rTdT [recombinant Terminal Deoxynucleotidyl Transferase] in 98µL equilibration buffer)
- Stop reaction by immersing the slides in 2x SSC 15min at RT
- 3x wash in PBS 5min at RT

Blocking

- Block in 0.3% H_2O_2 in PBS 5min at RT
- 3x wash in PBS 5min at RT

Binding

- Add streptavidin-HRP (1:500 in PBS); incubate 30min at RT
- 3x wash in PBS 5min at RT

Develop

- Develop with TSA-FITC 1:500 in amplification diluent [Perkin Elmer Ref. NEL753001KT]
- 3x wash in PBS rocking 5min at RT, protected from light

Perform ccas3 staining

- Block unspecific antibody binding by incubating in blocking solution (0.3% Triton X-100 5% non-fat milk in PBS) O/N at 4°C
- Incubate primary antibody [ccas3, Cell Signalling Ref. 9661] 1:500 in blocking solution 3h at RT
- 5x wash in PBS rocking 5min at RT, protected from light
- Incubate secondary antibody [DaR-546, Life Technologies Ref. A-10040] 1:1000 in PBS 2h at RT
- 5x wash in PBS rocking 5min at RT, protected from light

Nuclei counterstaining and mounting

- Add 500µL DAPI 1:2000 in water / well [5mg/mL Invitrogen Ref. D1306]; incubate 10min at RT, protected from light
- 3x wash in PBS 5min at RT, protected from light
- Mount in ProLong® Diamond (with DAPI) [Thermo Scientific Ref. P36971] onto a slide
- Pictures were obtained with a TCS SP5 Upright Confocal Microscope, using the Leica Application Suite software

MM13. qRT-PCR

In molecular biology, quantitative real time polymerase chain reaction (qRT-PCR) is a technique based on the PCR, which is used to amplify and simultaneously quantify a targeted DNA fragment. It enables both detection and quantification (as an absolute number of copies or relative amount when normalized to DNA input or additional normalizing genes) of one or more specific sequences in a DNA sample.

Starting material was either freshly isolated crypts or adenoma cells, or 3D cultures (see above). Total RNA was extracted using the RNeasy Mini Kit [Qiagen Ref. 74104], following manufacturer's instructions, eluting in 30µL of RNase-free H_2O. Then, samples were quantified with a NanoDrop spectrophotometer [Thermo Scientific]. RNAs were retrotranscribed using the First Strand cDNA Synthesis Kit [GE Healthcare Life Sciences Ref. 27-9261-01], following manufacturer's instructions. The product of the cDNA reaction was usually diluted 1:20 and used for subsequent PCR analysis. qRT-PCR was performed in the LightCycler480 system, using a SYBR Green I Master Kit [Roche Ref. 04887352001]. The primers used are listed in the table below:

Target	Species	Sense (5'-3')	Antisense (5'-3')
Gapdh	Mouse	TGTTCCTACCCCCAATGTGT	TGTGAGGGAGATGCTCAGTG
β2m	Mouse	CTGACCGGCCTGTATGCTAT	CAGTCTCAGTGGGGGTGAAT
Villin	Mouse	CACCTTTGGAAGCTTCTTCG	CTCTCGTTGCCTTGAACCTC
Lgr5	Mouse	CGTCTTGCTGGAAATGCTTTGAC	AAGGCGTAGTCTGCTATGTGGTG
Olfm4	Mouse	GCTGGAAGTGAAGGAGATGC	ACAGAAGGAGCGCTGATGTT
Ascl2	Mouse	AGCATGGAAGCACACCTTG	AAGTGGACGTTTGCACCTTC
Bmi1	Mouse	CCAATGAAGACCGAGGAGAA	TTTCCGATCCAATCTGCTCT
c-Myc	Mouse	GCTGGAGATGATGACCGAGT	AACCGCTCCACATACAGTCC
EphB2	Mouse	TTCTCACCTCAGTTCGCCTCTG	CAAACCCCCGTCTGTTACATACG
Hopx	Mouse	GAGGACCAGGTGGAGATCCT	TCCGTAACAGATCTGCATTCC
Lrig1	Mouse	CCAAAAGCTGCATGAGTTGA	GCACCACTGGTATCCTCGAT
mTert	Mouse	AGGGTAAGCTGGTGGAGGTT	GATGCTCTGCTCGATGACAA
p16Ink4a	Mouse	GTACCCCGATTCAGGTGATG	TCGCACGATGTCTTGATGTC
p19Arf	Mouse	CATGTTGTTGAGGCTAGAGAGG	ACCAGCGTGTCCAGGAAG
Hes1	Mouse	CGGCATTCCAAGCTAGAGAAGG	GGTAGGTCATGGCGTTGATCTG
Atoh1	Mouse	GCTTCCTCTGGGGGTTACTC	CTGTGGGATCTGGGAGATGT
Lyz1	Mouse	AGACCGAAGCACCGACTATG	CGGTTTTGACATTGTGTTCG
Syp	Mouse	CTCCTCGGCTGAATTCTTTG	CCACATGAAAGCGAACACTG
Muc5	Mouse	AATCAGATGGGCTGTGTTCC	TCAGCACATAGGTGCAGTCC
Dll1	Mouse	GGGCCTTTTCTGCAACCAAG	TATACCCAGGTCGGCAGGAA
Dll4	Mouse	ACCTTTGGCAATGTCTCCAC	TTGGATGATGATTTGGCTGA

(table continued on the next page)

Target	Species	Sense (5'-3')	Antisense (5'-3')
Jag1	Mouse	GACCAGAACGGCAACAAAACTTGCA	TTGGTCTCACAGAGGCACTGCCAGG
Jag2	Mouse	GGACCAGCAGGGCCTCGTGAAT	CGAGTTCCAGTGTGACGCCTAC
Cd44	Mouse	CTCCAGACAACCACCAGGAT	ATCCGTTCTGAAACCACGTC
Cd133	Mouse	ACGTTTGTTGTTGGTGCAAA	TCTCAAGCTGAAAAGCAGCA
β-*ACTIN*	Human	CGCAAGTACTCCGTGTGGA	CGGCCACATTGTGAACTTTG
C-MYC	Human	CGTGGTATGTATGGGAGATGGCAG	GGACAGTAGGAAAGGAAGTGGGATG
EPHB2	Human	CCAGACAAGCATCCAGGAGAAGTTG	AGATTGGGGAACCGACAGTGAAGG
BMI1	Human	CACCAGAGAGATGGACTGACAAATG	TGAGGAAACTGTGGATGAGGAGAC
HES1	Human	TACCTCTCTCCTTGGTCCTGGAAC	CAGATGCTGTCTTTGGTTTATCCG

Table MM5 | qRT-PCR primers.

MM14. Sequential chromatin-immunoprecipitation (ChIP)

Chromatin immunoprecipitation is a technique used to analyse the association of proteins to the chromatin. By doing two sequential immunoprecipitations in the same sample, the purpose was to detect co-existence of Notch1 and β-catenin at the chromatin level, in the Bmi1 promoter.

Starting material was freshly isolated crypts (see **MM9** above).

Cross-link

- Add 1/10 of cross-link solution to crypt suspension (in PBS) to a final concentration of 0.5% formaldehyde [Sigma Ref.252549]. Cross-link solution contains [50mM HEPES pH 8.0, 10mM NaCl, 1mM EDTA, 0.5mM EGTA, 5.55% formaldehyde, in H_2O]. Incubate 10min gently rocking at RT.
- Stop the cross-linking reaction by adding 1/10 stop solution. Stop solution contains [1.25M Glycine, 10mM Tris-HCl pH 8.0, in H_2O]. Incubate 5min gently rocking at RT.

Wash

- Spin down the crypts by centrifuging 5min at 1000rpm. Discard supernatant (SN).
- Rinse twice with ice-cold PBS supplemented with 0.5mM EDTA and protease inhibitors (1 tablet/0.5L PBS) [Complete Mini, Roche Ref. 11836153001].

Lysis

- Lyse cell pellets with 1mL lysis buffer, which contains [10mM Tris-HCl pH 8.0, 0.25% Triton X-100, 10mM EDTA, 0.5mM EGTA, 10mM Na-butyrate, 20mM β-glycerol-phosphate, 0.1mM Na-orthovanadate, protease inhibitors, in H_2O]. Incubate 20min on ice.
- Centrifuge 4min at 3000rpm. Discard SN.

Wash

- Resuspend pellet in ice-cold washing buffer, which contains [sonication buffer (see below) plus an extra 0.1M NaCl].
- Centrifuge 4min at 3000rpm. Discard SN.

Sonication

- Resuspend nuclei in 800uL ice-cold sonication buffer, that contains [10mM Tris-HCl pH 8.0, 0.1M NaCl, 1mM EDTA, 0.5mM EGTA, 10mM Na-butyrate, 20mM β-glycerol-phosphate, 0.1mM Na-orthovanadate, protease inhibitors, in H_2O]. Add 80uL 10% sodium dodecyl sulphate (SDS), to a final concentration of 1%.
- Sonicate cells at medium power with a 0.5 interval using a Bioruptor Sonicator [Diagenode] during 10min, to generate 500 to 1500bp DNA fragments.
- Centrifuge at maximum speed for 30min at 20-25°C. Collect the SN to a new tube (it contains the soluble chromatin). The black pellet should be discarded.

SDS wash

- Dilute the SN 10-fold with sonication buffer to reduce the concentration of SDS to 0.1%.
- Concentrate the samples using a Vivaspin 20 column [Sartorius Ref. VS2032], centrifuging at 3400rpm at 20°C to a final volume of 0.5-0.8mL.
- Adjust the concentrated chromatin solution to RIPA buffer by adding 0.1% deoxycholate (DOC), 140mM NaCl and 1% Triton X-100.

Preclearing

- Preclear the chromatin twice by adding 1% BSA, 1µg salmon sperm DNA, unspecific pre-immune IgG (volume and species according to

the experimental antibodies) and 60µL of 50:50 protein A/G sepharose [GE Healthcare, Refs. 17-0618-01 and 17-0780-01]. Incubate rotating 2h at 4°C.
- Centrifuge 2min at 3000rpm and recover SN. Collect input (50µL) at this step after second preclearing (and continue processing them at the "Revert crosslink" step below).

Immunoprecipitation (1)

- Add 2µg of first target antibody (β-catenin, see **Table MM6**) and the corresponding pre-immune control IgG to 800µL of chromatin suspension.
- Incubate rotating O/N at 4°C.
- Pull down the IgG-chromatin complexes by adding 60µL 50:50 protein A/G sepharose, adding 1% BSA and 1µg salmon sperm DNA.
- Incubate rotating 2h at 4°C.
- Centrifuge 2min at 1000rpm. Discard the unbound fraction (SN).

Wash

Centrifuge 1min at 1000rpm and discard the SN after each washing step.

- 2x wash with ice-cold RIPA buffer [0.1% DOC, 0.1% SDS, 1% Triton X-100, 10mM Tris-HCl pH 8.0, 140mM NaCl, 1mM EDTA, 0.25mM EGTA, 10mM Na-butyrate, 0.1mM Na-orthovanadate, in H_2O].
- 2x wash with ice-cold RIPA-sodium buffer [RIPA buffer plus 1M NaCl].
- 1x wash with LiCl buffer [0.25M LiCl, 1% Nonidet P-40, 1% DOC, 10mM Tris-HCl pH 8.0, 1mM EDTA, 1mM EGTA, 10mM Na-butyrate, 0.1mM Na-orthovanadate, in H_2O].
- 1x wash with TE buffer [10mM Tris-HCl pH 8.0, 1mM EDTA, in H_2O].

Elute the first ChIP

- Resuspend the chromatin-protein-antibody-G/A sepharose complexes in 20-30µL 10mM Dithiothreitol (DTT) and incubate 30min at 37°C.
- Centrifuge 2min at 3000rpm and recover SN. Dilute 25 times in RIPA buffer.

Immunoprecipitation (2)

- Add 5µL/IP of second target antibody (Notch1, see **Table MM6**).
- Incubate rotating O/N at 4°C.
- Pull down the IgG-chromatin complexes by adding 40µL 50:50 protein A/G sepharose.
- Incubate rotating 2h at 4°C.
- Centrifuge 2min at 3000rpm. Discard the unbound fraction (SN).

Antibody	Company	Reference	Species	Dilution
Cleaved Notch1	abcam	ab8925	Rabbit	5µL/IP
β-catenin	BD Biosciences	61054	Mouse	2µg/IP
Rabbit IgG	Sigma	I 8140	Rabbit	2µg/IP
Mouse IgG	Sigma	I 8765	Mouse	2µg/IP

Table MM6 | Antibodies used in the sequential ChIP.

Wash

- 2x wash with ice-cold RIPA buffer. Centrifuge 1min at 1000rpm and discard the SN.

Elute the second ChIP

- Add 100µL elution buffer [10mM Tris-HCl pH 8.0, 1mM EDTA, 1% SDS, 30mM NaCl 20µM β-glycerol-phosphate, 10µM Na-butyrate, in H_2O]. Incubate rotating 60min at RT.
- Centrifuge 2min at 100rpm and recover the SN, this is the product of your sequential ChIP.

Revert crosslink

- Revert crosslink by incubating the obtained solution (and inputs) O/N at 65°C.
- Add 0.5µg/µL Proteinase K [Roche Ref. 03115828001] and incubate 2h at 55°C.

Purify

- Purify the DNA using the GFX Kit [GE Healthcare Life Sciences Ref. 28-9034-71], following the manufacturer's instructions, eluting in 50µL of RNAse-free water.

Quantitative PCR amplification of the DNA sequences

- Detect the presence of promoter regions in the eluted DNA using the primers indicated in **Table MM7**. qPCR was performed in the LightCycler480 system, using a SYBR Green I Master Kit [Roche Ref. 04887352001].

Primer pair	Sense (5'-3')	Antisense (5'-3')
mBmi1p pp2	TGAGCGTCTTCAAGCCCTAT	CACACCTTTCCCGAAACACT
mBmi1p pp4	CCTTGTGGGTAAGGAATGGA	TTATTCCACTTGCCCTTTGG
mBmi1p pp6	GCCACGGACGTAGTGAGTTT	GATTTCTGCGTGATGTGCAG

Table MM7. Primer sequences used in the sequential ChIP assay. "pp" indicates "primer pair".

MM15. Co-immunoprecipitation (CoIP) and Western Blot (WB)

When a cell is lysed under non-denaturing conditions, many protein-protein associations that exist within the intact cell are conserved. Thus we can detect and identify physiologically relevant protein-protein interactions.

Start with a freshly isolated crypt suspension (see **MM9** above).

Cell extract preparation

- 2x wash cells in PBS, pelleting them down by centrifuging at 1200rpm 5min. Discard supernatant (SN).
- Resuspend crypt pellet in 1mL ice-cold CoIP lysis buffer (1mM EDTA, 0.1mM Na-orthovanadate (Na_3VO_4), 0.5% Triton X-100, 20mM β-glycerol-phosphate, 0.2mM PMSF, protease inhibitor cocktail, in PBS)
- Incubate 20min on ice.
- Centrifuge at maximum speed for 15min at 4°C and recover SN to a new tube. Keep 100µL of this lysate as input.

Blocking and conjugation of the beads

- Block 50µL protein A/G sepharose beads per sample, with 5µg BSA in IPP buffer (10mM Tris-HCl pH8.0, 500mM NaCl, 0.1% Nonidet P-40, 5mM EDTA, 50mM NaF, 0.4mM Na-orthovanadate, 1mM PMSF, 10µg/mL leupeptin, 10µg/mL aprotinin) and conjugate with 2µg of

the desired antibody or an irrelevant IgG as a negative control (see **Table MM8**).
- Incubate rotating 1h at 4°C.

Immunoprecipitation

- Add the lysate obtained at the first step to the antibody-conjugated sepharose beads.
- Incubate rotating 2h at 4°C.

Wash

- 5x wash in 1mL CoIP buffer (20mM HEPES pH 7.0, 2mM EGTA, 2mM $MgCl_2$, 1mM PMSF, protease inhibitor cocktail, in H_2O) pelleting the proteins-antibody-protein A/G sepharose complexes down by centrifuging at 1000rpm 2min. Discard SN every time.

Elution

- Prepare the samples for analysis by Western Blot by directly incubating the beads in 60µL sample loading buffer (50mM Tris-HCl pH 6.8, 1.4M β-mercaptoehtanol, 2% SDS, 0.1% bromophenol blue, 10% glycerol, in H_2O) and boiling for 4min.

Western Blot

- Electrophoresis and gel transfer: separate the samples by 10% polyacrylamide gel electrophoresis (SDS-PAGE) and transfer to a PVDF membrane [Millipore Ref. IPVH00010].
- Block the PVDF membrane with 5% non-fat milk in TBS-T buffer (50mM Tris-HCl pH 8.0, 150mM NaCl, 0.05% Tween 20, in H_2O) rocking 1h at RT.
- Incubate the membrane with the primary antibody in blocking solution (see **Table MM8**) rocking O/N at 4°C.
- 5x wash in TBS-T buffer rocking 5min at RT.
- Incubate the membrane with the secondary antibody (HRP-conjugated) in blocking solution (see **Table MM8**) rocking 1h at RT.
- 5x wash in TBS-T buffer rocking 5min at RT.
- Incubate the membrane with ECL solution [Biological Industries Ref. 20-500-120], that contains a chemiluminescent HRP substrate.

- Develop the chemiluminescent signal in an autoradiography film [GE Healthcare Ref. 28906835].

Antibody	Company	Reference	Species	Dilution	Step
β-catenin	Sigma	C2206	Rabbit	2µL/IP	IP
IgG	Sigma	I 8140	Rabbit	2µL/IP	IP
β-catenin	Sigma	C2206	Rabbit	1:4000	WB
ICN1 (Cleaved Notch1)	Cell Signaling	#2421	Rabbit	1:800	WB
anti-Rabbit-HRP (2ary)	Dako	P0448	Goat	1:100	WB

Table MM8 | Antibodies used in the CoIP and WB.

MM16. Cell lines and reagents

All cells were grown in Dulbecco's modified Eagle's medium (DMEM) [Invitrogen] supplemented with 10% fetal bovine serum (FBS) [Biological Industries], 4.5g/L glucose [Life Technologies], 2mM L-glutamine [Biological Industries], 56U/mL penicillin and 56µg/mL streptomycin [Biological Industries]. Cells were grown in an incubator at 37°C and 5% CO_2.

For luciferase assays human HEK293T and NIH/3T3 were used [ATCC Refs. CRL-3216 and CRL-1658]. For Figure R5, the human CRC cell line Ls174T was used [ATCC Ref. CL-188].

Dr. Verónica Rodilla generated the stable clones. In brief, for the generation of Ls174T/dnTCF4/N1ICD clones, N1ICD plasmid was transfected to Ls174T/dnTCF4 cells [L8 clones (Van de Wetering et al. 2002), kindly provided by Dr. Hans Clevers, Hubrecht Institute, Utrecht, Netherlands] using PEI (See **MM17** below). Stable transfectants were obtained after selection with 1mg/mL G418 [Geneticin, Gibco Ref. 11811031], 5µg/mL Blasticidine [InvivoGen Ref. ant-bl] and 100µg/ml Zeocin [InvivoGen Ref. ant-zn] and screened by western blot and immunofluorescence after doxycycline treatment [1µg/mL, Sigma Ref. D9891]. Clones with highest dnTCF4 and N1ICD expression were selected.

MM17. Transfection

Transfection is the process of introducing nucleic acids into cells. In cell biology research, the term is used for non-viral methods in eukaryotic cells.

For this, we used PEI [Polyethylenimine, Linear, MW 25.000, Polysciences Inc. Ref. 23996]. PEI is a high-charge cationic polymer that readily binds highly anionic substrates, such as DNA and other negatively charged molecules. It works as a carrier vector.

Transfection

- At least 6h prior to transfection, starve the cells by changing their medium to serum-free DMEM. Add 9/10 of the final volume only (for example, 900µL/well in a 12-well plate for luciferase assays)
- Dilute 3-5µL PEI per µg of DNA into 1/10 of the final volume in serum-free DMEM (for example in 100µL/well in a 12-well plate for luciferase assays)
- Mix gently and incubate 5 min at RT
- Add x ug of DNA, mix and incubate 20min at RT
- Add the solution to the culture plate or well
- O/N after transfection, change the medium to DMEM-10%FBS
- Analyse 48h after transfection

MM18. Luciferase Assay

Luciferase assay can be used to measure promoter activity. In this case, we cloned 2.5kb of the proximal human *Bmi1* promoter region into a luciferase reporter vector. Specifically, we cloned the region from -2009 to +484 around the TSS (transcription start site) of the human Bmi1 genomic region into the pGL2 basic vector [Promega Ref. E1641]. Insertion was verified by sequencing using the GLprimer1 and GLprimer2 [Promega Refs. E1651 and E1661]. Consensus binding sites for Rbpj, Tcf/Lef and Hes1 were found using the MatInspector from Genomatix.

By using chemical inhibitors, co-transfecting different expression vectors (of specific proteins or dominant negative forms) or shRNAs, we tried to modulate the promoter activity that was measured by luciferase activity.

A β-galactosidase expressing vector is co-transfected along with the luciferase reporter vector to measure its activity as a transfection control.

The starting material is 30.000 HEK293T or 15.000 NIH/3T3 cells/well in 1mL DMEM-10% FBS in a 12 well-plate, transfected the day after (see Transfection Protocol in **MM17**) in triplicates, and the assay was performed 48h after transfection. When indicated, HEK293T cells were treated with 50µM DAPT [ɣ-secretase inhibitor IX from Calbiochem, now at Merck Millipore Ref. 565770] 72h prior to the assay or 0.66µM PKF115-584 [β-catenin/Tcf-Lef inhibitor, kindly given by Novartis] 24h before.

Vectors used

Vector	Detailed name	Description	Reference
Bmi1-luc	pGL2b-hBmi1pro-2,5kb	The region from -2009 to +484 around the TSS of the human Bmi1 genomic region as a luciferase reporter	(Lopez-Arribillaga et al. 2014)
β-gal	RSV-β-galactosidase	β-galactosidase is expressed under the control of a constitutively active promoter, used for transfection efficiency control	(Flug et al. 1987)
ICN1	pCS2-N1ΔE	Transcriptionally active Notch1, lacking the extracellular domain	(Kopan et al. 1996)
β-cat	pCDNA3-β-cat S37I	Non-phosphorylatable (non-degradable) form of active β-catenin	Kindly donated by A. Garcia de Herreros
Mam	pCMV2-Maml1	Mastermind-like1, coactivator of ICN1-mediated transcription	(Wu et al. 2000)
dnRbpj	pCMXN-dnRBP	Dominant negative form of Rbpj (R218H), unable to bind DNA but able to bind ICN1	(Chung et al. 1994; Kato et al. 1997)
dnTCF4	pCDNA4TO-dnTCF4	Dominant negative form of Tcf4, able to bind DNA but unable to bind β-cat	(Van de Wetering et al. 2002)
dnMam	PeGFP-dnMaml1-GFP	Dominant negative form of MAML1, residues 13 to 74; can interact with CSL and ICN1 but lacks the TAD domain and is unable to recruit co-activators	(Weng et al. 2003)
shHes1	MISSION shRNA, TRCN0000018989 (human)	shRNA against the 3' UTR region of the human HES1 gene	Sigma

Table MM9 | Vectors used in the luciferase assays.

Prepare cell lysates

- Wash cells twice with PBS; dry well
- Add 100µL of reporter lysis buffer 1x per well [Promega Ref. E3971]

- Incubate 10 min rocking at RT
- Incubate 10 min at -80°C, to ensure that membranes are broken
- Thaw at RT (or 5min at 37°C)
- Scrape the well and collect each sample to a 1,5mL tube
- Centrifuge 10 min at maximum speed (13200 or 14000 rpm); collect the supernatant to a new tube

Measure β-galactosidase activity

- In a flat-bottom 96-well plate, place 10µL (HEK293T) or 20µL (NIH/3T3) of the lysate and 10µL or 20µL of the reporter lysis buffer for the blank measure
- At a constant pace, add 100µL of the β-gal substrate to each well [2.6mM ONPG (O-Nitrophenyl-β-D-galactopyranoside), $MgCl_2$, 43mM β-mercaptoethanol, in 1mM 0.1M phosphate buffer (Na_2HPO_4:NaH_2PO_4) pH 7.4]
- Protect reaction from light and wait at RT until it turns yellow
- At the same constant pace, add 100µL 1M Na_2CO_3, to stop the reaction
- Measure OD at 420nm; this is the transfection efficiency control

Measure luciferase activity

- Place 10µL (HEK293T) or 20µL (NIH/3T3) of the lysate into luminometer tubes
- Add 50µL luciferase substrate [Promega Ref. E1501]
- Measure RLU/s (relative luminescent units per second) in the luminometer; this is the promoter activity measurement

MM19. Flow cytometry

Flow cytometry is an analytical cell-biology technique that utilizes light to count and profile cells in a heterogeneous suspension. It is a very potent technique that offers a "high-throughput" (for a large number of cells) automated quantification of fluorescent signals from individual cells. We relied on the gradient expression of EphB2 [with the same approach as Jung and colleagues had with human colonic epithelium (Jung et al. 2011)] to distinguish between $EphB2^{hi}$ (including post-mitotic Paneth

cells and ISCs), EphB2^{med} (including most of the TA cells) and explore the cell cycle status inside those populations.

Starting material is freshly isolated crypts (See **MM9**). The protocol that we used was adapted from (Merlos-Suárez et al. 2011).

Obtain a single cell suspension

- Incubate crypts in 0.4mg/mL Dispase I [Sigma Ref. D4818], 0.8U/µL DNase I [Sigma Ref. D4513] in HBSS 30min at 37°C
- Add FBS to 5% to stop the enzymatic reaction
- Filter through 100µm-70µm-40µm pore diameter cell strainers [Falcon Refs. 352360/50/40]
- Centrifuge 5min at 1200rpm at 4°C; discard SN
- Resuspend single cell pellet in blocking solution (20% FBS, 140nM ROCK inhibitor, [Y-27632, Sigma Ref. Y0503] in PBS); incubate 20min at RT
- 1x wash in 10% FBS in PBS plus 140nM ROCK inhibitor
- Centrifuge 5min at 1200rpm at 4°C; discard SN

Immunostaining

- Incubate cells in primary antibody solution (10% FBS, 140nM ROCK inhibitor, in PBS) (see **Table MM10**); incubate 30min at RT
- 1x wash in 10% FBS in PBS plus 140nM ROCK inhibitor
- Centrifuge 5min at 1200rpm at 4°C; discard SN
- Incubate cells in secondary antibody solution solution (10% FBS, 140nM ROCK inhibitor, in PBS) (see **Table MM10**); incubate 40min on ice
- 1x wash in 10% FBS in PBS plus 140nM ROCK inhibitor
- Centrifuge 5min at 1200rpm at 4°C; discard SN

Hoechst staining

Hoechst 33342 [BD Pharmingen Ref. 561908] stains live cells and is used for cell cycle analysis.

- Incubate cells in Hoechst solution (10% FBS, 140nM ROCK inhibitor, 10µg/mL Hoechst 33342 in PBS) (see **Table MM10**); incubate 1h at 37°C
- 1x wash in 10% FBS in PBS plus 140nM ROCK inhibitor

Analyse by flow cytometry

- Samples were analysed in a LSRFortessa analyser [BD Biosciences]

Category	Reagent	Company	Reference	Species	Dilution
1ary ab	**EphB2**	R&D Systems	AF467	Goat	1:200
2ary ab	**DαG-488**	Life Technologies	A-11055	Donkey	1:1000
DNA dye	**Hoechst 33342**	BD Pharmingen	561908		1:100

Table MM10 | Reagents used in flow cytometry analysis.

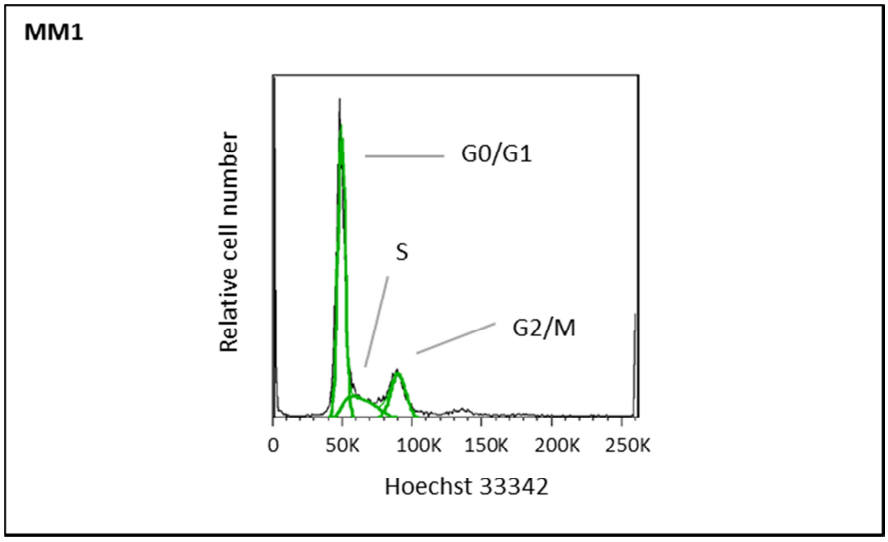

Figure MM1 | Sample plot of cell cycle analysis by flow cytometry using Hoechst 33342. Adapted from BD Biosciences' website. Representation of the different cell cycle phases in which cells can be found depending on their DNA content.

PREVIOUS WORK (PART I)

Notch and Wnt pathways are simultaneously required to maintain the intestinal stem cell compartment in vivo

A plausible explanation for the coexistence of active Notch and Wnt signalling in the intestinal stem/progenitor compartment would be that one of the signalling pathways was upstream of the other. To investigate this possibility, a former member of our lab analysed a set of gain- and loss-of-function mutants generated at the *Ecole Polytechnique Federale de Lausanne*, under supervision of Dr. Freddy Radtke. Specifically, a tamoxifen-inducible Cre recombinase driven by the *Villin* promoter (*Villin*-CreER^{T2}) was used to conditionally delete lox-P flanked sites in the intestinal epithelium (el Marjou et al. 2004). This construct is based on a fusion of the Cre protein with a mutant ligand-binding domain of the human oestrogen receptor, which -although insensitive to normal oestrogen- is able to respond to the oestrogen analogue tamoxifen. Being under the control of the *Villin* promoter, the fusion protein is expressed in all intestinal epithelial cells, including stem and progenitor cells. In the absence of tamoxifen, the mutant oestrogen receptor domain retains the fusion protein in the cytosol. Upon exposure and binding to tamoxifen, the fusion protein translocates to the nucleus where the Cre is able to recognise two 34-bp loxP sites and excise the intervening DNA sequence. The *Villin*-CreER^{T2} mice were crossed with mice carrying "floxed" alleles[16] for Notch and Wnt signalling pathway members to yield gain- and loss-of-function single and composite mutants. To generate a Notch LOF / Wnt GOF mutant, *Rbpj*^{lox} alleles that delete *Rbpj* and shut down Notch signalling (Notch OFF) were combined with a *Ctnnb1*$^{lox(ex3)}$ allele where the exon 3 of β-catenin is deleted, giving rise to a non-degradable active form of the protein (hereon called *Ctnnb1*^{active}, for sake of simplicity) (Wnt ON). To generate a Wnt LOF / Notch GOF mutant, *Ctnnb1*^{lox} alleles were used to delete the effector of Wnt β-catenin (Wnt OFF) combined with a knock-in in the constitutive Rosa26 locus of an active form of Notch1 (the intracellular domain of Notch1, ICN1) preceded by an stop codon flanked by loxP sites, called *R26-LSL-ICN1* (*ICN1*, for simplicity) (Notch ON). Single and compound mutants were generated by crossing these mouse strains, tamoxifen was

[16] Alleles with flanking loxP sites in specific genetic regions.

administered to induce Cre recombinase activity, and 3-4 days after induction the intestinal tissue was collected for analysis.

We (and others) previously demonstrated that genetic depletion of Notch signalling resulted in the complete loss of ISC markers and the intestinal stem cell function (Pellegrinet et al. 2011; Riccio et al. 2008). To study the status of the intestinal stem/progenitor compartment, we first analysed the paraffin-embedded intestinal tissue by *in situ* hybridization (ISH). Confirming the Notch-dependent ISC phenotype, Notch LOF mutants displayed an absence of the ISC markers *Lgr5*, *Olfm4* and *Ascl2* mRNA from the crypt base [**FIGURE P1**, see *Rbpj*^{lox}]. We found that this phenotype was not rescued by Wnt GOF [**FIGURE P1**, see *Rbpj*^{lox}*;Ctnnb1*^{active}]. As a control, constitutive activation of β-catenin alone led to the expansion of the undifferentiated crypt compartment, accompanied by ectopic expression of *Olfm4*, *Lgr5* and *Ascl2* [**FIGURE P1**, see *Ctnnb1*^{active}]. Wnt LOF also led to a loss of expression of the indicated ISC markers, even in the presence of Notch GOF (not shown). Loss of the ISC/progenitor compartment after shutting down either Notch or Wnt signalling in the intestinal epithelium would lead to the inability to self-renew the tissue. Mice were killed barely 3-4 days after induction of Cre activity, previous to intestinal damage, and hematoxylin/eosin (HE) staining of the intestinal sections indicate that the tissue is mostly undamaged at the analysed stage [**FIGURE P1**].

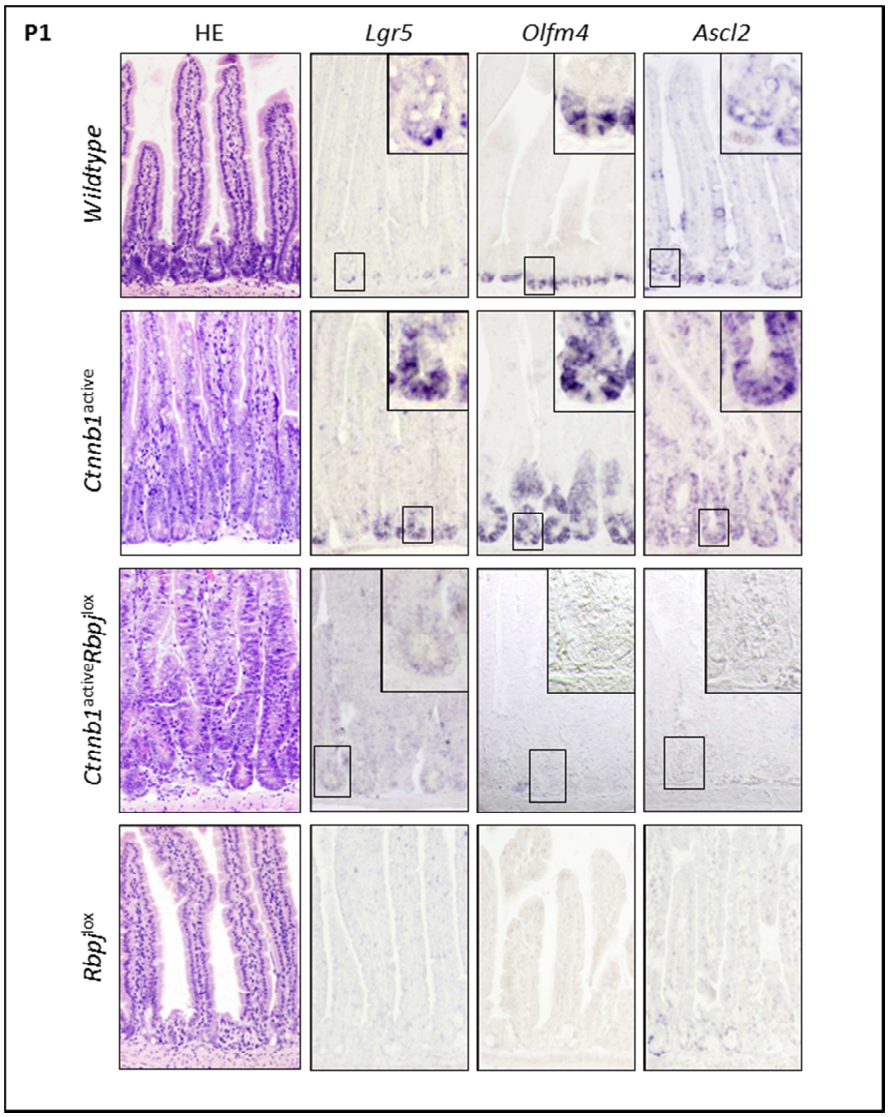

FIGURE P1 | ISH of ISC markers. mRNA expression pattern of *Lgr5*, *Olfm4* and *Ascl2* in intestinal paraffin sections from indicated genotypes. HE: Haematoxylin and Eosin staining to determine tissue architecture. These experiments were performed by Dr. Verónica Rodilla.

To confirm the levels of ISC marker mRNA seen by ISH, we performed qRT-PCR analyses of crypt enriched fractions of the indicated phenotypes [FIGURE P2]. qRT-PCR analyses confirmed that knockout of *Rbpj* or *Ctnnb1* resulted in complete loss of *Lgr5*, *Olfm4* and *Ascl2* ISC marker expression, that was not rescued by ectopic activation of the complementary pathway and was indicative of the loss of the ISC compartment.

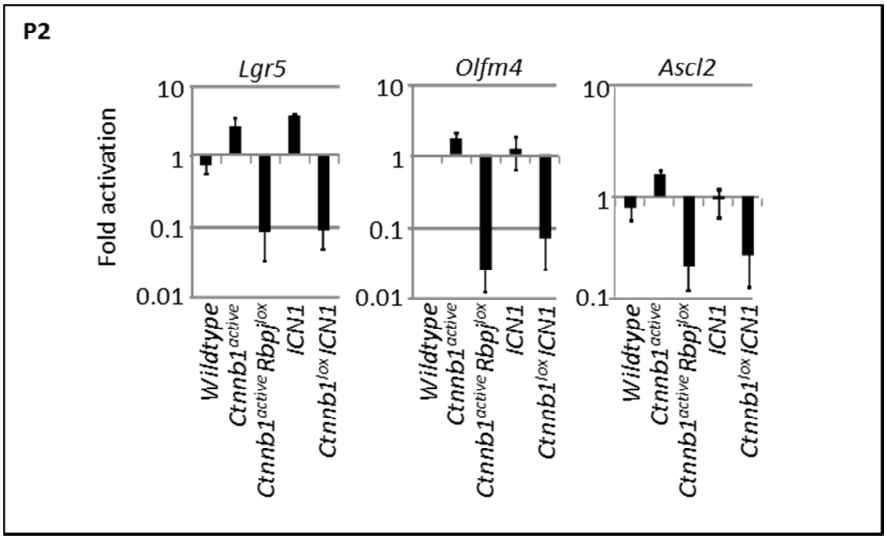

FIGURE P2 | qRT-PCRs of ISC markers. Expression levels of *Lgr5*, *Olfm4* and *Ascl2* in isolated crypts from indicated genotypes, relative to *Villin*. These experiments were performed by Dr. Verónica Rodilla.

RESULTS (PART I)

López-Arribillaga E, Rodilla V, Pellegrinet L, Guiu J, Iglesias M, Roman AC, Gutarra S, González S, Muñoz-Cánoves P, Fernández-Salguero P, Radtke F, Bigas A, Espinosa L. Bmi1 regulates murine intestinal stem cell proliferation and self-renewal downstream of Notch. *Development.* 2015 Jan 1;142(1):41-50. doi: 10.1242/dev.107714.

Notch and Wnt pathways are simultaneously required to maintain the intestinal stem cell compartment in vivo (continuation)

Alcian blue staining is widely used for identification of goblet cells in intestinal sections, since as a basic dye has high affinity for the acidic mucopolysaccharides that they accumulate and secrete. A combined immunohistochemistry (IHC) assay for the proliferation marker Ki67 with Alcian blue staining of paraffin sections further confirmed that post-mitotic goblet cells accumulate in the small intestinal crypts of Notch LOF mutants, associated with a marked reduction of the proliferative compartment [**FIGURE R1**, see *Rbpj*^{lox}]. Interestingly, in the crypts of the composite *Rbpj*^{lox};*Ctnnb1*^{active} mutants, both the goblet cell differentiation imposed by Notch LOF and the reduction in the number of proliferating ISC/progenitor cells were significantly rescued, leading to values comparable to the wildtype (WT) intestine, although still reduced compared with the single *Ctnnb1*^{active} mice [**FIGURE R1**]. This reveals that Wnt GOF partially compensates the effect of Notch LOF, without rescuing the loss of the ISC compartment.

Taken together, these results indicate that rather than by a hierarchical relationship, **simultaneous activation of Notch and Wnt is required to maintain the ISC/progenitor compartment homeostasis**.

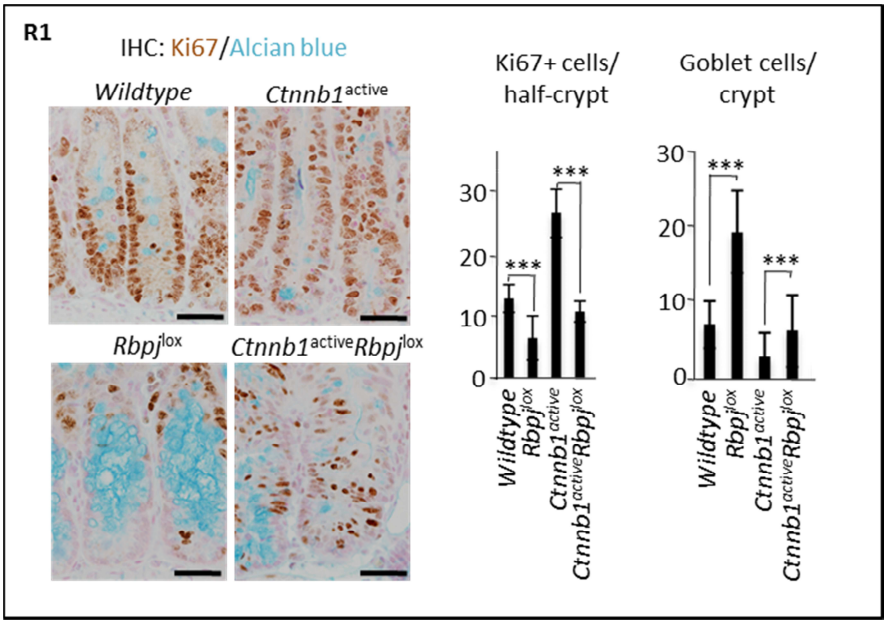

FIGURE R1 | Ki67/Alcian blue staining and quantification graphs. IHC against Ki67 was performed in paraffin sections of intestines of the indicated genotypes followed by staining with Alcian blue to identify goblet cells. Nuclei were counterstained with Nuclear Fast Red. Scale bar equals 50µm. In the graphs, columns represent the average quantification of >30 crypts of at least 2 samples for each indicated genotype and error bars represent the standard deviation. Statistical significance was assessed using the Student's T Test. *P<0.05, **P<0.01 and ***P<0.001.

We then performed an IHC against Lysozyme 1 to detect Paneth cells and surprisingly found a similar increase in number associated both to Notch LOF or Wnt GOF and even a further increase in the composite Notch LOF / Wnt LOF mutant [FIGURE R2]. However, in the active β-catenin mutants (both single and double with *Rbpj*^{lox}) it was clear that Paneth cells were abnormally distributed along the crypt-villus axis, suggestive of a **defect in compartmentalization** (Batlle et al. 2002).

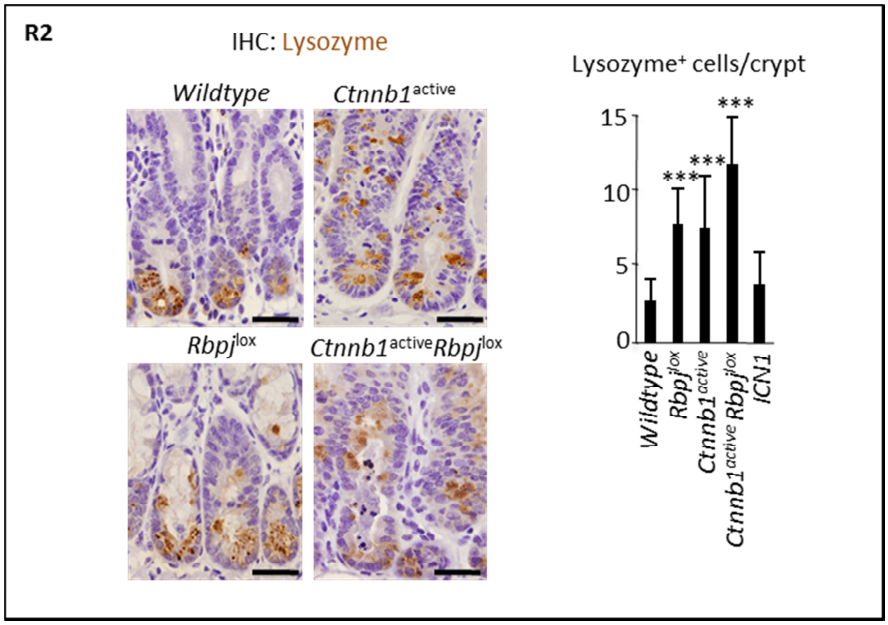

FIGURE R2 | Lysozyme staining and quantification graphs. IHC against Lysozyme 1 was performed in paraffin sections of intestines of the indicated genotypes to identify Paneth cells. Nuclei were counterstained with haematoxylin. Scale bar equals 50µm. In the graphs, columns represent the average quantification of >30 crypts of at least 2 samples for each indicated genotype and error bars represent the standard deviation. Statistical significance was assessed using the Student's T Test. *P<0.05, **P<0.01 and ***P<0.001.

Notch and β-catenin cooperate in the transcriptional activation of a subset of ISC genes

To understand the mechanism behind the simultaneous requirement for Notch and Wnt pathways in the ISC/progenitor compartment, we took advantage of a previously identified Notch and β-catenin-dependent transcriptional signature described in colorectal cancer cells (Rodilla et al. 2009). The signature was described using an *in vitro* model that in a way resembles the aforementioned in vivo LOF / GOF rescue experiments. Briefly, the Ls174T cell line that displayed high levels of active ICN1 and nuclear β-catenin was used. Specifically, it was a stable line able to express a dominant negative form of TCF4 (Wnt LOF) upon doxycycline treatment. This cell line was treated with the ɣ-secretase inhibitor DAPT to block Notch activity (Notch LOF). Blocking one of the pathways or both simultaneously prior to a microarray analysis, our group was able to describe a set of genes whose transcription was dependent on both pathways. More precisely, we focused on the genes whose expression in Ls174T/dnTCF4(+DOX) was not rescued by ectopic expression of ICN1 (Wnt LOF / Notch GOF). Among those genes, first we focused on three that were known to or could be related to ISC function: C-MYC, EPHB2 and BMI1. We validated their expression by qRT-PCR in the same cell line system. The expression of neither of them was rescued by ectopic activation of Notch in the absence of Wnt signalling [**FIGURE S1**]. As a control, expression of *HES1*, a classical Notch target was rescued upon expression of ICN1. This denotes that **Notch and Wnt signalling are required simultaneously to allow transcription of genes important for ISC function**.

Next, we needed to confirm that the cooperative transcriptional regulation of Bmi1 by Notch and Wnt also occurred *in vivo* under homeostatic conditions. For that, we analysed the expression pattern of the Bmi1 protein in the composite LOF/GOF mutants by IHC and found that ectopic activation of neither pathway rescued the loss of expression caused by absence of signalling of the complementary one [**FIGURE R3**]. By qRT-PCR analysis, we confirmed that mRNA expression was not recovered accordingly [**FIGURE R3**]. This corroborated that, ***in vivo* and in**

non-tumoural conditions also, Notch and Wnt signalling pathways need to be active for *Bmi1* to be expressed.

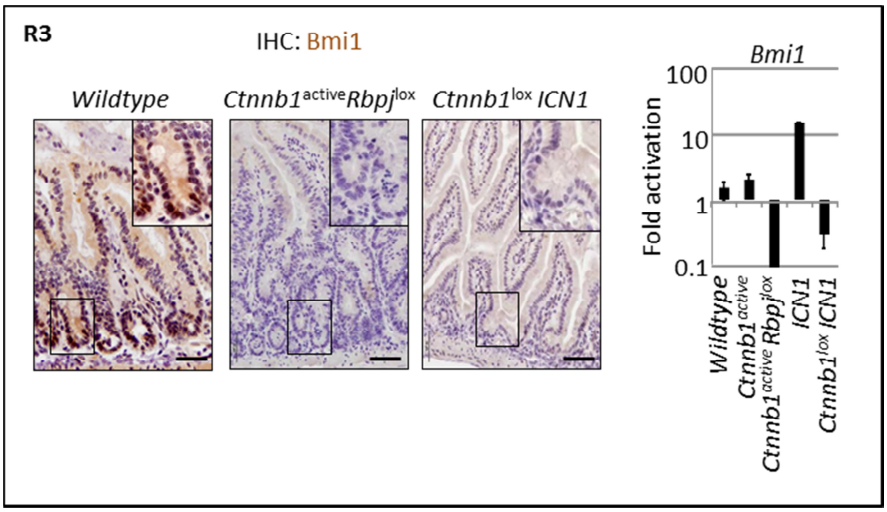

FIGURE R3 | Bmi1 staining and mRNA quantification. IHC against Bmi1 was performed in paraffin sections of intestines of the indicated genotypes. Nuclei were counterstained with haematoxylin. Scale bar equals 50µm. The graph indicates the expression level (qRT-PCR) of *Bmi1* in isolated crypts from indicated genotypes, relative to *Villin*.

We then decided to delve into the crosstalk between Notch and Wnt signalling at the transcriptional level upon Bmi1. Irrefutable proof that they are concurrently regulating transcription of a target gene would be that their effectors coexisted at its promoter region. Using the Genomatix software, we identified several adjacent Tcf and Rbpj consensus binding sites in the regulatory region of the murine *Bmi1* gene [depicted in **FIGURE R4**]. These sites were validated by a sequential chromatin immunoprecipitation (ChIP) in purified murine intestinal crypts. In particular, recruitment of Notch and β-catenin proteins was detected in a predicted region close to the TSS that contained both consensus binding sequences [**FIGURE R4**, see pp2]. This result validates that the effectors of the pathways **ICN1 and β-catenin concur in a region of the Bmi1 promoter** close to the TSS.

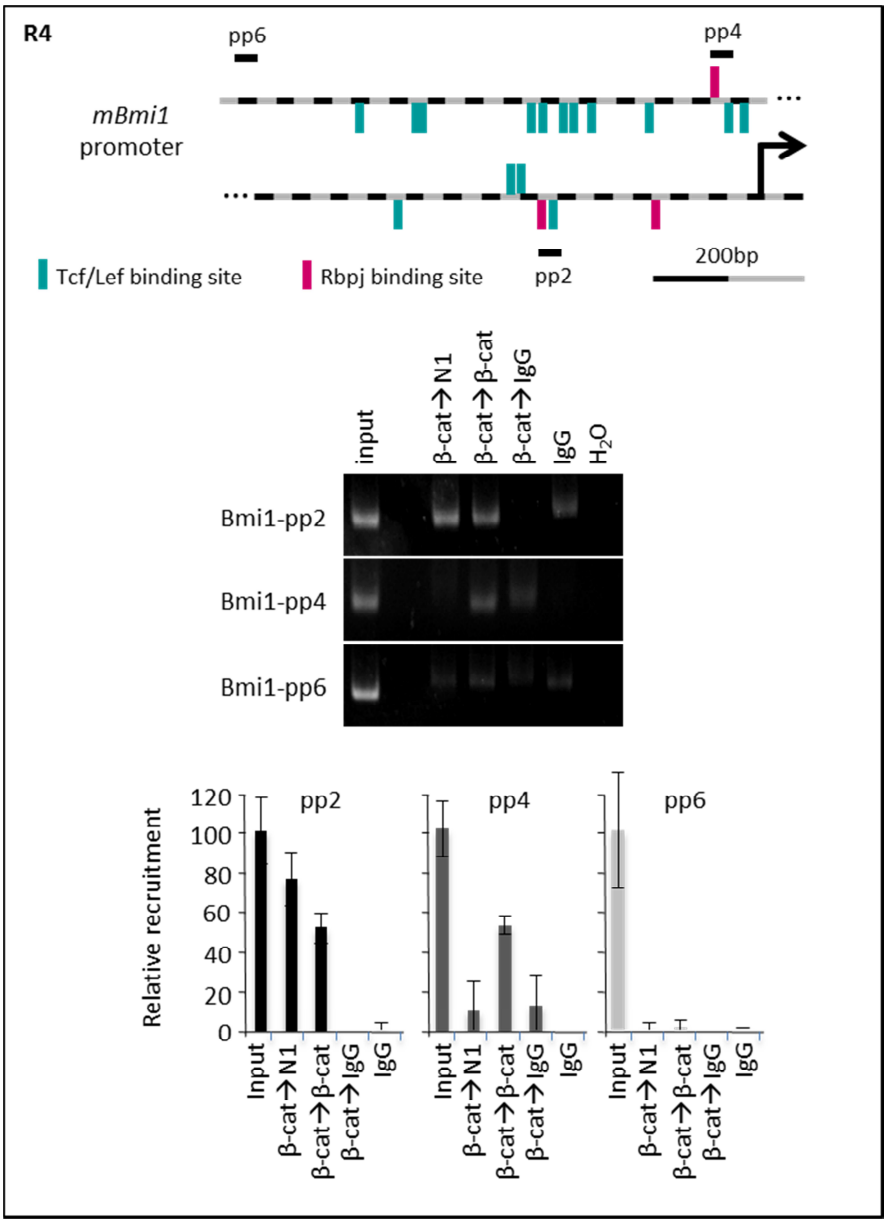

FIGURE R4 | ICN1 and β-catenin concur at the chromatin level in the *Bmi1* promoter. From top to bottom: Schematic representation of the murine *Bmi1* promoter indicating the consensus sites for Tcf and Rbp, and the position of the primer pairs used for the ChIP analysis. Sequential ChIP assay of the *Bmi1* promoter with the indicated antibodies. Chromatin was isolated from murine intestinal crypts and after precipitation a quantitative PCR was performed with the depicted primer pairs. Graphs indicate the densitometric quantification of β-catenin and β-catenin/Notch1 co-recruitment to the Bmi1 promoter region as determined by quantitative PCR analysis.

Another experiment that further supports the functional interplay between both pathways in the intestinal stem/progenitor compartment is a co-precipitation of protein extracts from isolated murine intestinal crypts that demonstrated that **ICN1 and β-catenin can in interact at the protein level** [FIGURE R5].

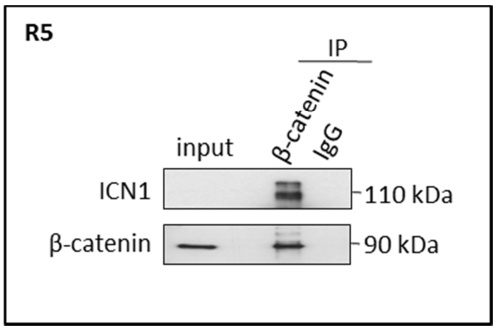

FIGURE R5 | ICN1 and β-catenin co-IP. Total cell extracts from isolated crypts were precipitated using an anti-β-catenin antibody. Precipitates were analysed by Western Blotting for the presence of active (cleaved) Notch1.

Then, we generated a reporter construct carrying 2.5kb of the proximal human *Bmi1* promoter, including the putative Rbpj and TCF consensus sites, fused to the luciferase gene [FIGURE R6].

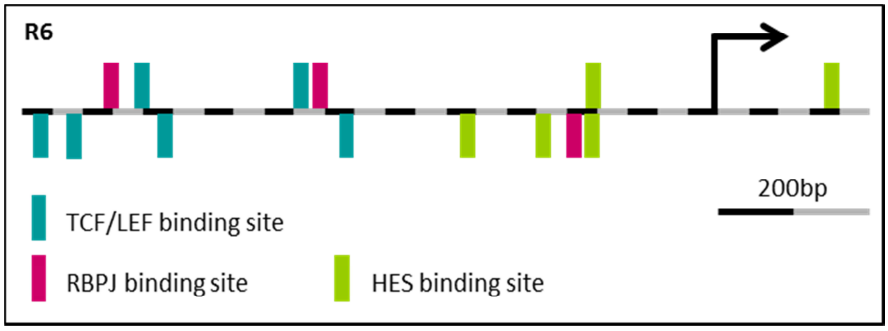

FIGURE R6 | The human *Bmi1* promoter. Schematic representation of the human *Bmi1* promoter region, depicting the consensus sites for TCF, RBP and HES. Arrow indicates TSS.

First, we tried silencing the promoter by pharmacological inhibition. Treatment with the γ-secretase inhibitor DAPT that blocks Notch signalling or with the small molecule PKF115-584 that blocks the interaction of β-catenin with TCF and hence blocks Wnt signalling was sufficient to repress transcription driven by the *Bmi1* promoter [FIGURE R7]. Ectopic expression of the dominant negative forms of the transcription factors of either pathway (Rbpj and TCF4) was also capable of repressing transcription driven by the *Bmi1* promoter [FIFURE R7].

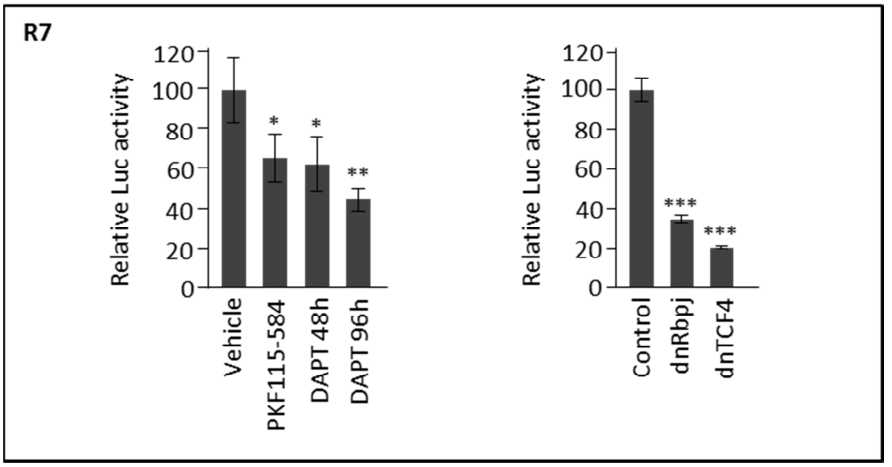

FIGURE R7 | Silencing the *Bmi1* promoter by pharmacological inhibition and dnTF. ***Bmi1*** promoter activity assay with the indicated treatments or constructs. Left graph shows pharmacologic inhibition of β-cat/Tcf-Lef by treatment with PKF or inhibition of Notch signalling with DAPT. Right graph shows inhibition of *Bmi1* promoter activity by co-transfection with dominant negative forms of the transcription factors Rbpj and TCF4 (see MM18). Error bars represent the standard deviation and statistical significance was determined using Student's t-test. *P<0.05, **P<0.01 and ***P<0.001.

Next, we sought to activate the *Bmi1* promoter activity. Although neither active ICN1 nor β-catenin alone could induce *Bmi1* directed transcription, the coactivator Mam was able to enhance the *Bmi1* promoter activity considerably, and seemed to be able to do so independently of Rbpj or TCF4 [**FIGURE R8**, see columns 5 and 6]. This suggested that **Mam might be a limiting factor** for the activation of the *Bmi1* promoter in the tested cell lines (HEK293T and NIH/3T3).

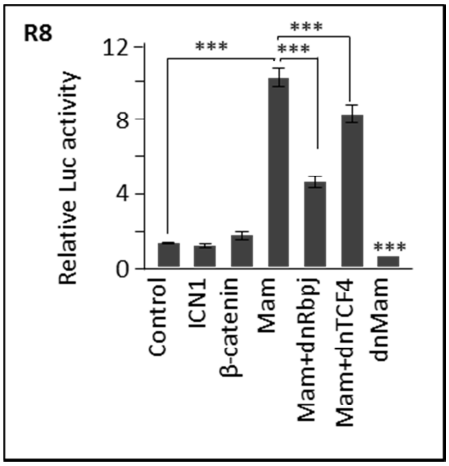

FIGURE R8 | Activating the *Bmi1* promoter with Mam. ***Bmi1*** promoter activity assay with the indicated constructs (see MM18). ICN1 and β-cat alone are unable to activate *Bmi1* promoter activity, Maml seems to be a limiting factor. Error bars represent the standard deviation and statistical significance was determined using Student's t-test. *P<0.05, **P<0.01 and ***P<0.001.

On the other hand, even taking into consideration the fact that Mam could be a limiting factor, the inability to further activate the promoter by ectopic expression of ICN1 and β-catenin still struck us as odd. Transcriptional repression through the specific Notch target Hes1 protein is a widely used mechanism for attenuating Notch-dependent transcription (Krejcí et al. 2009). Indeed, we found several HES consensus binding sites near the TSS in the *Bmi1* promoter [FIGURE R6], and we functionally tested them in the reporter activity assays. Ectopic Hes1 expression totally abolished *Bmi1* promoter driven transcription, whereas knockdown of *Hes1* by shRNA not only increased *Bmi1* promoter reporter activity, but also facilitated its activation by ICN1, β-catenin and Mam [FIGURE R9].

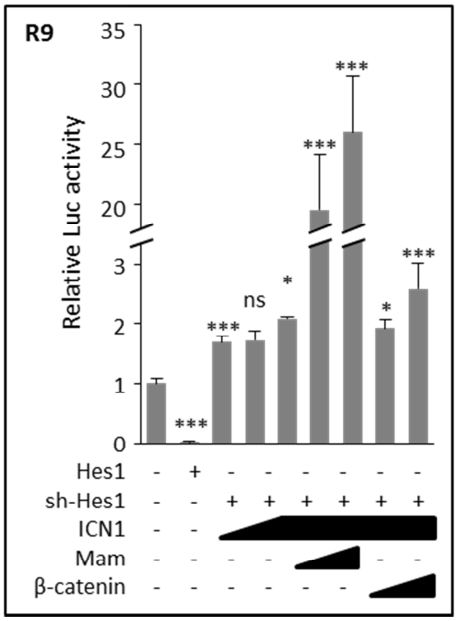

FIGURE R9 | Activating the *Bmi1* promoter after silencing *Hes1*. ***Bmi1*** promoter activity assay with the indicated constructs (See MM18). Increasing concentrations of ICN1, Mam and β-catenin were transfected. Error bars represent the standard deviation and statistical significance was determined using Student's t-test. *P<0.05, **P<0.01 and ***P<0.001.

Taking these results together, we propose a model of **cooperative regulation of *Bmi1* transcription positively regulated by ICN1, β-catenin and Mam, where Hes1 comes into play to repress and fine-tune *Bmi1* levels in response to Notch and Wnt pathway activation**, as reported in other incoherent feed-forward loop systems [FIGURE R10].

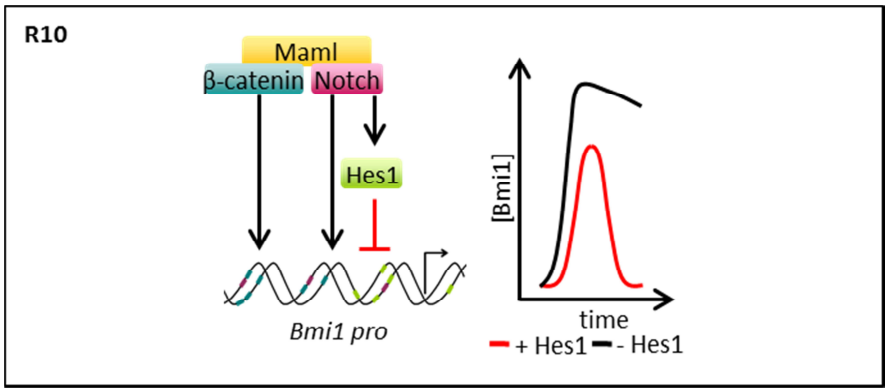

FIGURE R10 | Molecular model of the regulation of the *Bmi1* promoter by Notch, β-catenin and Hes1 (I1-FFL). The graph shows the hypothetical *Bmi1* expression levels in the presence (red) or absence (black) of Hes1, when both the Notch and Wnt-β-catenin pathways are active.

Bmi1 *deficient mice display intestinal defects that resemble a Notch LOF phenotype*

Bmi1 deficient mice are born at Mendelian ratios but die prematurely (around 2-3 months of age) presenting growth retardation and stem cell associated defects (see INTRODUCTION). Thanks to a collaboration established with Dr. Pura Muñoz-Cánoves, we analysed the intestine of the total *Bmi1* KO mice at 2-3 months of age, before they presented neurological symptoms indicative of an imminent death. We found that the small intestine was significantly shortened compared to wildtype littermates (35.88±2.3cm in the WT and 28.33±2.5 cm in the KO, p<0.001) [FIGURE R11].

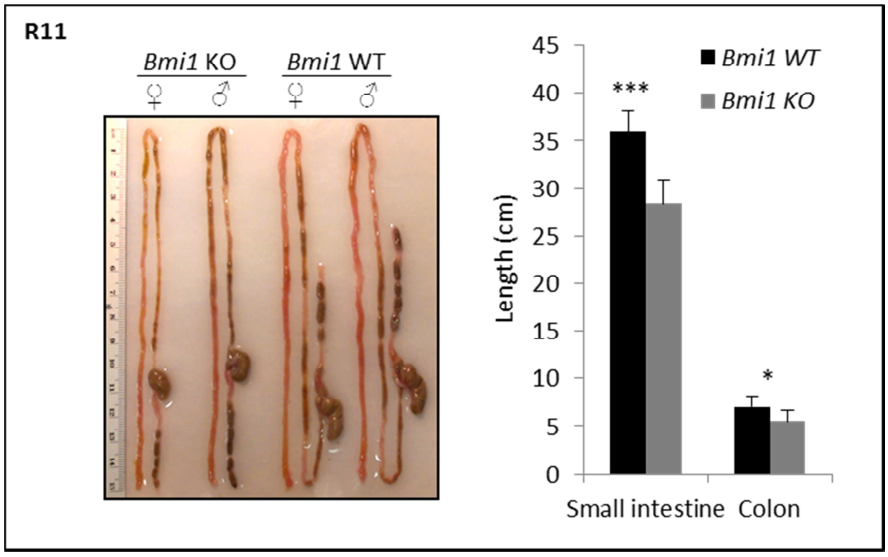

FIGURE R11 | Macroscopic analysis of the *Bmi1 KO* intestines. On the left, photographs of intestines from 2-month-old mice of the indicated phenotypes and sex. On the right, length in centimetres of the indicated regions and genotypes. Bars indicate average length, error bars standard deviation, and statistical significance was assessed using the Student's T test. *P<0.05, **P<0.01 and ***P<0.001.

A similar (although milder) defect was found in the colon (7.05±1.0cm in the WT and 5.5±1.2cm in the KO, p=0.04) [FIGURE R11].

At the moment of doing this experiments, we thought that Bmi1 was not expressed in the colon, but the development of better antibodies for its detection by IHC allowed us (and others, see INTRODUCTION) to confirm that Bmi1 was indeed also expressed in colonic epithelial intestinal cells [FIGURE R12].

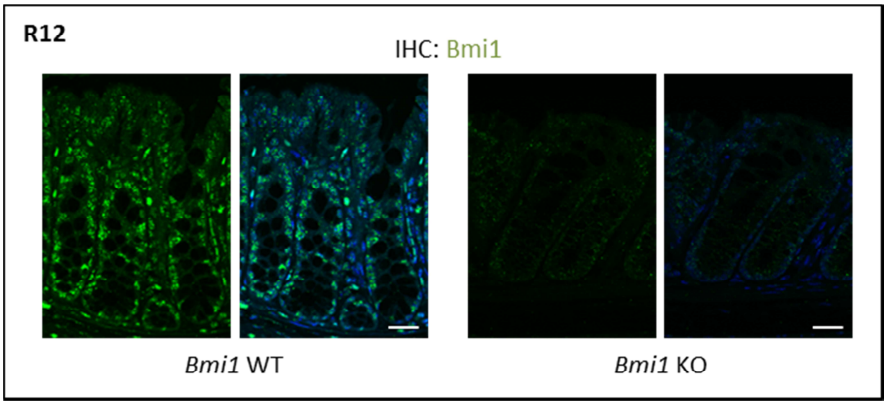

FIGURE R12 | Bmi1 staining in the colon. Confocal images of intestinal sections stained for Bmi1 (green) of the indicated genotypes. Nuclei were counterstained with DAPI (shown in blue, right picture for each genotype). Scale bar equals 25µm.

Interestingly, not only were intestines overall shorter along the anterior-posterior axis, which could be due to systemic effects (see DISCUSSION), but when we measured the crypt-villus axis it was also shortened in the *Bmi1* KO mice, compared to wildtype littermates; that is, they were also thinner [FIGURE R13].

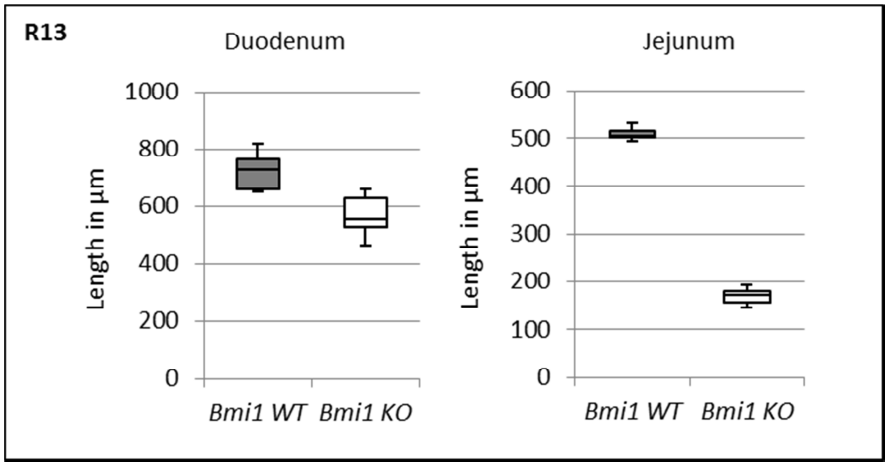

FIGURE R13 | Measurement of the crypt-villus axis. Box plots depicting differences in the crypt-villus axis length between the wildtype and the mutant genotypes.

Next, we explored the proliferative status of the intestinal epithelium. As described above, we first performed a Ki67/Alcian blue staining, to visualize proliferating cells together with post-mitotic goblet cells [FIGURE R14]. We observed a reduction in cycling Ki67^{+} cells in both the small intestine and the colon of *Bmi1* KO animals, when compared to their wildtype littermates. This reduction was statistically significant, as indicated by the quantification graphs on FIGURE R15, and comparable to the reduction observed in the mutants where RBP, was specifically deleted in the intestinal epithelium [for an image, refer to FIGURE R1]. We also observed a moderate but still significant increase in the number of goblet cells, **partially resembling the RBP deficient phenotype (Notch LOF)**.

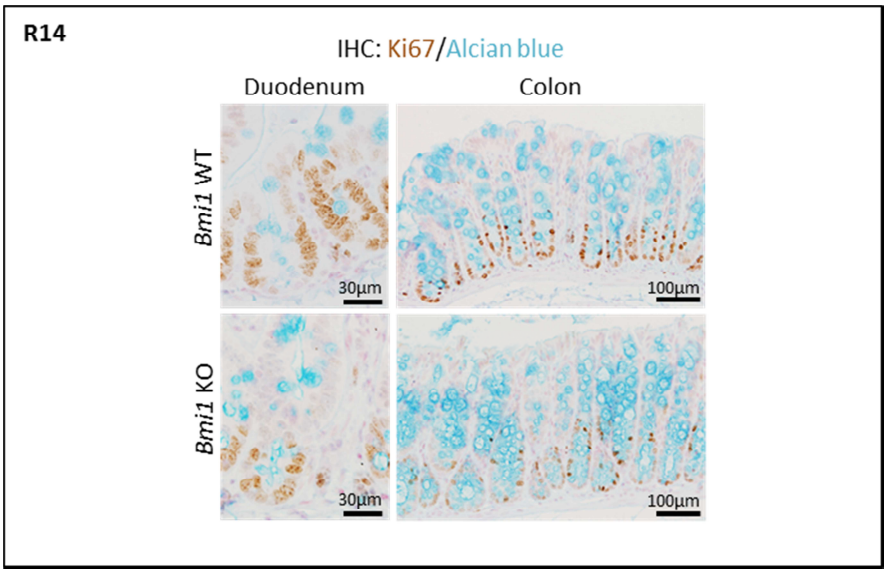

FIGURE R14 | Ki67/alcian blue staining. IHC-P against Ki67 was performed in paraffin sections of intestines of the indicated genotypes followed by staining with Alcian blue to identify goblet cells. Nuclei were counterstained with Nuclear Fast Red.

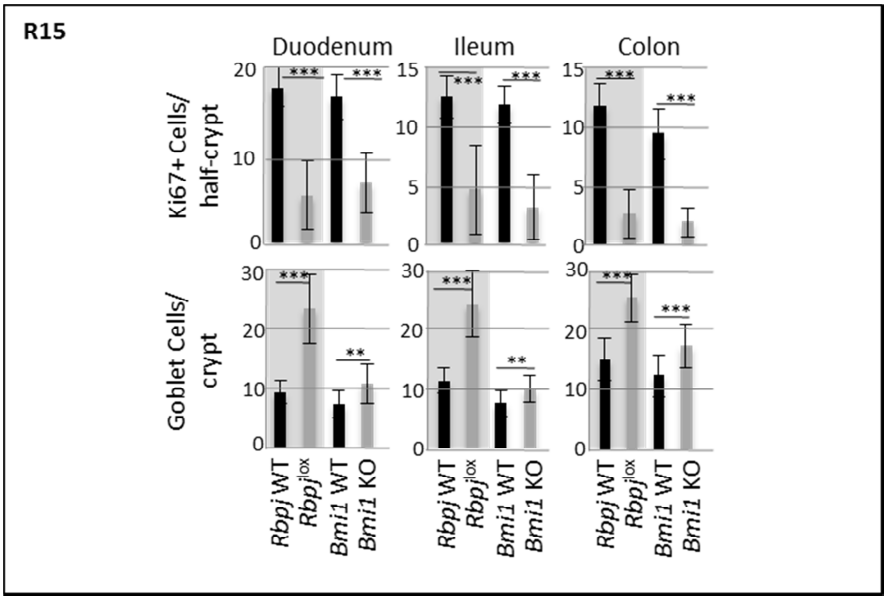

FIGURE R15 | Ki67/alcian blue staining: quantification graphs. From *Bmi1* KO intestinal sections. RBP KO quantifications are also included for comparison (see pictures in FIGURE R3). Columns represent the average quantification of >30 crypts of at least 2 samples for each indicated genotype and error bars represent the standard deviation. Statistical significance was assessed using the Student's T Test. *P<0.05, **P<0.01 and ***P<0.001.

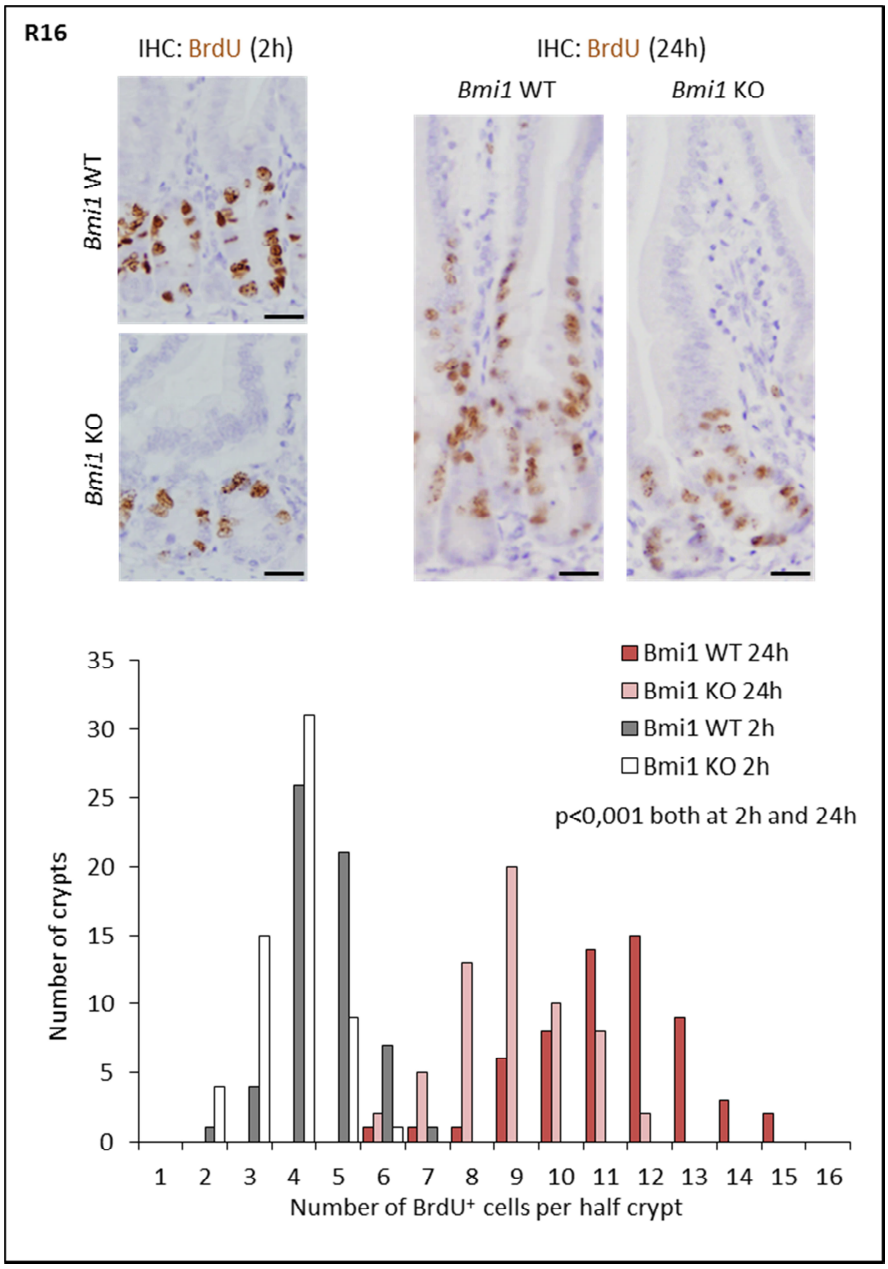

FIGURE R16 | BrdU staining 2h vs. 24h chase. Mice were injected with a single pulse of BrdU and intestines were embedded in paraffin for histological analysis. Upper panels show representative micrographs of BrdU staining at the indicated time points. Scale bar corresponds to 25µm. Lower graph shows distribution of $BrdU^+$ cell number per half crypt. In each case, more than 60 crypts were counted.

The proliferation status was also assessed by a bromodeoxyuridine (BrdU) incorporation assay. BrdU staining corroborated that **Bmi1-deficient intestinal epithelial cells are significantly less proliferative than their wildtype counterparts**, and most likely show a delay in their migration capacity [see FIGURE R16, 24h after BrdU injection].

To further explore which compartments are specifically affected by *Bmi1* deficiency, we performed a double staining of BrdU (IHC) and *Olfm4* (ISH) in the intestines collected 2h after the BrdU pulse. This staining proved that **defects in proliferation affected both the ISC** (3.1±2.2 BrdU and Olfm4 double positive cells in the WT compared with 1.0±1.6 in the KO; P<0.001) **and, to a minor extent, the transit-amplifying compartment** (6.9±3.4 BrdU-positive cells in the WT compared with 6.3±3.6 in the KO, P=0.17) [FIGURE R17].

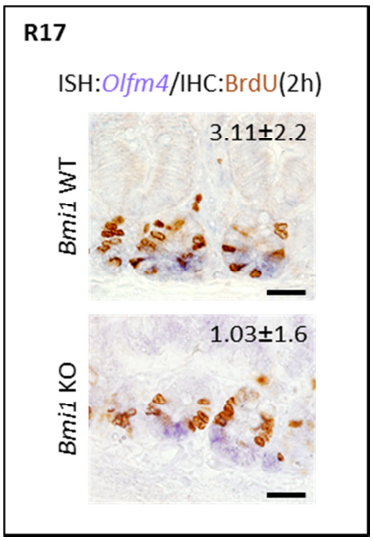

FIGURE R17 | Double staining of BrdU (IHC) and *Olfm4* (ISH). Mice were injected with a single pulse of BrdU and intestines were embedded in paraffin for histological analysis. First, the ISH against *Olfm4* was performed, then the IHC-P staining for BrdU (See MM7 and 8), nuclei were not counterstained. Numbers indicate average and standard deviation of double BrdU/Olfm4 positive cells per crypt. 30 crypts were counted per each genotype (n=2). Scale bar equals 30µm. This experiment was performed in collaboration with Dr. Jordi Guiu.

We obtained similar results when we analysed the cell cycle profile of intestinal crypt populations classified according to the surface marker EphB2. ISCs were included in the EphB2^{High} population and most of the TA cells were included in the EphB2^{Medium} population (Jung et al. 2011).We observed a **decrease in actively cycling ISCs** (33.3% in the WT EphB2^{High} cells in S/G2/M compared to 16.2% in the KO) while TA cells remained unchanged (25.9% in the WT EphB2^{Medium} cells in S/G2/M compared to 27.4% in the KO) [FIGURE R28].

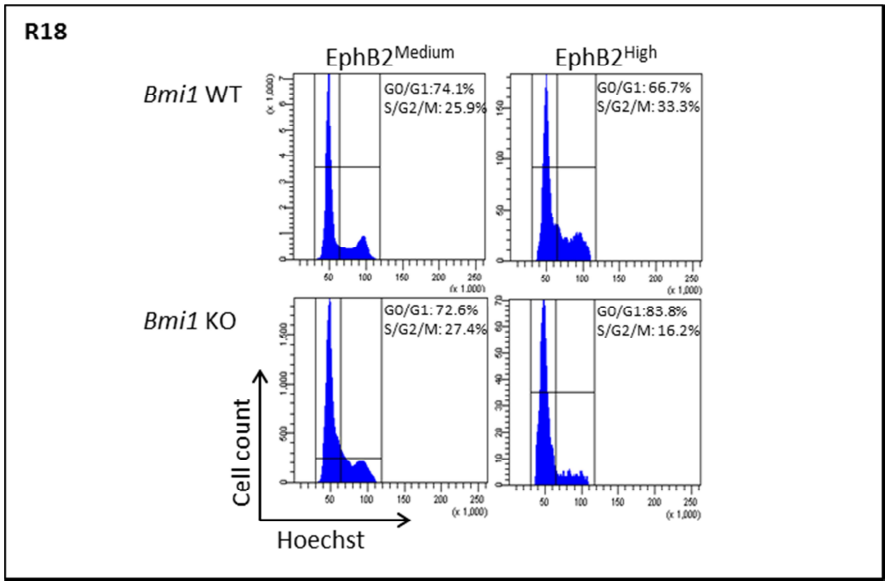

FIGURE R18 | Cell cycle profile of EphB2 medium and high populations. Staining and cell cycle analysis was performed in cells from freshly isolated crypts (See MM19). EphB2^{hi} includes post-mitotic Paneth cells and ISCs, EphB2^{med} includes most of the TA cells. A representative experiment of two is shown. This was performed in collaboration with Dr. Jordi Guiu.

The defects observed in the *Bmi1* KO adult intestines were already appreciable at the time of birth, both macroscopically [FIGURE R19] and at the level of proliferation [FIGURE R20]. Ki67 staining of paraffin sections of **post-natal *Bmi1* KO intestines showed a decrease in proliferating cells** at the intervillous regions [see FIGURE R20][17].

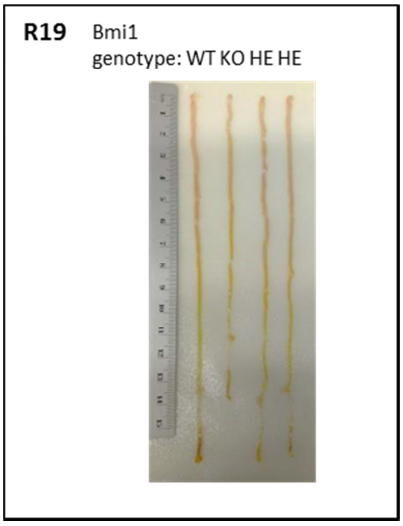

FIGURE R19 | Photograph of P3 *Bmi1* KO intestines. Defects in total intestinal length are observed at the time of birth (postnatal day 3) already in the Bmi1-deficient mice.

[17] Even after birth, proper crypts are still not observed, since intestinal epithelium maturation takes two more weeks post-natally. Passing of food (milk) plays an essential role in this maturation process.

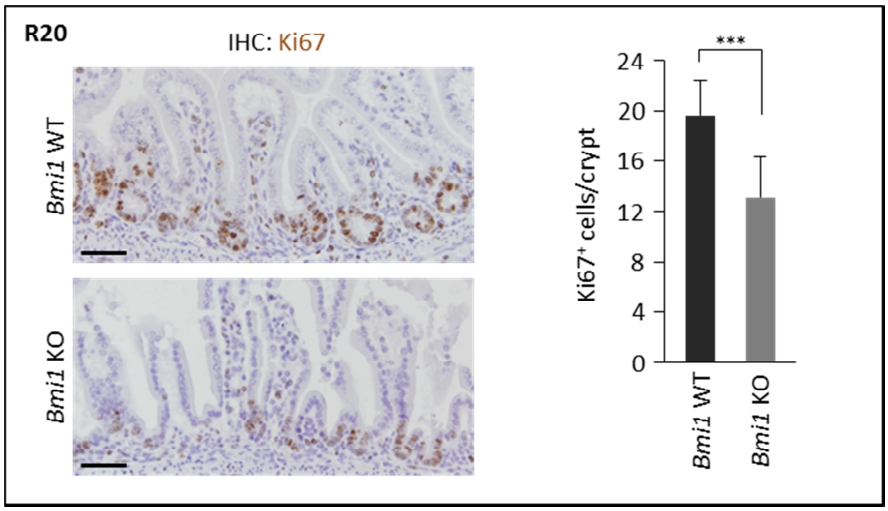

FIGURE R20 | Ki67 staining and quantification graph pf P3 *Bmi1* KO intestines. IHC-P against Ki67 was performed in paraffin sections of intestines of the indicated genotypes. Nuclei were counterstained with haematoxylin. Scale bar equals 50µm. In the graphs, columns represent the average quantification of >30 crypts of at least 2 samples for each indicated genotype and error bars represent the standard deviation. Statistical significance was assessed using the Student's T Test. *P<0.05, **P<0.01 and ***P<0.001.

Interestingly, this defect in proliferation capacity of the *Bmi1* KO intestinal epithelium was also observed as early as 15.5 days post-coitum in the developing embryos, which coincides with the onset of villogenesis, and was even more notable 24h later in development, at stage E16.5 [FIGURE R21].

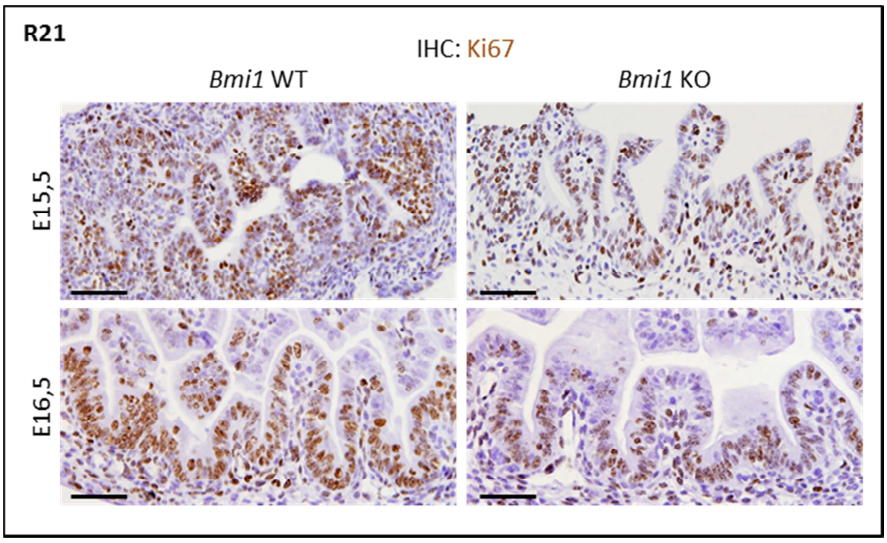

FIGURE R21 | Ki67 staining of E15,5 and E16,5 *Bmi1* KO intestines. IHC against Ki67 was performed in paraffin sections of intestines of the indicated genotypes and developmental stages. Nuclei were counterstained with haematoxylin. Scale bar equals 50µm.

Surprisingly, however, even though *Bmi1*-deficient ISCs show an impaired proliferation, they are still present and express normal levels of most ISC markers. An ISH for *Lgr5* or *Olfm4* showed no differences in their expression level or pattern between *Bmi1* KO and WT intestines [FIGURE R22]. *Lgr5* mRNA levels were also unchanged when tested by qRT-PCR in crypt-enriched fractions [FIGURE R23]. Other relevant double Notch/Wnt targets (*c-Myc* and *EphB2*) were similarly expressed in *Bmi1* KO and WT crypts, as were quiescent ISC markers *Hopx* and *Lrig1*. We only found a **decrease in *mTert* expression levels in *Bmi1* KO intestinal crypts**, compared to the WT. This, at least, hinted a possible functional defect of *Bmi1* KO ISCs, in addition to their proliferative disadvantage.

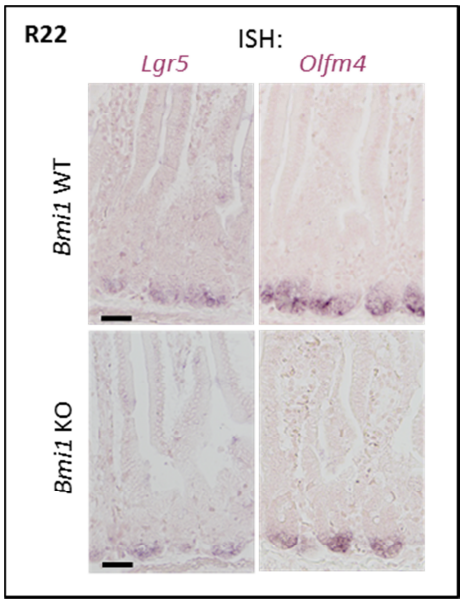

FIGURE R22 | ISH of *Lgr5* and *Olfm4* in *Bmi1* KO adult intestines. ISH against *Lgr5* and *Olfm4* was performed in paraffin sections of intestines of the indicated genotypes. Scale bar equals 25µm. This experiment was performed in collaboration with Dr. Jordi Guiu.

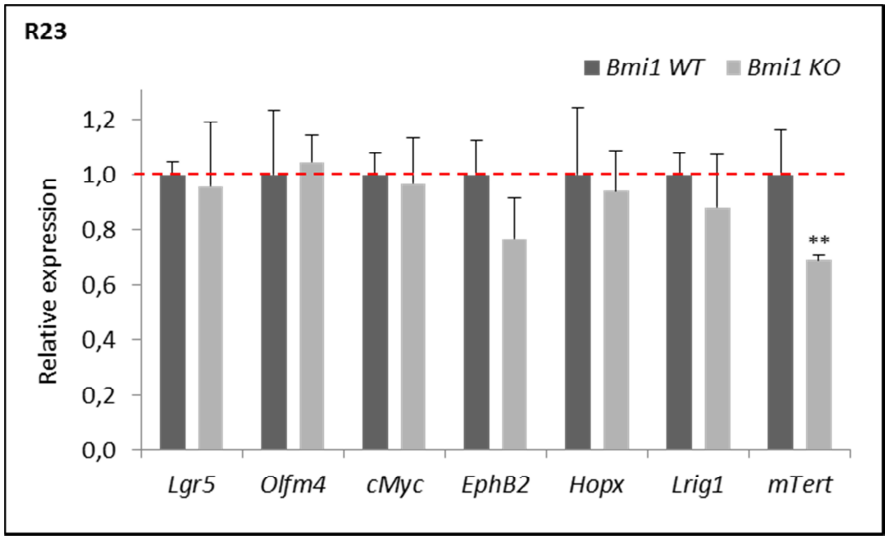

FIGURE R23 | Expression analysis of ISC markers in *Bmi1* KO crypt fractions. RNA was extracted from freshly isolated crypts of the indicated genotypes (2 mice per genotype). Quantification was done by qRT-PCR. Expression relative to *Gapdh* is graphed. Columns indicate the average quantification and error bars represent the standard deviation. Statistical significance was assessed using the Student's T Test. *P<0.05, **P<0.01 and ***P<0.001.

Next, we sought possible downstream effectors of Bmi1 that could in part explain functionally the defects seen in *Bmi1*-deficient ISCs. The first thing we looked at was the classical *Cdkn2a* locus, which is kept silenced when Bmi1 is present and represses transcription of $p16^{INK4a}$ and the alternative reading frame product $p19^{ARF}$. As we expected, $p16^{INK4a}$ protein was greatly accumulated in the crypts of *Bmi1* KO mice [FIGURE R24, left panel; see FIGURE R30 for quantification]. When tested at the mRNA level, both transcriptional products of the locus were vastly upregulated in the *Bmi1* KO crypts [FIGURE R24, right panel].

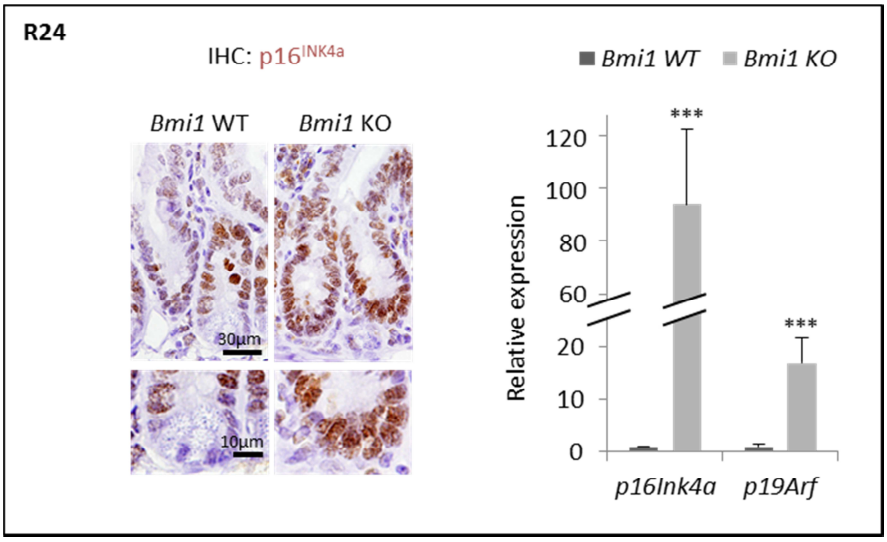

FIGURE R24 | $p16^{INK4a}$ staining and expression analysis of ISC $p16^{INK4a}$ and $p19^{ARF}$ in *Bmi1* KO samples. Left panel shows $p16^{INK4a}$ expression in the crypt region of intestinal paraffin sections of the indicated genotypes. Lower photographs show a magnification of the bottom crypt area. Right panel shows $p16^{INK4a}$ and $p19^{ARF}$ mRNA levels relative to *Gapdh* in freshly isolated crypt enriched fractions of the indicated genotypes. Columns indicate average of two animals from each genotype, and error bars indicate standard deviation. Statistical significance was assessed using the Student's T test. *P<0.05, **P<0.01 and ***P<0.001.

We also confirmed that in the Notch OFF genotype where Bmi1 expression is lost due to the absence of Notch signalling and in the composite Notch OFF / Wnt ON genotype, where Bmi1 expression is not rescued, $p16^{INK4a}$ protein was also accumulated in the intestinal crypts

[FIGURE R25], almost to the same extent as in the *Bmi1* KO intestines [FIGURE R26].

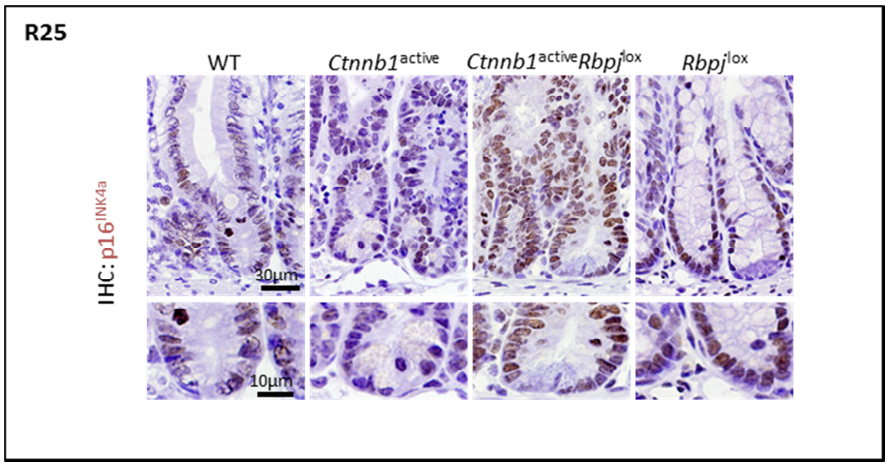

FIGURE R25 | p16^{INK4a} staining. IHC staining against p16^{INK4a} was performed in paraffin sections of intestines of the indicated genotypes. Lower photographs show a magnification of the bottom crypt area.

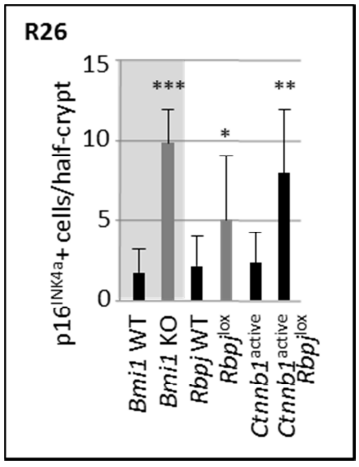

FIGURE R26 | Quantification graphs for p16^{INK4a} IHC-P. Representative images are shown in FIGURES R24 and R25. Columns represent the average quantification of >30 crypts of at least 2 samples for each indicated genotype and error bars represent the standard deviation. Statistical significance was assessed using the Student's T Test. *P<0.05, **P<0.01 and ***P<0.001.

In parallel to the proliferation defect that is detectable already during embryogenesis, p16^{INK4a} accumulation was also prominent in *Bmi1* KO foetal intestines at developmental stage E15.5 [FIGURE R27], at the onset of villogenesis. An additional control of Bmi1 expression by IHC (and lack thereof in the KO animals) was included in this experiment.

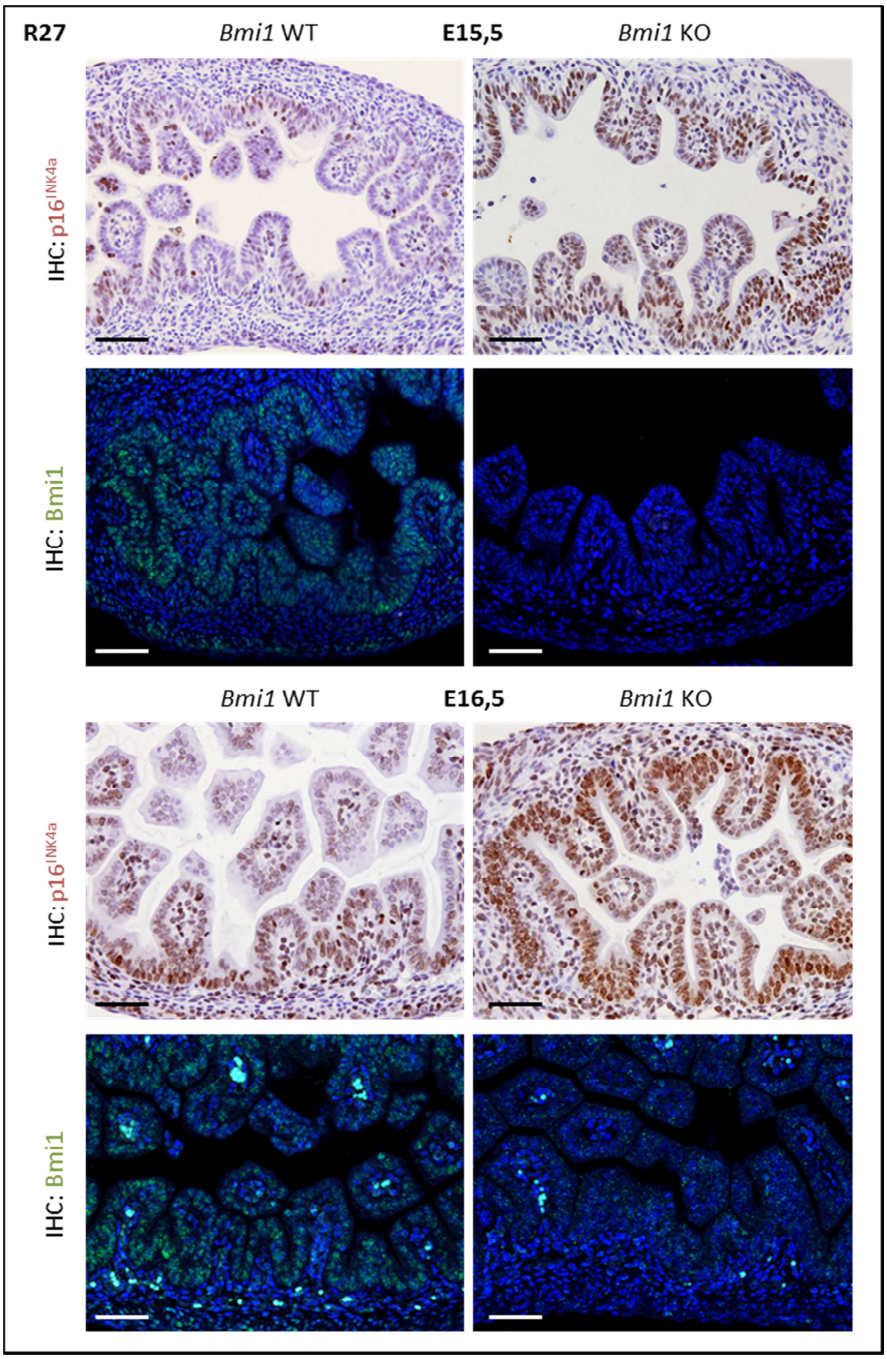

FIGURE R27 | p16^{INK4a} and Bmi1 staining. IHC staining against p16^{INK4a} and Bmi1 was performed in paraffin sections of foetal intestines of the indicated genotypes at the indicated developmental time. Scale bars equal 50µm.

These results together reveal that **the *Cdkn2a* locus is remarkably de-repressed in the absence of Bmi1**, leading to accumulation of *p16*^{INK4a} and *p19*^{ARF}.

Because Bmi1 is involved in the regulation of stem cell compartments in other tissues, we considered the possibility that the intestinal defects observed in the total *Bmi1* KO could be systemic instead of tissue-autonomous. To test this, we generated a *Villin*-Cre;*Bmi1*$^{lox/lox}$ mouse line in which the Bmi1 gene was specifically deleted in the intestinal epithelium. IHC analysis of 3- to 4-week-old intestinal specific *Bmi1* deficient mice revealed a significant accumulation of p16^{INK4a} along the crypt-villus axis, associated with a reduction in the number of proliferating Ki67-positive cells [FIGURE R28].

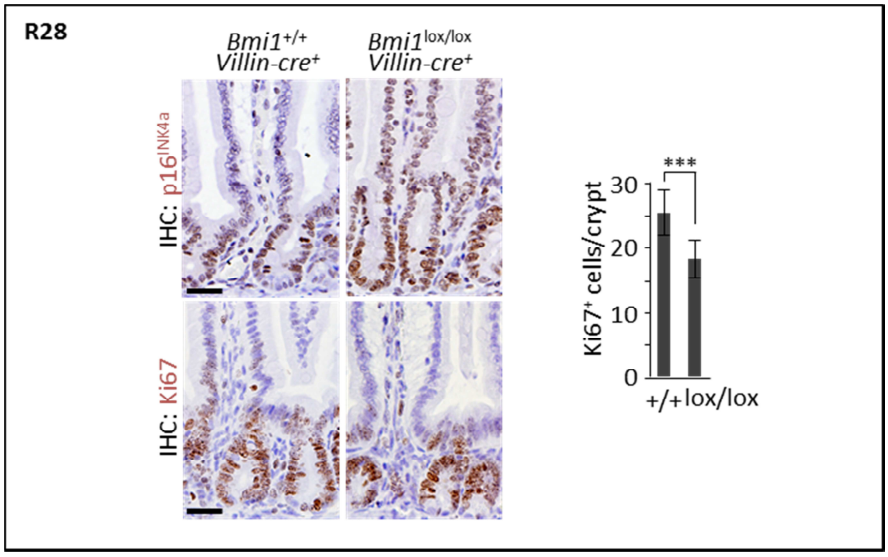

FIGURE R28 | p16^{INK4a} and Ki67 staining and quantification graph. IHC staining against p16^{INK4a} and Ki67 was performed in paraffin sections of intestines of the indicated genotypes. Scale bar equals 30µm. Right panel shows quantification graph where columns represent the average quantification of >30 crypts of at least 2 samples for each indicated genotype and error bars represent the standard deviation. Statistical significance was assessed using the Student's T Test. *P<0.05, **P<0.01 and ***P<0.001.

The Bmi1-*deficient phenotype mimics that of Notch inhibition with respect to the self-renewal and DNA repair capacity of ISCs*

We then used an *in vitro* culture system that allows ISCs to grow in 3D structures as organoids, resembling the crypt-villus organization of the intestinal epithelium (Sato et al. 2009). Isolated crypts can be cultured in an extracellular matrix-based hydrogel (Matrigel®), which facilitates anchorage-independent growth into 3D structures, in a serum-free medium, which enriches for stem cells and prevents differentiation. The serum-free medium is complemented with growth factors (EGF and basic FGF), the BMP inhibitor Noggin, the Wnt agonist R-Spondin1 and the ROCK inhibitor Y-27632, to prevent anoikis[18], among other supplements (to see a detailed composition of the medium see MATERIALS and METHODS). Moreover, this culture system allows for serial passage and indefinite maintenance of ISC-derived intestinal organoids.

We found that serially replated wildtype organoids (after the 10th passage) contain a high number of Bmi1-expressing cells [**FIGURE R29**, upper panel], which seem to be decreased upon Notch inhibition by DAPT treatment [**FIGURE R29**, lower panel]. This decrease in Bmi1-expressing cells occurred before the failure of organoid growth that follows 3-4 days after DAPT treatment [**FIGURE R30**]. Bmi1 mRNA levels dropped already 48h after DAPT treatment [**FIGURE R31**], but the fact that the protein is still detectable 72h after treatment may be due to its stability.

[18] From the Ancient Greek word ἄνοικος (ánoikos), which means "without a home". It is actually a pseudo-Greek coinage intended to have the sense of "homelessness", by ἀν- "without", οἰκ- "house", and -ις (extracted from -σις "trait, attribute". Anoikis is a form of programmed cell death induced by lack of correct cell or extracellular matrix attachment.

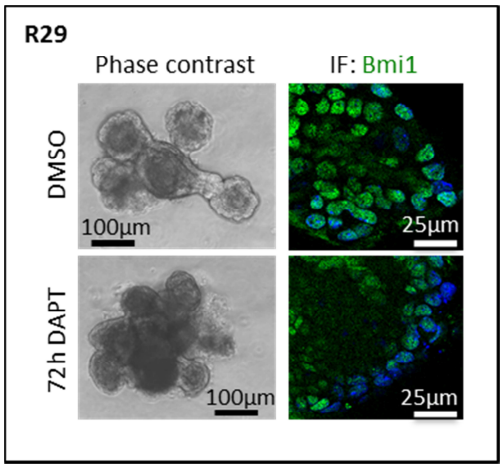

FIGURE R29 | Bmi1 IF in organoids treated with DAPT. Micrographs showing intestinal organoids 72h after vehicle (DMSO) or 50µM DAPT treatment. Right panels show IF staining of Bmi1, note the decreased number of Bmi1^{+} cells.

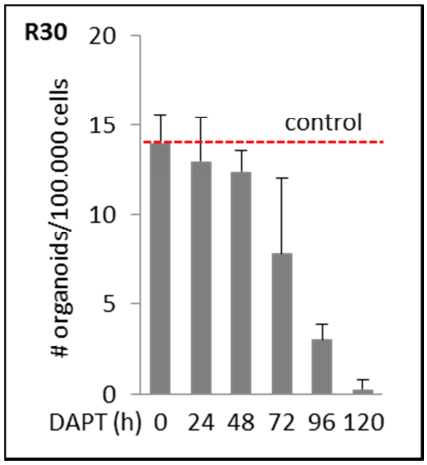

FIGURE R30 | Number of organoids treated with DAPT. Number of organoids in DAPT-treatment vs. vehicle treated conditions decreases over time. The concentration of DAPT was 50µM. Columns represent average of two independent experiments and error bars the standard deviation.

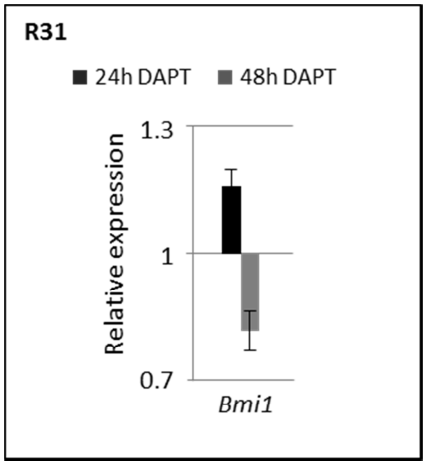

FIGURE R31 | *Bmi1* qRT-PCR in organoids treated with DAPT. 50µM DAPT treatment decreases Bmi1 transcript levels at 48h. RNA was extracted from DAPT- and vehicle-treated organoids at different times of treatment. Quantification was done by qRT-PCR. Expression relative to housekeeping average (*Gapdh* and β*2m*) is represented. Columns indicate the average quantification and error bars represent the standard deviation.

When we checked transcriptional changes after DAPT treatment, we found that there is an increase in *p16*^{INK4a} and *p19*^{ARF} levels [FIGURE R32], concomitant with the decrease in *Bmi1* mRNA levels [See FIGURE R31]. Interestingly, as early as 12h after initiation of Notch inhibition, the levels of a classical Notch target gene, *Hes1*, drop drastically [FIGURE R32]. Furthermore, the levels of expression of the stem cell markers *Ascl2* and *Olfm4* also sink 12h after DAPT treatment, suggesting a stem-cell failure [FIGURE R32].

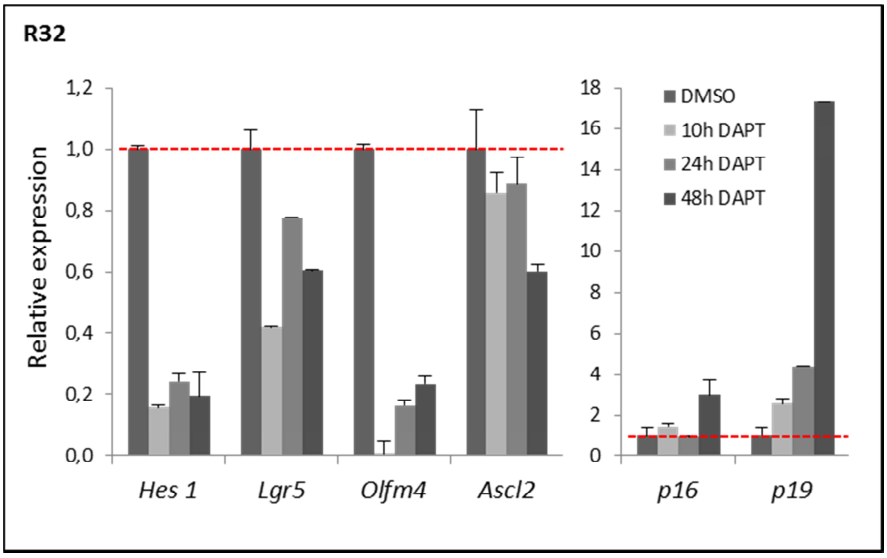

FIGURE R32 | qRT-PCR in organoids treated with DAPT. 50µM DAPT treatment decreases Notch target Hes1 transcript levels as well as stem cell marker levels. Bmi1-targets *p16*^{INK4a} and *p19*^{ARF} are de-repressed in the presence of the Notch inhibitor DAPT. RNA was extracted from DAPT- and vehicle-treated organoids at different times of treatment. Quantification was done by qRT-PCR. Expression relative to housekeeping average (*Gapdh* and β*2m*) is represented. Columns indicate the average quantification (vehicle-treated condition is normalised to 1, indicated by the dashed red line) and error bars represent the standard deviation.

These results highlight the **requirement of Notch signalling for the *in vitro* culture of intestinal organoids**, and suggest that some of the defects can be due to the decrease in Bmi1 levels upon Notch inhibition.

We subsequently tried to culture *Bmi1*-deficient intestinal crypts as organoids, and were surprised to find that they were able to do so, despite the defects that they displayed *in vivo* (reduced proliferation and accumulation of $p16^{INK4a}$ and $p19^{ARF}$). However, since conventional *Bmi1* KO animals live well until around 2 months of age, it is clear that they maintain a certain intestinal epithelial renewal capacity. Hence, we speculated whether we needed to force the system to discover the extent of Bmi1-dependence for ISCs.

When we tested the long-term replating ability of the organoids, even though at early passages *Bmi1* KO organoids divided with a similar ratio to WT counterparts, their replating ability started declining after the 7^{th} passage and they failed to survive longer than passage 15-16 [**FIGURES R33 and S3**]. This was indicative of a **defective long-term self-renewal capacity**. While FIGURE 33 shows the cumulative number of organoids along the culture passages, FIGURE S3 depicts the ratio between the average numbers of *Bmi1* KO organoids relative to the WT organoids obtained at every passage.

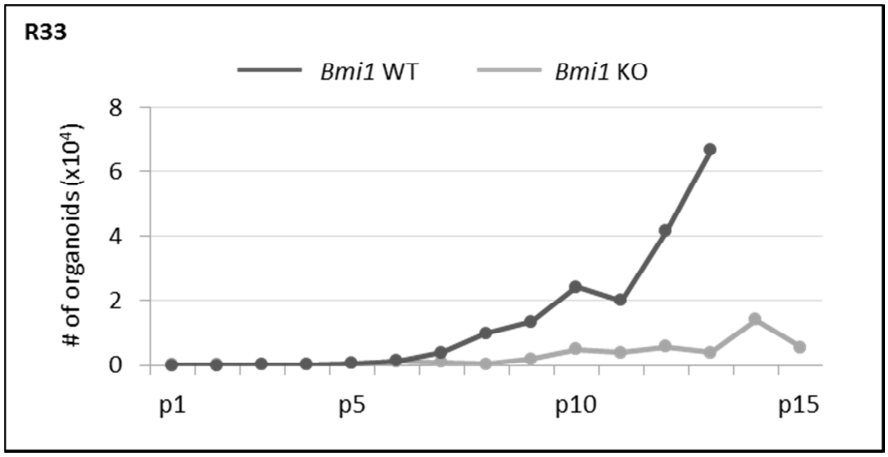

FIGURE R33 | *Bmi1* WT and KO organoid growth curve along culture passages. The cumulative number of organoids obtained from WT and Bmi1-deficient crypt cells after passage is plotted.

To uncover the cause of *Bmi1* KO organoid failure at long-term replating, we performed a Terminal deoxynucleotidyl transferase (TdT) dUTP Nick-End Labeling (TUNEL) assay along with a staining for active (cleaved) caspase 3 at passage 14. We discovered that *Bmi1* KO organoids accumulated TUNEL-positive cells in what still seemed their intact monolayer of epithelial cells, that were mostly negative for active (cleaved) caspase 3 [FIGURE R34]. Note that cells that are dying by apoptosis both in the WT and *Bmi1* KO organoids are double positive for TUNEL staining and active (cleaved) caspase 3 and being released to the lumen of the 3D structure. This result suggested that ***Bmi1* KO organoids accumulated DNA breaks independently of an apoptotic program**.

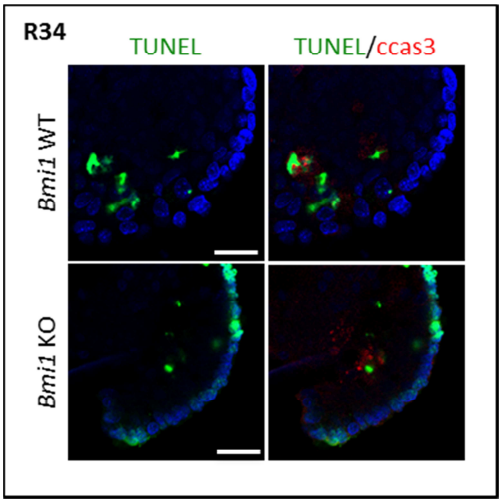

FIGURE R34 | TUNEL/ccas3 in p14 *Bmi1* KO organoids. Double TUNEL/ccas3 staining was performed in WT and Bmi1-deficient organoids (See MM12) of late passages (p14). Scale bar equals 25µm. $TUNEL^{+}/ccas3^{+}$ cells secreted to the lumen of the organoids are normal occurring apoptotic cells. Note the $TUNEL^{+}/ccas3^{-}$ cells that have accumulated DNA damage in the seemingly intact epithelium of the *Bmi1* KO organoids.

Accumulation of DNA breaks could result from a defective DNA damage repair. To test this possibility, first we explored what was the DNA damage status under basal conditions. We did so by performing an IHC against phosphorylated histone H2A.X (ɣH2A.X). Following DNA double strand breaks (DSBs), kinases from the PI3K pathway ataxia telangiectasia mutated (ATM) and ATM-Rad3-related (ATR) phosphorylate H2A.X on Serine 139[19]. Phosphorylated H2A.X is known as ɣH2A.X. A single DSB can

[19] ATM seems to predominantly phosphorylate H2A.X in response to ionizing radiation (Burma et al. 2001) while ATR is related to defects in DNA replication (at the sites of stalled replication forks and replication blocks) (Ward & Chen 2001).

induce phosphorylation of many H2A.X molecules in the surrounding nucleosomes, hence giving rise to discrete γH2A.X foci at the damage site, hallmark of the very early steps of the cellular response to DSBs (Rogakou et al. 1999).

Under basal conditions, there are several cells in the crypts with γH2A.X foci, but these mostly disappear in the differentiated cells along the villus, indicating that the DSB has been successfully repaired [FIGURE R35]. PP2A is the phosphatase responsible of de-phosphorylating γH2A.X after the DNA damage has been resolved (Chowdhury et al. 2005). In the *Bmi1* KO or intestinal-epithelial *Rbpj* KO, however, some cells seem to accumulate γH2A.X to the point where the entire nucleus is stained [FIGURE R35]. This implies that **in the absence of Bmi1 or Notch signalling the DNA damage cannot be successfully repaired**.

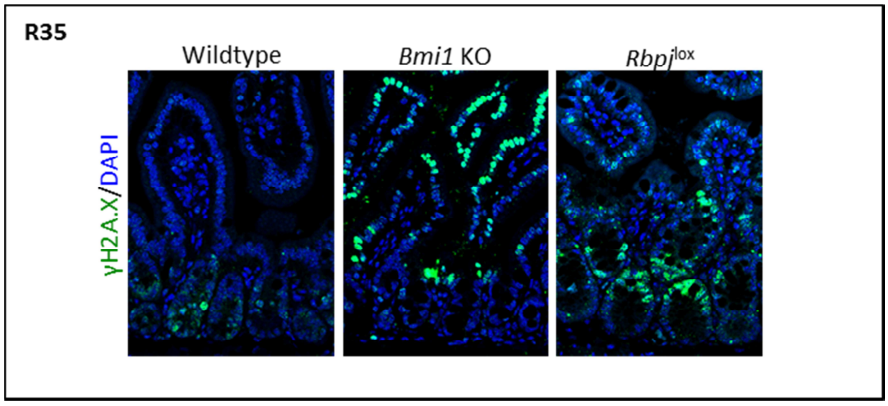

FIGURE R35 | γH2A.X IHC-P in *Bmi1* KO and *RBP* KO. IHC-P staining against γH2A.X was performed in paraffin sections of intestines of the indicated genotypes. Scale bar equals 50µm.

We then determined the DNA repair capacity of *Bmi1*-deficient intestinal cells in response to ɣ-radiation *in vivo*. We irradiated the whole body of *Bmi1* WT or KO littermates with 12 Gy (which is a lethal irradiation) and killed the mice to collect the intestines and process for IHC 2 hours later. By staining for ɣH2A.X we found that the WT intestines greatly accumulated ɣH2A.X in the villus region, indicating unrepaired DNA breaks. However, intestinal crypt cells only showed discrete ɣH2A.X foci (as shown before in FIGURE R40 under basal conditions) as a result of efficient DNA repair, as had been previously reported (Hua et al. 2012). In contrast, *Bmi1*-deficient intestines displayed an intense homogeneous ɣH2A.X staining pattern arising from the base of the crypts to the top of the villi [FIGURE R36]. This evidences that **Bmi1 is involved in regulating DNA damage repair in intestinal crypt cells *in vivo***, which is consistent with the known role of Bmi1 in DNA damage repair through H2A monoubiquitylation (See INTRODUCTION).

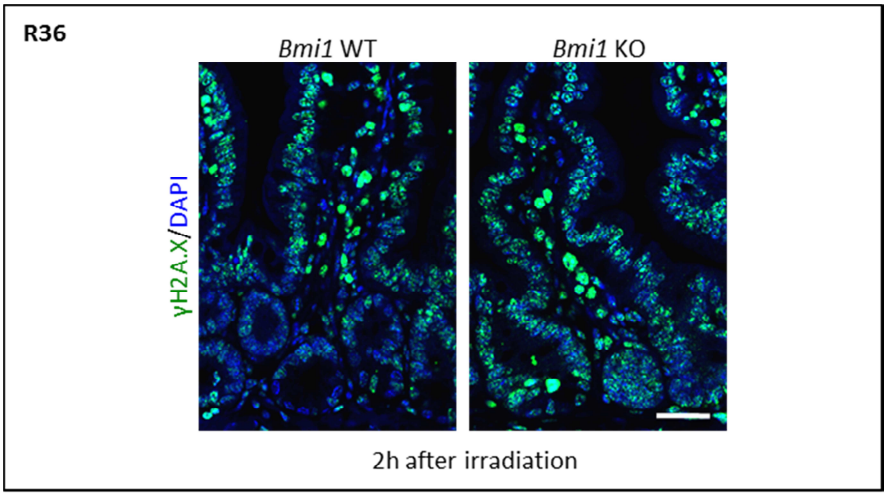

FIGURE R36 | ɣH2A.X IHC-P 2h after irradiation. IHC-P staining against γH2A.X was performed in paraffin sections of intestines collected 2h after whole-body irradiation (12Gy) of animals of the indicated genotypes. Scale bar equals 50µm.

We confirmed the requirement of Bmi1 for efficient DNA damage repair in ISCs *in vitro* by using the organoid culture system. When we irradiated pre-formed organoids with 2 Gy and studied recovery at 2 or 5 hours post-irradiation, we found that WT organoids displayed abundant γH2A.X foci 2 hours after irradiation that were completely resolved 5 hours after irradiation. *Bmi1*-deficient organoids, instead, displayed nuclei full of γH2A.X even 5 hours after irradiation [FIGURE R37, left panels]. Interestingly, the success of the DNA damage repair was assessed functionally by measuring the resistance of the organoids to the irradiation [FIGURE R37, right panel]. *Bmi1*-deficient organoids were sensitive to ionizing radiations as low as 0.5 Gy, where only half of them were able to survive. These results demonstrate that **Bmi1 is also necessary for proper DNA damage repair in ISCs *in vitro***.

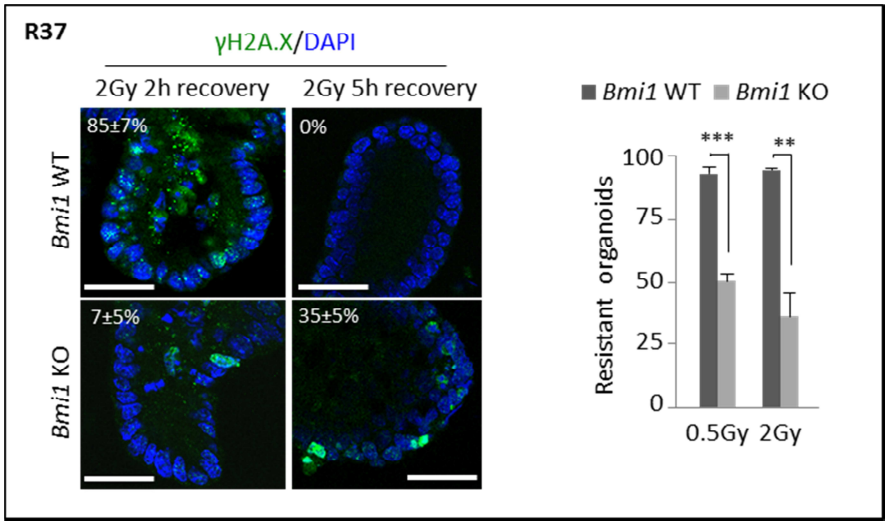

FIGURE R37 | γH2A.X IF and *Bmi1* KO organoid failure upon irradiation. Organoids were irradiated at 0.5 or 2.0 Gy and 2h or 5h after they were processed for IF against γH2A.X. Left panel shows representative pictures of the 2.0 Gy condition for the indicated genotypes. Scale bars equal 50μm. In parallel, after irradiation organoids were replated to test their survival, which is represented on the right panel as a total number of organoids. Columns represent the average quantification for each indicated genotype and error bars represent the standard deviation. Statistical significance was assessed using the Student's T Test. *P<0.05, **P<0.01 and ***P<0.001.

Interestingly, we could partially reproduce the phenotype observed in *Bmi1*-deficient organoids when we treated WT organoids with DAPT. Vehicle treated organoids, formed γH2A.X foci that were efficiently resolved 5 hours after irradiation. DAPT treated organoids, in contrast, still displayed unresolved γH2A.X foci / full nuclei 5 hours after recovery from irradiation, similarly to *Bmi1*-deficient organoids [**FIGURE R38**, compare to FIGURE R42]. We hypothesised that the extent of unresolved DNA damage is not as high in DAPT-treated organoids, because 48h after DAPT treatment (which is when the organoids were irradiated) there are still residual levels of Bmi1 protein that could contribute to DNA damage repair (see FIGURE R33). Nevertheless, these results indicate **that Notch signalling is necessary for DNA damage repair in ISCs *in vitro***, most probably through Bmi1 as a downstream effector.

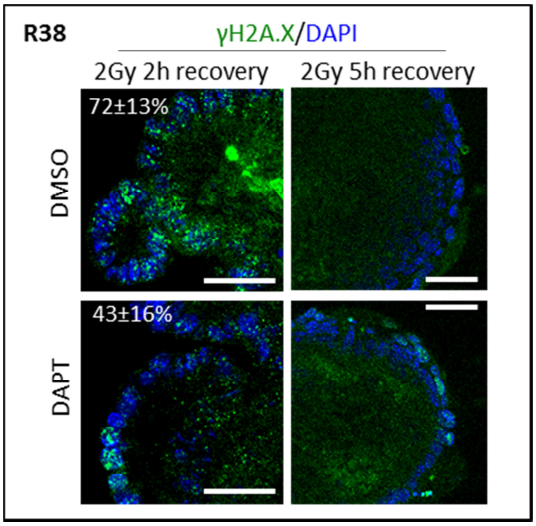

FIGURE R38 | γH2A.X IF in organoids treated with DAPT. Prior to irradiation, organoids were treated for 48h with 50μM DAPT (or vehicle, DMSO). Then, they were irradiated at 2.0 Gy and 2h or 5h after they were processed for IF against γH2A.X. Scale bars equal 50μm.

Indeed, we have observed that under basal conditions there is Notch1 activity in intestinal crypts [FIGURE R39, left panel]. Strikingly, after irradiation, the number of cleaved-Notch1-positive crypt cells seems to increase [FIGURE R39, right panel].

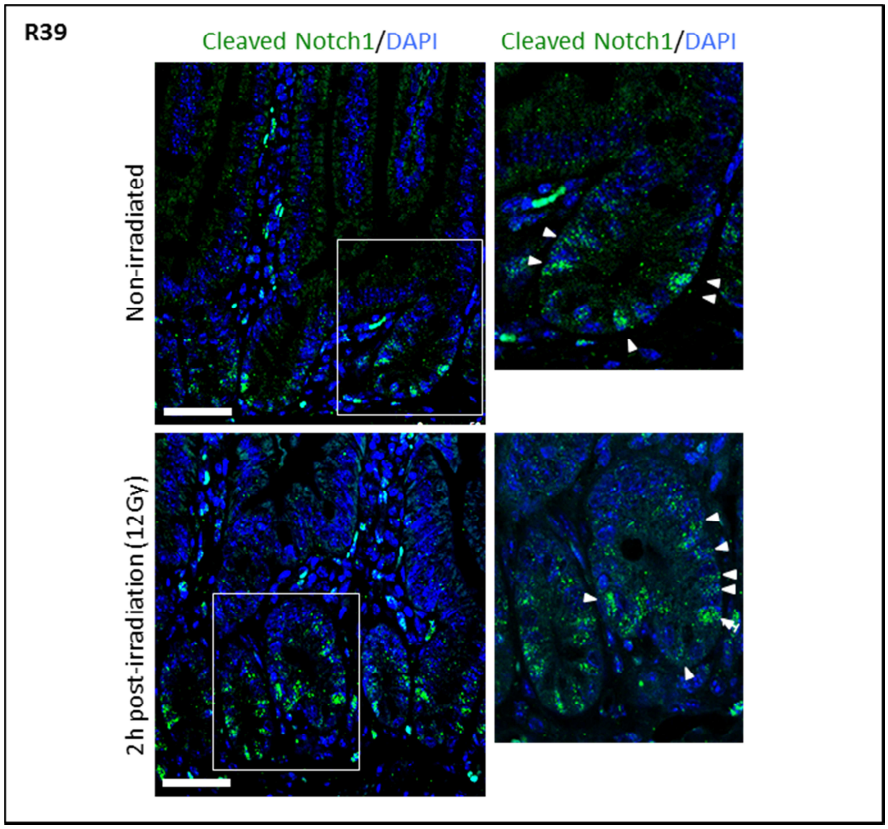

FIGURE R39 | ICN1 IHC-P after irradiation. IHC-P staining against cleaved Notch1 (ICN1) was performed in paraffin sections of wildtype intestines collected 2h after whole-body irradiation (12Gy). Scale bar equals 50µm. Although not quantified, note the increased number of active Notch1 cells after irradiation (white arrowheads indicate $ICN1^{+}$ nuclei).

What we can conclude from this set of experiments is that Notch and Wnt signalling pathways are essential for the integrity of ISCs and they are so because they cooperatively regulate a set of genes important for their function. This cooperation involves an interaction of the effectors of the pathway ICN1 and β-catenin at the chromatin level. We have identified *Bmi1* as a target of both signalling pathways and demonstrated that it is essential for the proper proliferation, cell cycle progression and self-renewal capacity of ISCs. Moreover, Bmi1 not only participates in ISC maintenance through the regulation of its classical target locus *Cdkn2a*, but it also does so by its role in DNA damage repair. These conclusions are summarized in the model represented in FIGURE R40.

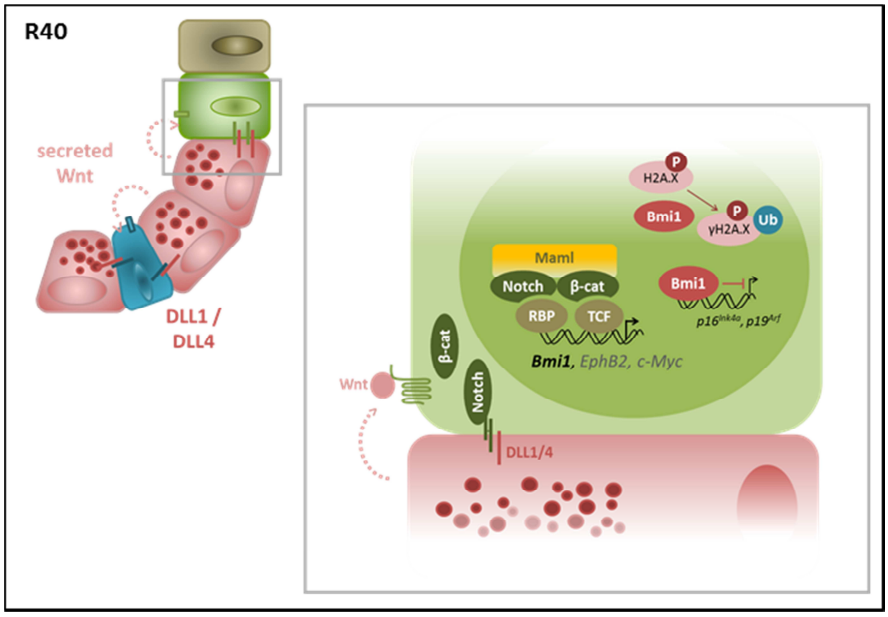

FIGURE R40 | Bmi1 regulates murine intestinal stem cell proliferation and self-renewal downstream of Notch (and β-catenin). Paneth cells (red) provide Wnt and Notch ligands to the neighbouring ISCs, where together they activate transcription of genes relevant for ISC function. Among those, Bmi1 is crucial for their survival by inhibiting its classical target locus *Cdkn2a* (encoding for $p16^{INK4a}$ and $p19^{ARF}$), allowing for cell cycle progression when necessary and preventing senescence. Moreover, it also helps maintain ISCs in homeostasis by exerting alternative functions in DNA damage repair, facilitating the recruitment of the DDR (DNA damage repair) machinery.

SUPPLEMENTARY FIGURES

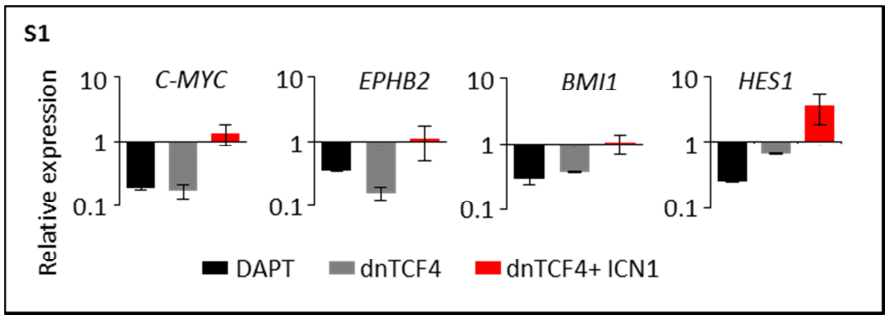

FIGURE S1 | qRT-PCRs of genes related to ISC function. Expression levels of *C-MYC*, *EPHB2, BMI* and *HES1* in Ls174T/dnTCF4 cells treated for 48h with DAPT (Notch/γ-secretase inhibitor) or with doxycycline (to induce expression the dnTCF4 construct and inhibit Wnt signalling) and Ls174T/dnTCF4/ICN1 cells treated for 48h with doxycycline (to inhibit Wnt signalling and induce expression of active ICN1). Expression is shown relative to β-*ACTIN levels*. In summary: BLACK bars Notch LOF; GREY bars Wnt LOF; RED bars Wnt LOF / Notch GOF. This experiment was performed by Dr. Verónica Rodilla.

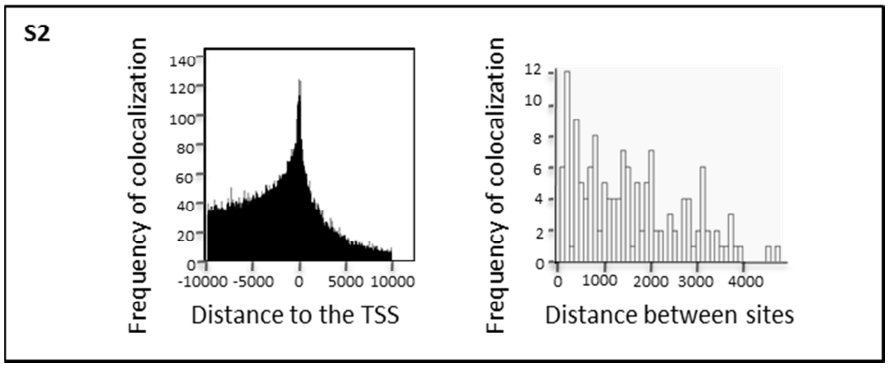

FIGURE S2 | RBPJ and TCF biding sites across the genome. Bioinformatic analysis of the whole human genome sequence demonstrating that TCF and RBPJ binding consensus colocalised close to the TSS of the gene promoters (left) and determine the presence of adjacent consensus sequences (right). This experiment was performed in collaboration with Dr. Pedro Fernández Salguero.

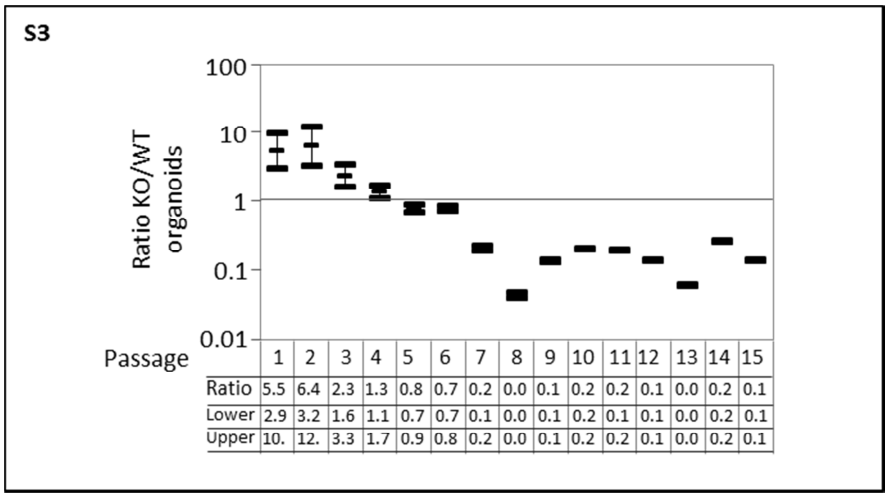

FIGURE S3 | Representation in ratio of *Bmi1* KO vs. WT organoid growth curve along passages. Quantification of the average number of organoids obtained from *Bmi1* KO and *Bmi1* WT crypt cells. The ratio between the average number of KO and WT organoids obtained at the different passages (from a minimum of 3 wells counted) is represented. Note the inverted ratio after passage 7. This analysis was performed by Angel Carlos Roman.

PREVIOUS WORK (PART II)

The second part of this thesis focuses on why Notch signalling through Jagged 1 (Jag1) is necessary for intestinal tumours. Our previous work demonstrated that in CRC, Wnt/β-catenin signalling drives expression of the Notch ligand *Jag1* (Rodilla et al. 2009), creating a context where both signalling pathways are also active, in a similar manner to ISCs. Moreover, just deleting a copy of Jag1 in the mouse model for intestinal tumorigenesis *Apc*$^{Min/+}$ significantly reduced their polyp burden, highlighting the requirement of Notch signalling as an essential modulator of Wnt/β-catenin-mediated tumorigenesis. Nevertheless, that bulk of evidence was generated using a general *Jag1* heterozygous mouse model, because the total KO is embryonic lethal (Xue et al. 1999).

Deletion of Jag1 *does not disturb intestinal homeostasis but affects intestinal tumour initiation*

Following this line of work, we analysed the expression levels of the Notch ligands *Dll1*, *Dll4*, *Jag1* and *Jag2* in the different compartments of the intestinal epithelium of the *Apc*$^{Min/+}$ mice. We found that although all ligands were expressed in the crypt compartment, **only *Jag1* seemed to be expressed in the adenomas** [FIGURE P3].

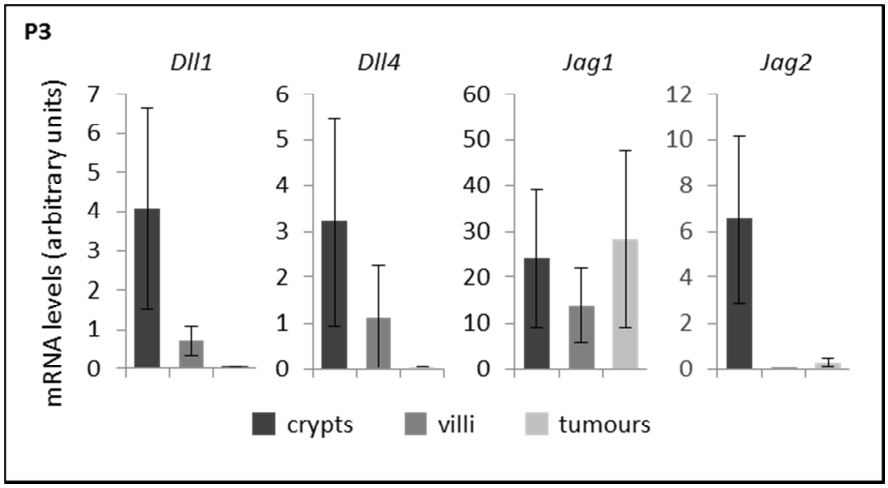

FIGURE P3 | Notch ligand expression in *Apc*$^{Min/+}$ intestinal epithelial compartments. RNA was extracted from freshly isolated crypts/villi/adenomas of wildtype mice (See MM9). Quantification was done by qRT-PCR. Expression relative to *Villin* is shown. Columns indicate the average quantification and error bars represent the standard deviation. This experiment was performed by Dr. Verónica Rodilla.

Thus, to overcome *Jag1* KO-associated embryonic lethality and discard possible systemic effects of *Jag1* haploinsufficiency, we generated an intestinal epithelial specific *Jag1* deficient mouse strain, by crossing *Jag1*$^{lox/lox}$ with *Villin*-Cre mice. A lox-stop-lox-YFP knock-in in the Rosa26 locus was also introduced as a reporter for Cre activity. Intestinal epithelial *Jag1* deficient mice (R26-LSL-YFP;*Jag1*$^{lox/lox}$;*Villin*-Cre^{+}, hereon *Jag1*$^{\Delta IEC}$) are viable and born at Mendelian ratios. By analysing YFP expression by IHC, we confirmed that the Cre recombinase was expressed in the entire intestinal epithelium, including the long-lived Paneth cells [FIGURE P4].

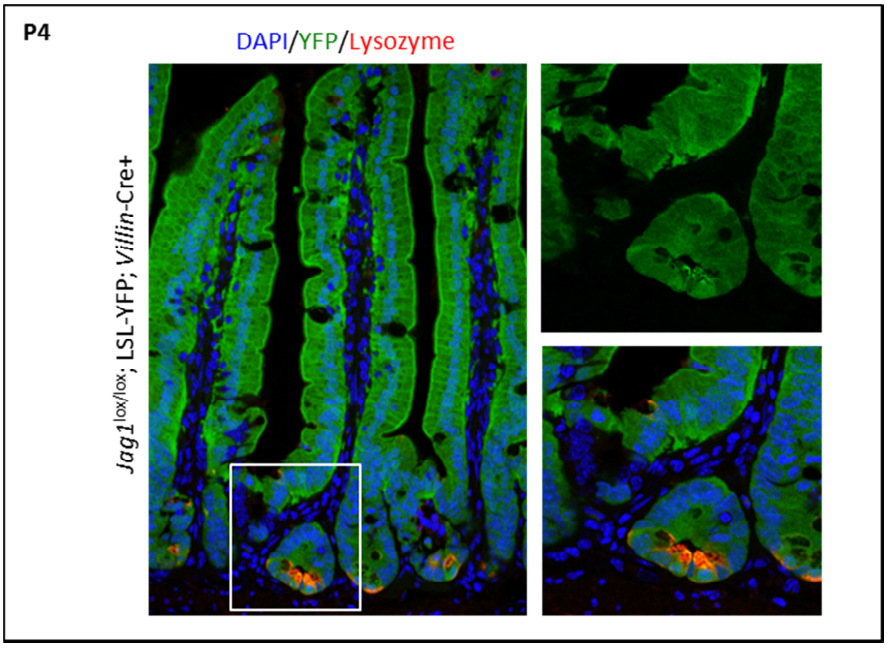

FIGURE P4 | YFP/Lyz1 double IHC in *Jag1*$^{\Delta IEC}$ sections. YFP staining as a reporter of Cre expression in the intestinal epithelium under the control of the *Villin* promoter. Cre activity is evident in all the cells of the crypt, including the Paneth cells (Lyz1^{+} in red). Right panels show a magnification of a YFP^{+} CBC ISC between two Paneth cells. Images were obtained in an Olympus BX-61 at 200X and 400X magnifications. This experiment was performed by Dr. Verónica Rodilla.

Before crossing them with the *Apc*$^{Min/+}$ mice, we assessed their intestinal function by measuring weight gain along their lifespan. We confirmed that ***Jag1*$^{\Delta IEC}$ mice gained weight at the same ratio than their WT littermates** [FIGURE P5]. Indeed, recent work deriving from a collaboration with our group uncovered that Jag1 is dispensable for the maintenance of intestinal homeostasis (Pellegrinet et al. 2011), confirming our results that *Jag1*$^{\Delta IEC}$ mice were functionally healthy.

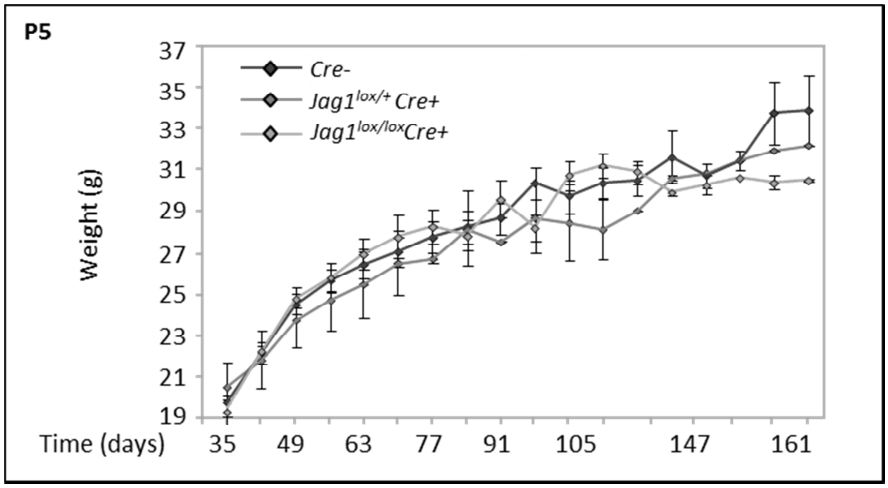

FIGURE P5 | Weight gain graph of *Jag1*$^{\Delta IEC}$ mice compared to their heterozygous or WT littermates. The weight of mice of the indicated genotypes was monitored for 6 months, as a surrogate measure of intestinal function. This experiment was performed by Dr. Verónica Rodilla.

So next we set out to cross our *Jag1*$^{\Delta IEC}$ mice with the *Apc*$^{Min/+}$ mice. We found that not only **their polyp burden was reduced** [FIGURE P6], but that the few adenomas that arose in the *Jag1*$^{\Delta IEC}$;*Apc*$^{Min/+}$ mice were also smaller (not depicted).

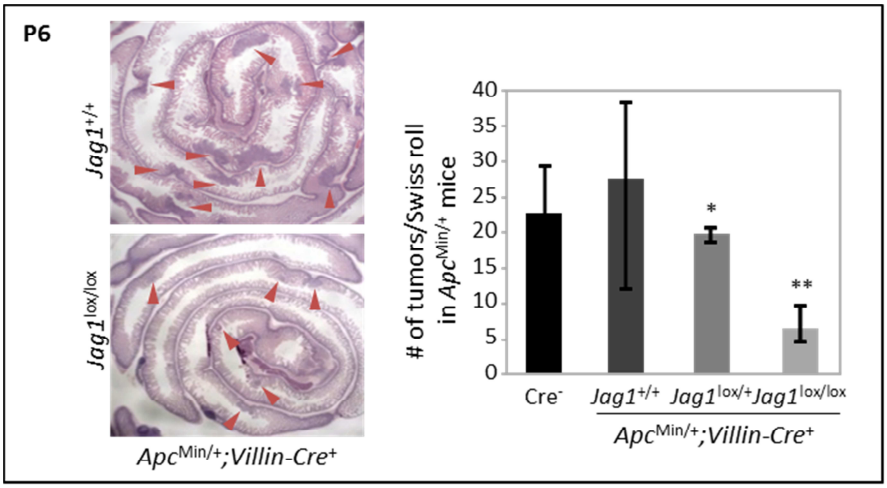

FIGURE P6 | Swiss roll and tumour number quantification in *Jag1*$^{\Delta IEC}$;*Apc*$^{Min/+}$ mice. The number of intestinal tumours is reduced in the absence of intestinal epithelial Jag1. Red arrowheads indicate tumours. Right graph shows the quantification, columns indicate average number of tumours and error bars the standard error of the mean. Statistical significance was assessed using the Student's T Test. *P<0.05, **P<0.01 and ***P<0.001.This experiment was performed by Dr. Verónica Rodilla.

When we analysed *Jag1*$^{\Delta IEC}$;*Apc*$^{Min/+}$ adenomas in depth and compared them to the Jag1 WT *Apc*$^{Min/+}$ adenomas, we discovered that, as expected, they displayed less active Notch 1 protein (by IHC against the cleaved form of Notch1, ICN1) [FIGURE P7]. They were also proliferating less (by IHC against Ki67) and exhibited lower c-Myc protein levels, when compared to their WT counterparts [FIGURE P7].

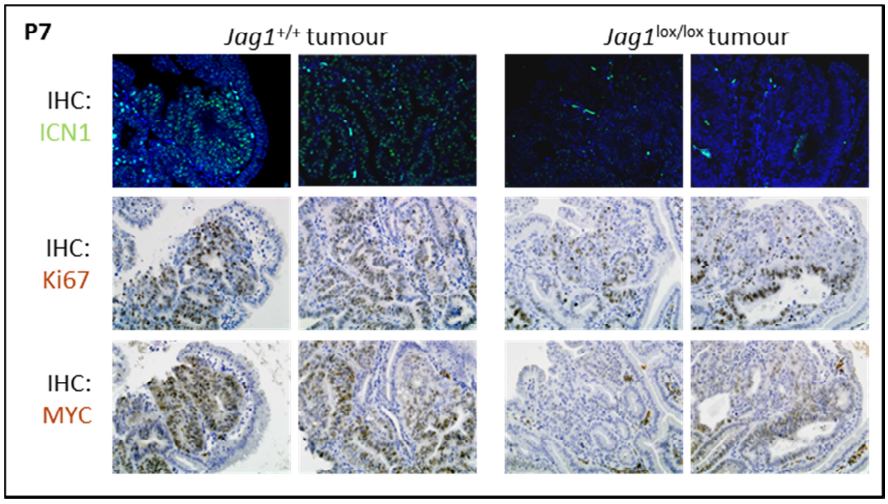

FIGURE P7 | ICN1, Ki67 and c-Myc IHC-P in *Jag1*$^{\Delta IEC}$;*Apc*$^{Min/+}$ sections. IHC-P against cleaved Notch1 (active), Ki67 and c-Myc was performed in paraffin sections of intestines of the indicated genotypes. Nuclei were counterstained with haematoxylin. Representative pictures of adenomas are shown. This experiment was performed by Dr. Verónica Rodilla.

By qRT-PCR analysis we also found that in *Jag1*$^{\Delta IEC}$ adenomas, compared to the WT counterparts: (1) Hes1 mRNA was reduced, indicating decreased Notch1 transcriptional activity, (2) double Notch and Wnt targets *Bmi1*, *EphB2* and *c-Myc* expression levels were also lower, and (3) ISC and/or CSC markers *Lgr5* and *Cd44* were less expressed as well [FIGURE P8]. In summary, **Jag1-deficient adenomas have a lower degree of active Notch1, proliferate less and exhibit reduced expression of ISC/CSC genes**.

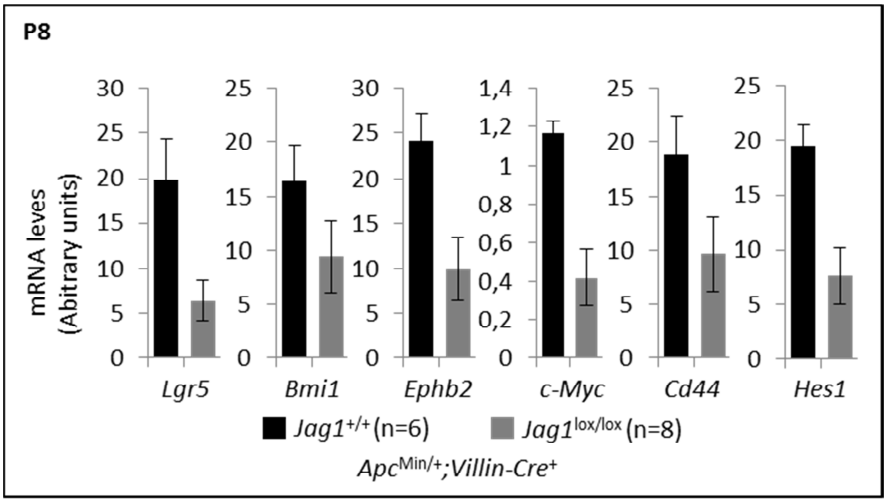

FIGURE P8 | qRT-PCRs in in *Jag1*$^{\Delta IEC}$;*Apc*$^{Min/+}$ adenomas. RNA was extracted from freshly isolated adenomas of wildtype mice (See MM9). Quantification was done by qRT-PCR. Expression relative to *Gapdh* is shown. Columns indicate the average quantification and error bars represent the standard error of the mean. This experiment was performed by Dr. Verónica Rodilla.

Taking these results together, we demonstrate that **Jag1-mediated Notch signalling downstream of Wnt/β-catenin is essential to maintain certain properties essential for the adenoma cell survival**, such as their proliferative capacity and ISC/CSC-associated gene expression.

RESULTS (PART II)

Adenoma cells require Notch signalling to grow in vitro

To confirm the requirement of Notch signalling for adenoma stemness, we resorted to the *in vitro* culture system of adenoma cells taking advantage of our knowledge from ISCs and other CSCs. As mentioned in the introduction, CSCs are characterized (in part) by their ability to grow in 3D structures without attachment to a culture plate, in serum-free conditions. We tried to grow adenoma cells in non-adherent culture plates in serum-free media supplemented with growth factors EGF and FGFb, but they failed to do so. The most plausible explanation is that adenoma cells are pre-cancerous and have not developed malignant qualities enough to allow them to grow in CSC-friendly conditions (in which colorectal cancer cell lines and advanced-stage patient samples can grow). To overcome this problem, we applied what we had learned from normal ISC *in vitro* culture system and plated adenoma cells in Matrigel® and supplemented the medium as we did for organoids. In contrast to the mini-gut like structures that ISCs form, "adenoma stem cells" grew as round cyst-like structures or spheroids [**FIGURE R41**].

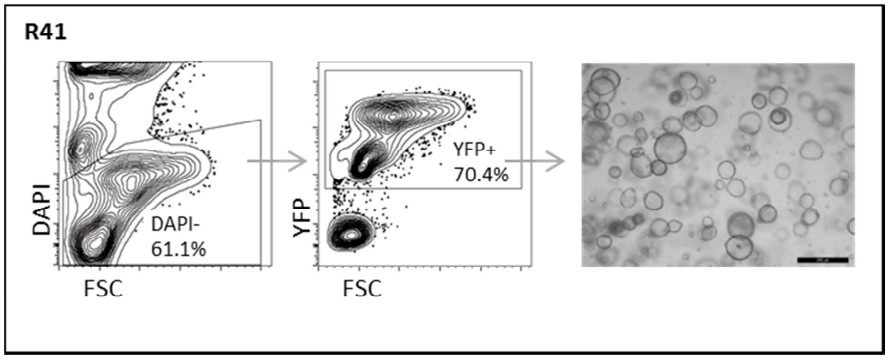

FIGURE R41 | Sorting IECs from *Apc*$^{Min/+}$ adenomas and growing them as spheroids in ISC culture conditions. Adenomas from a YFP$^{lox/lox}$;*Jag1*$^{+/+}$;*Apc*$^{Min/+}$;*Villin*-Cre^{+} can be isolated and cells can be processed for FACS (fluorescence-activated cell sorting), based on their YFP expression (indicating their epithelial origin). Scale bar equals 200µm.

To characterise these adenoma spheroids we performed a series of stainings by immunofluorescence. E-cadherin staining confirmed their epithelial origin. EphB2, CD44 and Bmi1 expression indicated that they were enriched in (if not all) stem-like cells. Several cells also seem to express the Notch1 receptor. And spheroids displayed a homogeneous expression pattern of Jag1 and Dll4 (see DISCUSSION). Sparse expression pattern of differentiation markers Muc2 (goblet cells), Lyz1 (Paneth cells), Syp (enteroendocrine cells) and CAII (absorptive cells) confirmed that the vast majority of the cells that formed the spheroids were indeed undifferentiated cells [FIGURE R42].

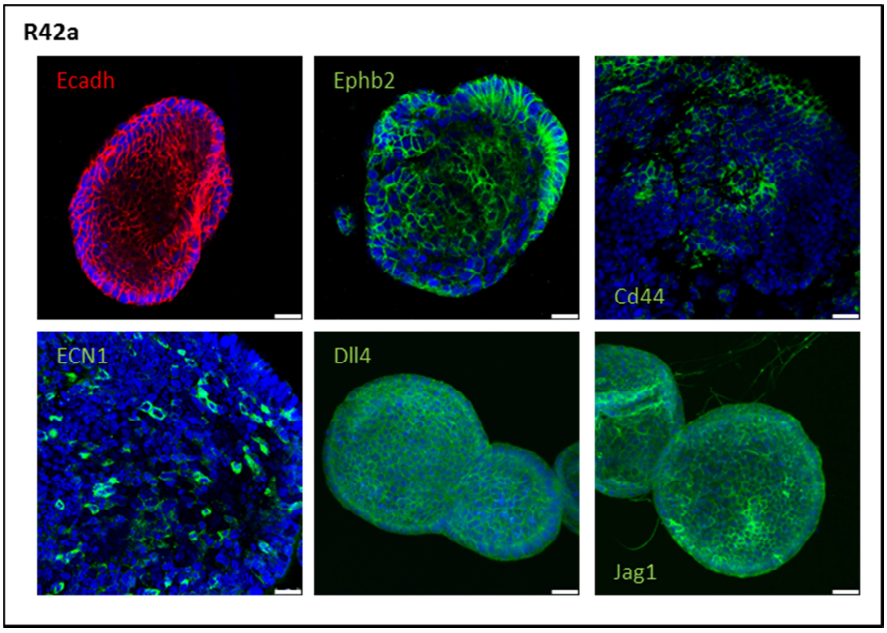

FIGURE R42 | Spheroid IF panel. Characterisation of *Apc*$^{Min/+}$ spheroids (cells were isolated as on MM9 and seeded unsorted as indicated on MM10). Immunostaining was performed as described on MM11. Panel **a** shows staining for Ecadh (epithelial marker); EphB2 and Cd44 as CSC markers; ECN1, Dll4 and Jag1 as members of the Notch signalling pathway. Panel **b** (on next page) shows Bmi1, Ki67 (proliferation marker), and differentiation markers of several intestinal epithelial cell lineages: CAII for absorptive cells, Lyz1 for Paneth cells, Muc2 for goblet cells and Syp for enteroendocrine cells. Arrowheads indicate discrete differentiated cells. Spheroids are epithelial in origin, predominantly formed by undifferentiated cells. Scale bar equals 25µm.

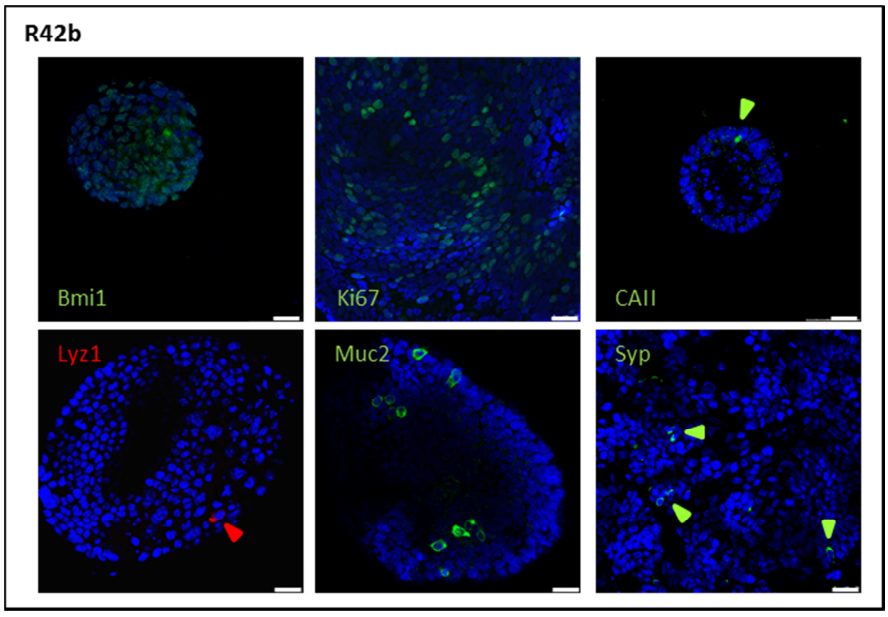

Next, we treated the spheroids with DAPT to shut Notch signalling off. We found that **inhibition of Notch signalling hampered the growth of adenoma spheroids** [FIGURE R43]. When we treated with DAPT, the total number of 3D structures that were formed was significantly reduced and the formation of big spheroids (>50µm) was almost abolished. Their replating ability was also greatly affected (not shown).

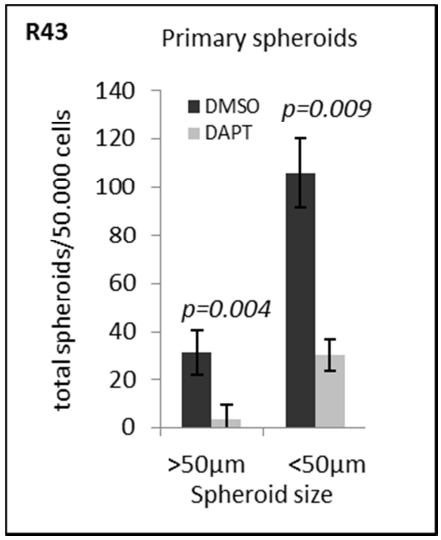

FIGURE R43 | Spheroids treated with DAPT have impaired growth. MIACs from *Apc*$^{Min/+}$ mice were isolated as on MM9 and seeded unsorted as indicated on MM10. Total number of spheroids was quantified and classified according to their size in the presence of vehicle (DMSO) or 50µM DAPT. Columns indicate average number of spheroids. Error bars represent the standard deviation. Statistical significance was assessed using the Student's T Test.

Interestingly, 72h of DAPT treatment reduced Notch target Hes1 expression, as well as the mRNA levels of stem cell markers [FIGURE R44], and halted proliferation of spheroid cells, as measured by Ki67 staining [FIGURE R45].

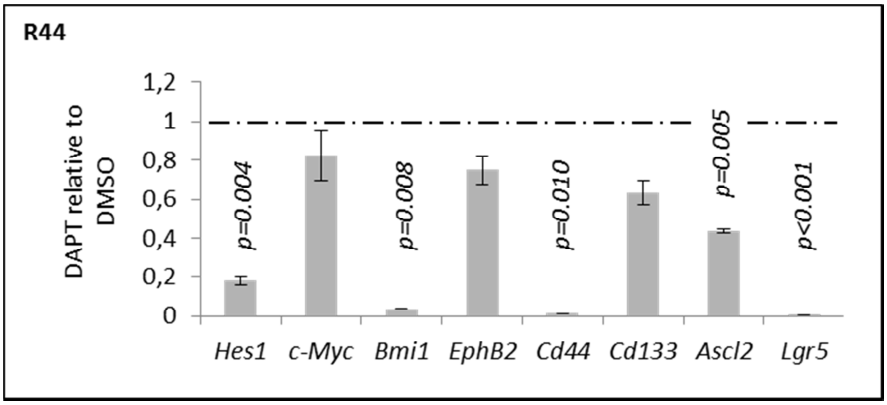

FIGURE R44 | qRT-PCR of spheroids treated with DAPT. Spheroids were treated for 72h with 50µM DAPT (or DMSO for vehicle treated conditions) and collected for RNA isolation. qRT-PCR was performed as described on MM13. Total mRNA levels were normalised to *Gapdh* expression. Columns indicate expression levels of indicated gene in DAPT relative to DMSO-treated. Error bars represent the standard deviation. Statistical significance was assessed using the Student's T Test.

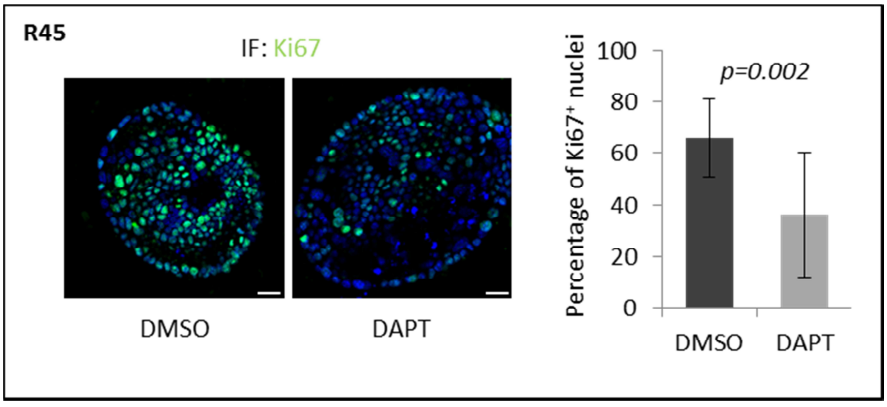

FIGURE R45 | Ki67 IF and quantification graph of spheroids treated with DAPT. Spheroids were treated for 48h with 50µM DAPT (or DMSO for vehicle treated conditions) prior to immunostaining (as described on MM11). Left panel shows representative images. Scale bars represent 25µm. Right graph shows quantification of $Ki67^+$ nuclei in each condition. Columns indicate the quantification of 3 independent experiments. Error bars represent the standard deviation. Statistical significance was assessed using the Student's T Test.

Abrogation of Jag1-mediated Notch signalling restrains the stem cell potential of intestinal adenoma cells in vitro

So far, we knew that Notch signalling through Jag1 was necessary for adenoma formation *in vivo* and that Notch signalling was also essential for adenoma cells to grow *in vitro*. So the next step was to try to grow *in vitro* the cells from the few adenomas that arose in the *Jag1*$^{\Delta IEC}$;*Apc*$^{Min/+}$ mice. When we seeded comparable amounts of *Apc*$^{Min/+}$ adenoma cells from *Jag1*$^{WT/IEC\text{-}HET}$ or *Jag1*$^{\Delta IEC}$ backgrounds, the latter failed to grow [FIGURE R46], indicating that **Jag1 was also essential for the *in vitro* growth of adenoma cells**.

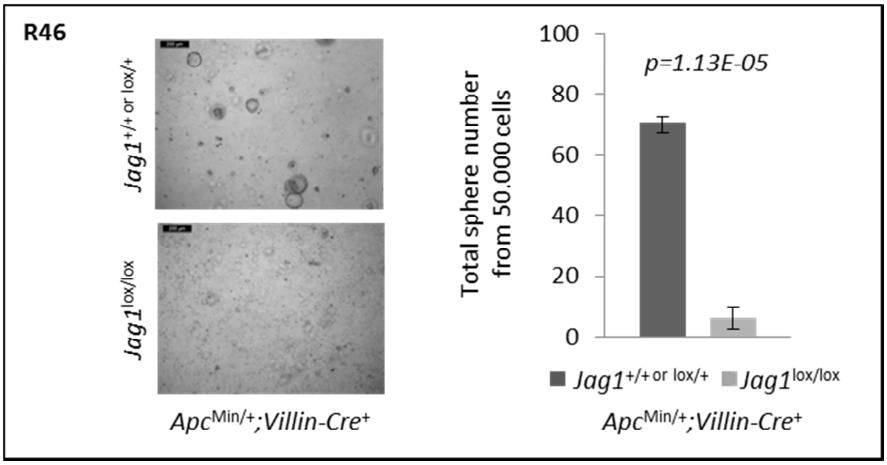

FIGURE R46 | *Jag1* deletion in vivo and spheroid count. Spheroid forming efficiency of *Jag1*$^{\Delta IEC}$;*Apc*$^{Min/+}$ cells is greatly impaired. Left shows representative images of the spheroid cultures from MIACs with the indicated genotypes. Scale bar equals 200µm. Right panel shows the total number of spheroid quantification from 3 independent experiments. Error bars represent the standard deviation. Statistical significance was assessed using the Student's T Test.

Next we generated a *Apc*$^{Min/+}$;*Jag1*$^{lox/lox}$;β-*actin*-CreERT mouse line to allow for time-controlled deletion of *Jag1*. In the absence of external stimuli, *Jag1* remains WT in all the cells and adenomas can be formed normally in the *Apc*$^{Min/+}$ background. This allowed us to culture adenoma cells and promote *Jag1* deletion in preformed spheroids upon exposure to 4-hydroxytamoxifen (4OHT), an active metabolite of the oestrogen homolog tamoxifen, that has more affinity for the ER than tamoxifen *in vitro*. When we treated preformed spheroids with 4OHT to induce *Jag1* deletion, they collapsed [FIGURE R47], suggesting that ***Jag1*** **was indispensable for the maintenance of adenoma spheroids**.

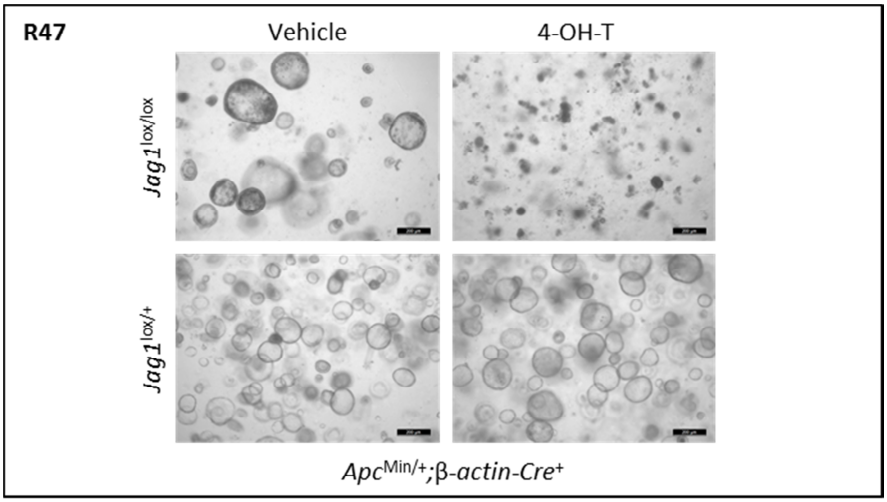

FIGURE R47 | *Jag1* deletion in vitro. Isolating MIACs from a *Apc*$^{Min/+}$;*Jag1*$^{lox/lox\ or\ +}$;β-*actin*-CreERT background allows for Jag1 deletion once they have been pre-formed by the addition of 4-hydroxytamoxifen (4-OH-T). Spheroids were left to be formed after passaging for three days and then treated with 5μM 4-OH-T (or ethanol for vehicle-treated) for 72h. A representative experiment from n>3 is shown. Scale bar equals 200μm.

When we analysed changes in gene expression at different time points after *Jag1* deletion, prior to spheroid death, we found that *Hes1* was downregulated, revealing the inactivation of Notch signalling. Moreover, double Notch and Wnt targets *Bmi1*, *EphB2* and *c-Myc* expression also decreased, and ISC markers *Hopx*, *Lrig1* and *mTert* were also diminished [FIGURE R48]. This result indicates that **Notch signalling through Jag1 in adenoma spheroids is necessary to maintain their stemness**.

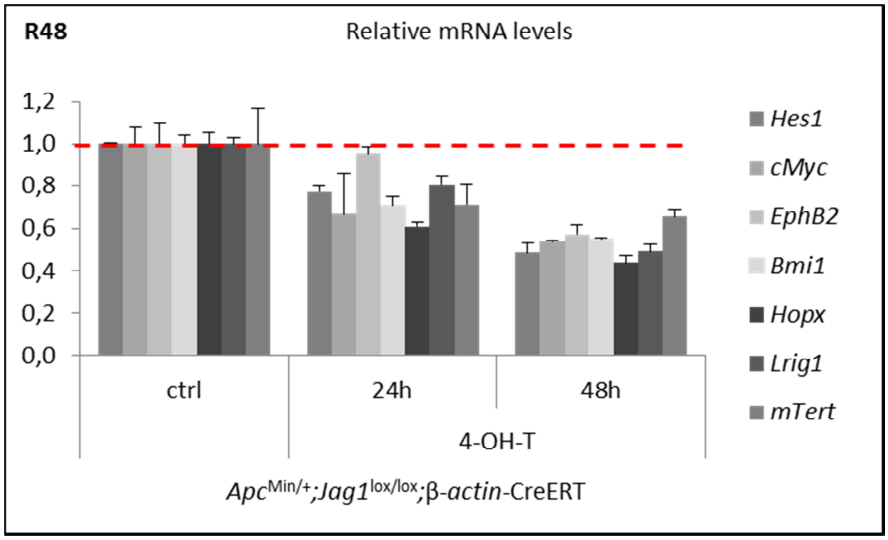

FIGURE R48 | qRT-PCRs of 4OHT treated spheroids. MIACs from the indicated genotype were cultured as spheroids for three days prior to 4-OH-T treatment for the indicated times. Expression relative to HK average (β*2m* and *Gapdh*) is shown, normalised to 1 in the vehicle-treated. One representative experiment from three is depicted. Error bars represent the standard deviation.

To have a deeper understanding of why spheroids die when *Jag1* is deleted, we performed various stainings. Detection of Ki67 by IF showed that 4OHT-treated spheroids proliferated significantly less [FIGURE R49]. By staining against active (cleaved) caspase 3, it also seemed that their apoptotic rate was increased, but this was difficult to quantify, since apopototic cells and other cell remnants are being released into the lumen of the spheroids [FIGURE R50].

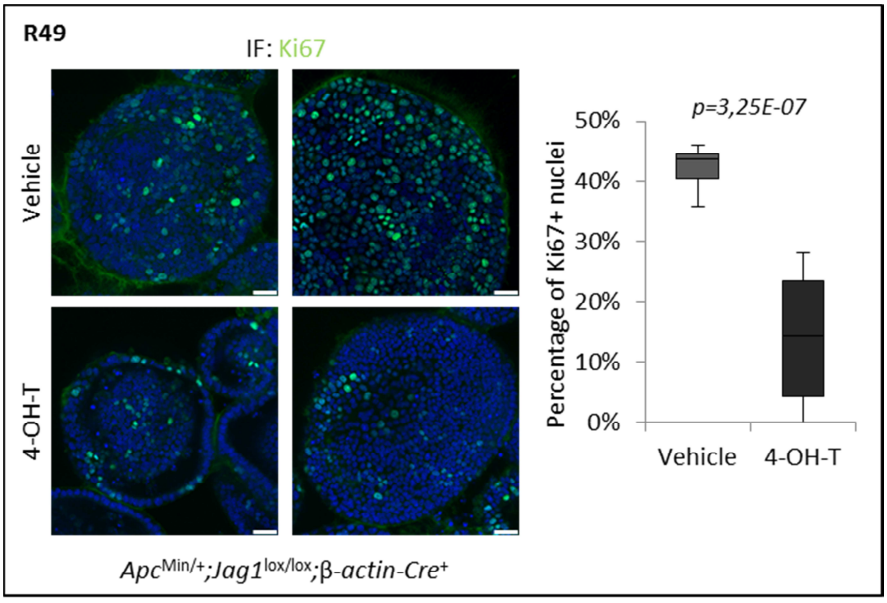

FIGURE R49 | Ki67 IF in 48h 4-OH-T treated spheroids and quantification box plots. Spheroids were treated for 48h with 5µM 4-OH-T (or ethanol for vehicle treated conditions) prior to immunostaining (as described on MM11). Left panel shows representative images. Scale bars represent 25µm. Right graph shows quantification of $Ki67^{+}$ nuclei in each condition. Columns indicate the quantification of 3 independent experiments. Error bars represent the standard deviation. Statistical significance was assessed using the Student's T Test.

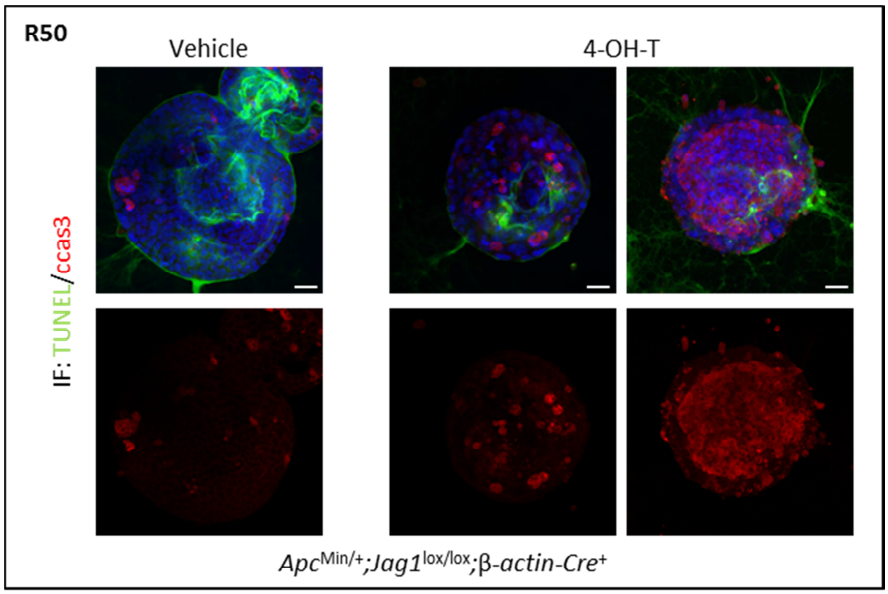

FIGURE R50 | TUNEL/ccas3 IF in 48h 4-OH-T treated spheroids. Spheroids were treated for 48h with 5µM 4-OH-T (or ethanol for vehicle treated conditions) prior to immunostaining (as described on MM12). Scale bars represent 25µm.

Moreover, when we checked for differentiation markers, such as Lyz1 for Paneth cells, despite being very rare in untreated spheroids, abundant Lyz1^{+} cells appeared in the 4OHT-treated spheroids [FIGURE R51].

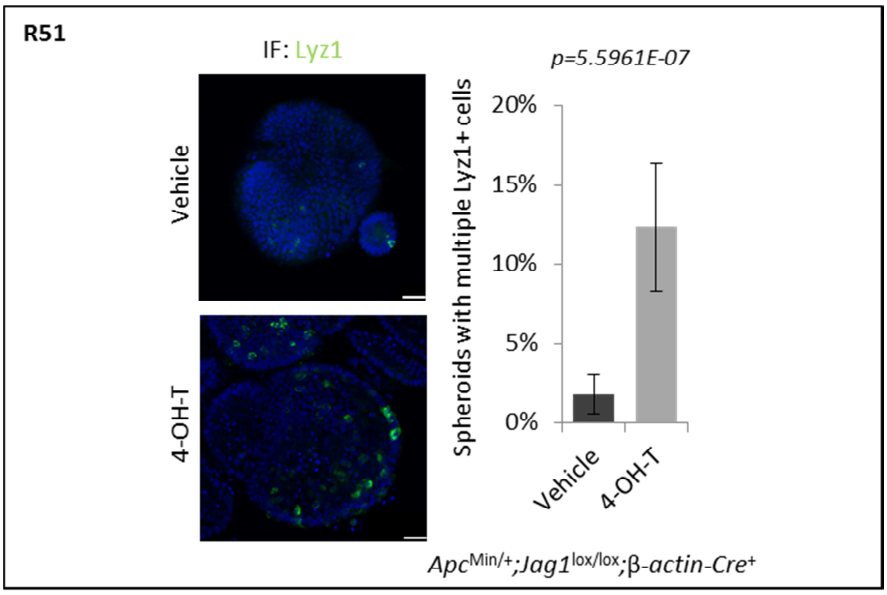

FIGURE R51 | Lyz1 IF after 4OHT treatment and quantification graph. Spheroids were treated for 48h with 5µM 4-OH-T (or ethanol for vehicle treated conditions) prior to immunostaining (as described on MM11). Left panel shows representative images. Scale bars represent 25µm. Right graph shows quantification of Lyz1^{+} cells in each condition. Columns indicate the quantification of 2 independent experiments. Error bars represent the standard deviation. Statistical significance was assessed using the Student's T Test.

Taken together, these results indicate that **Jag1 is necessary for the maintenance of adenoma cells in an undifferentiated, proliferative state *in vitro***. When *Jag1* is deleted in preformed spheroids, they stop proliferating, differentiate and probably have a higher rate of apoptosis.

As a proof of concept, spheroid collapse can be prevented by cultivating them in the presence of soluble Jag1 [FIGURE R52].

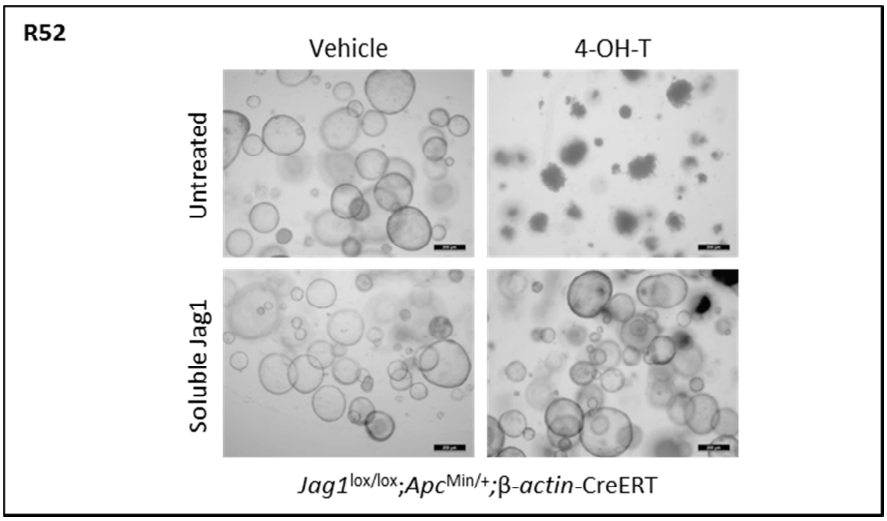

FIGURE R52 | *Jag1* deletion rescue with soluble Jag1. Spheroids were seeded in the absence or presence of soluble Jag1 (See MM10) and left to grow for three days. Then , they were treated with 5μM 4-OH-T (or ethanol for vehicle-treated) for 72h. A representative experiment from n>3 is shown. Scale bar equals 200μm.

Normal stem cells can also be cultured ex vivo in 3D, and they grow as organoids (or mini-guts). These, unlike spheroids, contain multiple differentiated cells, such as $Muc2^+$ goblet cells and $Lyz1^+$ Paneth cells [**FIGURE R53**]. When we analysed Notch ligand expression by IF, we found that both organoids coming from ISCs and spheroids coming from MIACs contain similar levels of Jag1 and Dll4 [**FIGURE R54**]. Then, we assessed the expression of Manic Fringe (Mfng) in our 3D cultures, as a candidate that could mediate the differential requirement of Jag1 by adenoma cells. We found that organoids displayed detectable levels of Mfng, but spheroids strikingly did not [**FIGURE R55**].

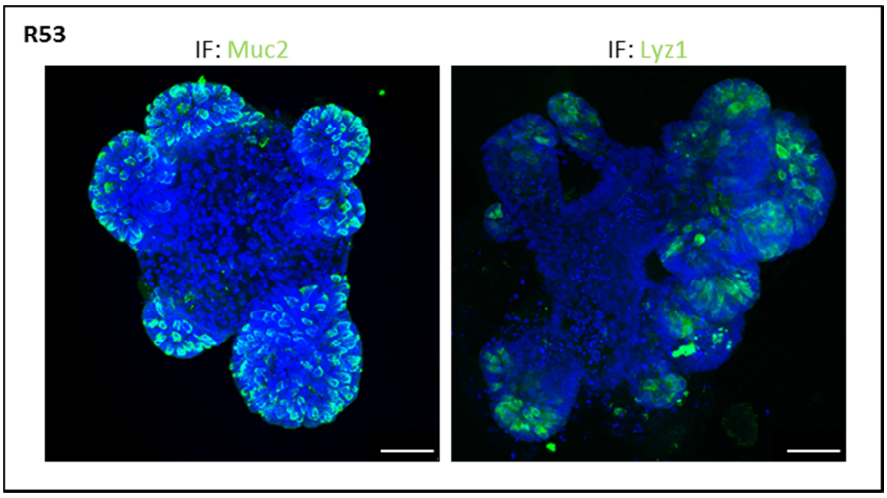

FIGURE R53 | Muc2 and Lyz1 staining in WT organoids. Crypts were isolated as on MM9 and seeded unsorted as indicated on MM10. Immunostaining was performed as described on MM11. On the left, staining for Muc2 for goblet cells. On the right, Lyz1 staining for Paneth cells. Scale bar equals 50µm.

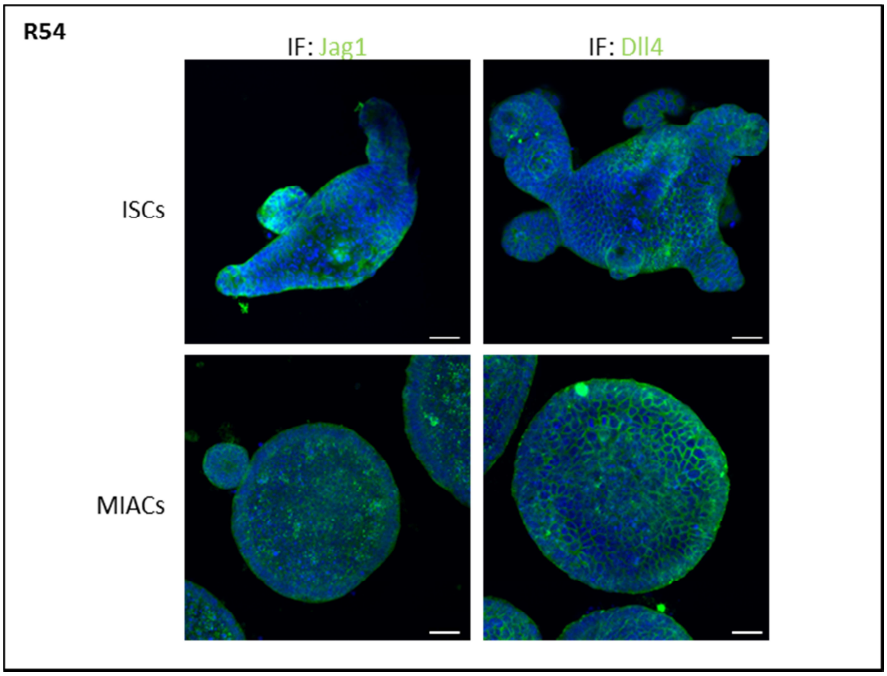

FIGURE R54 | Jag1 and Dll4 staining in organoids vs. spheroids. Crypts and MIACs were isolated as on MM9 and seeded unsorted as indicated on MM10. Immunostaining was performed as described on MM11. Scale bar equals 25µm.

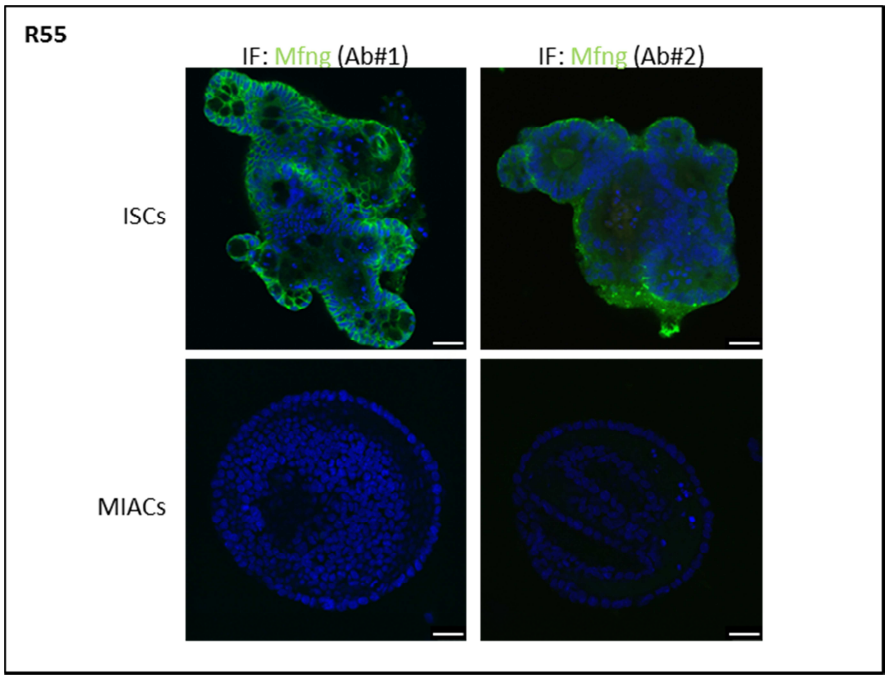

FIGURE R55 | Mfng staining in organoids vs. spheroids. Crypts and MIACs were isolated as on MM9 and seeded unsorted as indicated on MM10. Immunostaining was performed with two different antibodies as described on MM11. Scale bar equals 25µm.

Apc$^{Min/+}$ tumours, by IHC, display heterogeneous levels of Mfng expression [**FIGURE R56**].

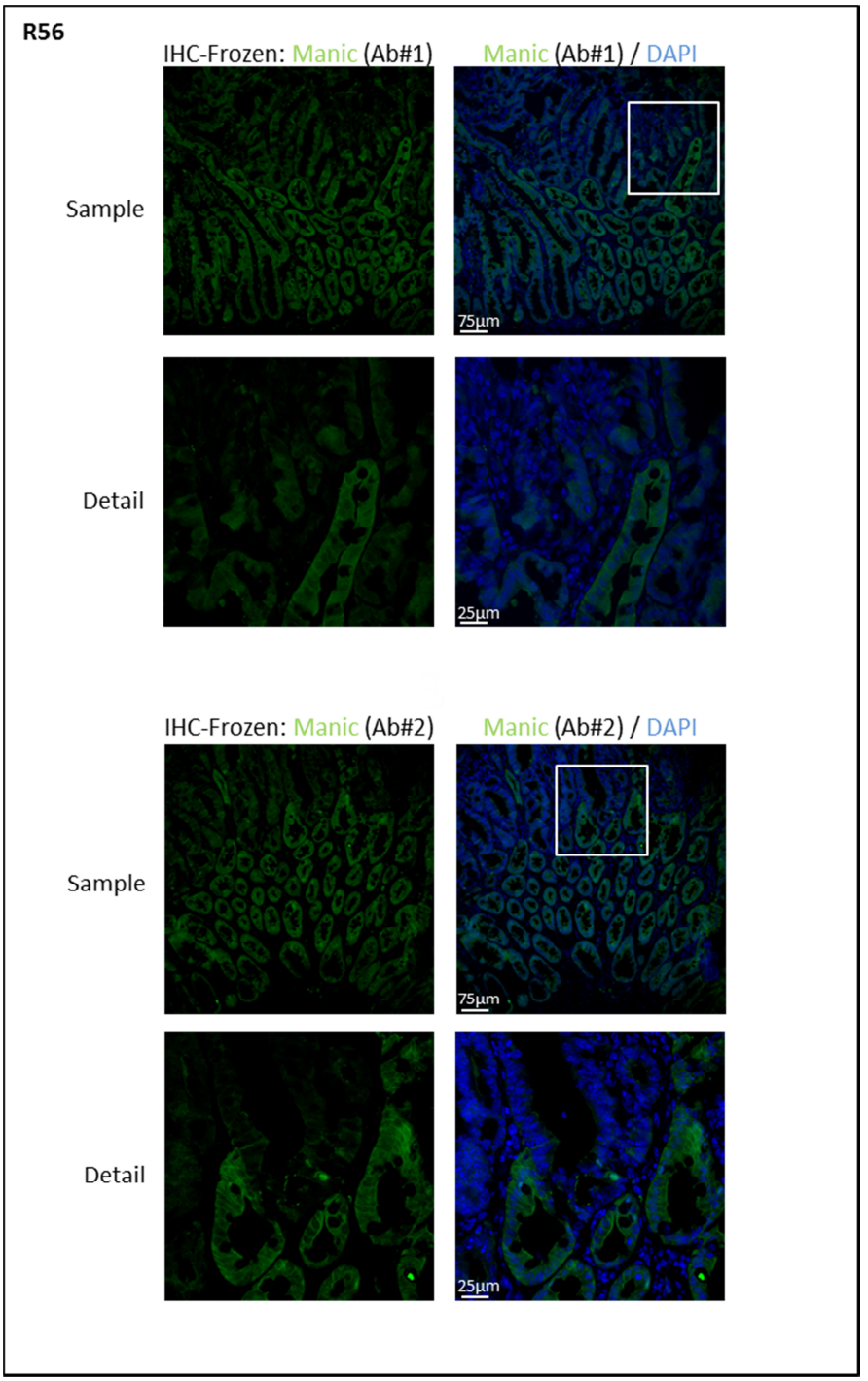

FIGURE R56 | Mfng expression in *Apc*$^{Min/+}$ adenomas. IHC-F was performed with two different antibodies as described on MM6. Pictures show representative adenomas.

DISCUSSION

Notch signalling in intestinal homeostasis

With the first part of this work we have demonstrated the complex interplay between Wnt and Notch signalling pathways in the intestinal epithelium. We show that in normal ISCs both pathways are simultaneously required to activate transcription of genes relevant for ISC function. Indeed, *c-Myc*, *EphB2* and *Bmi1* were known targets of the Wnt/β-catenin signalling pathway (He et al. 1998; Batlle et al. 2002; Yu et al. 2012), and Myc was also known to be regulated by Notch in other tissues (Klinakis et al. 2006; Palomero et al. 2006; Weng et al. 2006). Therefore, we wanted to highlight the requirement of Notch signalling for their transcription in the intestinal crypt compartment. vanDussen and colleagues had shown that Notch activity was necessary for CBC maintenance and proliferation, but failed to provide a molecular mechanism that explained why (VanDussen et al. 2012). They speculated that morphological changes that Paneth cells suffered upon Notch inhibition may result in alteration of important niche signals that are required for CBC stem cell homeostasis. They had observed that blocking Notch resulted in fewer stem cells, due to reduced proliferation, increased differentiation and apoptotic cell loss. And although they identified *Olfm4* as a target of Notch in CBCs, its intestinal function remains obscure and it is not clear how it can contribute to stemness.

The requirement of Notch activity in the undifferentiated cells of the intestinal epithelium was difficult to prove due to the extensive differentiation of cells into the secretory lineage (mainly mucus-secreting goblet cells), which exhausted the stem/progenitor pool. But importantly, Wnt pathway overactivation, even if it partially compensates the effect of Notch LOF, is not sufficient to rescue the loss of the ISC compartment (at the levels of cell proliferation or ISC marker expression). This suggests that they co-regulate the transcription of some genes essential for ISC maintenance. Indeed, in tumour cells we previously demonstrated a cooperative transcriptional regulation of *C-MYC*, *EPHB2* and *BMI1* by Notch and Wnt. In fact, transcriptional co-regulation by Notch and Wnt might be a conserved evolutionary strategy, since Rbpj and Tcf binding consensus are not randomly distributed throughout the genome [**FIGURE S2**]. Instead, they cluster together in

the promoter region of multiple genes. This would fall into the first category of crosstalk between Wnt and Notch signalling pathways that Collu and colleagues proposed and gathered several examples for (Collu et al. 2014).

If we focus in non-pathological conditions, c-Myc and EphB2 particularly were known to play a functional role in the intestinal stem/progenitor compartment. Under canonical Wnt activity, c-Myc is necessary to maintain ISCs in a proliferative, undifferentiated state (Pinto et al. 2003). On the other hand, β-catenin/TCF-mediated transcription of the EphB2 and EphB3 efrin receptors also takes place in the undifferentiated crypt compartment of the intestine, and is necessary for its correct compartmentalization – the gradient that they create (inverse with their ligands) is essential for Paneth cells to migrate downwards (Batlle et al. 2002) to constitute the niche of ISCs. As mentioned in the introduction, Bmi1 was postulated as an ISC marker but its functional significance for this population remained unexplored. Hence, we focused our efforts in exploring the functional role of Bmi1 in intestinal homeostasis.

First, by chromatin immunoprecipitation we demonstrated that ICN1 and β-catenin (effectors of the Notch and Wnt pathway, respectively) concur in a region of the proximal Bmi1 promoter. Using luciferase promoter activity assays, we determine that the mechanism by which these two pathways co-regulate Bmi1 expression is through an incoherent feed forward loop. In this context, ICN1 and β-catenin positively regulate transcription of Bmi1, but at the same time, when the Notch-target Hes1 levels increase, it can also bind its putative sites in the proximal Bmi1 promoter and block its expression. In other words, Notch activation induces positive and negative signals in the Bmi1 gene, resulting in a so-called type I incoherent feed forward loop (I1-FFL; Mangan and Alon 2003). Our prediction is that this would allow the fine-tuning of Bmi1 levels through time (or position). This type of transcriptional regulation has been proposed for another Notch target gene, *Gata2*, in the embryonic site of hematopoietic stem cell generation (Guiu et al. 2013). Notch1 itself has also been proposed to be a target of one of these loops in intestinal and colorectal cancer stem cells, but at the level of regulation by microRNAs. Bu and colleagues first demonstrated that miR-

34a targeted the Notch mRNA in the progeny of CoCSCs that was more differentiated, while the CoCSC that did not retain the miR-34a maintained high levels of Notch and its self-renewal capacity (Bu et al. 2013). More recently, they have shown that miR-34a not only suppresses Notch directly but upregulates Notch indirectly via inhibition of Numb, and they have suggested that this mechanism generates a better Notch bimodal switch with more clearly defined levels between cells (Bu et al. 2016). Interestingly, they proposed this mechanism for CoCSCs but also for ISCs in response to an inflammatory stimulus.

Going back to Bmi1 regulation by Notch signalling, Yu and colleagues already anticipated that Notch could also be involved indirectly in regulating Bmi1 transcription through KLF4 (Yu et al. 2012). They showed that KLF4 directly binds to the BMI1 promoter and represses its expression. And KLF4 itself is also regulated by Notch in the intestine (Ghaleb et al. 2008; Zheng et al. 2009), where the Notch target HES1 represses its expression. KLF4 is necessary for terminal goblet cell differentiation (Katz et al. 2002), but whether its expression is controlled by Math1 remains unknown.

Bmi1 functionality in maintaining intestinal homeostasis

In an effort to understand the functional relevance of Bmi1 expression in the undifferentiated crypt compartment, we analysed the intestinal epithelium of total *Bmi1* KO mice. We found that the intestine of the *Bmi1* KO mice is shorter and thinner, compared to their WT littermates, which correlates with a reduction in the number of proliferating cells. Defects in crypt-villus axis length can be explained by reduced proliferation of the ISC/progenitor compartment. Pulse/chase experiments following single BrdU administration allowed us to measure not only the cycling status of crypt cells but also their migration capacity just by studying the distribution of $BrdU^+$ cells along the crypt-villus axis. Our results suggested a reduced migratory capacity of *Bmi1* KO epithelial cells when compared to WT cells, which could be partially explained by a lack of a "pushing force" from the bottom of the crypt due to the lower number of cells proliferating in that region. On the other hand, the use of total Bmi1 knockout mice did not allow us to exclude the participation of

systemic effects in all the observed phenotypes including the decreased total length of the intestine, since *Bmi1* KO mice are overall smaller than their WT littermates. Supporting the idea that reduced intestinal size had a systemic component, tissue-specific *Bmi1* KO intestines do not display a reduction in length. Yet, around time of death, total *Bmi1* KO mice display a decrease in body weight (not shown), which is in general considered readout of defective intestinal function.

Nevertheless, different ISC markers were still detected in the Bmi1 deficient mice and the integrity of intestinal tissue was maintained for almost three months. This, together with the fact that Bmi1 deficiency only partially overlaps with the Notch LOF phenotype, highlights the relevance of other Notch target genes in the maintenance of the ISC pool, such as EphB2 and c-Myc.

By specifically looking at the effects of *Bmi1* deletion into the intestinal stem/progenitor cells (as determined by expression of *Olfm4* and high levels of EphB2), we confirmed that the number of cycling cells was significantly reduced in this particular compartment. But can we consider that stem cell function is affected in the Bmi1 deficient mice if they can still maintain the integrity of the tissue for at least three months? To answer this question, we cultured ISCs ex-vivo as organoids to force their self-renewal requirements by serially replatings. We found that even though Bmi1 KO ISCs are able to give rise to organoids for a few passages, their growing ability decreases and they do not survive longer than passage 15-16. This indicates that Bmi1-deficient cells display a defect in their long-term self-renewal capacity.

What were the downstream effectors of Bmi1 that could explain the proliferation and self-renewal defects in ISCs? Bmi1, as a member of the PRC1 complex, participates in the addition of repressive marks to histones across the genome. One of the best-characterised target of PRC1-mediated silencing is the *Cdkn2a* locus, which can give rise to two different transcripts: $p16^{INK4a}$ and $p19^{ARF}$ ($p14^{ARF}$ in humans). We found that these classical targets are upregulated in the Bmi1 KO cells, both in the adult intestines and already detected during the developmental stages when ISCs are being determined. So, similarly to what was

described for HSCs (Janzen et al. 2006), ISC self-renewal is probably affected due to the elevated levels of p16. Interestingly, in the Notch OFF genotype and the composite Notch OFF / Wnt ON genotype, where Bmi1 is not expressed, p16 levels are also elevated. These results confirm that Notch, through Bmi1, is able to ensure ISC self-renewal capacity by repressing the *Cdkn2a* locus.

In a recent report Chiacchiera and colleagues showed that the Polycomb Complex PRC1 preserves ISC identity by suppressing non-tissue-specific transcription, hence ensuring proper Wnt/β-catenin transcriptional activity (Chiacchiera et al. 2015). Specifically, what they analysed are the effects of inactivating the catalytic subunits Ring1a and Ring1b and found a general transcriptional effect that was Cdkn2a-independent (because it is also detected in the *Cdkn2a*-null background). In this work, loss of PRC1 activity lead to a massive upregulation of several DNA-binding transcription factors, many of which were known to negatively regulate β-catenin transcriptional activity, such as HOXB13 (Jung et al. 2005), RUNX3 (Ito et al. 2008), Sox17 (Sinner et al. 2007), Zic2 (Pourebrahim et al. 2011) and Zic3 (Fujimi et al. 2012). In particular, Zics bind the β-catenin/Tcf7l2 complex in ISCs and inhibit its transcriptional activity (Chiacchiera et al. 2015). However, to our knowledge the existence of this general genome-wide effect (likely as a result of deficient H2A ubiquitination) does not undermine or exclude the relevance of Bmi1-mediated maintenance of ISCs through regulation of the *Cdkn2a* locus.

What does accumulation of p16 and p19 mean functionally? In the case of $p16^{INK4a}$, this is a cyclin-dependent kinase inhibitor that functions blocking CDK4, therefore capable of inducing cell cycle arrest in G1 phase. $p19^{ARF}$ functions as an stabilizer of the tumour suppressor protein p53 as it can interact with and sequester the E3 ubiquitin ligase MDM2 (responsible of the degradation of p53). p53, that is stabilised in response to DNA damage (and other deleterious stimuli), can induce cell cycle arrest [by activating transcription of $p21^{CIP}$, another CDK inhibitor

(el-Deiry et al. 1993; Harper et al. 1993)[20]] and apoptosis [by activating transcription of BAX, which forms a heterodimer with and antagonises the apoptosis repressor Bcl-2 (Miyashita et al. 1994)]. So p19, indirectly through p53 and p21 can also induce cell cycle arrest. Accumulation of p16 and p19 occur physiologically with ageing and p16 is related to senescence (Krishnamurthy et al. 2004) and, in consequence, so is Bmi1 (Park et al. 2004).

Another phenomenon that we observed when culturing Bmi1 KO organoids was the accumulation of unresolved DNA damage. This fits with alternative functions that have been previously described for Bmi1 in facilitating DNA damage repair. Bmi1 localised to sites of damage and when it was absent, the repair machinery could not be efficiently recruited (Facchino et al. 2010; Ismail et al. 2010). Indeed, Ismail and colleagues showed that in the absence of BMI1 cells accumulated ɣH2A.X foci. Consistent with this data, we found that Bmi KO organoids were particularly sensitive to ionizing radiations. Thus, 5h after a low-dose radiation such as 0.5 Gy, organoid cells displayed nuclei full of ɣH2A.X and only half of them were able to survive after replating.

Our results were not only confirmed in vitro, using the organoid culture system, but we observed similar results in vivo. Specifically, we found that p16 and p19 are also accumulated in the Bmi1 KO intestinal crypt cells, as shown by IHC and/or qRT-PCR, and upon whole body irradiation they show a massive accumulation of ɣH2A.X foci (not detected in the WT). This indicates that in the intestinal stem / progenitor compartment, Bmi1 is also regulating cell cycle progression and senescence as well as proper DNA damage repair, essential mechanisms to ensure stem cell self-renewal and maintenance. This would be in agreement with the identification of the $Bmi1^+$ cells as a radioresistant population with capacity to replace $Lgr5^+$ cells after radiation (Yan et al. 2012).

[20] Both in the same issue of Cell in 1993. El-Deiry and colleagues identified p21/WAF1 as a p53 target and Harper and colleagues described the function of p21 as an inhibitor of G1 CDKs.

Most importantly, comparable defects were observed when we abrogated Notch signalling with various approaches, suggesting that Notch signalling, by ensuring transcription of Bmi1, is upstream controlling these relevant functions. For instance, after treating organoids with DAPT we observed a decrease in Bmi1 transcript levels, concomitant with an increase in p16 and p19 levels. In this case we do see that other stem cell markers such as *Ascl2* and *Olfm4* are repressed when Notch signalling is inhibited. The decrease in *Olfm4* levels was expected since *Olfm4* is a direct target of Notch (VanDussen et al. 2012). *Ascl2*, on the other hand, is known to be regulated by Wnt signalling (Jubb et al. 2006; Van der Flier et al. 2007), but not by Notch (van der Flier, van Gijn, et al. 2009). So, its reduction suggests that the stemness is also affected when Notch signalling is abrogated in vitro. DAPT-treated organoids also fail to repair gamma-irradiation-induced DNA damage as efficiently as their vehicle-treated counterparts. And again in vivo, in the absence of DNA damaging stimuli, *Rbpj*-deficient intestines also accumulate γH2A.X-filled nuclei, suggestive of unresolved DNA-damage.

Interestingly, although Notch1 activity ($ICN1^+$) can be easily detected in the intact intestinal crypt cells, the number of $ICN1^+$ cells in this compartment was significantly increased after irradiation. Whether upregulation of Notch activity is a possible protective mechanism to ensure proper DNA damage repair or whether this is as result of an expansion of the $ICN1^+$ ISC compartment after irradiation remains to be explored. It is possible that $ICN1^+$ cells represent some type of radioresistant population that is expanded after irradiation. In the same direction, several reports have shown that Notch family member expression levels and/or activity can be increased after irradiation in breast cancer stem cells (Phillips et al. 2006; Lagadec et al. 2013), in lung cancer (Mizugaki et al. 2012), in osteoblasts (Yang et al. 2013), and in glioma stem cells (Saito et al. 2015). Several of these reports indeed suggest that Notch signalling might be mediating resistance to radiotherapy, and suggest a regime of GSI treatment to radiosensitize the remaining cells. Thus, it is possible that in the intestinal crypt compartment Notch might be playing a similar protective role, to ensure proper DNA damage through Bmi1. Multiple evidences currently support the existence of CSCs responsible for tumour persistence, metastasis and

chemotherapy resistance (Visvader & Lindeman 2008), and share biological features with normal ISCs including transcriptional programs (Merlos-Suárez et al. 2011). Whether this is happening in colorectal cancer remains to be explored, but it seems that Wnt and Notch are also regulating transcription of a subset of genes in CRC that might confer them stem-cell characteristics.

As mentioned, we have here shown that Notch activity, indirectly through Bmi1, facilitates DNA damage repair. However, a recent report from Vermezovic and colleagues has shown that Notch can also function as a direct negative regulator of the DNA damage response (Vermezovic et al. 2015). Specifically, they show that Notch1 can interact directly with ATM, inhibiting its kinase activity and observe an inverse correlation between Notch1 levels/activity???? and ATM activation in human breast cancer. In contrast, they also find that inhibition of Notch1 by GSI in the presence of DNA damage leads to increased radiosensitivity in an ATM-dependent manner in T-ALL cells. Thus, whereas Inhibition of ATM kinase activity by Notch delays or impede DNA damage repair, Notch inhibition can induce cell apoptosis in an ATM-dependent manner. If both mechanisms, activation of Bmi1 and inhibition of ATM coexisted in CRC cells, it would be possible that Notch activity would elicit opposing effects upon DNA damage. Thus, it would be important to investigate whether Notch inhibition increase CRC cell sensitivity to radiotherapy, both by a mechanism involving less efficient DNA damage repair (Bmi1 dependent) and ATM-mediated apoptosis. Our results indicate that Bmi1 is actually a target of Wnt and Notch signalling in CRC and others have shown its relevance in tumorigenesis, where Bmi1 knockdown decreases the growth of CRC cell line-derived xenografts (Yu et al. 2012). Thus, analysing this level of cross-regulation between Notch and Wnt signalling in CRC would be of great interest.

Concerns regarding lineage tracing

We are nowhere near to describing a true and definitive ISC marker and there is still great controversy in the field. Although it is not the focus of this work, a recent publication is worth discussing with regard to lineage tracing in the intestinal epithelium aiming to discover ISC markers. Zhu

and colleagues elegantly demonstrated that apoptosis plays an important role in controlling lineage tracing from different ISC populations in the mouse intestine (Zhu et al. 2013). They showed that $Bmi1^+$ cells are tamoxifen-sensitive, and enter apoptosis when mice are injected the standard dose of tamoxifen (50mg/kg). If apoptosis is prevented by overexpression of Bcl2 or knockout of Chk2, $Bmi1^+$ cells are readily traced whereas $Lgr5^+$ cells significantly reduce their lineage tracing ability in long-term tracing experiments. These results should be taken into account for future lineage tracing experiments that are normally done using tamoxifen. Instead, the use of *Ah*-Cre mice could be taken into consideration, where Cre expression is inducible from a cytochrome P450 promoter element (CYP1A1 promoter) that is transcriptionally up-regulated in response to lipophilic xenobiotics such as β-napthoflavone (Ireland et al. 2004).

Nevertheless, studies addressing the functional characterization of the intestinal stem/progenitor compartment in general are essential (1) to give a molecular insight into how ISCs differ from CRC cells, as well as (2) to provide a better understanding of how ISCs are maintained for future studies in the field of regenerative medicine.

Notch signalling in colorectal cancer

In the second part of this thesis, we focused on further studying another crosstalk that our group had previously described. In CRC, tumour associated β-catenin induces transcription of the notch ligand Jag1 (Rodilla et al. 2009).

First, we set up the in vitro culture system for adenoma cells, based on the culture of ISCs as organoids, to enrich it in cells with stem cell properties. Adenoma stem-like cells obtained from $Apc^{Min/+}$ adenomas were grown as spheroids, without generating the crypt-like pocket structures [as reported by (Sato et al. 2011)]. These spheroids are formed by epithelial cells, and enriched in stem-like cells (by expression of EphB2, Cd44 and Bmi1). In concordance, they display very few terminally differentiated cells, as demonstrated by staining with markers of different lineages. Several cells seem to express the Notch1 receptor and

interestingly there is homogeneous expression of the Notch ligands Jag1 and Dll4. Unfortunately, we were unable to perform the active ICN1 staining in these structures, spheroids were sensitive to Notch inhibition by DAPT displaying reduced proliferation and stem cell marker expression [as reported for organoids by (VanDussen et al. 2012)].

Importantly, we found that epithelial-specific deletion of *Jag1* is sufficient to inhibit intestinal tumour formation and growth of adenoma cells as spheroids in the $Apc^{Min/+}$ background. This inhibition is associated with Notch-target gene downregulation and loss of the ISC signature in vivo, which suggests a role for Jag1-mediated Notch signalling in tumour initiation. By deleting Jag1 once the spheroids were pre-formed, we also highlight the necessity of Jag1-mediated Notch signalling in cancer cell maintenance. Jag1 deletion in spheroids arrests cell cycle and increases apoptotic cell death, concomitantly with a reduction in stem cell marker expression. We detect an increase in secretory-type enriched spheroids in about 10 % of the cases after Jag1 deletion. Unexpectedly, we were unable to detect $Muc2^{+}$ goblet cells in these cultures. We hypothesise that upon clonal expansion and selection of stem-cell enriched spheroids the ability to form fully-differentiated goblet cells has been lost.

Why are spheroids so sensitive to Jag1 deletion if they express Dll4 as well? When we looked at ligand expression in the organoids coming from normal ISCs, we found that, similar to $Apc^{Min/+}$ spheroids, they also express homogeneous levels of the Notch ligands Jag1 and Dll4. But, at least in vivo, ISCs seem to be refractory to Jag1 deletion because they rely on Dll1 and Dll4 signals (Pellegrinet et al. 2011). There is a group of proteins, the Fringe glycosyltransferases, which confer ligand specificity to the Notch receptors: addition of sugar moieties by Fringe proteins favours the association of Notch with the Delta-like ligands while blocking its interaction with Serrate. Interestingly, when we assessed expression of Manic Fringe (Mfng) in our 3D cultures we found that organoids displayed detectable levels of Mfng, but spheroids did not. Thus, our explanation is that in the absence of Mfng, the Notch receptor does not have the right post-translational modifications to signal through Dll4 and become addicted to Jagged1.

Mfng in *Apc*$^{Min/+}$ adenomas seems to be expressed in a heterogeneous manner. At the bottom, expression seems to be comparable to the levels in the crypts, where we expected to find Fringe proteins that modify the Notch receptors to be able to respond to the Delta-like ligands presented by the Paneth cells. In the bulk of the tumour, instead, there are "ribbons" that seem to have lost Mfng expression. Whether these are the more malignant portions of the adenomas remain to be explored. Another thing that we will study in the future is the status of Mfng expression in colorectal tumours from patients and to correlate it with overall or disease-free survival. It is possible that loss-of-Mfng might be a bad-prognosis marker.

What are the clinical implications of these findings? Of course, we cannot overexpress Mfng in tumours that have lost its expression and become addicted to Jag1, but there are other possibilities that can be explored. These are the current Notch-based therapies that are being tested or studied for treating human colorectal cancer:

General Notch Inhibition

The use of GSI inhibitors in anti-cancer therapy has been extensively investigated. Preclinical research has consistently shown that GSI treatment can revert tumorigenesis through a mechanism involving both anti-angiogenic and anti-CSC activities (Kalén et al. 2011; Arcaroli et al. 2012; Ramakrishnan et al. 2012; Palagani et al. 2012; Hassan et al. 2013; Miyamoto et al. 2013; Tanaka et al. 2015; Pant et al. 2016). GSI treatment also prevents Notch1 activation by chemotherapy thus sensitizing colon cancer cells to the treatment with oxaliplatin and 5-FU (Meng et al. 2009). However, GSI-associated toxicity is still a major drawback that needs further investigation (Pant et al. 2016). GSI-associated toxicity is reduced by intermittent dosing and ameliorated by glucocorticoid co-treatment (Real et al. 2009; Samon et al. 2012). In fact, glucocorticoids have demonstrated their efficacy even when administered after GSI treatment (Wei et al. 2010).

Targeting Notch Receptors

It is expected that targeting Notch receptors (or ligands) would result in a more specific and less toxic attenuation of Notch activity. Indeed, several monoclonal antibodies selectively targeting Notch 1-3 have been already generated and are being tested for their clinical applications (Li et al. 2008; Lin et al. 2010; Wu et al. 2010; Tran et al. 2013; Lafkas et al. 2015). Specific antibodies blocking Notch1 (Wu et al. 2010) showed reduced intestinal toxicity due to Notch1 and Notch2 redundancy in this tissue (Riccio et al. 2008). However, it is not known whether only Notch1 participates on CRC since previous studies from our group indicate that Notch2 is also active in cancer cells (Rodilla et al. 2009).

Targeting Notch Ligands

In addition to Notch receptors, Notch ligands can also be targeted using therapeutic antibodies. DLL4 Is expressed at sites of angiogenesis (Mailhos et al. 2001). Importantly, in human CRC, DLL4 expressed in stromal cells can activate Notch1 in surrounding tumour tissue (Sonoshita et al. 2011). Demcizumab, a humanized monoclonal antibody targeting DLL4 was shown to reduce tumour size in patients with previously treated solid tumours (10/55 colorectal tumours) (Smith et al. 2014). Hoey and colleagues elegantly demonstrated that in a parallel way to inhibiting Notch, blocking Dll4 not only inhibits tumour growth by blocking angiogenesis, but also reduces CSC frequency (Hoey et al. 2009). Combination of anti-DLL4 antibodies with irinotecan produced a significant decrease of CSC activity, and promoted apoptosis in a xenograft model of early passage patient-derived CRC (Fischer et al. 2011). Other antibodies against Dll4 (REGN1035 and REGN421) revealed a potent anti-tumour activity in renal carcinoma patient-derived tumours that was enhanced by VEGF signalling inhibition (Miles et al. 2014), likely related with reduced angiogenesis. Neutralizing Dll4 signal with a humanized anti-Dll4-selective antibody (YW152F) caused defective endothelial cell differentiation both in vitro and in vivo, and inhibited tumour growth in several tumour models without affecting intestinal differentiation (Ridgway et al. 2006). These particular effects could be therapeutically exploited for treating the CMS4 subtype of CRC (see

below). However, DLL4 blockade can also disrupt normal organ homeostasis and induce vascular tumours (Yan et al. 2010), thus raising serious concerns about its therapeutic potential.

Targeting the transcriptional complex

Another attractive method for inhibiting Notch signal is by blocking its nuclear transcriptional complex. In this sense, it was shown that a 62-amino-acid peptide derived from the NOTCH co-activator MAML1 was capable of forming a transcriptionally inert nuclear complex with NOTCH1 and CSL, and specifically inhibit the growth of murine and human NOTCH1-transformed T-ALL cells (Weng et al. 2003). More recently, a synthetic peptide called SAHM1 has been shown to prevent the assembly of a transcriptionally active Notch1 complex in T-ALL cells. Treatment of leukemic cells with SAHM1 resulted in the transcriptional suppression of NOTCH-dependent genes, and showed a specific anti-proliferative effect in both cultured cells and in a mouse model of NOTCH1-driven T-ALL (Moellering et al. 2009). Cell-permeable peptides such as SAHM1, which impede the formation of protein complexes, could be extremely advantageous owing to their small size and their ability to interfere with specific protein surfaces, which should impact on their target selectivity.

Colorectal cancer subtypes

Recently, a novel molecular classification has been established that permits the stratification of most CRCs in four subtypes with distinguishable features (Guinney et al. 2015): CMS1 (for consensus molecular subtype 1), includes tumours with microsatellite instability and an important immune activation; CMS2, the most frequent (37%) is characterized by an epithelial phenotype and a marked activation of the WNT and MYC pathways; CMS3, still epithelial but with significant metabolic alterations; and CMS4 includes the more mesenchymal tumours, with high TGF activity, and stromal and vascular invasion. Interestingly, colorectal tumours classified into the CSM2 subtype, with marked activation of the WNT pathway, also display an increased NOTCH pathway activation signature, reinforcing the idea of a crosstalk between

these two pathways in the intestinal tumorigenic context as well. It is tempting to speculate that CMS2 tumours that are associated to high WNT activity would be more Jagged1-dependent, being *Jag1* a target of β-catenin, whereas CMS4 tumours would depend on Delta ligands that are highly expressed in the endothelial infiltrate that is characteristic of this tumour subtype (Mailhos et al. 2001; Sonoshita et al. 2011). In agreement with this idea, we found that MFNG is downregulated in CMS2 (data not shown).

Hence, it would be of paramount importance (1) to molecularly characterize each patient's tumour, and for those who fall into the CMS2 subtype, (2) the fact that Jag1 is dispensable for the maintenance of intestinal homeostasis (Pellegrinet et al. 2011), making it a suitable target for therapy. We therefore propose the study of using anti-Jag1 blocking antibodies for these specific tumours, and to limit their availability to the intestinal epithelium, where it seems to be dispensable, to avoid blocking Jag1-mediated Notch signalling where it is important.

CONCLUSIONS

CONCLUSIONS

Part I

1. Notch and Wnt signalling are required simultaneously to allow transcription of genes important for ISC function, such as Bmi1
2. ICN1 and β-catenin, effectors of the Notch and Wnt pathways respectively, concur in a region of the Bmi1 promoter and can interact at the protein level in crypt cells
3. Cooperative regulation of Bmi1 transcription is positively regulated by ICN1 and β-catenin, and negatively regulated by the Notch target Hes1, fine-tuning Bmi1 levels in response to Notch and Wnt pathway activation (forming an incoherent feed forward type I loop)
4. *Bmi1* deficient intestines partially recapitulate the Notch-LOF phenotype
5. *Bmi1*-deficient intestinal epithelial cells are significantly less proliferative (including ISCs) than their wildtype counterparts, and the defects are already detected at the onset of villogenesis
6. Although ISC marker expression remains largely unaltered, *Bmi1*-deficient cells display reduced levels of *mTert*
7. The *Cdkn2a* locus is remarkably de-repressed in the absence of Bmi1
8. *Bmi1*-deficient organoids are defective in defective long-term self-renewal capacity, likely because they accumulate DNA damage
9. Bmi1 is involved in regulating DNA damage repair in intestinal crypt cells

Part II

1. Intestinal-specific deletion of Jag1 does not affect homeostasis, but reduces tumour initiation
2. The few tumours that arise in the Jag1-deficient background are less proliferative and express less stem cell markers
3. Adenoma cells require Jag1-mediated notch signalling to grow in vitro
4. Adenoma spheroids and ISC organoids express similar levels of Notch ligands Jag1 and Dll4
5. A possible candidate that mediates the differential requirement for Jag1 in intestinal adenomas is Mfng

BIBLIOGRAPHY

BIBLIOGRAPHY

Aberle, H. et al., 1997. beta-catenin is a target for the ubiquitin-proteasome pathway. *The EMBO journal*, 16(13), pp.3797–804.

Acar, M. et al., 2008. Rumi is a CAP10 domain glycosyltransferase that modifies Notch and is required for Notch signaling. *Cell*, 132(2), pp.247–58.

del Alamo, D. & Mlodzik, M., 2006. Frizzled/PCP-dependent asymmetric neuralized expression determines R3/R4 fates in the Drosophila eye. *Developmental cell*, 11(6), pp.887–94.

Albig, A.R. et al., 2008. Microfibril-associate glycoprotein-2 (MAGP-2) promotes angiogenic cell sprouting by blocking notch signaling in endothelial cells. *Microvascular research*, 76(1), pp.7–14.

Albuquerque, C. et al., 2002. The "just-right" signaling model: APC somatic mutations are selected based on a specific level of activation of the beta-catenin signaling cascade. *Human molecular genetics*, 11(13), pp.1549–1560.

Alves-Guerra, M.C., Ronchini, C. & Capobianco, A.J., 2007. Mastermind-like 1 is a specific coactivator of ??-catenin transcription activation and is essential for colon carcinoma cell survival. *Cancer Research*, 67(18), pp.8690–8698.

Amsen, D. et al., 2007. Direct regulation of Gata3 expression determines the T helper differentiation potential of Notch. *Immunity*, 27(1), pp.89–99.

Androutsellis-Theotokis, A. et al., 2006. Notch signalling regulates stem cell numbers in vitro and in vivo. *Nature*, 442(7104), pp.823–6.

Aparicio, J. et al., 2005. FOLFOX alternated with FOLFIRI as first-line chemotherapy for metastatic colorectal cancer. *Clinical colorectal cancer*, 5(4), pp.263–7.

Arcaroli, J.J. et al., 2012. ALDH+ tumor-initiating cells exhibiting gain in NOTCH1 gene copy number have enhanced regrowth sensitivity to a γ-secretase inhibitor and irinotecan in colorectal cancer. *Molecular oncology*, 6(3), pp.370–81.

Arranz, L. et al., 2012. Bmi1 is critical to prevent Ikaros-mediated lymphoid priming in hematopoietic stem cells. *Cell cycle (Georgetown, Tex.)*, 11(1), pp.65–78.

Artavanis-Tsakonas, S., Muskavitch, M.A. & Yedvobnick, B., 1983. Molecular cloning of Notch, a locus affecting neurogenesis in Drosophila melanogaster. *Proceedings of the National Academy of Sciences of the United States of America*, 80(7), pp.1977–81.

Asfaha, S. et al., 2015. Krt19+/Lgr5− Cells Are Radioresistant Cancer-Initiating Stem Cells in the Colon and Intestine. *Cell Stem Cell*, 16(6), pp.627–638.

Axelrod, J.D. et al., 1996. Interaction between Wingless and Notch signaling pathways mediated by dishevelled. *Science (New York, N.Y.)*, 271(5257), pp.1826–32.

Ayyanan, A. et al., 2006. Increased Wnt signaling triggers oncogenic conversion of human breast epithelial cells by a Notch-dependent mechanism. *Proceedings of the National Academy of Sciences of the United States of America*, 103(10), pp.3799–804.

Baladrón, V. et al., 2005. dlk acts as a negative regulator of Notch1 activation through interactions with specific EGF-like repeats. *Experimental cell research*, 303(2), pp.343–59.

Bänziger, C. et al., 2006. Wntless, a conserved membrane protein dedicated to the secretion of Wnt proteins from signaling cells. *Cell*, 125(3), pp.509–22.

Barker, N. et al., 2009. Crypt stem cells as the cells-of-origin of intestinal cancer. *Nature*, 457(7229), pp.608–11.

Barker, N. et al., 2007. Identification of stem cells in small intestine and colon by marker gene Lgr5. *Nature*, 449(7165), pp.1003–1007.

Barolo, S. et al., 2000. A notch-independent activity of suppressor of hairless is required for normal mechanoreceptor physiology. *Cell*, 103(6), pp.957–69.

Bartscherer, K. et al., 2006. Secretion of Wnt ligands requires Evi, a conserved transmembrane protein. *Cell*, 125(3), pp.523–33.

Batlle, E. et al., 2002. β-catenin and TCF mediate cell positioning in the intestinal epithelium by controlling the expression of EphB/EphrinB. *Cell*, 111(2), pp.251–263.

Behrens, J. et al., 1996. Functional interaction of beta-catenin with the transcription factor LEF-1. *Nature*, 382(6592), pp.638–42.

Belenkaya, T.Y. et al., 2008. The retromer complex influences Wnt secretion by recycling wntless from endosomes to the trans-Golgi network. *Developmental cell*, 14(1), pp.120–31.

Benhattar, J. et al., 1996. p53 mutations as a possible predictor of response to chemotherapy in metastatic colorectal carcinomas. *International journal of cancer*, 69(3), pp.190–2.

Bessho, Y. et al., 2003. Periodic repression by the bHLH factor Hes7 is an essential mechanism for the somite segmentation clock. *Genes & development*, 17(12), pp.1451–6.

Bevins, C.L., 2004. The Paneth cell and the innate immune response. *Current opinion in gastroenterology*, 20(6), pp.572–80.

Bevins, C.L. & Salzman, N.H., 2011. Paneth cells, antimicrobial peptides and maintenance of intestinal homeostasis. *Nature reviews. Microbiology*, 9(5), pp.356–368.

Bhanot, P. et al., 1996. A new member of the frizzled family from Drosophila functions as a Wingless receptor. *Nature*, 382(6588), pp.225–30.

Bizzozero, G., 1892. Über die schlauchförmigen Drüsen des Magendarmkanals und Beziehungen ihres Epithels zu dem Oberflächenepithel der Schleimhaut. *Arch. Mikrosk. Anat.*, 40, pp.325–375.

Bjerknes, M. & Cheng, H., 1981. The stem-cell zone of the small intestinal epithelium. I. Evidence from Paneth cells in the adult mouse. *The American journal of anatomy*, 160(1), pp.51–63.

Blaumueller, C.M. et al., 1997. Intracellular cleavage of Notch leads to a heterodimeric receptor on the plasma membrane. *Cell*, 90(2), pp.281–91.

Bokemeyer, C. et al., 2009. Fluorouracil, leucovorin, and oxaliplatin with and without cetuximab in the first-line treatment of metastatic colorectal cancer. *Journal of clinical oncology : official journal of the American Society of Clinical Oncology*, 27(5), pp.663–71.

Boland, P.M. & Fakih, M., 2014. The emerging role of neoadjuvant chemotherapy for

rectal cancer. *Journal of gastrointestinal oncology*, 5(5), pp.362–73.

Bossmann, B. & Haschen, R.J., 1983. Release of enzymes from rat jejunal mucosa by bile salts. *Journal of clinical chemistry and clinical biochemistry. Zeitschrift für klinische Chemie und klinische Biochemie*, 21(1), pp.1–9.

Bray, S.J., 2006. Notch signalling: a simple pathway becomes complex. *Nature reviews. Molecular cell biology*, 7(9), pp.678–89.

Bray, S.J. et al., 2008. The atypical mammalian ligand Delta-like homologue 1 (Dlk1) can regulate Notch signalling in Drosophila. *BMC developmental biology*, 8, p.11.

Brou, C. et al., 2000. A novel proteolytic cleavage involved in Notch signaling: the role of the disintegrin-metalloprotease TACE. *Molecular cell*, 5(2), pp.207–16.

Brückner, K. et al., 2000. Glycosyltransferase activity of Fringe modulates Notch-Delta interactions. *Nature*, 406(6794), pp.411–5.

Bruggeman, S.W.M. et al., 2005. Ink4a and Arf differentially affect cell proliferation and neural stem cell self-renewal in Bmi1-deficient mice. *Genes and Development*, 19(12), pp.1438–1443.

Bu, P. et al., 2013. A microRNA miR-34a-regulated bimodal switch targets notch in colon cancer stem cells. *Cell Stem Cell*, 12(5), pp.602–615.

Bu, P. et al., 2016. A miR-34a-Numb Feedforward Loop Triggered by Inflammation Regulates Asymmetric Stem Cell Division in Intestine and Colon Cancer. *Cell stem cell*, 18(2), pp.189–202.

Buchwald, G. et al., 2006. Structure and E3-ligase activity of the Ring-Ring complex of polycomb proteins Bmi1 and Ring1b. *The EMBO journal*, 25(11), pp.2465–74.

Bunz, F. et al., 1999. Disruption of p53 in human cancer cells alters the responses to therapeutic agents. *The Journal of clinical investigation*, 104(3), pp.263–9.

Burma, S. et al., 2001. ATM phosphorylates histone H2AX in response to DNA double-strand breaks. *The Journal of biological chemistry*, 276(45), pp.42462–7.

Candy, P.A. et al., 2013. Notch-induced transcription factors are predictive of survival and 5-fluorouracil response in colorectal cancer patients. *British journal of cancer*, 109(4), pp.1023–30.

Cao, R., Tsukada, Y.-I. & Zhang, Y., 2005. Role of Bmi-1 and Ring1A in H2A ubiquitylation and Hox gene silencing. *Molecular cell*, 20(6), pp.845–54.

Carmon, K.S. et al., 2011. R-spondins function as ligands of the orphan receptors LGR4 and LGR5 to regulate Wnt/beta-catenin signaling. *Proceedings of the National Academy of Sciences of the United States of America*, 108(28), pp.11452–11457.

Cavallo, R.A. et al., 1998. Drosophila Tcf and Groucho interact to repress Wingless signalling activity. *Nature*, 395(6702), pp.604–8.

Chanrion, M. et al., 2014. Concomitant Notch activation and p53 deletion trigger epithelial-to-mesenchymal transition and metastasis in mouse gut. *Nature communications*, 5, p.5005.

Chastagner, P., Israël, A. & Brou, C., 2008. AIP4/Itch regulates Notch receptor degradation in the absence of ligand. *PloS one*, 3(7), p.e2735.

Chastagner, P., Israël, A. & Brou, C., 2006. Itch/AIP4 mediates Deltex degradation through the formation of K29-linked polyubiquitin chains. *EMBO reports*, 7(11), pp.1147–

53.

Chen, F. et al., 2002. Hop is an unusual homeobox gene that modulates cardiac development. *Cell*, 110(6), pp.713–23.

Cheng, H. & Leblond, C.P., 1974. Origin, differentiation and renewal of the four main epithelial cell types in the mouse small intestine. V. Unitarian Theory of the origin of the four epithelial cell types. *The American journal of anatomy*, 141(4), pp.537–561.

Chiacchiera, F. et al., 2015. Polycomb Complex PRC1 Preserves Intestinal Stem Cell Identity by Sustaining Wnt/β-Catenin Transcriptional Activity. *Cell Stem Cell*, pp.1–13.

Chowdhury, D. et al., 2005. gamma-H2AX dephosphorylation by protein phosphatase 2A facilitates DNA double-strand break repair. *Molecular cell*, 20(5), pp.801–9.

Chu, D. et al., 2010. High level of Notch1 protein is associated with poor overall survival in colorectal cancer. *Annals of surgical oncology*, 17(5), pp.1337–42.

Chung, C.N. et al., 1994. Site-directed mutagenesis study on DNA binding regions of the mouse homologue of Suppressor of Hairless, RBP-J kappa. *Nucleic acids research*, 22(15), pp.2938–44.

Clevers, H., 2011. The cancer stem cell: premises, promises and challenges. *Nature medicine*, 17(3), pp.313–319.

Clevers, H., 2006. Wnt/??-Catenin Signaling in Development and Disease. *Cell*, 127(3), pp.469–480.

Clevers, H.C. & Bevins, C.L., 2013. Paneth cells: maestros of the small intestinal crypts. *Annual review of physiology*, 75, pp.289–311.

Cohen, M.H. et al., 2007. FDA drug approval summary: bevacizumab plus FOLFOX4 as second-line treatment of colorectal cancer. *The oncologist*, 12(3), pp.356–61.

Colak, S. & Medema, J.P., 2014. Cancer stem cells - important players in tumor therapy resistance. *FEBS Journal*, 281(21), pp.4779–4791.

Collu, G.M. et al., 2012. Dishevelled limits Notch signalling through inhibition of CSL. *Development (Cambridge, England)*, 139(23), pp.4405–15.

Collu, G.M., Hidalgo-Sastre, A. & Brennan, K., 2014. Wnt-Notch signalling crosstalk in development and disease. *Cellular and Molecular Life Sciences*, pp.3553–3567.

Coudreuse, D.Y.M. et al., 2006. Wnt gradient formation requires retromer function in Wnt-producing cells. *Science (New York, N.Y.)*, 312(5775), pp.921–4.

Couturier, L., Mazouni, K. & Schweisguth, F., 2013. Numb localizes at endosomes and controls the endosomal sorting of notch after asymmetric division in Drosophila. *Current biology : CB*, 23(7), pp.588–93.

Crabtree, M. et al., 2003. Refining the relation between “first hits” and “second hits” at the APC locus: the “loose fit” model and evidence for differences in somatic mutation spectra among patients. *Oncogene*, 22(27), pp.4257–4265.

Cui, X.-Y. et al., 2004. NB-3/Notch1 pathway via Deltex1 promotes neural progenitor cell differentiation into oligodendrocytes. *The Journal of biological chemistry*, 279(24), pp.25858–65.

Cunliffe, R.N. et al., 2001. Human defensin 5 is stored in precursor form in normal Paneth

cells and is expressed by some villous epithelial cells and by metaplastic Paneth cells in the colon in inflammatory bowel disease. *Gut*, 48(2), pp.176–85.

Van Cutsem, E. et al., 2009. Cetuximab and chemotherapy as initial treatment for metastatic colorectal cancer. *The New England journal of medicine*, 360(14), pp.1408–17.

Dai, Y. et al., 2014. Silencing of Jagged1 inhibits cell growth and invasion in colorectal cancer. *Cell death & disease*, 5, p.e1170.

Dalerba, P. et al., 2007. Phenotypic characterization of human colorectal cancer stem cells. *Proceedings of the National Academy of Sciences of the United States of America*, 104(24), pp.10158–10163.

Daniels, D.L. & Weis, W.I., 2005. Beta-catenin directly displaces Groucho/TLE repressors from Tcf/Lef in Wnt-mediated transcription activation. *Nature structural & molecular biology*, 12(4), pp.364–71.

Davidson, G. et al., 2005. Casein kinase 1 gamma couples Wnt receptor activation to cytoplasmic signal transduction. *Nature*, 438(7069), pp.867–72.

Deckx, R.J., Vantrappen, G.R. & Parein, M.M., 1967. Localization of lysozyme activity in a Paneth cell granule fraction. *Biochimica et biophysica acta*, 139(1), pp.204–7.

Dexter, J.S., 1914. The Analysis of a Case of Continuous Variation in Drosophila by a Study of Its Linkage Relations. *The American Naturalist*, 48(576), pp.712–758.

Dick, J.E., 2008. Stem cell concepts renew cancer research. *Blood*, 112(13), pp.4793–4807.

Douillard, J.-Y. et al., 2010. Randomized, phase III trial of panitumumab with infusional fluorouracil, leucovorin, and oxaliplatin (FOLFOX4) versus FOLFOX4 alone as first-line treatment in patients with previously untreated metastatic colorectal cancer: the PRIME study. *Journal of clinical oncology : official journal of the American Society of Clinical Oncology*, 28(31), pp.4697–705.

Dow, L.E. et al., 2015. Apc Restoration Promotes Cellular Differentiation and Reestablishes Crypt Homeostasis in Colorectal Cancer. *Cell*, 161(7), pp.1539–1552.

Doyle, T.G., Wen, C. & Greenwald, I., 2000. SEL-8, a nuclear protein required for LIN-12 and GLP-1 signaling in Caenorhabditis elegans. *Proceedings of the National Academy of Sciences of the United States of America*, 97(14), pp.7877–81.

Drost, J. et al., 2015. Sequential cancer mutations in cultured human intestinal stem cells. *Nature*, 521(7550), pp.43–7.

Eiraku, M. et al., 2005. DNER acts as a neuron-specific Notch ligand during Bergmann glial development. *Nature neuroscience*, 8(7), pp.873–80.

el-Deiry, W.S. et al., 1993. WAF1, a potential mediator of p53 tumor suppression. *Cell*, 75(4), pp.817–25.

Eleftheriou, A., Yoshida, M. & Henderson, B.R., 2001. Nuclear export of human beta-catenin can occur independent of CRM1 and the adenomatous polyposis coli tumor suppressor. *The Journal of biological chemistry*, 276(28), pp.25883–8.

Engelstoft, M.S. et al., 2013. Enteroendocrine cell types revisited. *Current Opinion in Pharmacology*, 13(6), pp.912–921.

van Es, J.H. et al., 2012. Dll1+ secretory progenitor cells revert to stem cells upon crypt damage. *Nature Cell Biology*, 14(10), pp.1099–1104.

van Es, J.H. et al., 2005. Notch/gamma-secretase inhibition turns proliferative cells in intestinal crypts and adenomas into goblet cells. *Nature*, 435(7044), pp.959–963.

Escobar, M. et al., 2011. Intestinal epithelial stem cells do not protect their genome by asymmetric chromosome segregation. *Nature communications*, 2, p.258.

Espinosa, L. et al., 2003. Phosphorylation by glycogen synthase kinase-3β down-regulates Notch activity, a link for Notch and Wnt pathways. *Journal of Biological Chemistry*, 278(34), pp.32227–32235.

Estrach, S. et al., 2006. Jagged 1 is a beta-catenin target gene required for ectopic hair follicle formation in adult epidermis. *Development (Cambridge, England)*, 133(22), pp.4427–38.

Facchino, S. et al., 2010. BMI1 confers radioresistance to normal and cancerous neural stem cells through recruitment of the DNA damage response machinery. *The Journal of neuroscience : the official journal of the Society for Neuroscience*, 30(30), pp.10096–10111.

Fagotto, F., Glück, U. & Gumbiner, B.M., 1998. Nuclear localization signal-independent and importin/karyopherin-independent nuclear import of β-catenin. *Current Biology*, 8(4), pp.181–190.

Fatehullah, A., Tan, S.H. & Barker, N., 2016. Organoids as an in vitro model of human development and disease. *Nature Cell Biology*, 18(3), pp.246–254.

Fearon, E.R., 2011. Molecular genetics of colorectal cancer. *Annual review of pathology*, 6, pp.479–507.

Fearon, E.R. & Vogelstein, B., 1990. A genetic model for colorectal tumorigenesis. *Cell*, 61(5), pp.759–767.

Fender, A.W. et al., 2015. Notch-1 promotes stemness and epithelial to mesenchymal transition in colorectal cancer. *Journal of cellular biochemistry*, 116(11), pp.2517–27.

Feng, Y. et al., 2011. Mutant KRAS promotes hyperplasia and alters differentiation in the colon epithelium but does not expand the presumptive stem cell pool. *Gastroenterology*, 141(3), pp.1003–1013.e1–10.

Ferlay, J. et al., 2013. GLOBOCAN 2012 v1.0, Cancer Incidence and Mortality Worldwide: IARC CancerBase No. 11 [Internet]. *Lyon, France: International Agency for Research on Cancer;* Available at: http://globocan.iarc.fr [Accessed April 17, 2015].

Fernandez-Valdivia, R. et al., 2011. Regulation of mammalian Notch signaling and embryonic development by the protein O-glucosyltransferase Rumi. *Development (Cambridge, England)*, 138(10), pp.1925–34.

Fischer, A. & Gessler, M., 2007. Delta-Notch--and then? Protein interactions and proposed modes of repression by Hes and Hey bHLH factors. *Nucleic acids research*, 35(14), pp.4583–96.

Fischer, M. et al., 2011. Anti-DLL4 inhibits growth and reduces tumor-initiating cell frequency in colorectal tumors with oncogenic KRAS mutations. *Cancer research*, 71(5), pp.1520–5.

Fleming, R.J. et al., 1990. The gene Serrate encodes a putative EGF-like transmembrane protein essential for proper ectodermal development in Drosophila melanogaster. *Genes & development*, 4(12A), pp.2188–201.

van der Flier, L.G., Haegebarth, A., et al., 2009. OLFM4 Is a Robust Marker for Stem Cells in Human Intestine and Marks a Subset of Colorectal Cancer Cells. *Gastroenterology*, 137(1), pp.15–17.

Van der Flier, L.G. et al., 2007. The Intestinal Wnt/TCF Signature. *Gastroenterology*, 132(2), pp.628–32.

van der Flier, L.G., van Gijn, M.E., et al., 2009. Transcription Factor Achaete Scute-Like 2 Controls Intestinal Stem Cell Fate. *Cell*, 136(5), pp.903–912.

Flug, F. et al., 1987. cis-acting elements of the rat growth hormone gene which mediate basal and regulated expression by thyroid hormone. *The Journal of biological chemistry*, 262(13), pp.6373–82.

Fodde, R., Smits, R. & Clevers, H., 2001. APC, signal transduction and genetic instability in colorectal cancer. *Nature reviews. Cancer*, 1(1), pp.55–67.

Foltz, D.R. et al., 2002. Glycogen synthase kinase-3beta modulates notch signaling and stability. *Current biology : CB*, 12(12), pp.1006–11.

Fre, S. et al., 2009. Notch and Wnt signals cooperatively control cell proliferation and tumorigenesis in the intestine. *Proceedings of the National Academy of Sciences of the United States of America*, 106(15), pp.6309–6314.

Fryer, C.J. et al., 2002. Mastermind mediates chromatin-specific transcription and turnover of the Notch enhancer complex. *Genes & development*, 16(11), pp.1397–411.

Fryer, C.J., White, J.B. & Jones, K.A., 2004. Mastermind recruits CycC:CDK8 to phosphorylate the Notch ICD and coordinate activation with turnover. *Molecular cell*, 16(4), pp.509–20.

Fujimi, T.J., Hatayama, M. & Aruga, J., 2012. Xenopus Zic3 controls notochord and organizer development through suppression of the Wnt/β-catenin signaling pathway. *Developmental biology*, 361(2), pp.220–31.

Galceran, J. et al., 2004. LEF1-mediated regulation of Delta-like1 links Wnt and Notch signaling in somitogenesis. *Genes & development*, 18(22), pp.2718–23.

Le Gall, M., De Mattei, C. & Giniger, E., 2008. Molecular separation of two signaling pathways for the receptor, Notch. *Developmental biology*, 313(2), pp.556–67.

Gao, W. et al., 2013. Isolation and phenotypic characterization of colorectal cancer stem cells with organ-specific metastatic potential. *Gastroenterology*, 145(3), pp.636–46.e5.

Gerbe, F. et al., 2011. Distinct ATOH1 and Neurog3 requirements define tuft cells as a new secretory cell type in the intestinal epithelium. *Journal of Cell Biology*, 192(5), pp.767–780.

Gerbe, F., Legraverend, C. & Jay, P., 2012. The intestinal epithelium tuft cells: Specification and function. *Cellular and Molecular Life Sciences*, 69(17), pp.2907–2917.

Gersemann, M. et al., 2012. Olfactomedin-4 is a glycoprotein secreted into mucus in active IBD. *Journal of Crohn's & colitis*, 6(4), pp.425–34.

Ghaleb, A.M. et al., 2008. Notch inhibits expression of the Krüppel-like factor 4 tumor suppressor in the intestinal epithelium. *Molecular cancer research : MCR*, 6(12), pp.1920–7.

Ginjala, V. et al., 2011. BMI1 is recruited to DNA breaks and contributes to DNA damage-induced H2A ubiquitination and repair. *Molecular and cellular biology*, 31(10), pp.1972–1982.

Glinka, A. et al., 1998. Dickkopf-1 is a member of a new family of secreted proteins and functions in head induction. *Nature*, 391(6665), pp.357–62.

Glinka, A. et al., 2011. LGR4 and LGR5 are R-spondin receptors mediating Wnt/β-catenin and Wnt/PCP signalling. *EMBO reports*, 12(10), pp.1055–1061.

Gordon, W.R. et al., 2015. Mechanical Allostery: Evidence for a Force Requirement in the Proteolytic Activation of Notch. *Developmental Cell*, 33(6), pp.729–736.

Gregorieff, A. & Clevers, H., 2005. Wnt signaling in the intestinal epithelium: From endoderm to cancer. *Genes and Development*, 19(8), pp.877–890.

Gu, B. et al., 2013. Chromatin effector Pygo2 mediates wnt-notch crosstalk to suppress luminal/alveolar potential of mammary stem and basal cells. *Cell Stem Cell*, 13(1), pp.48–61.

Guilmeau, S. et al., 2008. Intestinal deletion of Pofut1 in the mouse inactivates notch signaling and causes enterocolitis. *Gastroenterology*, 135(3), pp.849–60, 860.e1–6.

Guinney, J. et al., 2015. The consensus molecular subtypes of colorectal cancer. *Nature Medicine*, 21(11), pp.1350–6.

Guiu, J. et al., 2013. Hes repressors are essential regulators of hematopoietic stem cell development downstream of Notch signaling. *The Journal of experimental medicine*, 210(1), pp.71–84.

Guiu, J. et al., 2014. Identification of Cdca7 as a novel Notch transcriptional target involved in hematopoietic stem cell emergence. *The Journal of experimental medicine*, 211(12), pp.2411–23.

Gur, G. et al., 2004. LRIG1 restricts growth factor signaling by enhancing receptor ubiquitylation and degradation. *The EMBO journal*, 23(16), pp.3270–81.

Han, H. et al., 2002. Inducible gene knockout of transcription factor recombination signal binding protein-J reveals its essential role in T versus B lineage decision. *International immunology*, 14(6), pp.637–45.

Hao, H.-X. et al., 2012. ZNRF3 promotes Wnt receptor turnover in an R-spondin-sensitive manner. *Nature*, 485(7397), pp.195–200.

Harada, N. et al., 1999. Intestinal polyposis in mice with a dominant stable mutation of the beta-catenin gene. *The EMBO journal*, 18(21), pp.5931–42.

Harley, C.B., Futcher, A.B. & Greider, C.W., 1990. Telomeres shorten during ageing of human fibroblasts. *Nature*, 345(6274), pp.458–60.

Harper, J.W. et al., 1993. The p21 Cdk-interacting protein Cip1 is a potent inhibitor of G1 cyclin-dependent kinases. *Cell*, 75(4), pp.805–16.

Hart, M. et al., 1999. The F-box protein beta-TrCP associates with phosphorylated beta-catenin and regulates its activity in the cell. *Current biology : CB*, 9(4), pp.207–10.

Hassan, K.A. et al., 2013. Notch pathway activity identifies cells with cancer stem cell-like properties and correlates with worse survival in lung adenocarcinoma. *Clinical cancer research : an official journal of the American Association for Cancer Research*, 19(8), pp.1972–80.

Hayashi, S. & McMahon, A.P., 2002. Efficient recombination in diverse tissues by a tamoxifen-inducible form of Cre: a tool for temporally regulated gene activation/inactivation in the mouse. *Developmental biology*, 244(2), pp.305–18.

Hayward, P. et al., 2005. Notch modulates Wnt signalling by associating with Armadillo/beta-catenin and regulating its transcriptional activity. *Development (Cambridge, England)*, 132(8), pp.1819–30.

Hayward, P., Balayo, T. & Arias, A.M., 2006. Notch synergizes with axin to regulate the activity of Armadillo in Drosophila. *Developmental Dynamics*, 235(10), pp.2656–2666.

Hayward, P., Kalmar, T. & Arias, A.M., 2008. Wnt/Notch signalling and information processing during development. *Development (Cambridge, England)*, 135(3), pp.411–424.

He, T.C. et al., 1998. Identification of c-MYC as a target of the APC pathway. *Science (New York, N.Y.)*, 281(5382), pp.1509–12.

Hinck, L., Nelson, W.J. & Papkoff, J., 1994. Wnt-1 modulates cell-cell adhesion in mammalian cells by stabilizing beta-catenin binding to the cell adhesion protein cadherin. *The Journal of cell biology*, 124(5), pp.729–41.

Hirata, H. et al., 2002. Oscillatory expression of the bHLH factor Hes1 regulated by a negative feedback loop. *Science (New York, N.Y.)*, 298(5594), pp.840–3.

Hoey, T. et al., 2009. DLL4 blockade inhibits tumor growth and reduces tumor-initiating cell frequency. *Cell stem cell*, 5(2), pp.168–77.

Hori, K. et al., 2011. Synergy between the ESCRT-III complex and Deltex defines a ligand-independent Notch signal. *The Journal of cell biology*, 195(6), pp.1005–15.

Hsu, S.Y., Liang, S.G. & Hsueh, A.J., 1998. Characterization of two LGR genes homologous to gonadotropin and thyrotropin receptors with extracellular leucine-rich repeats and a G protein-coupled, seven-transmembrane region. *Molecular endocrinology (Baltimore, Md.)*, 12(12), pp.1830–1845.

Hu, Q.-D. et al., 2003. F3/contactin acts as a functional ligand for Notch during oligodendrocyte maturation. *Cell*, 115(2), pp.163–75.

Hua, G. et al., 2012. Crypt base columnar stem cells in small intestines of mice are radioresistant. *Gastroenterology*, 143(5), pp.1266–1276.

Huang, E.H. et al., 2009. Aldehyde dehydrogenase 1 is a marker for normal and malignant human colonic stem cells (SC) and tracks SC overpopulation during colon tumorigenesis. *Cancer research*, 69(8), pp.3382–9.

Huelsken, J. et al., 2001. beta-Catenin controls hair follicle morphogenesis and stem cell differentiation in the skin. *Cell*, 105(4), pp.533–45.

Ichii, S. et al., 1993. Detailed analysis of genetic alterations in colorectal tumors from patients with and without familial adenomatous polyposis (FAP). *Oncogene*, 8(9), pp.2399–2405.

Ikeda, S. et al., 1998. Axin, a negative regulator of the Wnt signaling pathway, forms a complex with GSK-3beta and beta-catenin and promotes GSK-3beta-dependent phosphorylation of beta-catenin. *The EMBO journal*, 17(5), pp.1371–84.

Ireland, H. et al., 2004. Inducible Cre-mediated control of gene expression in the murine gastrointestinal tract: effect of loss of beta-catenin. *Gastroenterology*, 126(5),

pp.1236–46.

Ismail, H. et al., 2010. BMI1-mediated histone ubiquitylation promotes DNA double-strand break repair. *Journal of Cell Biology*, 191(1), pp.45–60.

Iso, T., Kedes, L. & Hamamori, Y., 2003. HES and HERP families: multiple effectors of the Notch signaling pathway. *Journal of cellular physiology*, 194(3), pp.237–55.

Itasaki, N. et al., 2003. Wise, a context-dependent activator and inhibitor of Wnt signalling. *Development (Cambridge, England)*, 130(18), pp.4295–305.

Ito, K. et al., 2008. RUNX3 attenuates beta-catenin/T cell factors in intestinal tumorigenesis. *Cancer cell*, 14(3), pp.226–37.

Ito, S., 1965. The enteric surface coat on cat intestinal microvilli. *The Journal of cell biology*, 27(3), pp.475–91.

Itzkovitz, S. et al., 2011. Single-molecule transcript counting of stem-cell markers in the mouse intestine. *Nature Cell Biology*, 14(1), pp.106–114.

Jacobs, J.J. et al., 1999. The oncogene and Polycomb-group gene bmi-1 regulates cell proliferation and senescence through the ink4a locus. *Nature*, 397(6715), pp.164–168.

Janzen, V. et al., 2006. Stem-cell ageing modified by the cyclin-dependent kinase inhibitor p16INK4a. *Nature*, 443(7110), pp.421–426.

Jarriault, S. et al., 1995. Signalling downstream of activated mammalian Notch. *Nature*, 377(6547), pp.355–358.

Järvi, O. & Keyrilainen, O., 1955. On the cellular structures of the epithelial invasions in the glandular stomach of mice caused by intramural application of 20-methylcholanthrene. *Acta Pathol. Microbiol. Scand.*, 111(Suppl), pp.72–73.

Jayasena, C.S. et al., 2008. Notch signaling augments the canonical Wnt pathway to specify the size of the otic placode. *Development (Cambridge, England)*, 135(13), pp.2251–61.

Jensen, J. et al., 2000. Control of endodermal endocrine development by Hes-1. *Nature genetics*, 24(1), pp.36–44.

Jho, E. et al., 2002. Wnt/beta-catenin/Tcf signaling induces the transcription of Axin2, a negative regulator of the signaling pathway. *Molecular and cellular biology*, 22(4), pp.1172–83.

Jin, Y.H. et al., 2009. Beta-catenin modulates the level and transcriptional activity of Notch1/NICD through its direct interaction. *Biochimica et biophysica acta*, 1793(2), pp.290–9.

Johnston, S.H. et al., 1997. A family of mammalian Fringe genes implicated in boundary determination and the Notch pathway. *Development (Cambridge, England)*, 124(11), pp.2245–54.

Jubb, A.M. et al., 2006. Achaete-scute like 2 (ascl2) is a target of Wnt signalling and is upregulated in intestinal neoplasia. *Oncogene*, 25(24), pp.3445–57.

Jung, C. et al., 2005. HOXB13 is downregulated in colorectal cancer to confer TCF4-mediated transactivation. *British journal of cancer*, 92(12), pp.2233–9.

Jung, P. et al., 2011. Isolation and in vitro expansion of human colonic stem cells. *Nature Medicine*, 17(10), pp.1225–1227.

Kalén, M. et al., 2011. Gamma-secretase inhibitor treatment promotes VEGF-A-driven blood vessel growth and vascular leakage but disrupts neovascular perfusion. *PloS one*, 6(4), p.e18709.

Kato, H. et al., 1997. Involvement of RBP-J in biological functions of mouse Notch1 and its derivatives. *Development (Cambridge, England)*, 124(20), pp.4133–41.

Katoh, M., 2005. WNT/PCP signaling pathway and human cancer (review). *Oncology reports*, 14(6), pp.1583–8.

Katz, J.P. et al., 2002. The zinc-finger transcription factor Klf4 is required for terminal differentiation of goblet cells in the colon. *Development (Cambridge, England)*, 129(11), pp.2619–28.

Kiernan, A.E., Xu, J. & Gridley, T., 2006. The Notch ligand JAG1 is required for sensory progenitor development in the mammalian inner ear. *PLoS genetics*, 2(1), p.e4.

Kim, H. et al., 2012. Notch1 counteracts WNT / -catenin signaling through chromatin modi cation in colorectal cancer. *The Journal of clinical investigation*, 122(9), pp.3248–3259.

Kim, K.-A. et al., 2005. Mitogenic influence of human R-spondin1 on the intestinal epithelium. *Science (New York, N.Y.)*, 309(5738), pp.1256–9.

Kishi, N. et al., 2001. Murine homologs of deltex define a novel gene family involved in vertebrate Notch signaling and neurogenesis. *International journal of developmental neuroscience : the official journal of the International Society for Developmental Neuroscience*, 19(1), pp.21–35.

Kishida, S. et al., 1998. Axin, a negative regulator of the wnt signaling pathway, directly interacts with adenomatous polyposis coli and regulates the stabilization of beta-catenin. *The Journal of biological chemistry*, 273(18), pp.10823–6.

Kitagawa, M. et al., 1999. An F-box protein, FWD1, mediates ubiquitin-dependent proteolysis of beta-catenin. *The EMBO journal*, 18(9), pp.2401–10.

Klein, T. & Arias, A.M., 1999. The vestigial gene product provides a molecular context for the interpretation of signals during the development of the wing in Drosophila. *Development (Cambridge, England)*, 126(5), pp.913–25.

Klinakis, A. et al., 2006. Myc is a Notch1 transcriptional target and a requisite for Notch1-induced mammary tumorigenesis in mice. *Proceedings of the National Academy of Sciences of the United States of America*, 103(24), pp.9262–7.

Klingelhoefer, L. & Reichmann, H., 2015. Pathogenesis of Parkinson disease-the gut-brain axis and environmental factors. *Nature reviews. Neurology*, 11(11), pp.625–36.

Kohn, A.D. & Moon, R.T., Wnt and calcium signaling: beta-catenin-independent pathways. *Cell calcium*, 38(3-4), pp.439–46.

Koo, B.-K. et al., 2005. Mind bomb 1 is essential for generating functional Notch ligands to activate Notch. *Development (Cambridge, England)*, 132(15), pp.3459–70.

Koo, B.-K. et al., 2012. Tumour suppressor RNF43 is a stem-cell E3 ligase that induces endocytosis of Wnt receptors. *Nature*, 488(7413), pp.665–669.

Kopan, R. et al., 1996. Signal transduction by activated mNotch: importance of proteolytic processing and its regulation by the extracellular domain. *Proceedings of the National Academy of Sciences of the United States of America*, 93(4), pp.1683–8.

Korinek, V. et al., 1997. Constitutive transcriptional activation by a beta-catenin-Tcf complex in APC-/- colon carcinoma. *Science (New York, N.Y.)*, 275(5307), pp.1784–1787.

Korinek, V. et al., 1998. Depletion of epithelial stem-cell compartments in the small intestine of mice lacking Tcf-4. *Nature genetics*, 19(4), pp.379–83.

Krejcí, A. et al., 2009. Direct response to Notch activation: signaling crosstalk and incoherent logic. *Science signaling*, 2(55), p.ra1.

Krishnamurthy, J. et al., 2004. Ink4a/Arf expression is a biomarker of aging. *The Journal of clinical investigation*, 114(9), pp.1299–307.

Kwon, C. et al., 2009. A regulatory pathway involving Notch1/beta-catenin/Isl1 determines cardiac progenitor cell fate. *Nature cell biology*, 11(8), pp.951–7.

Kwon, C. et al., 2011. Notch post-translationally regulates β-catenin protein in stem and progenitor cells. *Nature cell biology*, 13(10), pp.1244–51.

Lafkas, D. et al., 2015. Therapeutic antibodies reveal Notch control of transdifferentiation in the adult lung. *Nature*, 528(7580), pp.127–131.

Lagadec, C. et al., 2013. Radiation-induced Notch signaling in breast cancer stem cells. *International journal of radiation oncology, biology, physics*, 87(3), pp.609–18.

Lai, E.C., 2005. The ubiquitin ligase Drosophila Mind bomb promotes Notch signaling by regulating the localization and activity of Serrate and Delta. *Development*, 132(10), pp.2319–2332.

de Lau, W. et al., 2011. Lgr5 homologues associate with Wnt receptors and mediate R-spondin signalling. *Nature*, 476(7360), pp.293–297.

Lee, G. et al., 2009. Response of small intestinal epithelial cells to acute disruption of cell division through CDC25 deletion. *Proceedings of the National Academy of Sciences of the United States of America*, 106(12), pp.4701–4706.

Levy, D.B. et al., 1994. Inactivation of both APC alleles in human and mouse tumors. *Cancer Research*, 54(22), pp.5953–5958.

Li, K. et al., 2008. Modulation of Notch signaling by antibodies specific for the extracellular negative regulatory region of NOTCH3. *The Journal of biological chemistry*, 283(12), pp.8046–54.

Li, L. & Clevers, H., 2010. Coexistence of quiescent and active adult stem cells in mammals. *Science (New York, N.Y.)*, 327(5965), pp.542–545.

Li, V.S.W. et al., 2012. Wnt signaling through inhibition of β-catenin degradation in an intact Axin1 complex. *Cell*, 149(6), pp.1245–56.

Lin, L. et al., 2010. Targeting specific regions of the Notch3 ligand-binding domain induces apoptosis and inhibits tumor growth in lung cancer. *Cancer research*, 70(2), pp.632–8.

Liu, C. et al., 2002. Control of beta-catenin phosphorylation/degradation by a dual-kinase mechanism. *Cell*, 108(6), pp.837–47.

Liu, W. et al., 2006. The glycoprotein hGC-1 binds to cadherin and lectins. *Experimental cell research*, 312(10), pp.1785–97.

Logeat, F. et al., 1998. The Notch1 receptor is cleaved constitutively by a furin-like convertase. *Proceedings of the National Academy of Sciences of the United States*

of America, 95(14), pp.8108–12.

Lopez-Arribillaga, E. et al., 2014. Bmi1 regulates murine intestinal stem cell proliferation and self-renewal downstream of Notch. *Development*, 142(1), pp.41–50.

Loregger, A. et al., 2015. The E3 ligase RNF43 inhibits Wnt signaling downstream of mutated β-catenin by sequestering TCF4 to the nuclear membrane. *Science Signaling*, 8(393), pp.ra90–ra90.

Lu, J. et al., 2013. Endothelial Cells Promote the Colorectal Cancer Stem Cell Phenotype through a Soluble Form of Jagged-1. *Cancer Cell*, 23(2), pp.171–185.

Van Der Lugt, N.M.T. et al., 1994. Posterior transformation, neurological abnormalities, and severe hematopoietic defects in mice with a targeted deletion of the bmi-1 proto-oncogene. *Genes and Development*, 8(7), pp.757–769.

Luo, F. et al., 2007. Conditional expression of mutated K-ras accelerates intestinal tumorigenesis in Msh2-deficient mice. *Oncogene*, 26(30), pp.4415–27.

Luo, F. et al., 2011. Synergism between K-rasVal12 and mutant Apc accelerates murine large intestinal tumourigenesis. *Oncology reports*, 26(1), pp.125–33.

Mabbott, N. a et al., 2013. Microfold (M) cells: important immunosurveillance posts in the intestinal epithelium. *Mucosal immunology*, 6(4), pp.666–77.

MacDonald, B.T., Tamai, K. & He, X., 2009. Wnt/??-Catenin Signaling: Components, Mechanisms, and Diseases. *Developmental Cell*, 17(1), pp.9–26.

Mailhos, C. et al., 2001. Delta4, an endothelial specific notch ligand expressed at sites of physiological and tumor angiogenesis. *Differentiation; research in biological diversity*, 69(2-3), pp.135–44.

Mangan, S. & Alon, U., 2003. Structure and function of the feed-forward loop network motif. *Proceedings of the National Academy of Sciences of the United States of America*, 100(21), pp.11980–5.

el Marjou, F. et al., 2004. Tissue-specific and inducible Cre-mediated recombination in the gut epithelium. *Genesis*, 39(3), pp.186–193.

Martinez, A.-M. et al., 2009. Polyhomeotic has a tumor suppressor activity mediated by repression of Notch signaling. *Nature genetics*, 41(10), pp.1076–82.

Masi, G. et al., 2006. First-line 5-fluorouracil/folinic acid, oxaliplatin and irinotecan (FOLFOXIRI) does not impair the feasibility and the activity of second line treatments in metastatic colorectal cancer. *Annals of oncology : official journal of the European Society for Medical Oncology / ESMO*, 17(8), pp.1249–54.

Matano, M. et al., 2015. Modeling colorectal cancer using CRISPR-Cas9–mediated engineering of human intestinal organoids. *Nature Medicine*, 21(3), pp.256–62.

McGill, M.A. et al., 2009. Numb regulates post-endocytic trafficking and degradation of Notch1. *The Journal of biological chemistry*, 284(39), pp.26427–38.

Meng, R.D. et al., 2009. gamma-Secretase inhibitors abrogate oxaliplatin-induced activation of the Notch-1 signaling pathway in colon cancer cells resulting in enhanced chemosensitivity. *Cancer research*, 69(2), pp.573–82.

Merlos-Suárez, A. et al., 2011. The intestinal stem cell signature identifies colorectal cancer stem cells and predicts disease relapse. *Cell Stem Cell*, 8(5), pp.511–524.

Miles, K.M. et al., 2014. Dll4 blockade potentiates the anti-tumor effects of VEGF

inhibition in renal cell carcinoma patient-derived xenografts. *PloS one*, 9(11), p.e112371.

Miyamoto, A. et al., 2006. Microfibrillar proteins MAGP-1 and MAGP-2 induce Notch1 extracellular domain dissociation and receptor activation. *The Journal of biological chemistry*, 281(15), pp.10089–97.

Miyamoto, S., Nakanishi, M. & Rosenberg, D.W., 2013. Suppression of colon carcinogenesis by targeting Notch signaling. *Carcinogenesis*, 34(10), pp.2415–23.

Miyashita, T. et al., 1994. Tumor suppressor p53 is a regulator of bcl-2 and bax gene expression in vitro and in vivo. *Oncogene*, 9(6), pp.1799–805.

Mizugaki, H. et al., 2012. γ-Secretase inhibitor enhances antitumour effect of radiation in Notch-expressing lung cancer. *British journal of cancer*, 106(12), pp.1953–9.

Moellering, R.E. et al., 2009. Direct inhibition of the NOTCH transcription factor complex. *Nature*, 462(7270), pp.182–8.

Molofsky, A. V et al., 2005. Bmi-1 promotes neural stem cell self-renewal and neural development but not mouse growth and survival by repressing the p16Ink4a and p19Arf senescence pathways. *Genes & development*, 19(12), pp.1432–1437.

Moloney, D.J. et al., 2000. Fringe is a glycosyltransferase that modifies Notch. *Nature*, 406(6794), pp.369–75.

Montgomery, R.K. et al., 2011. Mouse telomerase reverse transcriptase (mTert) expression marks slowly cycling intestinal stem cells. *Proceedings of the National Academy of Sciences of the United States of America*, 108(1), pp.179–184.

Morin, P.J. et al., 1997. Activation of beta-catenin-Tcf signaling in colon cancer by mutations in beta-catenin or APC. *Science (New York, N.Y.)*, 275(5307), pp.1787–1790.

Mumm, J.S. et al., 2000. A ligand-induced extracellular cleavage regulates gamma-secretase-like proteolytic activation of Notch1. *Molecular cell*, 5(2), pp.197–206.

Munemitsu, S. et al., 1995. Regulation of intracellular beta-catenin levels by the adenomatous polyposis coli (APC) tumor-suppressor protein. *Proceedings of the National Academy of Sciences of the United States of America*, 92(7), pp.3046–3050.

Muñoz, J. et al., 2012. The Lgr5 intestinal stem cell signature: robust expression of proposed quiescent "+4" cell markers. *The EMBO Journal*, 31(14), pp.3079–3091.

Murayama, M. et al., 2009. Musashi-1 suppresses expression of Paneth cell-specific genes in human intestinal epithelial cells. *Journal of gastroenterology*, 44(3), pp.173–82.

Murtaugh, L.C. et al., 2003. Notch signaling controls multiple steps of pancreatic differentiation. *Proceedings of the National Academy of Sciences of the United States of America*, 100(25), pp.14920–5.

Nacerddine, K. et al., 2012. Akt-mediated phosphorylation of Bmi1 modulates its oncogenic potential, E3 ligase activity, and DNA damage repair activity in mouse prostate cancer. *The Journal of clinical investigation*, 122(5), pp.1920–1932.

Nagel, A.C. et al., 2005. Hairless-mediated repression of notch target genes requires the combined activity of Groucho and CtBP corepressors. *Molecular and cellular biology*, 25(23), pp.10433–41.

Nakanishi, Y. et al., 2013. Dclk1 distinguishes between tumor and normal stem cells in the intestine. *Nature genetics*, 45(1), pp.98–103.

Neumann, J. et al., 2011. SOX2 expression correlates with lymph-node metastases and distant spread in right-sided colon cancer. *BMC cancer*, 11, p.518.

Nichols, J.T. et al., 2007. DSL ligand endocytosis physically dissociates Notch1 heterodimers before activating proteolysis can occur. *The Journal of cell biology*, 176(4), pp.445–58.

Noguera-Troise, I. et al., 2006. Blockade of Dll4 inhibits tumour growth by promoting non-productive angiogenesis. *Nature*, 444(7122), pp.1032–7.

Nusse, R. & Varmus, H.E., 1982. Many tumors induced by the mouse mammary tumor virus contain a provirus integrated in the same region of the host genome. *Cell*, 31(1), pp.99–109.

Nüsslein-Volhard, C. & Wieschaus, E., 1980. Mutations affecting segment number and polarity in Drosophila. *Nature*, 287(5785), pp.795–801.

O'Brien, C.A. et al., 2007. A human colon cancer cell capable of initiating tumour growth in immunodeficient mice. *Nature*, 445(7123), pp.106–110.

O'Neil, J. et al., 2007. FBW7 mutations in leukemic cells mediate NOTCH pathway activation and resistance to gamma-secretase inhibitors. *The Journal of experimental medicine*, 204(8), pp.1813–24.

Oguro, H. et al., 2006. Differential impact of Ink4a and Arf on hematopoietic stem cells and their bone marrow microenvironment in Bmi1-deficient mice. *The Journal of experimental medicine*, 203(10), pp.2247–2253.

Okajima, T. & Irvine, K.D., 2002. Regulation of notch signaling by o-linked fucose. *Cell*, 111(6), pp.893–904.

Okochi, M. et al., 2002. Presenilins mediate a dual intramembranous gamma-secretase cleavage of Notch-1. *The EMBO journal*, 21(20), pp.5408–16.

Ordentlich, P. et al., 1998. Notch inhibition of E47 supports the existence of a novel signaling pathway. *Molecular and cellular biology*, 18(4), pp.2230–9.

Ouellette, A.J. et al., 1992. Purification and primary structure of murine cryptdin-1, a Paneth cell defensin. *FEBS letters*, 304(2-3), pp.146–8.

Palagani, V. et al., 2012. Epithelial mesenchymal transition and pancreatic tumor initiating CD44+/EpCAM+ cells are inhibited by γ-secretase inhibitor IX. *PloS one*, 7(10), p.e46514.

Palomero, T. et al., 2006. NOTCH1 directly regulates c-MYC and activates a feed-forward-loop transcriptional network promoting leukemic cell growth. *Proceedings of the National Academy of Sciences of the United States of America*, 103(48), pp.18261–6.

Pan, M.R. et al., 2011. Monoubiquitination of H2AX protein regulates DNA damage response signaling. *Journal of Biological Chemistry*, 286(32), pp.28599–28607.

Paneth, J., 1888. Ueber die secernirenden Zellen des Dünndarm-Epithels. *Arch. Mikrosk. Anat.*, 31, pp.113–191.

Pang, R. et al., 2010. A subpopulation of CD26 + cancer stem cells with metastatic capacity in human colorectal cancer. *Cell Stem Cell*, 6(6), pp.603–615.

Pant, S. et al., 2016. A first-in-human phase I study of the oral Notch inhibitor, LY900009, in patients with advanced cancer. *European journal of cancer (Oxford, England : 1990)*, 56, pp.1–9.

Park, I.-K., Morrison, S.J. & Clarke, M.F., 2004. Bmi1, stem cells, and senescence regulation. *The Journal of clinical investigation*, 113(2), pp.175–9.

Park, J.-I. et al., 2009. Telomerase modulates Wnt signalling by association with target gene chromatin. *Nature*, 460(7251), pp.66–72.

Paulus, U. et al., 1993. The differentiation and lineage development of goblet cells in the murine small intestinal crypt: experimental and modelling studies. *Journal of cell science*, 106 (Pt 2, pp.473–483.

Pelaseyed, T. et al., 2014. The mucus and mucins of the goblet cells and enterocytes provide the first defense line of the gastrointestinal tract and interact with the immune system. *Immunological Reviews*, 260(1), pp.8–20.

Pellegrinet, L. et al., 2011. Dll1- and Dll4-mediated notch signaling are required for homeostasis of intestinal stem cells. *Gastroenterology*, 140(4), pp.1230–1240.

Petcherski, A.G. & Kimble, J., 2000. LAG-3 is a putative transcriptional activator in the C. elegans Notch pathway. *Nature*, 405(6784), pp.364–8.

Phillips, T.M., McBride, W.H. & Pajonk, F., 2006. The response of CD24(-/low)/CD44+ breast cancer-initiating cells to radiation. *Journal of the National Cancer Institute*, 98(24), pp.1777–85.

Pietrantonio, F. et al., 2015. First-line anti-EGFR monoclonal antibodies in panRAS wild-type metastatic colorectal cancer: A systematic review and meta-analysis. *Critical reviews in oncology/hematology*, 96(1), pp.156–66.

Pinson, K.I. et al., 2000. An LDL-receptor-related protein mediates Wnt signalling in mice. *Nature*, 407(6803), pp.535–8.

Pinto, D. et al., 2003. Canonical Wnt signals are essential for homeostasis of the intestinal epithelium. *Genes & development*, 17(14), pp.1709–13.

Pita-Fernández, S. et al., 2015. Intensive follow-up strategies improve outcomes in nonmetastatic colorectal cancer patients after curative surgery: a systematic review and meta-analysis. *Annals of oncology : official journal of the European Society for Medical Oncology / ESMO*, 26(4), pp.644–656.

Pitsouli, C. & Delidakis, C., 2005. The interplay between DSL proteins and ubiquitin ligases in Notch signaling. *Development (Cambridge, England)*, 132(18), pp.4041–50.

Plaks, V., Kong, N. & Werb, Z., 2015. The Cancer Stem Cell Niche: How Essential Is the Niche in Regulating Stemness of Tumor Cells? *Cell Stem Cell*, 16(3), pp.225–238.

Port, F. et al., 2008. Wingless secretion promotes and requires retromer-dependent cycling of Wntless. *Nature cell biology*, 10(2), pp.178–85.

Potten, C.S. et al., 2003. Identification of a putative intestinal stem cell and early lineage marker; musashi-1. *Differentiation; research in biological diversity*, 71(1), pp.28–41.

Potten, C.S. & Loeffler, M., 1987. A comprehensive model of the crypts of the small intestine of the mouse provides insight into the mechanisms of cell migration and the proliferation hierarchy. *Journal of theoretical biology*, 127(4), pp.381–391.

Potten, C.S., Owen, G. & Booth, D., 2002. Intestinal stem cells protect their genome by

selective segregation of template DNA strands. *Journal of cell science*, 115(Pt 11), pp.2381–2388.

Pourebrahim, R. et al., 2011. Transcription factor Zic2 inhibits Wnt/β-catenin protein signaling. *The Journal of biological chemistry*, 286(43), pp.37732–40.

Powell, A.E. et al., 2012. The pan-ErbB negative regulator lrig1 is an intestinal stem cell marker that functions as a tumor suppressor. *Cell*, 149(1), pp.146–158.

Qiu, L. et al., 2000. Recognition and ubiquitination of Notch by Itch, a hect-type E3 ubiquitin ligase. *The Journal of biological chemistry*, 275(46), pp.35734–7.

Ramain, P. et al., 2001. Novel Notch alleles reveal a Deltex-dependent pathway repressing neural fate. *Current biology : CB*, 11(22), pp.1729–38.

Ramakrishnan, V. et al., 2012. MRK003, a γ-secretase inhibitor exhibits promising in vitro pre-clinical activity in multiple myeloma and non-Hodgkin's lymphoma. *Leukemia*, 26(2), pp.340–8.

Rand, M.D. et al., 2000. Calcium depletion dissociates and activates heterodimeric notch receptors. *Molecular and cellular biology*, 20(5), pp.1825–35.

Rangarajan, A. et al., 2001. Notch signaling is a direct determinant of keratinocyte growth arrest and entry into differentiation. *The EMBO journal*, 20(13), pp.3427–36.

Real, P.J. et al., 2009. Gamma-secretase inhibitors reverse glucocorticoid resistance in T cell acute lymphoblastic leukemia. *Nature medicine*, 15(1), pp.50–8.

Reedijk, M. et al., 2008. Activation of Notch signaling in human colon adenocarcinoma. *International journal of oncology*, 33(6), pp.1223–9.

Riccio, O. et al., 2008. Loss of intestinal crypt progenitor cells owing to inactivation of both Notch1 and Notch2 is accompanied by derepression of CDK inhibitors p27Kip1 and p57Kip2. *EMBO reports*, 9(4), pp.377–383.

Ricci-Vitiani, L. et al., 2007. Identification and expansion of human colon-cancer-initiating cells. *Nature*, 445(7123), pp.111–115.

Ridgway, J. et al., 2006. Inhibition of Dll4 signalling inhibits tumour growth by deregulating angiogenesis. *Nature*, 444(7122), pp.1083–7.

Rijsewijk, F. et al., 1987. The Drosophila homolog of the mouse mammary oncogene int-1 is identical to the segment polarity gene wingless. *Cell*, 50(4), pp.649–57.

Robert-Moreno, A. et al., 2005. RBPjkappa-dependent Notch function regulates Gata2 and is essential for the formation of intra-embryonic hematopoietic cells. *Development (Cambridge, England)*, 132(5), pp.1117–26.

Roche, K.C. et al., 2015. SOX9 maintains reserve stem cells and preserves radioresistance in mouse small intestine. *Gastroenterology*, 149(6), pp.1553–1563.e10.

Rodilla, V. et al., 2009. Jagged1 is the pathological link between Wnt and Notch pathways in colorectal cancer. *Proceedings of the National Academy of Sciences of the United States of America*, 106(15), pp.6315–20.

Rogakou, E.P. et al., 1999. Megabase chromatin domains involved in DNA double-strand breaks in vivo. *The Journal of cell biology*, 146(5), pp.905–16.

Ronchini, C. & Capobianco, A.J., 2001. Induction of cyclin D1 transcription and CDK2 activity by Notch(ic): implication for cell cycle disruption in transformation by Notch(ic). *Molecular and cellular biology*, 21(17), pp.5925–34.

Rothenberg, M.E. et al., 2012. Identification of a cKit + colonic crypt base secretory cell that supports Lgr5 + stem cells in mice. *Gastroenterology*, 142(5), pp.1195–1205.e6.

Roura, S. et al., 2003. APC 3×15 β-catenin-binding domain potentiates β-catenin association to TBP and upregulates TCF-4 transcriptional activity. *Biochemical and Biophysical Research Communications*, 309(4), pp.830–835.

Rubinfeld, B. et al., 1993. Association of the APC gene product with beta-catenin. *Science (New York, N.Y.)*, 262(5140), pp.1731–1734.

Rulifson, E.J. & Blair, S.S., 1995. Notch regulates wingless expression and is not required for reception of the paracrine wingless signal during wing margin neurogenesis in Drosophila. *Development (Cambridge, England)*, 121(9), pp.2813–24.

Sacerdotti, C., 1894. Über die Entwicklung der Schleimzellen des Magendarmkanals. *Int. Mschr. Anat. Physiol.*, 11, pp.501–514.

Saito, N. et al., 2015. Effect of Notch expression in glioma stem cells on therapeutic response to chemo-radiotherapy in recurrent glioblastoma. *Brain tumor pathology*, 32(3), pp.176–83.

Sakanaka, C., Weiss, J.B. & Williams, L.T., 1998. Bridging of beta-catenin and glycogen synthase kinase-3beta by axin and inhibition of beta-catenin-mediated transcription. *Proceedings of the National Academy of Sciences of the United States of America*, 95(6), pp.3020–3.

Sakata, T. et al., 2004. Drosophila Nedd4 regulates endocytosis of notch and suppresses its ligand-independent activation. *Current biology : CB*, 14(24), pp.2228–36.

Samon, J.B. et al., 2012. Preclinical analysis of the γ-secretase inhibitor PF-03084014 in combination with glucocorticoids in T-cell acute lymphoblastic leukemia. *Molecular cancer therapeutics*, 11(7), pp.1565–75.

Sanders, P.G.T. et al., 2009. Ligand-independent traffic of Notch buffers activated Armadillo in Drosophila. *PLoS biology*, 7(8), p.e1000169.

Sangiorgi, E. & Capecchi, M.R., 2008. Bmi1 is expressed in vivo in intestinal stem cells. *Nature genetics*, 40(7), pp.915–920.

Sasai, Y. et al., 1992. Two mammalian helix-loop-helix factors structurally related to Drosophila hairy and Enhancer of split. *Genes and Development*, 6(12 PART B), pp.2620–2634.

Sato, A., 2007. Tuft cells. *Anatomical Science International*, 82(4), pp.187–199.

Sato, T. et al., 2011. Paneth cells constitute the niche for Lgr5 stem cells in intestinal crypts. *Nature*, 469(7330), pp.415–418.

Sato, T. et al., 2009. Single Lgr5 stem cells build crypt-villus structures in vitro without a mesenchymal niche. *Nature*, 459(7244), pp.262–265.

Schepers, a. G. et al., 2012. Lineage Tracing Reveals Lgr5+ Stem Cell Activity in Mouse Intestinal Adenomas. *Science*, 337(6095), pp.730–735.

Schepers, A.G. et al., 2011. Lgr5 intestinal stem cells have high telomerase activity and randomly segregate their chromosomes. *The EMBO journal*, 30(6), pp.1104–1109.

Schröder, N. & Gossler, A., 2002. Expression of Notch pathway components in fetal and adult mouse small intestine. *Gene expression patterns : GEP*, 2(3-4), pp.247–50.

Schuijers, J. et al., 2015. Ascl2 acts as an R-spondin/Wnt-responsive switch to control stemness in intestinal crypts. *Cell stem cell*, 16(2), pp.158–70.

Schwalbe, G., 1872. Beiträge zur Kenntniss der Drüsen in den Darmwandungen, insbesondere der Brunnerschen Drüsen. *Arch. Mikrosk. Anat.*, 8, pp.92–140.

Sethi, M.K. et al., 2010. Identification of glycosyltransferase 8 family members as xylosyltransferases acting on O-glucosylated notch epidermal growth factor repeats. *The Journal of biological chemistry*, 285(3), pp.1582–6.

Shan, M. et al., 2013. Mucus enhances gut homeostasis and oral tolerance by delivering immunoregulatory signals. *Science (New York, N.Y.)*, 342(6157), pp.447–53.

Sharma, M. et al., 2012. Specific armadillo repeat sequences facilitate β-catenin nuclear transport in live cells via direct binding to nucleoporins Nup62, Nup153, and RanBP2/Nup358. *The Journal of biological chemistry*, 287(2), pp.819–31.

Sharpless, N.E. et al., 2004. The differential impact of p16(INK4a) or p19(ARF) deficiency on cell growth and tumorigenesis. *Oncogene*, 23(2), pp.379–385.

Shen, B. et al., 2005. Human defensin 5 expression in intestinal metaplasia of the upper gastrointestinal tract. *Journal of clinical pathology*, 58(7), pp.687–94.

Sherr, C.J., 2001. The INK4a/ARF network in tumour suppression. *Nature reviews. Molecular cell biology*, 2(10), pp.731–737.

Shi, S. & Stanley, P., 2003. Protein O-fucosyltransferase 1 is an essential component of Notch signaling pathways. *Proceedings of the National Academy of Sciences of the United States of America*, 100(9), pp.5234–9.

Shin, C.H. et al., 2002. Modulation of cardiac growth and development by HOP, an unusual homeodomain protein. *Cell*, 110(6), pp.725–35.

Sinner, D. et al., 2007. Sox17 and Sox4 differentially regulate beta-catenin/T-cell factor activity and proliferation of colon carcinoma cells. *Molecular and cellular biology*, 27(22), pp.7802–15.

Smith, D.C. et al., 2014. A phase I dose escalation and expansion study of the anticancer stem cell agent demcizumab (anti-DLL4) in patients with previously treated solid tumors. *Clinical cancer research : an official journal of the American Association for Cancer Research*, 20(24), pp.6295–303.

Snippert, H.J. et al., 2009. Prominin-1/CD133 Marks Stem Cells and Early Progenitors in Mouse Small Intestine. *Gastroenterology*, 136(7), pp.2187–2194.e1.

Sonoshita, M. et al., 2015. Promotion of Colorectal Cancer Invasion and Metastasis through Activation of NOTCH-DAB1-ABL-RHOGEF Protein TRIO. *Cancer discovery*, 5(2), pp.198–211.

Sonoshita, M. et al., 2011. Suppression of colon cancer metastasis by aes through inhibition of notch signaling. *Cancer Cell*, 19(1), pp.125–137.

Sorkin, A. & von Zastrow, M., 2009. Endocytosis and signalling: intertwining molecular networks. *Nature reviews. Molecular cell biology*, 10(9), pp.609–22.

Sousa-Victor, P. et al., 2014. Geriatric muscle stem cells switch reversible quiescence into senescence. *Nature*, 506(7488), pp.316–21.

Specian, R.D. & Oliver, M.G., 1991. Functional biology of intestinal goblet cells. *The American journal of physiology*, 260(2 Pt 1), pp.C183–C193.

Srinivas, S. et al., 2001. Cre reporter strains produced by targeted insertion of EYFP and ECFP into the ROSA26 locus. *BMC developmental biology*, 1, p.4.

Städeli, R., Hoffmans, R. & Basler, K., 2006. Transcription under the control of nuclear Arm/beta-catenin. *Current biology : CB*, 16(10), pp.R378–85.

Stanley, P., 2007. Regulation of Notch signaling by glycosylation. *Current opinion in structural biology*, 17(5), pp.530–5.

Stanley, P. & Okajima, T., 2010. Roles of glycosylation in Notch signaling. *Current topics in developmental biology*, 92, pp.131–64.

De Strooper, B. et al., 1999. A presenilin-1-dependent gamma-secretase-like protease mediates release of Notch intracellular domain. *Nature*, 398(6727), pp.518–22.

Struhl, G. & Greenwald, I., 1999. Presenilin is required for activity and nuclear access of Notch in Drosophila. *Nature*, 398(6727), pp.522–5.

Su, L.K. et al., 1992. Multiple intestinal neoplasia caused by a mutation in the murine homolog of the APC gene. *Science (New York, N.Y.)*, 256(5057), pp.668–670.

Su, L.K., Vogelstein, B. & Kinzler, K.W., 1993. Association of the APC tumor suppressor protein with catenins. *Science (New York, N.Y.)*, 262(5140), pp.1734–1737.

Su, Y. et al., 2008. APC is essential for targeting phosphorylated beta-catenin to the SCFbeta-TrCP ubiquitin ligase. *Molecular cell*, 32(5), pp.652–61.

Sui, X. et al., 2015. p53 controls colorectal cancer cell invasion by inhibiting the NF-κB-mediated activation of Fascin. *Oncotarget*, 6(26), pp.22869–79.

Takeda, N. et al., 2011. Interconversion Between Intestinal Stem Cell Populations in Distinct Niches. *Science*, 334(6061), pp.1420–1424.

Takenobu, H. et al., 2011. CD133 suppresses neuroblastoma cell differentiation via signal pathway modification. *Oncogene*, 30(1), pp.97–105.

Tamai, K. et al., 2000. LDL-receptor-related proteins in Wnt signal transduction. *Nature*, 407(6803), pp.530–5.

Tanaka, S. et al., 2015. Strong therapeutic potential of γ-secretase inhibitor MRK003 for CD44-high and CD133-low glioblastoma initiating cells. *Journal of neuro-oncology*, 121(2), pp.239–50.

Tetteh, P.W. et al., 2016. Replacement of Lost Lgr5-Positive Stem Cells through Plasticity of Their Enterocyte-Lineage Daughters. *Cell Stem Cell*, 18(2), pp.203–13.

Thompson, B.J. et al., 2007. The SCFFBW7 ubiquitin ligase complex as a tumor suppressor in T cell leukemia. *The Journal of experimental medicine*, 204(8), pp.1825–35.

Tian, H. et al., 2012. A reserve stem cell population in small intestine renders Lgr5-positive cells dispensable. *Nature*, 482(7383), pp.120–120.

Timmerman, L.A. et al., 2004. Notch promotes epithelial-mesenchymal transition during cardiac development and oncogenic transformation. *Genes & development*, 18(1), pp.99–115.

Todaro, M. et al., 2014. CD44v6 is a marker of constitutive and reprogrammed cancer stem cells driving colon cancer metastasis. *Cell stem cell*, 14(3), pp.342–56.

Tran, I.T. et al., 2013. Blockade of individual Notch ligands and receptors controls graft-versus-host disease. *The Journal of clinical investigation*, 123(4), pp.1590–604.

Tsunematsu, R. et al., 2004. Mouse Fbw7/Sel-10/Cdc4 is required for notch degradation during vascular development. *The Journal of biological chemistry*, 279(10), pp.9417–23.

Valeri, N. et al., 2014. MicroRNA-135b promotes cancer progression by acting as a downstream effector of oncogenic pathways in colon cancer. *Cancer cell*, 25(4), pp.469–83.

Valk-Lingbeek, M.E., Bruggeman, S.W.M. & van Lohuizen, M., 2004. Stem cells and cancer; the polycomb connection. *Cell*, 118(4), pp.409–18.

VanDussen, K.L. et al., 2012. Notch signaling modulates proliferation and differentiation of intestinal crypt base columnar stem cells. *Development (Cambridge, England)*, 139(3), pp.488–97.

Vässin, H. et al., 1987. The neurogenic gene Delta of Drosophila melanogaster is expressed in neurogenic territories and encodes a putative transmembrane protein with EGF-like repeats. *The EMBO journal*, 6(11), pp.3431–40.

Vermezovic, J. et al., 2015. Notch is a direct negative regulator of the DNA-damage response. *Nature structural & molecular biology*, 22(5), pp.417–24.

Visvader, J.E. & Lindeman, G.J., 2008. Cancer stem cells in solid tumours: accumulating evidence and unresolved questions. *Nature reviews. Cancer*, 8(10), pp.755–768.

Walker, F. et al., 2011. LGR5 is a negative regulator of tumourigenicity, antagonizes wnt signalling and regulates cell adhesion in colorectal cancer cell lines. *PLoS ONE*, 6(7).

Wallberg, A.E. et al., 2002. p300 and PCAF act cooperatively to mediate transcriptional activation from chromatin templates by notch intracellular domains in vitro. *Molecular and cellular biology*, 22(22), pp.7812–9.

Wang, L. et al., 2014. Regulation of the phosphorylation and nuclear import and export of β-catenin by APC and its cancer-related truncated form. *Journal of cell science*, 127(Pt 8), pp.1647–59.

Wang, Y. et al., 1996. Identification of a GDP-L-fucose:polypeptide fucosyltransferase and enzymatic addition of O-linked fucose to EGF domains. *Glycobiology*, 6(8), pp.837–42.

Wang, Y. et al., 2001. Modification of epidermal growth factor-like repeats with O-fucose. Molecular cloning and expression of a novel GDP-fucose protein O-fucosyltransferase. *The Journal of biological chemistry*, 276(43), pp.40338–45.

Ward, I.M. & Chen, J., 2001. Histone H2AX is phosphorylated in an ATR-dependent manner in response to replicational stress. *The Journal of biological chemistry*, 276(51), pp.47759–62.

Waterhouse, C.C.M. et al., 2010. Secretory cell hyperplasia and defects in Notch activity in a mouse model of leukocyte adhesion deficiency type II. *Gastroenterology*, 138(3), pp.1079–90.e1–5.

Wehrli, M. et al., 2000. arrow encodes an LDL-receptor-related protein essential for Wingless signalling. *Nature*, 407(6803), pp.527–30.

Wei, P. et al., 2010. Evaluation of selective gamma-secretase inhibitor PF-03084014 for its antitumor efficacy and gastrointestinal safety to guide optimal clinical trial design. *Molecular cancer therapeutics*, 9(6), pp.1618–28.

Weng, A.P. et al., 2004. Activating mutations of NOTCH1 in human T cell acute

lymphoblastic leukemia. *Science (New York, N.Y.)*, 306(5694), pp.269–71.

Weng, A.P. et al., 2006. c-Myc is an important direct target of Notch1 in T-cell acute lymphoblastic leukemia/lymphoma. *Genes & development*, 20(15), pp.2096–109.

Weng, A.P. et al., 2003. Growth suppression of pre-T acute lymphoblastic leukemia cells by inhibition of notch signaling. *Molecular and cellular biology*, 23(2), pp.655–64.

van de Wetering, M. et al., 1997. Armadillo coactivates transcription driven by the product of the Drosophila segment polarity gene dTCF. *Cell*, 88(6), pp.789–99.

Van de Wetering, M. et al., 2002. The ??-catenin/TCF-4 complex imposes a crypt progenitor phenotype on colorectal cancer cells. *Cell*, 111(2), pp.241–250.

Wilkin, M.B. et al., 2004. Regulation of notch endosomal sorting and signaling by Drosophila Nedd4 family proteins. *Current biology : CB*, 14(24), pp.2237–44.

Wolfe, M.S. et al., 1999. Two transmembrane aspartates in presenilin-1 required for presenilin endoproteolysis and gamma-secretase activity. *Nature*, 398(6727), pp.513–7.

Wong, V.W.Y. et al., 2012. Lrig1 controls intestinal stem-cell homeostasis by negative regulation of ErbB signalling. *Nature Cell Biology*, 14(4), pp.401–408.

Wu, D. & Pan, W., 2010. GSK3: a multifaceted kinase in Wnt signaling. *Trends in biochemical sciences*, 35(3), pp.161–8.

Wu, L. et al., 2002. Identification of a family of mastermind-like transcriptional coactivators for mammalian notch receptors. *Molecular and cellular biology*, 22(21), pp.7688–700.

Wu, L. et al., 2000. MAML1, a human homologue of Drosophila mastermind, is a transcriptional co-activator for NOTCH receptors. *Nature genetics*, 26(4), pp.484–9.

Wu, X. et al., 2016. Autophagy regulates Notch degradation and modulates stem cell development and neurogenesis. *Nature Communications*, 7, p.10533.

Wu, Y. et al., 2010. Therapeutic antibody targeting of individual Notch receptors. *Nature*, 464(7291), pp.1052–7.

Wu, Z. et al., 2015. TPO-Induced Metabolic Reprogramming Drives Liver Metastasis of Colorectal Cancer CD110+ Tumor-Initiating Cells. *Cell stem cell*, 17(1), pp.47–59.

Xu, Q. et al., 2004. Vascular development in the retina and inner ear: control by Norrin and Frizzled-4, a high-affinity ligand-receptor pair. *Cell*, 116(6), pp.883–95.

Xue, Y. et al., 1999. Embryonic lethality and vascular defects in mice lacking the Notch ligand Jagged1. *Human molecular genetics*, 8(5), pp.723–30.

Yamamizu, K. et al., 2010. Convergence of Notch and beta-catenin signaling induces arterial fate in vascular progenitors. *The Journal of cell biology*, 189(2), pp.325–38.

Yamamoto, S., Charng, W.-L. & Bellen, H.J., 2010. Endocytosis and intracellular trafficking of Notch and its ligands. *Current topics in developmental biology*, 92, pp.165–200.

Yan, K., Chia, L. & Li, X., 2012. The intestinal stem cell markers Bmi1 and Lgr5 identify two functionally distinct populations. *Pnas*, 109(2), pp.466–471.

Yan, M. et al., 2010. Chronic DLL4 blockade induces vascular neoplasms. *Nature*, 463(7282), pp.E6–7.

Yan, S.-J. et al., 2004. Multiple signaling pathways and a selector protein sequentially

regulate Drosophila wing development. *Development (Cambridge, England)*, 131(2), pp.285–98.

Yang, B. et al., 2013. Effect of radiation on the Notch signaling pathway in osteoblasts. *International journal of molecular medicine*, 31(3), pp.698–706.

Yang, P.-T. et al., 2008. Wnt signaling requires retromer-dependent recycling of MIG-14/Wntless in Wnt-producing cells. *Developmental cell*, 14(1), pp.140–7.

Yang, Q. et al., 2001. Requirement of Math1 for secretory cell lineage commitment in the mouse intestine. *Science (New York, N.Y.)*, 294(5549), pp.2155–2158.

Yashiro-Ohtani, Y. et al., 2009. Pre-TCR signaling inactivates Notch1 transcription by antagonizing E2A. *Genes & development*, 23(14), pp.1665–76.

Ye, Y., Lukinova, N. & Fortini, M.E., 1999. Neurogenic phenotypes and altered Notch processing in Drosophila Presenilin mutants. *Nature*, 398(6727), pp.525–9.

Yokoya, F. et al., 1999. beta -Catenin Can Be Transported into the Nucleus in a Ran-unassisted Manner. *Molecular Biology of the Cell*, 10(4), pp.1119–1131.

Yu, T. et al., 2012. Regulation of the potential marker for intestinal cells, Bmi1, by ??-catenin and the zinc finger protein KLF4: Implications for colon cancer. *Journal of Biological Chemistry*, 287(6), pp.3760–3768.

Zacharek, S.J. et al., 2011. Lung stem cell self-renewal relies on BMI1-dependent control of expression at imprinted loci. *Cell Stem Cell*, 9(3), pp.272–281.

Zagouras, P. et al., 1995. Alterations in Notch signaling in neoplastic lesions of the human cervix. *Proceedings of the National Academy of Sciences of the United States of America*, 92(14), pp.6414–8.

Zecchini, V., Brennan, K. & Martinez-Arias, A., 1999. An activity of Notch regulates JNK signalling and affects dorsal closure in Drosophila. *Current biology : CB*, 9(9), pp.460–9.

Zeng, X. et al., 2005. A dual-kinase mechanism for Wnt co-receptor phosphorylation and activation. *Nature*, 438(7069), pp.873–7.

Zhai, L., Chaturvedi, D. & Cumberledge, S., 2004. Drosophila wnt-1 undergoes a hydrophobic modification and is targeted to lipid rafts, a process that requires porcupine. *The Journal of biological chemistry*, 279(32), pp.33220–7.

Zhang, Y. et al., 2010. Notch1 regulates the growth of human colon cancers. *Cancer*, 116(22), pp.5207–18.

Zheng, H. et al., 2009. KLF4 gene expression is inhibited by the notch signaling pathway that controls goblet cell differentiation in mouse gastrointestinal tract. *American journal of physiology. Gastrointestinal and liver physiology*, 296(3), pp.G490–8.

Zhou, J. et al., 2009. Notch and wingless signaling cooperate in regulation of dendritic cell differentiation. *Immunity*, 30(6), pp.845–59.

Zhu, L. et al., 2009. Prominin 1 marks intestinal stem cells that are susceptible to neoplastic transformation. *Nature*, 457(7229), pp.603–7.

Zhu, Y. et al., 2013. Apoptosis differently affects lineage tracing of lgr5 and bmi1 intestinal stem cell populations. *Cell Stem Cell*, 12(3), pp.298–303.

ARTICLE

Lopez-Arribillaga E, Rodilla V, Pellegrinet L, Guiu J, Iglesias M, Roman AC, et al. Bmi1 regulates murine intestinal stem cell proliferation and self-renewal downstream of Notch. Development. 2015 Jan 1;142(1):41–50. DOI: 10.1242/dev.107714